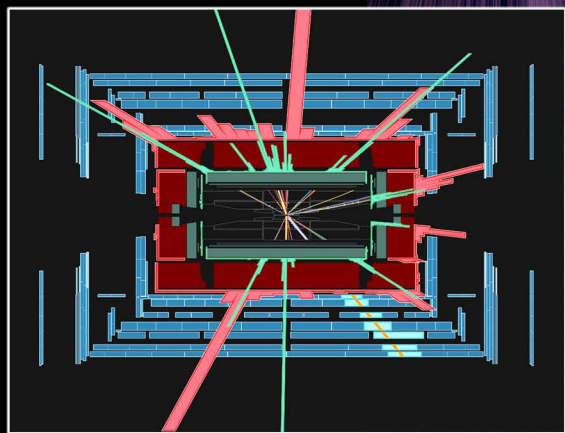
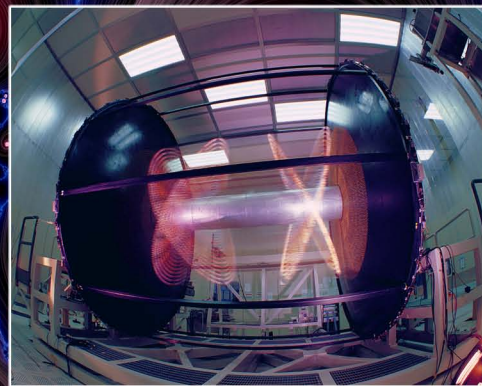


istituto nazionale di fisica nucleare
laboratori nazionali di Frascati

2004 ANNUAL REPORT



Cover:

Up – right: *The drift chamber of the KLOE experiment at the DAΦNE accelerator of the INFN – LNF.* (Photo Claudio Federici)

Middle: *A Japanese magnolia in blossom with the dome of the hall hosting the DAΦNE accelerator of the INFN – LNF in the background.* (Photo Rossana Morani)

Bottom – left: *A simulated event in the ATLAS detector at the CERN Large Hadron Collider in which a mini-blackhole is produced in the collision of two protons and immediately decays.* (Courtesy of the LNF ATLAS group)

Cover artwork: *Claudio Federici*

istituto nazionale di fisica nucleare
laboratori nazionali di Frascati

2004

ANNUAL REPORT

LNF-05/05 (IR)
April, 2005

Editor
Enrico Nardi

Technical Editor
Luigina Invidia

Published by
SIS-Pubblicazioni
P.O.Box 13 – I-00044 Frascati (Italia)

Available at www.lnf.infn.it/rapatt

Mario Calvetti
LNF Director (from November 2004)

Sergio Bertolucci
LNF Director (until October 2004)

Lucia Votano
Head, Research Division

Pantaleo Raimondi
Head, Accelerator Division (until August 2004)

Miro Andrea Preger
*Scientific Head, Accelerator Division
(from September 1, 2004)*

Claudio Sanelli
*Technical Head, Accelerator Division
(from September 1, 2004)*

LNF Scientific Coordinators

Maria Curatolo
Particle Physics

Marco Ricci
Astroparticle Physics

Valeria Muccifora
Nuclear Physics

Calogero Natoli
Theory and Phenomenology

Francesco Celani
Techn. and Interdisciplinary Research

FOREWORD

The Laboratori Nazionali di Frascati, situated on a hill just south of Rome, is the largest laboratory of the Italian Institute of Nuclear Physics.

The laboratory is organized into three sub-structures: the Accelerator Division, the Research Division and the Administration.

The Accelerator Division runs the DAΦNE accelerator complex, an $e^+ e^-$ storage ring used to produce Φ mesons at a high rate. Three experiments, KLOE, FINUDA, and DEAR, are used to study Φ and kaon decays.

A linear accelerator (the Linac) is used to accelerate electrons and positrons to fill the storage rings. The very clean electron and positron beams produced by the Linac, with variable energy between 50 and 850 MeV and variable intensity from 1 to 10^4 electrons per bunch at a rate of 50 Hz, can be deflected into an experimental area, the Beam Test Facility (BTF), where photon-tagged beams are also available.

The Accelerator Division is participating in the construction of the CNAO (Centro Nazionale Adroterapia Oncologica), a proton synchrotron used for medical purposes, in Pavia. A free electron laser, the SPARC project, is under construction at LNF, in collaboration with ENEA. Both projects should be completed by the end of the year 2007.

Physicists and engineers of the Accelerator Division also participate in research and development in the field of accelerator technology. The construction of CTF3, the CLIC Test Facility at CERN, the TTFII, the Tesla Test Facility at DESY, the work for the future World Linear Collider, and studies for a possible future Super B-factory, are all part of our research program.

The DAΦNE accelerator, which is continuously being improved, is also run to produce synchrotron radiation used by several experimental groups. The most intense infrared light for a synchrotron source is available at DAΦNE.

The Research Division is composed of physicists and engineers dedicated to experiments at LNF, at CERN (ATLAS, LHCb, DIRAC), at FNAL (CDFII), at SLAC (BABAR), at JLAB (AICE), at DESY (HERMES), in Grenoble (GRAAL), at the Laboratori Nazionali del Gran Sasso – LNGS (OPERA, ICARUS), at Cascina (VIRGO), in space born experiments within the WIZARD program, and also, locally, to search for gravitational waves with a cryogenic bar (NAUTILUS).

Among the most important scientific results obtained in the framework of the DAΦNE scientific program in the year 2004, I mention the measurements by the KLOE collaboration of V_{us} , important to verify the unitarity of the CKM matrix, and the measurement of the hadronic contributions to $g-2$. The measurement of the x-ray spectrum of kaonic hydrogen in DEAR and the observation of the first events from hypernuclei decays in FINUDA are also among the scientific highlights. Charged and monochromatic kaons produced by Φ decays constitute a unique tool for the study of hypernuclei. In 2004, DAΦNE reached a peak

luminosity of $1.3 \times 10^{32} \text{ cm}^{-2} \text{ s}^{-1}$, KLOE has collected about 750 pb^{-1} . The Frascati ATLAS group has completed the construction of the muon chambers and is now participating in the installation and testing of the detectors at CERN. The construction of the OPERA experiment continues at LNGS.

It is not up to the director, in this case, to judge the quality of the research performed by his laboratory: I leave such judgements to the reader.

The reader can find in this report a detailed description of the experimental and theoretical results obtained by the Research and Accelerator Divisions.

All this work was made possible by the devotion and dedication of many people; scientists, engineers, technicians, the administration, and the staff of the general services.

It is a fantastic adventure and a pleasure to be director of a laboratory with so many clever and dedicated people.

Prof. Mario Calvetti
Director of LNF

ACKNOWLEDGMENTS

Supervising the 2004 edition of the LNF annual report has given me the opportunity to appreciate the remarkably wide range of research activities that are being developed by LNF groups: from the larger groups cooperating with world-wide collaborations to small groups sometimes consisting of just a few researchers, the spectrum of scientific topics addressed is really vast, ranging from fundamental physics to the hi-tech frontier.

I would like to thank all the authors that contributed to this report, and in particular those that managed to submit their contribution within the scheduled deadline, notwithstanding the rather short notice.

My thanks go to Claudio Federici for the excellent design of the cover page, and to Stefano Bianco, Simone Dell'Agnello, Maria Curatolo, Maria Rita Ferrazza and Matthew Moulson for their help and suggestions. A special acknowledgment goes to Luigina Invidia for her very pleasant and productive collaboration in producing this report.

Finally, we all should thank the many colleagues whose activity, not being strictly related to scientific work, is not represented in this report: without their collaboration any kind of research at the LNF would hardly be possible.

Enrico Nardi
Editor

Laboratori Nazionali di Frascati

2004 ANNUAL REPORT

CONTENTS

<i>Foreword</i>	VII
<i>Acknowledgements</i>	IX
COMMUNICATION and OUTREACH	1
SCIENZA PER TUTTI	5
<i>1 – Particle Physics</i>	
ATLAS	9
BABAR	19
BTEV	27
CDF	33
E831	40
KLOE	42
LHC-b	55
<i>2 – Astroparticle Physics</i>	
ICARUS	65
LARES	67
NEMO	69
OPERA	70
PVLAS-DTZ	78
RAP-RD	80
ROG	82
VIRGO	88
WIZARD	90
<i>3 – Nuclear Physics</i>	
AIACE	93
FINUDA	99
GRAAL	106
HERMES	109
PANDA	119
SIDDHARTA	123
VIP	129

4 – Theory and Phenomenology

FA-51	131
LF-11	133
LF-21	141
MI-11	147
MI-12	148
PI-31	151

5 – Technological and Interdisciplinary Research

ARCHIMEDE	152
CAPIRE	154
CORA	157
DEUTER	159
E-CLOUD	163
FLUKA	166
FREETHAI	167
LAZIO-SiRad	172
MA-BO	174
MINCE	176
MIVEDE2	180
POLYX	181
SAFTA2	183
SI-RAD	187
SUE	189

6 – Accelerator Physics

DAΦNE	192
DAΦNE-BTF	207
DAΦNE-L Lab	213
GILDA	220
NTA CLIC	222
NTA TTF	224
SPARC	226

<i>LNF Publications</i>	236
--------------------------------------	-----

<i>Glossary</i>	245
------------------------------	-----

COMMUNICATION AND OUTREACH

R. Centioni, V. Ferretti (Art. 2222), S. Miozzi (Ass.), L. Sabatini, S. Vannucci (Resp.)
Office of Education and Public Relations
Scientific Information Service

The “Laboratori Nazionali di Frascati dell’INFN” (LNF) provide basic education in Physics for the general public, students and teachers. The LNF Educational and Public Relation programmes are made possible by the enthusiastic involvement of the laboratory graduate students, postdocs, researchers, engineers and technicians. This report describes the 2004 activity.

1 LNF guided tours, Scientific Week, Open Day and ScienzaOrienta

<http://www.lnf.infn.it/edu/>

A well established laboratory tradition: 4500 people/year for general public, students and teachers. Scientific coordinators: D. Babusci, L. Benussi, P. Gianotti, G. Mazzitelli, C. Petrascu, B. Sciascia. 81 volunteers have received 168 groups. A typical visit consists of:

- history of the laboratory;
- presentation of INFN-LNF activities on site and abroad;
- visit to the “en plein air museum”;
- visit to experimental areas.

LNF Scientific Week, Open day and ScienzaOrienta: 2500 visitors.

Most of LNF employees are in action to present their research center, answer questions and care for their guests. Since 1990 this is organized as:

- guided tours;
- conferences and public lectures;
- scientific videos;
- exhibitions of students’ projects;
- Open Day.

2 Outreach: Scientific Itineraries

The aim is to offer a more complete view of the scientific institutions operating in the area and improve the communication with the general public. In collaboration with:

- CNR Tor Vergata;
- ENEA Frascati;
- ESA-ESRIN Frascati;
- INAF Astronomical Observatory of Rome, Monte Porzio Catone;
- University of Rome Tor Vergata;
- COPIT, Rome;
- Frascati Municipality;
- International non-government organizations.



Figure 1: *LNF Tutor Danilo Babusci with summer stagists (photo by Roberto Baldini).*

3 High school students' programme

<http://www.lnf.infn.it/edu/stagelnf/>

Scientific Coordinator: L. Votano.

Goal: enable students to acquire the knowledge and understanding of INFN research activities.

- Winter stages, 2-4 weeks: 10 students with 6 tutors;
- Spring stages, 2-4 weeks: 37 students with 14 tutors;
- Summer stages, 1 week: 31 students with 5 tutors;
- INFN research and university course orientation, 2-3 days: 203 students with 7 tutors.

- Special Program for Primary School: QUASAR

<http://www.lnf.infn.it/edu/quasar/>

Care of F. Murtas and B. Sciascia.

Age: 8 - 14.

First meeting with the children at their school to introduce the world of research and some concepts of modern physics. Then, visit to the Frascati National Laboratories by small groups. Total of children and teachers in visit = 341.



Figure 2: *Margherita Hack with some participants at Incontri di Fisica 2004 (photo by Claudio Federici).*

4 High school teachers' programme: Incontri di Fisica

<http://www.lnf.infn.it/edu/incontri/>

Organizing Committee: S. Bertolucci, L. Votano (chair), D. Babusci, S. Bianco, L.E. Casano, R. Centioni, S. Miozzi, L. Sabatini, S. Vannucci.

- Lectures and Experiments for high-school science teachers and scientific journalists.
- Goal: stimulate teachers' professional training and provide an occasion for interactive and hands-on contact with the latest developments in physics.

Fourth edition (2004): 163 teachers, 75 students and 5 scientific journalists; 72 LNF Tutors (researchers, engineers and technicians).

5 General public programme

- Seminars

<http://www.lnf.infn.it/edu/seminaridivulgativi/>

Upon request, LNF researchers give seminars to high school students and general public on:

- INFN Activities and Elementary Particles;
- Modern Physics and Cosmology;
- Synchrotron Light;
- Gravitational waves.

- **Incontri con l'Autore**

<http://www.lnf.infn.it/edu/ica/>

Scientific coordinators: D. Babusci and C. Petrascu.

To disseminate the scientific culture by inviting an author presenting his recent book.

- Luisa Bonolis, M.G. Melchionni “Fisici Italiani del tempo presente”, LNF, February 18, 2004.
- David Goodstein “Il mondo in riserva. Energia, clima, il futuro della civiltà”, LNF, June 24, 2004.
- Luisa Bonolis, Carlo Bernardini and Enrico Agapito, film “Bruno Touschek e l’arte della fisica”, LNF, October 7, 2004.

6 Events

1. IV Incontro con la Scienza, Conference given by Prof. Franco Pacini, Frascati June 17, 2004.
2. V Incontro con la Scienza, Conference given by Prof. Antonino Zichichi Frascati November 9, 2004.
3. Christmas Concert, COROANAROMA LNF December 15, 2004.

Conferences

International conferences, workshops and schools hosted and organized by the LNF:

1. Les Rencontres de Physique de la Vallée d’Aoste, La Thuile, ITALY, February 29 - March 6, 2004.
2. AntiProton Annihilation at Darmstadt (PANDA), LNF, March 18-19, 2004.
3. Relativistic Channeling and Related Coherent Phenomena, LNF, March 23-26, 2004.
4. ELAN 2004, LNF, May 4-6, 2004.
5. LNF Spring School 2004, LNF, May 17-21, 2004.
6. Vulcano 2004, Vulcano, May 24-29, 2004.
7. Dafne 2004: Physics at Meson Factories, LNF, June 7-11, 2004.
8. Frontier Science 2004, LNF, June 14-19, 2004.
9. Transversity: new developments in nucleon spin structure, Trento, June 13-18, 2004.
10. Diffraction 2004, Cala Gonone Sardinia, September 18-23, 2004.
11. Nanotubes 2004, LNF, October 14-20, 2004.
12. Giornate di studio “Sicurezza degli apparati sperimentali e tecnologici dell’INFN”, LNF, October 25-27, 2004.
13. Channeling 2004, LNF, November 2-6, 2004.
14. ATLAS TDAQ Workshop, LNF, November 8-12, 2004.
15. 4th EuroGDR Meeting, LNF, November 25-27, 2004.

ScienzaPerTutti: A SCIENCE DISSEMINATION PROJECT

L. Benussi (Art. 23), H. Bilokon, F.L. Fabbri (Resp.), G. Isidori, G. Modestino,
G. Nicoletti, P. Patteri , C. Petrascu

1 Summary

ScienzaPerTutti is a communication and dissemination project about themes of science and, in more specific way, about those of physics addressed to the Italian general public with particular focus to the world of youth, to teachers and students. The project wants to constitute moments of direct dialog between the researchers and the non specialized public, actually the ultimate receiver, through the technological transfer, of the products of scientific research. At the same time, the project addresses itself to the galaxy of the youth world, offering, within the rigor of the contents, a humanized and user-friendly vision of science themes.

ScienzaPerTutti is articulated in:

- a web site: <http://scienzapertutti.lnf.infn.it/>,
- an annual contest adressed, to students and teachers of Italian school in the world,
- a series of public conferences on science frontiers.

The scientific research - and its technological evolvment reach - marks deeply our lives. It all leads to think that, beyond its own intrinsic value, the scientific progress will continue to produce even in the near future an enormous impact in society. Still, due to its formidable rhythm of growth, science disables the citizens - even those provided with a good cultural base- to keep in contact. The same instrument of communicating, the language - which becomes ever more specialized - constitutes an obstacle and contributes to increasing the distances between the producer and the consumer of science. As this awareness grows ScienzaPerTutti is an attempts to reunify for the Italian speaking public this fracture, and try to resolve the non easy task to bring the large public closer to the extraordinary challenge of modern physics through the stories of the scientific endeavors, of its men, of its machines and of its discoveries. The objective of the project ¹⁾ is to propagate the knowledge of some key meanings of physics, attempting to use an understandable language by a public mainly made up of students at high school level and curious about science. The philosophy inspiring the project is condensed within the logo-phrase of the web site: "-ScienzaPerTutti - where science can have an unexpected quality: to be fun".

2 Activities

The organizational structure of ScienzaPerTutti is made up of:

- (a) a promoting committee with the function of directing and guiding;
- (b) a scientific editorial board which has the responsibility of the preparation of all the published tests, of the monthly updating of the columns, of the addressing the questions sent by the web surfers to a group of experts and of completing their answers with glossary, addenda, references and graphs;
- (c) a group of more then 100 experts in different field of science which answer to the public;
- (d) external collaborators (university and high school professors or students) which help the scientific board.

In addition o this, it also counts on the collaboration of several project leaders and researchers invited by the scientific editorial board, who write articles about scientific arguments for non specialized readers.



Figure 1: *ScienzaPerTutti* homepage <http://scienzapertutti.lnf.infn.it> and the monthly accesses for the years 2003 and 2004.

The great dynamism of the site, with monthly updates and new contents, the interactivity of the editors and the experts with the web-surfers, the projects developed with the schools make *ScienzaPerTutti* a very active and lively community constituted of researchers, teachers, students, generic public.

Right from the appearance on the web, a large community of web surfers has greeted the site with great interest. The requests of daily access have grown from about 700 at the initial stage to 2700 by January 2005. The number of total requests cumulated in these two and half year is 2.179.762.

The site ranks absolute fifth in numbers of monthly access, among Italian sites that treat arguments of modern physics, preceded only by service sites like those of the INFN of the INFMM and the departments of the University of Bologna and Bari. About 67% of the accesses derive from dominions .it, 32% from dominions interbusiness.it, 11% from infn.it, 6% lnf.infn.it, and 3% from ch.it which shows participation by schools of Italian language in Switzerland too.

The experience accomplished during these two year of existence of *ScienzaPerTutti* has been very positive for different reasons: the goal of accesses, the loyalty of visitors, and the direct involvement of undergraduate schools and colleges. The texts of the *ScienzaPerTutti* site has been utilized as added teaching tools by more than 80 schools. About 700 students took part in the annual contest called by *ScienzaPerTutti* on themes as: the physics of the infinitesimal small (quarks and strings), the birth and evolution of the universe (big bang), the space messengers (neutrinos and cosmic rays), the particle accelerators machines, the quantum physics, the conservation of energy, the symmetry, the physics of chaos, and many others. The project will evolve in 2005 with the edition of the multilingual version (e), with the achievement of a modern experiment remotely operable ²⁾ via web offered to schools, and with the realization of specific projects to the celebration of the Year of Physics as, for instance, *12 Autobus* , *Einstein = Mc²* ³⁾.

(a) Promoting committee

R. Baldini, P. de Simone, E. Durante, F.L. Fabbri, G. Isidori, S. Ratti, P. Valente.

(b) Scientific editorial board

L. Benussi, H. Bilokon, P. de Simone, E. Durante, F. L. Fabbri, G. Modestino, G. Nicoletti, P. Patteri, C. Petrascu.

(c) Consultant experts

P. Agnoli, G. Amelino, R. Baiocchi, R. Baldini Celio, G. Barbiellini E. Basile, M. Basile, P. Belli, G. Bellini, S. Bellucci, H. Bilokon, S. Boffi, C. Bosio, C. Bruzzese, E. Burattini, G. Capon, M. Caponero, M. Casolino, P. Catone, F. Celani, O. Ciaffoni, I. Ciufolini, G. Corradi, L. Covi, S. D'Argenio, R. de Sangro, P. de Simone, P. di Nezza, U. Dosselli, E. Durante, A. Ereditato, A. Esposito, F. L. Fabbri, V. Fafone, M. Falcetta, A. Farina, F. Felli, M. L. Ferrer, P. Ferretti, L. Fo, P. Franzini, B. Gallavotti, M. Gasperini, M. Grandolfo, I. Iori, L. Iorio, G. Isidori, C. La Padula, C. Luci, V. Lucherini, M. Lusignoli, C. Matteuzzi, M. Mangano, G. Mannocchi, G. Mantovani, S. Marcello, I. Modena, G. Modestino, A. Moneti, G. Mussardo, G. P. Murtas, E. Nardi, C. Natoli, G. Nicoletti, L. Orr, M. Pallotta, E. Pallante, G. Pancheri, A. Paolozzi, E. Paris, L. Passamonti, P. Patteri, G. Penso, R. Peron, I. Peruzzi, C. Petrascu, M. Piccolo, G. Pizzella, F. Pompili, M. Primavera, L. Quintieri, S. Ratti, A. Reale, T. Regge, M. Ricci, E. Righi, F. Romano, F. Rosati, L. Ruggero, P. Santangelo, G. Saviano, C. Schaerf, L. Schirone, F. Sebastiani, A. Spallone, P. Spillantini, P. Strolin, G. Testera, S. Tomassini, L. Trasatti, L. Trentadue, G. Vilasi, F. Vissani, A. Venturelli.

(d) External collaborators

A. C. De Vitis (junior), F. R. Romano, E. Venturelli, A. Paolozzi, G. Bruzzese (engi. sec.).

(e) Multilingual versions

Portuguese: H. Bilokon, I. Bediaga (Rio de Janeiro), A. Maio (Lisbon).

Romanian: C. Petrascu, D. Sorghi.

French: F.L.Fabbri, L. Benussi C. Hadjidakis.

3 List of Conference Talks

- F.L. Fabbri, “La divulgazione in rete”, Alghero, LXXXVIII Congresso Nazionale SIF 2002.
- F.L. Fabbri, “ScienzaPerTutti: un progetto divulgativo in rete”, Parma, LXXXIX Congresso Nazionale SIF 2003.
- G. Modestino, “Il progetto ScienzaperTutti: un sito divulgativo in rete”, Brescia, XC Congresso Nazionale SIF, 2004.

References

1. L. Benussi *et al.*, Proceedings of “Expo e-learning2004” , Ferrara, October 2004.
2. F.L. Fabbri *et al.*, CRESCERE (Cosmic Rays in an European School Environment: a Remote Experiment), proposal to the European Commission under the call: FP6-2004-Mobility-13, FP6 – 019653.
3. <http://scienzapertutti.lnf.infn.it/wyp2005.html>

ATLAS

A. Antonelli, M. Antonelli, S. Argentati, M. Barone, M. Beretta, S. Bertolucci,
H. Bilokon, E. Capitolo (Tecn.), F. Cerutti, V. Chiarella, M. Curatolo, B. Dulach,
B. Esposito (Resp.), M.L. Ferrer, K. Kordas, P. Laurelli, G. Maccarrone, A. Martini, W. Mei,
G. Nicoletti, G. Pileggi (Tecn.), B. Ponzio (Tecn.), V. Russo (Tecn.), A. Sansoni,
T. Vassilieva (Tecn.), S. Ventura (Dott.)



Figure 1: *Status of the installation of the Atlas apparatus in the pit.*

1 Introduction

The Atlas experiment aims at covering the full physics potential at the LHC and is based on a general purpose apparatus of unprecedented performances and complexity to perform excellent inner tracking, electromagnetic and hadron calorimetry, muon measurement. A very large world-wide collaboration has shared the responsibility of the detector construction.

The LNF group has taken the responsibility of the construction of part of the precision tracking chambers of the Atlas muon spectrometer. The performance goal set for the muon spectrometer was to achieve in stand-alone mode a resolution $\delta p/p \simeq 10\%$ at $p_T = 1$ TeV in the measurement of the muon momenta. For that purpose a system of superconducting air core toroids, 1 for the barrel and 2 for the end-caps, has been designed, and tracking chambers of unprecedented resolution for such a large area detector have been developed ($40 \mu\text{m}$ resolution on single station point).

The Frascati group has participated in the design of the muon chambers with original contributions to the project, in particular developing the chamber assembly method and many production facilities, among which, particularly advanced from the point of view of technical achievement, is the fully automatic wiring machine.

The series production of muon chambers and the quality assurance and control of the production have been done using automated facilities, run via computer control, with limited human intervention. The facilities have been designed and realized by the Frascati group, with the instrumental collaboration of the Services and Workshops of the LNF Research Division.

Once the “bare” chambers are produced, the gas distribution system is mounted and the gas leak test is made; the Hedge-Hog FE Signal and HV boards are mounted; the Faraday cage is mounted; an electric integrity test and an HV test are made.

The bare chambers production work and the subsequent installation of services and test required about 4 year work at LNF with a team consisting of a few group technicians with the substantial addition of rotating short term temporary personnel, trained and guided by the group technicians. In the year 2004 the chamber construction phase was completed and the commissioning and integration was started at CERN. The installation in the Atlas pit is foreseen for the year 2005.

The picture in fig.1 show the status of advancement of the installation in the Atlas pit.

2 Chamber Production

The responsibility of the LNF group is the construction of all the BML (Barrel Middle Large) MDT (Monitoring Drift Tubes) chambers. They are 94 chambers which are to be located in the middle position of the 3-station chambers layout for the sagitta measurement and in between the toroid coils. The chambers cover an area of about 600 m^2 , with 6 sensitive detection planes along the track direction.

The chamber production has been going on for about 4 years and in the year 2004 has been completed. The picture in fig.2 show a set of chambers stored in the hall of the Capannone Gran Sasso at LNF.

3 Commissioning and Integration

The produced chambers are then shipped to CERN. Special transportation and storage frames have been designed for that purpose.

At CERN takes place the completion of the installation of services on the chambers. That concerns the active FE electronics, the so-called “mezzanine cards”, the mother boards of the CSM (chamber service module for the chamber read-out), the DCS components for the read-out of the alignment sensors and the temperature sensors, and the full cabling. The chambers undergo then a set of tests, in order to verify the integrity of all the components, their functionality and the correctness of the cabling connections. A gas leak test is also made. In fig.3 is a picture of a chamber showing the services installed.

Once the MDT chambers are completed and certified, they are to be integrated with two RPC (Resistive Plate Chambers) chambers, which are to provide the trigger on muons. The two RPC and the MDT chambers are assembled in one single mechanical package by means of special “common



Figure 2: *MDT Chambers in the storage frame in the hall of Capannone Gran Sasso at LNF.*

supports”, designed and built by the Frascati group, which guarantee the mechanical stability of the system and provide kinematical supports for the MDT chambers, to avoid producing deformations in the mechanics of the precision tracking chambers. The MDT-RPC integration is done by means of special tools, designed and built by the Frascati group.

The activity of commissioning and integration requires consistent man-power from the Institute to be located at CERN. In the year 2004 this phase of the activity started. At the end of the year the number of integrated MDT-RPC stations was 33. The picture in fig.4 show a set of MDT-RPC integrated stations in their storage frames.

4 Test beam

In the past years beam tests and cosmic ray tests have been performed in order to study the basic intrinsic performance of the muon detector and the system aspects of integrated components and subsystems. In the year 2004 a large scale system test of the ATLAS muon spectrometer on the H8 beam line at CERN has been completed. This test has been performed over four years. Its main goal was the study of the performance of the muon spectrometer in terms of momentum measurement and trigger capability and the integration of the different muon sub-systems (precision chambers, trigger chambers, alignment, DAQ, DCS and offline software) on a large test. The final setup achieved in 2004 included six barrel and six endcap precision chambers equipped with their optical alignment systems, two towers of barrel (RPC) and endcap trigger (TGC) chambers and two beam magnets in between precision chambers to measure the muon momenta. A picture of the 2004 setup is shown in fig.5.

The muon spectrometer system has also been integrated in 2004 in the test of a full slice of the ATLAS detector performed on the same beam line.

Most of the test objectives have been achieved as, to mention a few, the measurement of the sagitta resolution as a function of the muon momentum, the certification of the muon alignment systems and the test of the first level muon barrel and endcap trigger systems up to the Central Trigger Processor with a 25 ns bunched beam. This system test activities have been organized and supervised by a member of the Frascati group. The LNF group has also contributed to this activity, by providing two MDT chambers, fully equipped, integrating them with the RPCs, installing the two MDT-RPC stations on the test beam, taking care of the electric and gas connections and putting the chambers in operations. In addition to the participation in the data taking, there has

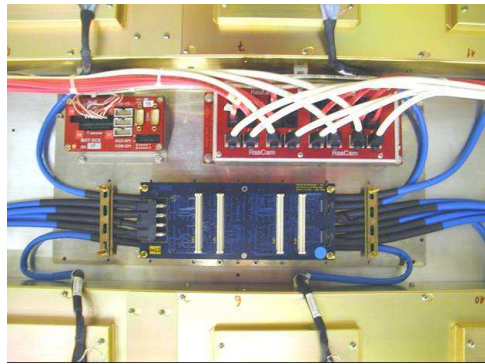
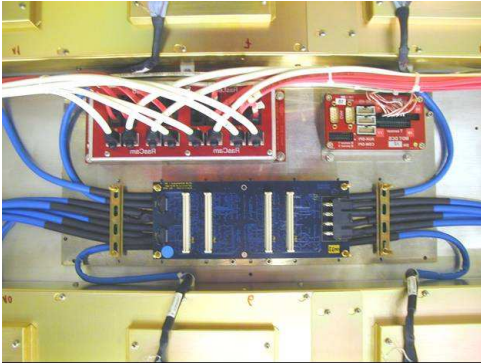
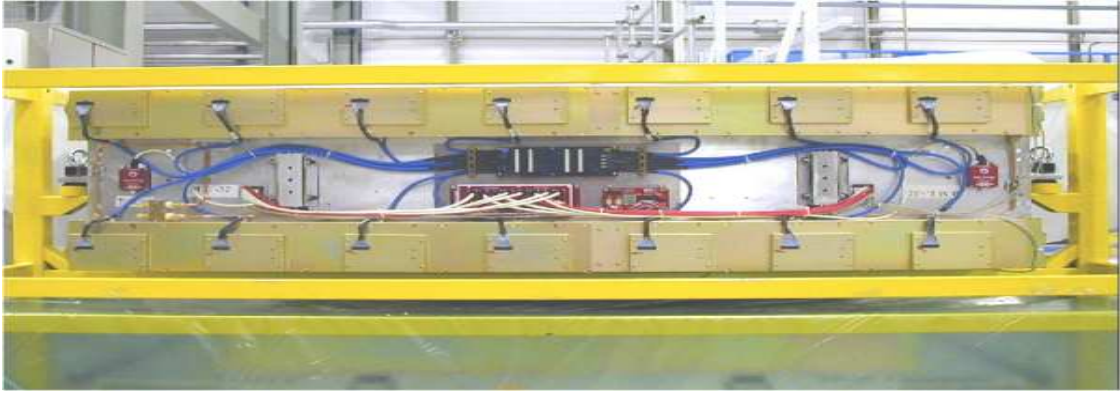


Figure 3: *Details of the services mounted on the MDT chambers.*



Figure 4: *MDT-RPC integrated station in the storage frame in the hall BB5 at CERN.*

also been an active involvement in the data analysis as explained in the following. The overall coordination of the muon collaboration test beam activity has been responsibility of a Frascati group member.

5 DAQ

The activity of the group in the trigger/DAQ area, started 3 years ago, has been pursued in the year 2004. The group has taken care of upgrading the DAQ component, that has been its responsibility, following the various upgrades of the new software releases of the DAQ system. The code which is responsibility of the Frascati group manages the on-line distribution of built events to be used for monitoring applications. The implementation makes use of the components of the “dataflow”, controlling the movement of event data, and of the on-line, related to run control, framework for communications, monitoring, error reporting. The new software has been used in the 2004 test beam, where a complete slice of Atlas was installed.

The last version of the Atlas software for the data acquisition was also installed in the cosmic ray station at Frascati. The system uses the software component called Rod Crate Daq (RCD) that the Atlas collaboration decided to develop during the last year in order to give the possibility to install small Readout systems using also non final readout hardware. At present our installation provides support for the old CSM module, TDC and different trigger boards. The software to acquire the V513 CAEN trigger module was completely developed by the group.

The reconfiguration of the system at the Frascati cosmic ray test station allows to read-out both MDT and RPC chambers, and make it possible to test full integrated MDT-RPC stations and to performe the off-line data processing using the standard Atlas offline software, i.e. in the Athena framework. The work for reconfiguring the DAQ was also very helpful in order to get a wide expertise on the DAQ system.

6 Computing, Software and Analysis

In view of the approaching of the completion of the detector construction and installation phase, and in preparation of the calibration runs and the first physics runs foreseen in the year 2007, the activity on computing, software and analysis has become more and more intense.



Figure 5: *Muon test setup at the H8 test beam at CERN.*

6.1 Computing

According to the computing model developed, the Atlas Collaboration is preparing itself to the tremendous task of the data processing and analysis by setting up computing centers, interconnected each other, following a scheme foreseeing one Tier0 at CERN, more Tier1 in National Institutions, a few Tier2 for each Tier1 and several Tier3. One of the 4 Atlas Tier2 foreseen for the INFN in Italy has been decided to be located at the LNF. The Atlas Frascati group has taken the responsibility of it with the necessary and instrumental support of the Computing Service of the LNF. The personnel in charge of the Frascati Atlas Tier2 is provided by both the Atlas Frascati group and the Computing Service.

In order to produce simulation events for many interesting channels and to reconstruct them for the subsequent analysis work, and in order to test at the same time the functionality of the Computing system being set up, the Atlas Collaboration has launched a large data production called “Data Challenge 2” (DC2). The Frascati Tier2 has been fully involved in DC2.

6.1.1 Frascati Atlas Tier2

In the year 2004 the first machines have been acquired to start setting up a PC Farm for the Frascati Tier2. The initial configuration was based on:

- 4 server HP Proliant (2 Xeon CPU 2.8 GHz) with 1 computing element and 3 working nodes;
- 1 server HP Proliant as storage element with 840 GB disk space;
- 1 server Dell (1 CPU P4 2.53 GHz) as LCFG server;
- 1 server Dell (1 CPU PIII 1 GHz) as UserInterface.

Subsequently the configuration has been slightly upgraded with the addition of 800 GB of storage and with the replacement of the Dell Server with an HP Proliant as LCFG server.

With this minimal starting configuration the Tier2 was put in the Grid network and used successfully in the Grid operation mode for the Atlas DC2.

6.1.2 Atlas Data Challenge 2

The Frascati Tier2 has been entirely dedicated to the Atlas DC2, and has been operated successfully, following the DC2 job submission. In fig.6 are reported as an example some job statistics.

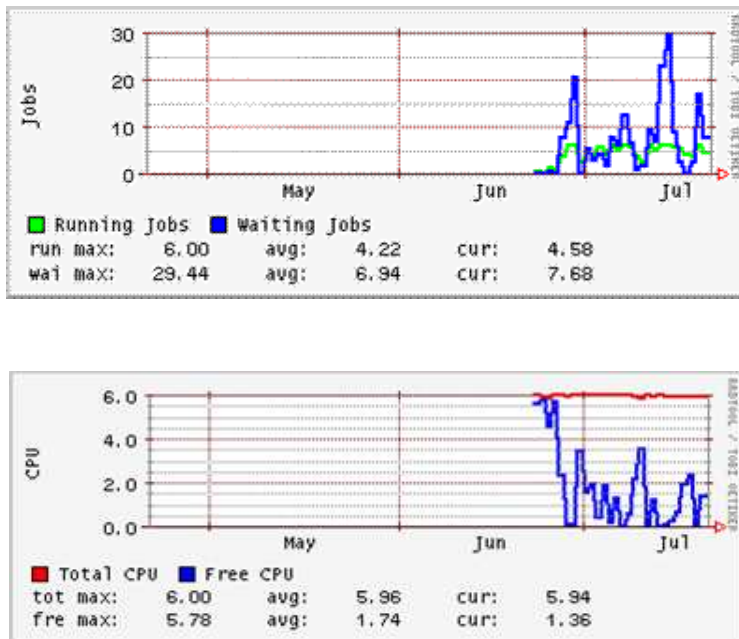


Figure 6: Job submission and CPU statistics of the Frascati Tier2 for the initial month of DC2.

6.2 Software and analysis

The work on software and analysis has concerned test beam data and simulated events, with the goal of studying detector performance and developing calibration algorithms, and also of investigating the physics potential of Atlas on the channels with muon signature and developing selection and analysis algorithms.

From the analysis of test beam data the efficiency and the noise of the individual channels and the efficiency of the track reconstruction was studied for the MDT chambers. The stability of the chamber response was checked over a month time period. Specific software was written to implement algorithms for a fast determination of noise and efficiency, in view of a possible use as on-line monitoring. This work was done using the Atlas software framework, called Athena, and the Atlas reconstruction software, and provided a way of testing it with real data, in real conditions, i.e. in presence of noise, inefficiency, using real calibration and alignment parameters. In such realistic conditions was determined the basic performance parameter of the Muon Spectrometer, that is the sagitta resolution. It was studied as a function of the beam momentum, as shown in fig.7. The muon momentum has been measured event by event by using the beam magnet installed in between the barrel precision chambers. The sagitta resolution turned out to be in agreement with the expected value of $50 \mu\text{m}$ for large muon momenta.

The determination of the spatial position measured by the chambers requires the knowledge of the $R(t)$ relations, giving the distance from the wire as a function of the drift time. The correct knowledge of the $R(t)$ relations is essential in order to achieve the resolution, that the detector can

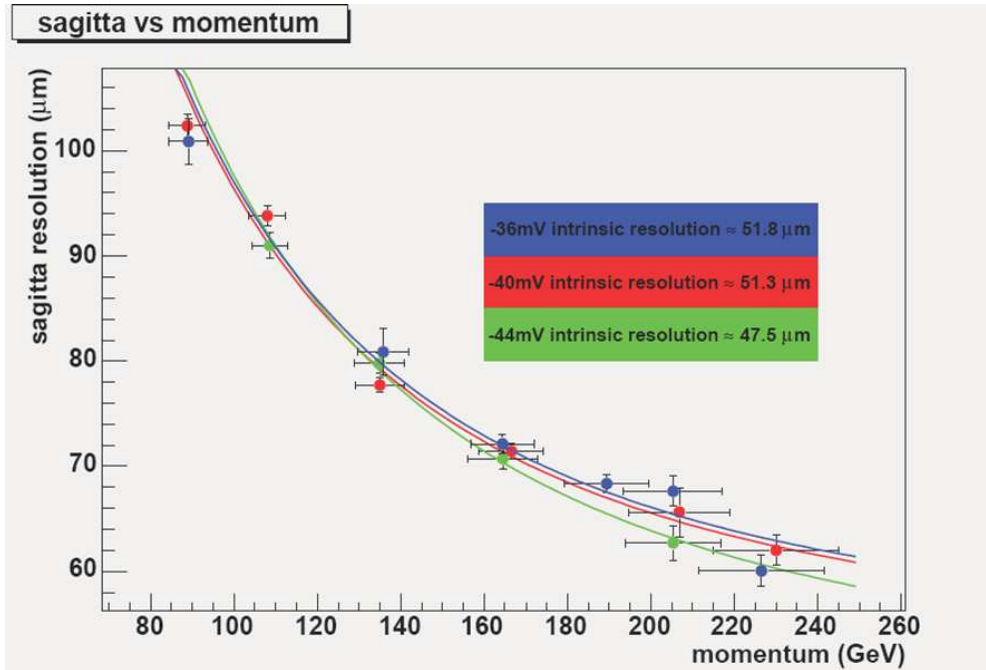


Figure 7: *Sagitta resolution as a function of the beam momentum for three values of the MDT threshold.*

potentially provide. A study was started in order to investigate how it is possible to determine the $R(t)$ relations from the inclusive drift time distribution, finding a method to correct for many effects, that make otherwise not enough precise such a determination. The use of the inclusive $R(t)$ distribution is for a fast determination of modifications in the $R(t)$ due to changes in the operation conditions. The precise determination in specific conditions is anyway to be achieved with autocalibration based on tracking residual minimization.

Besides the analysis of the test beam data and the study of the calibration algorithms and their performances, the activity in the area of software and analysis has also concerned the study of physics channels with simulated events.

The search for the Standard Model Higgs was studied in the 4μ decay channels. This study had two purposes: investigate the impact of the use of multivariate techniques (artificial Neural Network and likelihood based) to improve the rejection of the background with respect to simple cut based analysis and the impact of the change in detector layout and reconstruction software in the muon reconstruction performances reported in the Physics TDR. Concerning the first point in this study it has been shown that the transverse momentum and spin-CP characteristic of the signal can be used in the framework of the multivariate technique analyses to improve the rejection of the $ZZ^* \rightarrow 4\mu$ background. The new layout of the ATLAS detector used in this study has shown a degradation in the muon reconstruction performance with respect to the Physics TDR due to increased material in the Inner Detector and reduced geometrical acceptance of the muon spectrometer. The improvement due to the new analysis technique and the deterioration due to the new layout almost cancel out, and the performance in terms of discovery potential described in the Physics TDR is recovered. As an example the reconstructed 4 muons invariant mass for the Higgs signal with a mass of 130 GeV and for the different backgrounds is shown in fig.8 before (upper plot) and after (lower plot) applying a cut on the NN variable.

One of the two conveners of the ATLAS Higgs working group in 2004 was a member of the Frascati group.

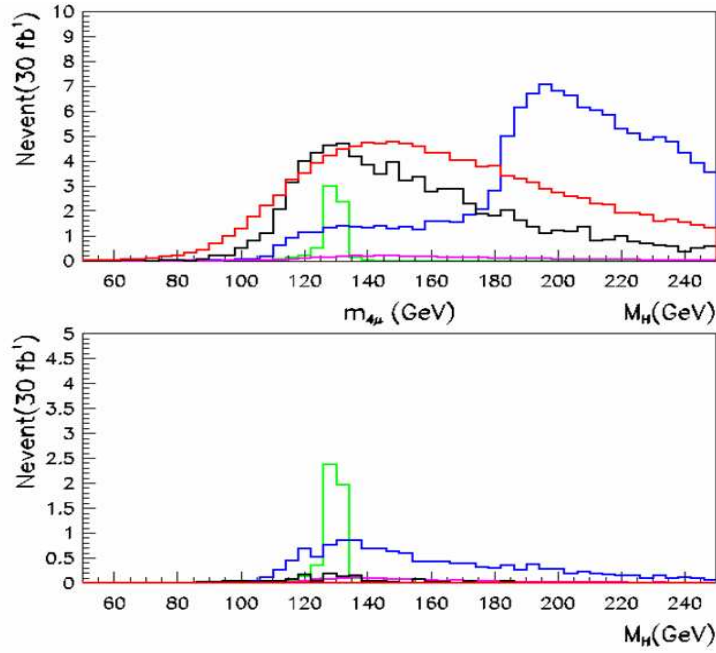


Figure 8: Event rate for the signal and various backgrounds before and after the analysis selection.

The production of the supersymmetric Higgs decaying into $\mu^+\mu^-$ was also studied. The full chain of the Atlas software was used starting from the generation. The simulation, using Geant4, and the reconstruction were run on the Grid. Standalone spectrometer and combined with inner detector reconstructions were tested for mass reconstruction and p_t , η distributions. In this work was also tested MatchMaker method to couple the reconstructed tracks to the simulated by minimization of the pairing parameter $R = \sqrt{(\Delta\eta^2 + \Delta\phi^2)}$. These studies were also used to validate the Atlas new software. The reconstructed Higgs mass obtained is shown in fig.9.

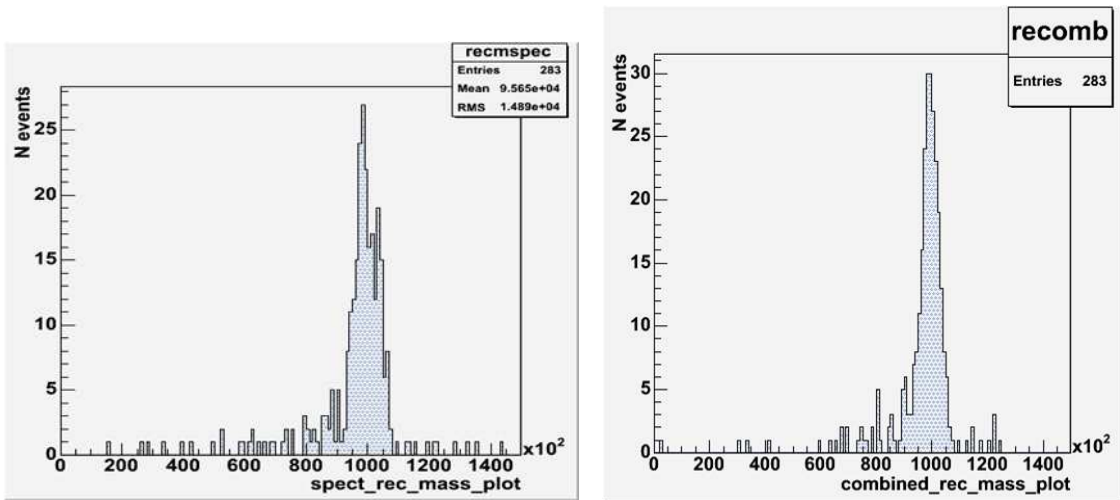


Figure 9: Reconstructed mass distribution for the $h_0 \rightarrow \mu^+\mu^-$ in the muon spectrometer and with the combined inner detector and muon detector reconstruction.

Due to the interest of the Frascati group in the physics of the channels with μ signature, and due to the fact that the group is heavily involved in the μ detector, the focus of the simulation studies has been basically on the events with muons in the final states. A more general project of simulation studies has been started with the goal of reviewing all the physics processes producing two muons in the final state, foreseen by the Standard Model and also from New Physics beyond

the Standard Model, in order to establish in various luminosity scenarios what can be measured and what are the optimal algorithms for event selection and for physical quantities measurement.

7 List of Conference Talks in year 2004

F. Cerutti, “Performance Studies of the monitored drift tubes of the Atlas muon spectrometer”, talk given at Vienna Wire-Chamber-Conference 2004.

References

1. M. Barone, F. Cerutti, B. Esposito, S. Giovannella, S. Ventura, “Study of noise and efficiency of MDT chambers on 2003 and 2004 H8 test beam data”, Atlas Note ATL-MUON-2004-025.
2. M. Beretta, S. Braccini, V. Chiarella, M. Curatolo, B. Esposito, M.L. Ferrer, A. Martini, G. Maccarrone, W. Mei, “Drift time response of the MDT chambers to a variation of the gas mixture”, Atlas Note ATL-MUON-2004-012.
3. M. Curatolo, C. Daly, B. Esposito, R. Ferrari, H.J. Lubatti, C. Petridou, H. Wellenstein, T. Zhao, B. Zhou, “Report of the MDT IHEP Beijing 2004 Site Review”, Atlas Note ATL-MUON-2004-013.
4. M. Antonelli, M. Barone, F. Cerutti, M. Curatolo, B. Esposito, “Long term stability and uniformity studies of MDT chambers in the H8 2003 system test”, Atlas Note ATL-MUON-2004-017.
5. E. Meoni, F. Cerutti, L. La Rotonda, “Search for the Standard Model $H \rightarrow ZZ^* \rightarrow 4\mu$ with multivariate techniques and GEANT3 based detector simulation”, Atlas Communication ATL-COM-PHYS-2004-040.
6. F. Cerutti, “Proposed measurement program for H8 2004 muon system test”, Atlas Communication ATL-COM-MUON-2004-006.
7. R. Sturrok *et al.*, “A step towards a computing Grid for the LHC experiments: Atlas Data Challenge 1”, CERN Preprint CERN-PH-EP-2004-028, Submitted to Nucl. Instrum. Methods Phys. Res.
8. N. Benekos *et al.*, “B-physics performance with initial and complete inner detector layouts in Data Challenge 1”, Atlas Communication ATL-COM-PHYS-2004-073.
9. F. Cerutti, “Performance Studies of the monitored drift tubes of the Atlas muon spectrometer”, Nucl. Instrum. Methods Phys. Res. **A535** (2004), 175-180.
10. H. P. Beck, “The base-line DataFlow system of the Atlas Trigger/DAQ”, Atlas Note ATL-DAQ-2004-006.

BaBar

F. Anulli (Ass.), R. Baldini Ferroli, A. Calcaterra, L. Daniello (Tecn.), R. de Sangro
G. Finocchiaro, P. Patteri, I. Peruzzi (Resp.), M. Piccolo, A. Zallo

1 Introduction

BaBar (in fig. 1) is the experiment running at the SLAC asymmetric B -factory PEP-II; the physics program is centered on, but not limited to, the study of the CP violation effects in the decay of neutral B mesons. The B system is the best suited to study CP violation because the expected effects are large, should appear in many final states and, most importantly, can be directly related to the Standard Model parameters. The large data sample now being collected has already allowed significant advances in a large number of topics in B , charm and top quark physics.

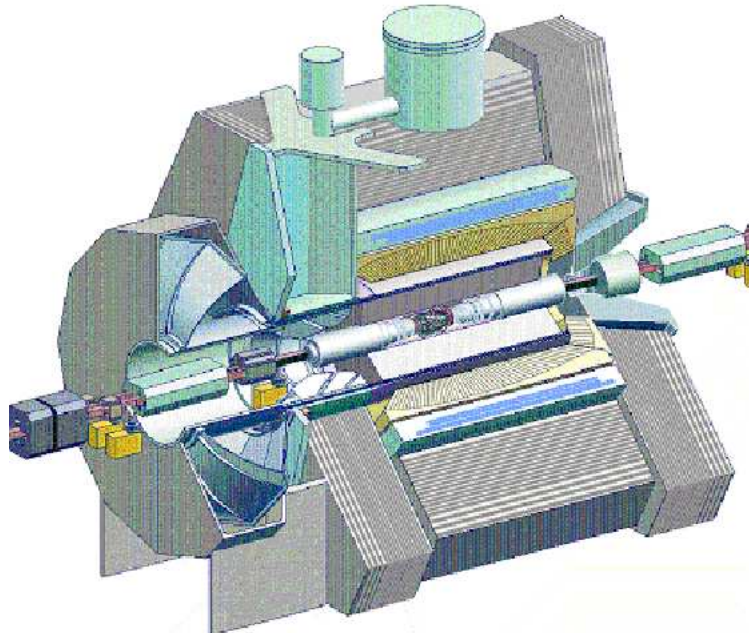


Figure 1: The BaBar Detector.

PEP-II is a two-ring e^+e^- storage ring, colliding 9 GeV electrons with 3.1 GeV positrons, energies chosen to maximize the production of B mesons. The c.m. energy corresponds to the mass of the $\Upsilon(4S)$ resonance which decays 50% in $B^+ B^-$, 50% in $B^0 \bar{B}^0$. The energy asymmetry is necessary in order to boost the B mesons momentum, so that the decay length can be measured with the accuracy needed to prove the CP violation effects.

The BaBar Collaboration includes about 560 physicists, with contributions from about 80 Institutions in 10 countries in North America, Europe, and Asia. Approximately half of the group are physicists from U.S. Universities and Laboratories, with the largest foreign contribution coming from Italy, with 12 INFN Institutions and more than 90 people.

The BaBar detector has been designed primarily for CP studies, but it is also serving well for the other physics objectives of the experiment. The asymmetry of the beam energies is reflected

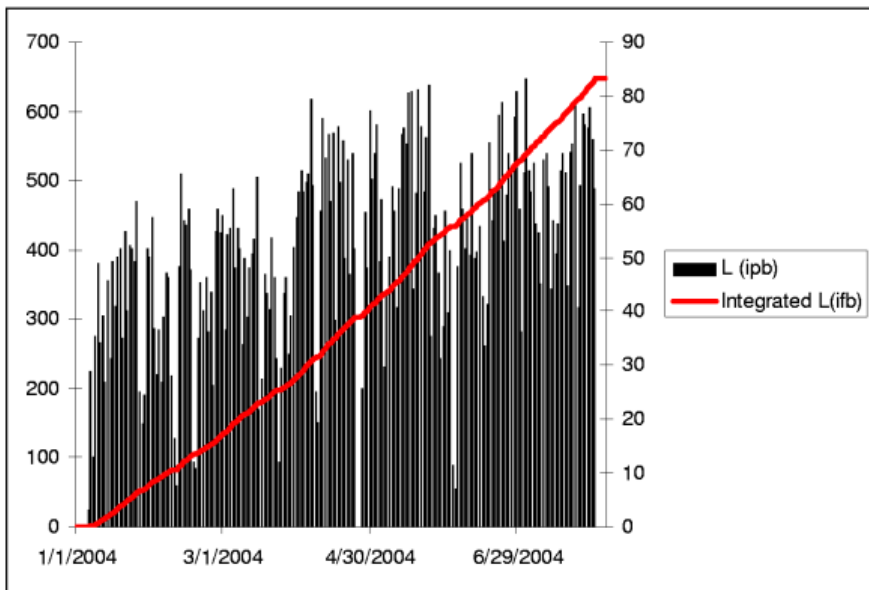


Figure 2: BaBar Luminosity in 2004.

in the detector design: the apparatus is centered 37 cm ahead of the collision point, along the direction of the high-energy beam, to increase forward acceptance. All services are placed on the opposite side of the detector, in order to minimize multiple scattering in the forward direction.

The momentum of the charged tracks is obtained from the curvature in a solenoidal field of 1.5 T and is measured in a low mass Drift Chamber. Different species of hadrons are identified in the DIRC, a dedicated device of a novel kind, based on the detection of Čerenkov light. Excellent photon detection and electron identification is provided by a CsI crystals electromagnetic calorimeter.

Muons and neutral hadrons are identified in the iron magnet's yoke, where a total thickness of 65 cm of Fe plates has been segmented in 18 slabs of graded thickness (from 2 to 10 cm) and instrumented with Resistive Plate Counters. This system, made of a 6-sided barrel, 2 endcaps and a double cylindrical layer inside the magnet coil, is called Instrumented Flux Return, or IFR. The final ingredient in the CP asymmetry measurements, the distance between the two decay vertices, is measured by a state of the art vertex detector, with five layers of double sided silicon strips.

2 Activity

Year 2004 data taking was very successful for BaBar; as seen in fig. 2, during the first 7 months of this year, before a 2-month shutdown for insertion of new detectors in the Instrumented Flux Return, more than $80fb^{-1}$ have been delivered by PEP-II and recorded by BaBar bringing the total data sample to almost $250fb^{-1}$.

Among the most important results published by BaBar in 2004 appear new and improved results on $\sin 2\beta$, systematic studies of many branching fractions for charmed mesons, discovery of a new narrow resonance, and the most precise measurement to date of the reaction $e^+e^- \rightarrow \pi^+ \pi^- \pi^0$.

In the next sections the items of analysis in which the Frascati group is more directly involved are shortly described.

3 Measurement of $\sin 2\beta$ with partial reconstruction of B mesons to the $D^{*+} D^{*-}$ decay

In 2004 this analysis has been advanced toward the final goal of publication. The main progress has been in the following areas:

- finalization of the event selection and a full review of the various part of the analysis, including tagging, vertexing etc.;
- finalization of the $\sin 2\beta$ fitting procedure, including toy Monte Carlo validation studies of the fit;
- inclusion of the full data set collected until July 2004, corresponding to BaBar data taking runs 1 through 4;
- beginning of the study of the systematic errors;

The parameter $\sin 2\beta$ is extracted from the CP and tag side vertices time difference Δt distribution of events selected using event topology and kinematic cuts.

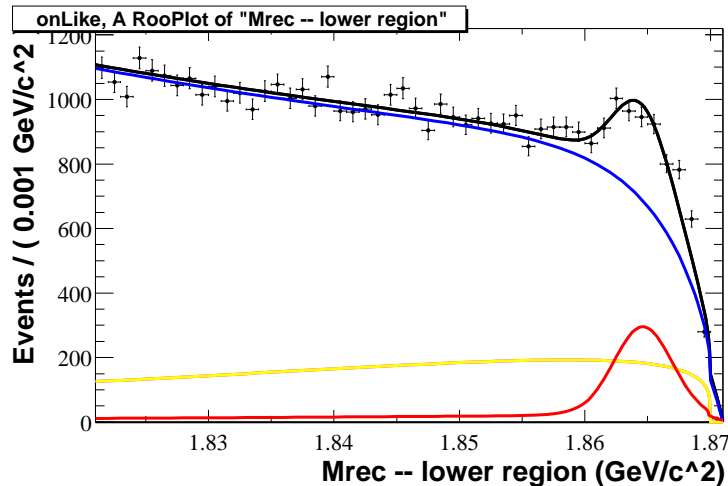


Figure 3: Missing mass for $B \rightarrow D^{*\pm} \pi^\mp (X)$. The curves represent the probability distribution functions (p.d.f.) for signal (red), continuum background (yellow), $B\bar{B}$ background (blue) and their sum (black).

In fig. 3 we show the recoil mass distribution of real data from RUN 1 through 4 (solid histogram), corresponding to $\approx 210 fb^{-1}$ of integrated luminosity. The presence of an excess of events in the signal region is evident, and a very preliminary fit to the data with a PDF (black curve), made of a signal component (red) plus a continuum (yellow) and a $B\bar{B}$ (blue) background component, has shown that the statistical power of this measurement is somewhat higher than that of the analysis made with the fully reconstructed sample. This is a very important result, as the two measurements of $\sin 2\beta$ can be regarded as almost independent of each other.

We also fit the time distribution in the data, and in fig. 4 we show a fit to the time difference distribution of data events including signal and background, for the full RUN 1-4 statistics. As the study of the systematic errors is still ongoing, the analysis at this stage can not yet quote a result for the CP violating parameter $\sin 2\beta$.

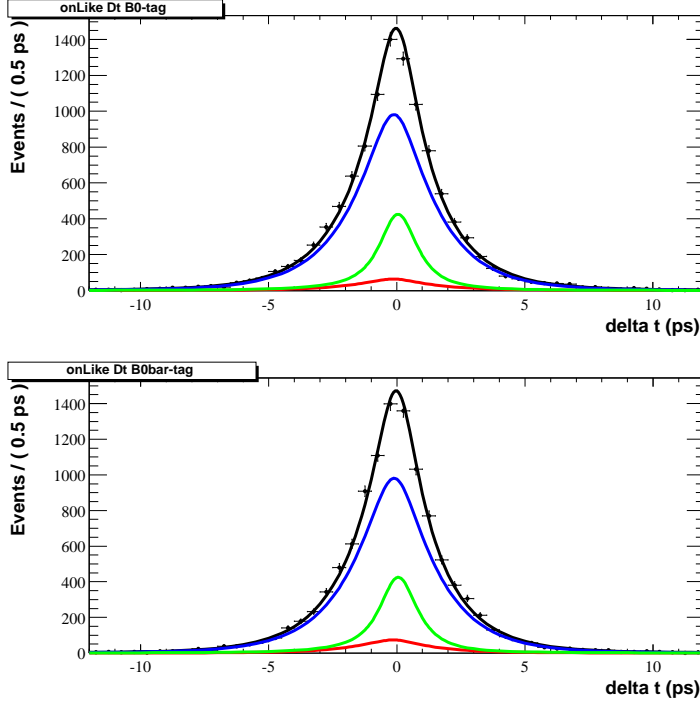


Figure 4: Δt fit to RUN 1-4 data. The curves represent the p.d.f.'s for signal (red), continuum background (green), $B\bar{B}$ background (blue) and their sum (black).

4 Measurement of the $B^0 \rightarrow D_s^{*+} D^{*-}$ and $D_s^+ \rightarrow \phi \pi^+$ branching fractions with partial reconstruction of B mesons to the $D_s^{*+} D^{*-}$ final state

During 2004, we finalized and submitted for publication the measurement of the branching fractions $\mathcal{B}(B^0 \rightarrow D_s^{*+} D^{*-})$ and $\mathcal{B}(D_s^+ \rightarrow \phi \pi^+)$, based on $123 \times 10^6 \Upsilon(4S) \rightarrow B\bar{B}$ decay events.

The $B^0 \rightarrow D_s^{*+} D^{*-} \rightarrow (D_s^+ \gamma)(\bar{D}^0 \pi^-)$ decay is reconstructed using two different methods. The first method combines the fully reconstructed D^{*-} decay with the photon from the $D_s^{*+} \rightarrow D_s^+ \gamma$ decay, without explicit D_s^+ reconstruction. Denoting the measured yield by \mathcal{N}_{D_s} , we can write:

$$\mathcal{B}(B^0 \rightarrow D_s^{*+} D^{*-}) \equiv \mathcal{B}_1 = \frac{\mathcal{N}_{D_s}}{\mathcal{K} \sum_i (\varepsilon_i \mathcal{B}_i)}. \quad (1)$$

Here $\mathcal{K} \equiv 2N_{B\bar{B}} f_{00} \mathcal{B}(D_s^{*+} \rightarrow D_s^+ \gamma) \mathcal{B}(D^{*-} \rightarrow \bar{D}^0 \pi^-)$, $N_{B\bar{B}}$ is the number of B -meson pairs, $f_{00} = 0.499 \pm 0.012$ ²⁾ is the fraction of $\Upsilon(4S) \rightarrow B^0 \bar{B}^0$ decays, \mathcal{B}_i is the branching fraction of \bar{D}^0 decay mode i , ε_i is the efficiency for partially reconstructing the B^0 with a photon, a low momentum (“soft”) pion and a \bar{D}^0 reconstructed in mode i .

The second method, based on full reconstruction of the $B^0 \rightarrow D_s^{*+} D^{*-}$ decay via $D_s^+ \rightarrow \phi \pi^+$ ($\phi \rightarrow K^+ K^-$), measures the branching fraction product $\mathcal{B}_2 \equiv \mathcal{B}(B^0 \rightarrow D_s^{*+} D^{*-}) \times \mathcal{B}(D_s^+ \rightarrow \phi \pi^+)$:

$$\mathcal{B}_2 = \frac{\mathcal{N}_{D_s \rightarrow \phi \pi}}{\mathcal{K} \mathcal{B}(\phi \rightarrow K^+ K^-) \sum_i (\varepsilon'_i \mathcal{B}_i)}, \quad (2)$$

where $\mathcal{N}_{D_s \rightarrow \phi \pi}$ is the number of reconstructed decays and ε'_i is the efficiency for fully reconstructing

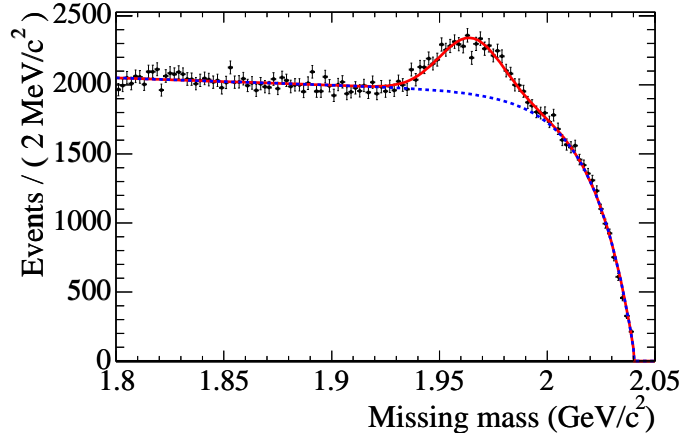


Figure 5: Fit (solid line) to the measured missing-mass distribution. The background component is shown as the dashed line.

the B^0 , including reconstruction of $\phi \rightarrow K^+K^-$. The $D_s^+ \rightarrow \phi\pi^+$ branching fraction is measured from the $\mathcal{B}_2/\mathcal{B}_1$ ratio:

$$\mathcal{B}(D_s^+ \rightarrow \phi\pi^+) = \frac{\mathcal{B}_2}{\mathcal{B}_1} = \frac{\mathcal{N}_{D_s \rightarrow \phi\pi} \sum_i (\varepsilon_i \mathcal{B}_i)}{\mathcal{N}_{D_s} \mathcal{B}(\phi \rightarrow K^+K^-) \sum_i (\varepsilon'_i \mathcal{B}_i)}, \quad (3)$$

where the factor \mathcal{K} drops out. Although the efficiencies ε_i and ε'_i are in general different, they include common factors and many systematic uncertainties cancel in the ratio.

To extract the signal in partially reconstructed events, we compute the “missing mass” recoiling against the $D^{*-}\gamma$ system, assuming that a $B^0 \rightarrow D^{*-}\gamma X$ decay took place:

$$m_{\text{miss}} = \sqrt{(E_B - E_{D^*} - E_\gamma)^2 - (\mathbf{p}_B - \mathbf{p}_{D^*} - \mathbf{p}_\gamma)^2}, \quad (4)$$

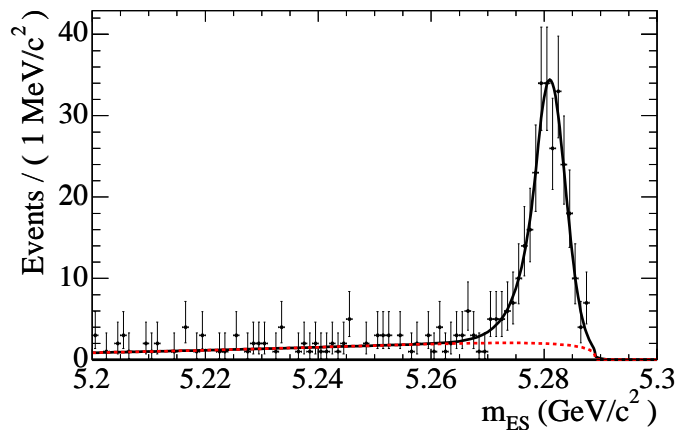


Figure 6: Fit (solid line) to the measured m_{ES} distribution. The background component is shown as the dashed line.

where all quantities are defined in the $\Upsilon(4S)$ center-of-mass (CM) frame.

We extracted the signal yield using an unbinned maximum-likelihood fit to the m_{miss} distribution. The signal peak is well described by a Gaussian probability density function. Fig. 5 shows the result of the fit to the missing-mass distribution.

The selection of D^{*-} candidates and most of the requirements on photon candidates are identical to those adopted in the partial reconstruction analysis. Due to the additional kinematical constraints on fully reconstructed B decays, the combinatorial background level is much smaller; we can therefore relax the requirement on E_γ , thus improving the statistical significance of our sample. From the fit to the data sample, shown in Fig. 6, we obtain (247 ± 19) events in the signal region defined as $m_{\text{ES}} > 5.27 \text{ GeV}/c^2$.

Comparing these two measurements provides a model-independent determination of the $D_s^+ \rightarrow \phi\pi^+$ branching fraction. We obtain $\mathcal{B}(B^0 \rightarrow D_s^{*+}D^{*-}) = (1.88 \pm 0.09 \pm 0.17)\%$ and $\mathcal{B}(D_s^+ \rightarrow \phi\pi^+) = (4.81 \pm 0.52 \pm 0.38)\%$, where the first uncertainties are statistical and the second systematic.

5 BaBar publications in 2004

- “Measurement of branching fractions in $B \rightarrow \phi K$ and $B \rightarrow \phi\pi$ and search for direct CP violation in $B^\pm \rightarrow \phi K^\pm$ ”, Phys. Rev. **D69:011102**, (2004).
- “ J/ψ production via initial state radiation in $e^+e^- \rightarrow \mu^+\mu^-\gamma$ at an e^+e^- center-of-mass energy near 10.6 GeV”, Phys. Rev. **D69:011103**, (2004).
- “Observation of a narrow meson decaying to $D_s^+ \pi^0 \gamma$ at a mass of 2.458 GeV/ c^2 ”, Phys. Rev. **D69:031101**, (2004).
- “Observation of the decay $B \rightarrow \rho^+\rho^-$ and measurement of the branching fraction and polarization”, Phys. Rev. **D69:031102**, (2004).
- “Measurement of branching fractions of color-suppressed decays of the B^0 meson in $D^{(*)0}\pi^0$, $D^{(*)0}\eta$, $D^{(*)0}\omega$, $D^{(*)0}\eta'$ ”, Phys. Rev. **D69:032004**, (2004).
- “Measurement of the branching fraction for $B^- \rightarrow D^0 K^{*-}$ ”, Phys. Rev. **D69:051101**, (2004).
- “Measurement of $\sin 2\beta$ with hadronic and previously unused muonic J/ψ decays”, Phys. Rev. **D69:052001**, (2004).
- “Measurement of the average ϕ multiplicity in B meson decay”, Phys. Rev. **D69:052005**, (2004).
- “Measurement of the B^+/B^0 production ratio from the $\Upsilon(4S)$ meson using $B^+ \rightarrow J/\psi K^+$ and $B^0 \rightarrow J/\psi K_S^0$ decays”, Phys. Rev. **D69:071101**, (2004).
- “Measurement of the branching fraction for $B^\pm \rightarrow \chi_{c0} K^\pm$ ”, Phys. Rev. **D69:071103**, (2004).
- “Search for the decay $B^0 \rightarrow \rho\bar{\rho}$ ”, Phys. Rev. **D69:091503**, (2004).
- “Measurements of moments of the hadronic mass distribution in semileptonic B decays”, Phys. Rev. **D69:111103**, (2004).
- “Measurement of the electron energy spectrum and its moments in inclusive $B \rightarrow X e \nu$ decays”, Phys. Rev. **D69:111104**, (2004).
- “Observation of $B \rightarrow \omega K^0$, $B^+ \rightarrow \eta\pi^+$, and $B^+ \rightarrow \eta K^+$ and Study of Related Decays”, Phys. Rev. Lett. **92:061801**, (2004).

- “Search for the Radiative Decays $B \rightarrow \rho\gamma$ and $B \rightarrow \omega\gamma$ ”, Phys. Rev. Lett. 92:111801, (2004).
- “Search for Lepton-Flavor Violation in the Decay $\tau^- \rightarrow \ell^- \ell^+ \ell^-$ ”, Phys. Rev. Lett. 92:121801, (2004).
- “Measurement of the Branching Fraction and Polarization for the Decay $B^- \rightarrow D^{*0} K^{*-}$ ”, Phys. Rev. Lett. 92:141801, (2004).
- “Limits on the Decay-Rate Difference of Neutral B Mesons and on CP , T , and CPT Violation in $B^0-\bar{B}^0$ Oscillations”, Phys. Rev. Lett. 92:181801, (2004).
- “Search for the Rare Leptonic Decay $B^+ \rightarrow \mu^+ \nu$ ”, Phys. Rev. Lett. 92:221803, (2004).
- “Study of $B^\pm \rightarrow J/\psi \pi^\pm$ and $B^\pm \rightarrow J/\psi K^\pm$ Decays: Measurement of the Ratio of Branching Fractions and Search for Direct CP Violation”, Phys. Rev. Lett. 92:241802, (2004).
- “Branching fraction measurements of $B \rightarrow \eta_c K$ decays”, Phys. Rev. D70:011101, (2004).
- “Limits on the decay-rate difference of neutral B mesons and on CP , T and CPT violation in $B^0-\bar{B}^0$ oscillations”, Phys. Rev. D70:012007, (2004).
- “ B meson decays to $\eta^{(\prime)} K^*$, $\eta^{(\prime)} \rho$, $\eta^{(\prime)} \pi^0$, $\omega \pi^0$, and $\phi \pi^0$ ”, Phys. Rev. D70:032006, (2004).
- “Study of the $e^+ e^- \rightarrow \pi^+ \pi^- \pi^0$ process using initial state radiation with BaBar”, Phys. Rev. D70:072004, (2004).
- “Search for $D^0-\bar{D}^0$ mixing using semileptonic decay modes”, Phys. Rev. D70:091102, (2004).
- “Measurements of neutral B decay branching fractions to $K_s^0 \pi^+ \pi^-$ final states”, Phys. Rev. D70:091103, (2004).
- “Search for the decay $B^0 \rightarrow J/\psi \gamma$ ”, Phys. Rev. D70:091104, (2004).
- “Measurement of the branching fractions for inclusive B^- and \bar{B}^0 decays to flavor-tagged D , D_s^+ and Λ_c ”, Phys. Rev. D70:091106, (2004).
- “Search for B -meson decays to two-body final states with $a_0(980)$ mesons”, Phys. Rev. D70:111102, (2004).
- “Measurement of branching fractions and CP and isospin asymmetries for $B \rightarrow K^* \gamma$ ”, Phys. Rev. D70:112006, (2004).
- “Determination of the Branching Fraction for $B \rightarrow X_c \ell \nu$ Decays and of $|V_{cb}|$ from Hadronic-Mass and Lepton-Energy Moments”, Phys. Rev. Lett. 93:011803, (2004).
- “Measurement of the Direct CP Asymmetry in $\rightarrow s \gamma$ Decays”, Phys. Rev. Lett. 93:021804, (2004).
- “Observation of the Decay $B \rightarrow J/\psi \eta K$ and Search for $X(3872) \rightarrow J/\psi \eta$ ”, Phys. Rev. Lett. 93:041801, (2004).
- “Study of High Momentum η' Production in $B \rightarrow \eta' X_c$ ”, Phys. Rev. Lett. 93:061801, (2004).
- “Measurement of the Time-Dependent CP Asymmetry in the $B^0 \rightarrow \phi K^0$ Decay”, Phys. Rev. Lett. 93:071801, (2004).

- “Bound on the Ratio of Decay Amplitudes for $\bar{B}^0 \rightarrow J/\psi K^{*0}$ and $B^0 \rightarrow J/\psi K^{*0}$ ”, Phys. Rev. Lett. 93:081801, (2004).
- “Measurement of the $B \rightarrow X_s \ell^+ \ell^-$ Branching Fraction with a Sum over Exclusive Modes”, Phys. Rev. Lett. 93:081802, (2004).
- “Search for B^0 Decays to Invisible Final States and to $\nu\bar{\nu}\gamma$ ”, Phys. Rev. Lett. 93:091802, (2004).
- “Direct CP Violating Asimmetry in $B^0 \rightarrow K^+ \pi^-$ Decays”, Phys. Rev. Lett. 93:131801, (2004).
- “Search for $B^\pm \rightarrow [K^\mp \pi^\pm]_D$ and Upper Limit on the $\rightarrow \check{A}$ Amplitude in $B^\pm \rightarrow DK^\pm$ ”, Phys. Rev. Lett. 93:131804, (2004).
- “Measurements of CP -Violating Asymmetries in $B^0 \rightarrow K_s^0 \pi^0$ Decays”, Phys. Rev. Lett. 93:131805, (2004).
- “Study of $B \rightarrow D_{sJ}^{*+} \bar{D}^{(*)}$ Decays”, Phys. Rev. Lett. 93:181801, (2004).
- “Branching Fractions and CP Asymmetries in $B^0 \rightarrow K^+ K^- K_s^0$ and $B^+ \rightarrow K^+ K_s^0 K_s^0$ ”, Phys. Rev. Lett. 93:181805, (2004).
- “Searches for B^0 Decays to Combinations of Two Charmless Isoscalar Mesons”, Phys. Rev. Lett. 93:181806, (2004).
- “Search for Flavor-Changing Neutral Current and Lepton-Flavor Violating Decays of $D^0 \rightarrow \ell^+ \ell^-$ ”, Phys. Rev. Lett. 93:191801, (2004).
- “Measurement of Time-Dependent CP -Violating Asymmetries in $B^0 \rightarrow K^{*0} \gamma(K^{*0} \rightarrow K_s^0 \pi^0)$ Decays”, Phys. Rev. Lett. 93:201801, (2004).
- “Study of the Decay $B^0 (\bar{B}^0) \rightarrow \rho^+ \rho^-$ and Constraints on the Cabbibo-Kobayashi-Maskawa Angle α ”, Phys. Rev. Lett. 93:231801, (2004).
- “Measurement of the $B^0 \rightarrow \phi K^{*0}$ Decay Amplitudes”, Phys. Rev. Lett. 93:231804, (2004).

References

1. PDG 2003.
2. The value for f_{00} quoted in the text is derived from the measurement of the ratio $\Gamma(\Upsilon(4S) \rightarrow B^+ B^-) / \Gamma(\Upsilon(4S) \rightarrow B^0 \bar{B}^0) = 1.006 \pm 0.048$ reported in B. Aubert *et al.* [BaBar Collab.], Phys. Rev. **D69**:071101, (2004).

BTeV

E. Basile² (Ass.), F. Bellucci³ (Ass.), M. Bertani, S. Bianco, M.A. Caponero¹ (Ass.),
D. Colonna¹ (Ass.), F. Di Falco² (Ass.), F.L. Fabbri (Resp.), F. Felli² (Ass.),
M. Giardoni, A. LaMonaca, F. Massa² (Ass.), G. Mensitieri³ (Ass.),
B. Ortenzi (Tecn.), M. Pallotta, A. Paolozzi² (Ass.), L. Passamonti (Tecn.),
D. Pierluigi (Tecn.), G. Saviano² (Ass.), S. Tomassini

¹*ENEA Centro Ricerche, Frascati;* ²*La Sapienza University, Rome;*

³*Federico II University, Naples*

The BTeV experiment is designed to challenge the Standard Model explanation of CP violation, mixing and rare decays of beauty and charm quark states. The Standard Model has been the baseline particle physics theory for several decades and BTeV aims to find out what lies beyond the Standard Model. In doing so, the BTeV results will also shed light on phenomena associated with the early universe such as why the universe is made up of matter and not anti-matter.

The BTeV Collaboration is a group of about 170 physicists drawn from more than 30 universities and physics institutes from Belarussia, Canada, China, Italy, Russia, and the United States of America. The Italian collaboration is composed about 40 physicists from Laboratori Nazionali di Frascati, University of Milan and INFN, and University of Bergamo.

The BTeV experiment will utilize the Tevatron proton-antiproton collider at the Fermi National Accelerator Lab, located in the far west suburbs of Chicago, Illinois in the USA. The experiment is still being developed; installation is scheduled to start in 2007, followed by commissioning in 2009.

1 The experiment

The Standard Model has been the backdrop of particle physics theory for more than a quarter of a century. It is a combination of three of the four known fundamental forces - electromagnetism, strong nuclear force, and weak nuclear force (gravity is the fourth). It also contains the fundamental particles which make up the universe which are the six quarks (up, down, charm, strange, top, beauty) and six leptons (electron, muon, tau, electron neutrino, muon neutrino, tau neutrino). All of these particles are partnered with antiparticles with opposite charge but the same mass. This model is very unsatisfying, however, because it asks more questions than it answers. The model does not tell us why there are three generations of quarks and three generations of leptons. The model also fails to predict the masses of these particles. It is believed by many that a more fundamental theory will be able to predict many of the parameters of the Standard Model which today must be measured by experiments. Physicists hope this more fundamental theory will also include the gravitational force which is not in the Standard Model.

BTeV is an experiment which is designed to deeply probe several aspects of the Standard Model. At the very least, BTeV will make very precise measurements of many Standard Model parameters. It is hoped that these precise measurements will reveal weaknesses in the Standard Model which will point the way to a more fundamental theory.

One of BTeV's main goals is to precisely measure CP violation in the beauty quark system. CP violation was first observed in strange quarks in 1963 and recently in beauty quarks at BaBar and Belle. CP violation causes particles and antiparticles to behave differently. There are two main reasons to study CP violation. The first reason is that many theories which provide extensions or replacements for the Standard Model predict effects in this realm. The second reason is that one of the big mysteries of the universe is why the universe is composed of matter instead of antimatter. The prevalence of matter over antimatter appears to require a large CP violating process sometime

during the early formation of the Universe. Although the levels of CP violation in the Standard Model are not large enough to explain this effect, it is the only place where CP violation has been observed and is therefore a natural place to look for more answers.

The BTeV detector is shown in Fig.1 a) and it is composed of a charged particle tracker, em calorimetry, Cerenkov particle identification detector, muon detection and data acquisition triggering. The charged particle tracker is composed of a pixel vertex detector and a magnetic forward spectrometer. The forward spectrometer is made of six stations of straw tubes and silicon microstrips.

The Frascati group has responsibility of the small-angle straw tube modules which hold the silicon microstrips. The Frascati group is also responsible of providing detector position monitoring of pixels, microstrips and straw-tubes by means of Fiber Bragg Grating sensors.

2 Activity during year 2004

The activity of the Frascati group related to the straws-microstrip interface stepped from conceptual design to prototyping during 2004. During the year, we realized several prototypes of the small-angle strawtube module able to hold the microstrip system. The baseline idea of such a *Module 0* is based on a straw-rohacell sandwich which is surrounded by a Carbon-Fiber Reinforced Plastic (CFRP) shell. Straws in Module 0 are kept in place with no mechanical tension. A detailed study was setup to investigate the effect of gas mixture composition on straws mechanical tension, which was recently shown to be affected in the case of kapton straws. The glueing technique was finalized by the choice of glue and spraying parameters.

Several straw module prototypes were built and tested on cosmic rays and on beam particles at the Frascati Beam Test Facility. Results show how the resolution performances of glued straws are comparable to the specifications.

The monitoring of sensitive components of pixels, microstrips and straws will be performed by position detectors using Fiber Bragg Grating (FBG) sensors as active components. FBG's are optical strain gauges with μ -strain sensitivity. During 2004 the main focus was concentrated on the development of the pixel repositioning system based on FBG. The system is composed of a Ω -like structure which follows the step-motor which locates the pixel system at each accelerator store. FBG sensors are glued on the structure, their strain measuring the repositioning of the pixel detector. Preliminary tests showed a precision of about $10\mu\text{m}$. The R&D program will continue in 2005 so to get to the required resolution of $4\text{-}5\mu\text{m}$. Besides, a detailed campaign of measurements was carried on the pixel carbon fiber mockup structure, in order to characterize its thermal and stress behaviour, and to validate the Finite Element Model simulations developed.

In order to verify the circularity of straws after glueing, x-ray tomographic techniques were developed in collaboration with groups in Bologna (F.Casali et al., INFN and University of Bologna; F.Baruffaldi et al., Laboratori Ospedale Rizzoli). Image analyses, pattern recognition and fitting code was developed, results show how glueing does not disrupt the straws circularity to better than $50\mu\text{m}$.

3 Outlook

In 2005 we plan to conclude the R& D projects undergoing, and to proceed to pre-production engineering for all subsystem. Straws MOX prototype will be tested at Fermilab. Tomographic facility able to scan 2.2 m long modules will be setup.

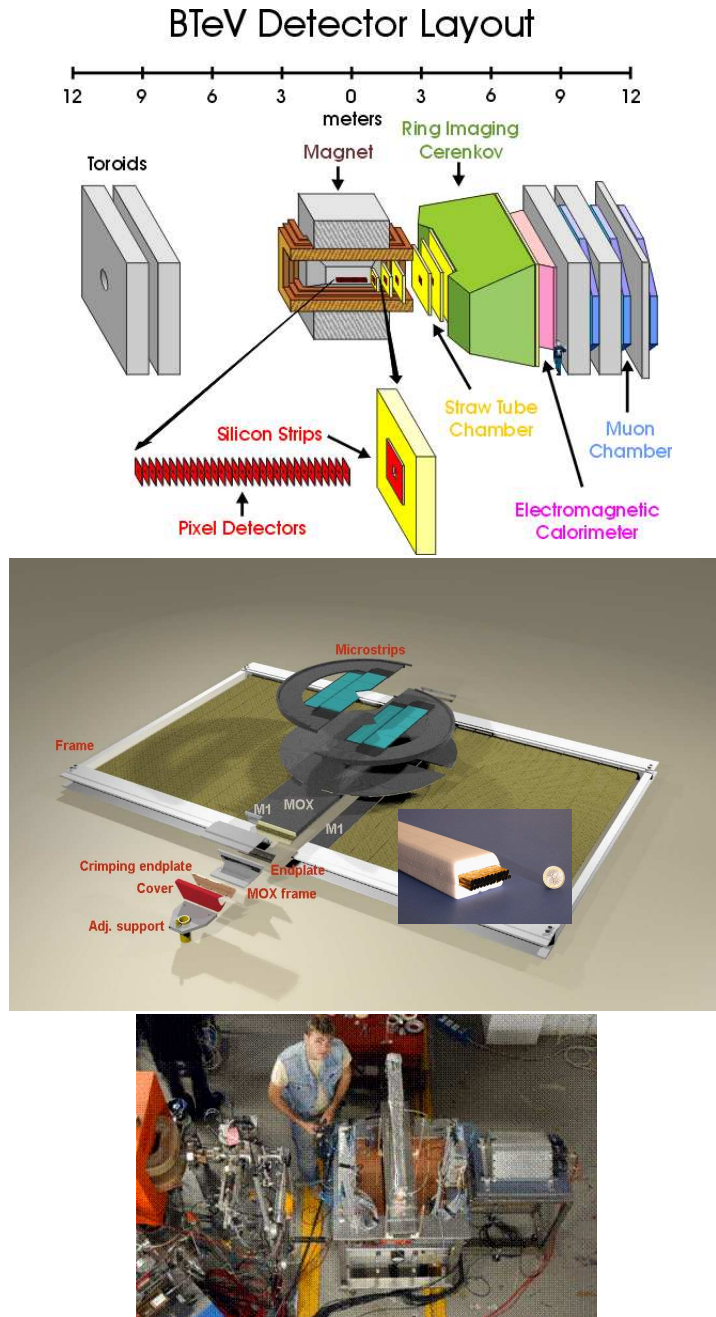


Figure 1: (a) The BTev detector; (b) Conceptual design of one straw tube station, including the CFRP Module 0 (inset: prototype of Module 0). (c) MOX prototype under test at BTF.

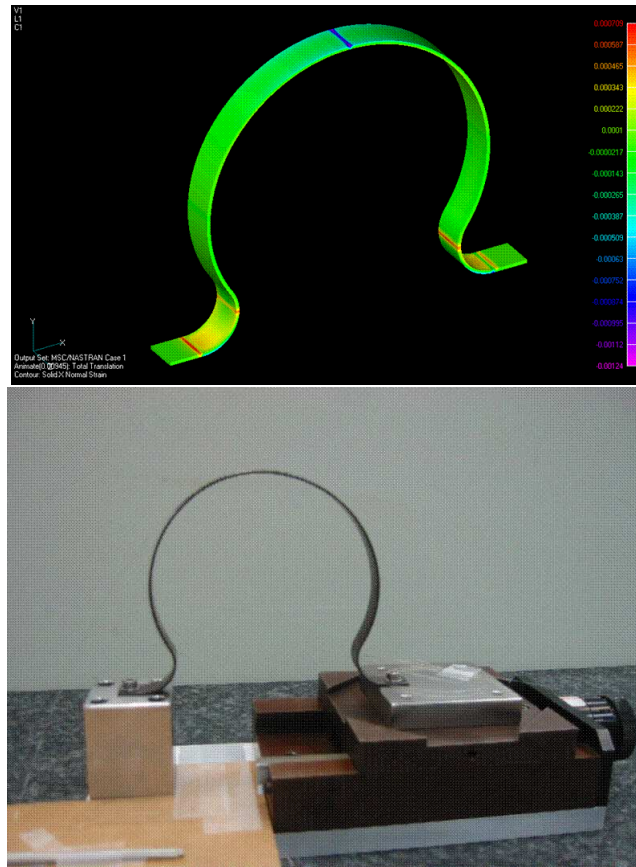


Figure 2: Ω -like pixel repositioning system employing FBG sensors. (top) FEA simulation; (bottom) prototype under test at Fermi SIDET Lab.

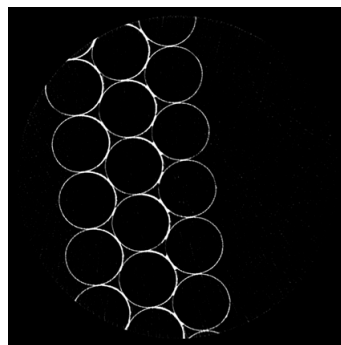


Figure 3: X-ray tomographic images of glued straws prototype of MOX module.

4 Conference Talks in 2004

- S.Bianco (on behalf of the BTeV Coll.) “Status of BTeV experiment at the Fermilab Tevatron”, presented at the Conference on Physics at LHC, 13-17 July 2004, Vienna, Austria, preprint LNF-04/1(P).
- E.Basile, F. Bellucci, M.Bertani, S.Bianco, M.A.Caponero, F. Di Falco, F.L.Fabbri, F.Felli, M.Giardoni, A. La Monaca, G.Mensitieri, B.Ortenzi, M.Pallotta, A.Paolozzi, L.Passamonti, D.Pierluigi, A.Russo and S.Tomassini, “Study of Tensile Response of Kapton and Mylar Strips to Ar and CO_2 Mixtures for the BTeV Straw Tube Detector”, presented by F. Di Falco at the Vienna Conference on Wire Chambers, Vienna (Austria) January 2004, preprint LNF-04/5(P).
- E. Basile *et al.*, “A New Configuration for a Strawtubes - Microstrips Detector”, presented by E. Basile at the IEEE04 Conference, Rome (Italy) October 2004, preprint LNF-04/19(P).

References

1. E. Basile *et al.*, “An unconventional approach for a straw tube - microstrip detector”, arXiv:physics/0412100.
2. E. Basile *et al.*, “A Novel Approach for an Integrated Straw Tube-Microstrip Detector”, preprint LNF-04-25(P).
3. E. Basile *et al.*, “A New Configuration for a Strawtubes - Microstrips Detector”, preprint LNF-04-19(P).
4. BTeV Note 3837-v3 “Tomography Activities for the MOX strawtube-microstrip module”, Giovanna Saviano, 12 Dec 2004.
5. BTeV Note 3487-v4 “Special strawtube module for forward silicon support - M0X”, Stefano Bianco, 13 Dec 2004.
6. BTeV Note 3488-v4 “Fiber Bragg Grating Sensors for BTeV tracking detectors - Summary of R&D results”, Stefano Bianco, 13 Dec 2004.
7. BTeV Note 3694-v1 “Brief report on Frascati straw group activities”, Stefano Bianco, 29 Nov 2004.
8. BTeV Note 3563-v2 “Status of BTeV Experiment at the Fermilab Tevatron”, Stefano Bianco, 30 Oct 2004.
9. BTeV Note 3415-v1 “Special Straw Module M0X”, Stefano Bianco, 17 Sep 2004.
10. BTeV Note 3255-v2 “Status of BTeV experiment at the Fermilab Tevatron”, Stefano Bianco, 16 Jul 2004.
11. BTeV Note 2391-v3 “Straws activity in Frascati”, Stefano Bianco, 11 Jan 2004.
12. BTeV Note 3482-v1 “FBG displacement monitoring by Omega-gauge - jul04”, M. A. Caponero, 24 Sep 2004.
13. BTeV Note 3481-v1 “FBG deformation monitoring of the Pixel Cylinder Support - test Jul04”, M. A. Caponero, 24 Sep 2004.

14. BTeV Note 3416-v1 “Fiber grating costs estimates”, M. A. Caponero, 17 Sep 2004.
15. BTeV Note 3414-v1 “Omega like displacement gauge: principle of operation”, M. A. Caponero, 17 Sep 2004.
16. BTeV Note 3404-v1 “ BTeV Frascati Status Report”, M. A. Caponero, 17 Sep 2004.
17. BTeV Note 2399-v9 “Alignment and Survey Task Force Report”, Herman Cease *et al.*, 03 May 2004.
18. BTeV Note 3011-v1 “Structural monitoring of PIXEL cylinder support by FBG - validation at SiDet CMM”, M. A. Caponero, 27 Apr 2004.
19. BTeV Note 2922-v2 “Fiber Bragg Grating Sensors for position monitoring of forward tracker in BTeV”, Stefano Bianco, 25 Apr 2004.
20. BTeV Note 2920-v1 “Special straw tube module for microstrip integration - M0X”, A. Paolozzi, 27 Sep 2004.
21. BTeV Note 2628-v1 “Microstrip-Straw (MIST) Prototype M0X”, A. Paolozzi, 24 May 2004.
22. BTeV Note 2303-v3 “Preliminary Results on a Study of Tensile Response of Kapton and Mylar Strips to Ar and CO₂ Mixtures for the BTeV Straw Tube Detector”, A. Paolozzi, 11 Jan 2004.

CDF

M. Barone (Ass.), M. Cordelli (Resp.), S. Dell'Agnello,
F. Happacher (Art. 23), S. Miscetti, A. Sansoni, I. Sfiligoi

1 Introduction

The TeVatron, with a $p\bar{p}$ collision energy of 1.98 TeV in the centre of mass system, is running with a record instantaneous luminosity, L , delivered to the experiments of $1.2 \times 10^{32} \text{ cm}^{-2}\text{s}^{-1}$, still below the designed one that is $2 \times 10^{32} \text{ cm}^{-2}\text{s}^{-1}$ (*vs.* $\sim 10^{31}$ of Run I). At the end of year 2004, the CDF experiment has collected on tape $\sim 600 \text{ pb}^{-1}$ (see Figure ??); during the whole Run I we collected $\sim 109 \text{ pb}^{-1}$. The instantaneous luminosity is still increasing during the first months of data taking of the year 2005; the goal is to integrate additional $\sim 470 \text{ pb}^{-1}$ by the experiments in 34 weeks during Fiscal Year 2005.

To reach high values of L it has been necessary to increase the number of p and \bar{p} bunches (N_b); this reflects in the shortening of the time interval between two adjacent bunch crossings, thus requiring the upgrade of the CDF detector. The Run I sub-detectors that were able to sustain this increase in luminosity without any major modification were the central calorimeters, electromagnetic and hadronic. They could work properly in the new Run after the renewal of all the front end electronics; indeed the integration time of charge signals has to be completed within the 132 ns window of the new machine clock (during Run I it was of 3.5 μs).

The CDF group of Frascati has built the hadronic calorimeter (the lead-scintillator based calorimeter in the central and end-wall region, CHA and WHA) and is responsible for its hardware maintenance and for its energy scale calibration.

We recall that to calibrate the calorimeter we profit of the following techniques:

- the ^{137}Cs sources system determines the absolute energy scale; this procedure relies on the test beam of '83 - '85 that used π 's with energy greater than 10 GeV;
- in Run II we use also Minimum Ionizing Particles (Mip's) energy deposition in the hadronic calorimeter looking at muons from J/Ψ 's decays to cross-calibrate;
- the N_2 laser system is often run to track the gains of the photomultipliers and it is a quick tool to check the functionality of the PM-ADMEM chain.

The group has also been involved in the calorimeter timing project, both for the hadron and electromagnetic compartments. The timing system in the hadronic calorimeters (CHA, WHA, PHA), is fully working since the beginning of year 2001. Our responsibility consisted in the design and realization of the fast discriminators VME boards, HADASD, the realization of the transition boards, TB, that connect the PM's cable signals to the backplane of the VME crates, and in the debugging and calibrations of the system. We fulfilled the boards installation and we keep calibrating the system determining the t_0 's, the dependence of the timing on the pulse-height (slewing corrections) together with the discriminators thresholds. All these calibrations taken regularly every $\sim 10 \text{ pb}^{-1}$ go into database tables and are picked during the offline reprocessing of the data.

During year 2004 we added the time information in the central and plug electromagnetic calorimeters (CEM, PEM).

The Frascati group designed and built the discriminator and transition boards for this system.

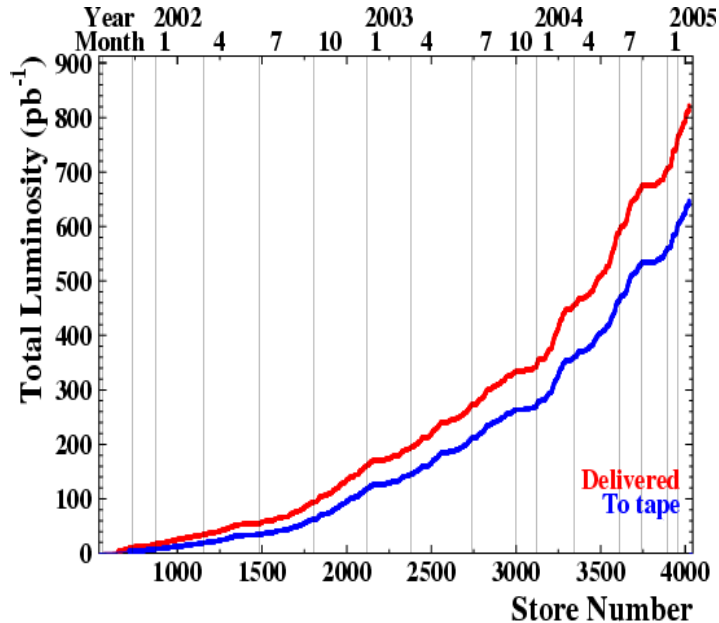


Figure 1: *Live integrated Luminosity vs time.*

During the shut-down of late 2004, we cabled the photomultipliers and installed all the VME boards for the whole CEM and PEM detectors. The system is working properly and it is calibrated using collision data the same way we calibrate the hadron timing system.

2 Calibrating the central hadron calorimeter

The main activity carried on during year 2004 has been the calibration of the central hadron calorimeters, CHA/WHA. The procedure to monitor the energy response of the calorimeters has been well established during year 2003.

For the WHA calorimeter the ^{137}Cs Sources system is fully working and therefore it can be used to set the absolute energy scale for all the towers; we have taken two ^{137}Cs Sources runs during April and September 2004 and we have accordingly computed two sets of Linear Energy Response:

$$LER = \frac{{}^{137}\text{Cs}(\text{test} - \text{beam})e^{-\Delta t/\tau}}{{}^{137}\text{Cs}(\text{today})},$$

that have been downloaded in the front end electronics to correct the raw ADMEM counts. This system effectively probes the behaviour of the calorimeter since the source runs in front of the inner scintillator plane of the wedges thus irradiating few of the scintillator/absorber layers of the calorimeter. In this way we monitor aging phenomena of the scintillator together with PM gain variations.

For the CHA calorimeter the source system is not mechanically reliable anymore and therefore we have decided to calibrate it looking at the energy deposition of Minimum Ionizing Particles (i.e. muons from J/Ψ decays).

We briefly recall the procedure to set the absolute calorimeter energy scale using Mip's. Looking at μ 's from the $\sim 81 \text{ pb}^{-1}$ dimuon trigger sample collected in Run Ib, we determined

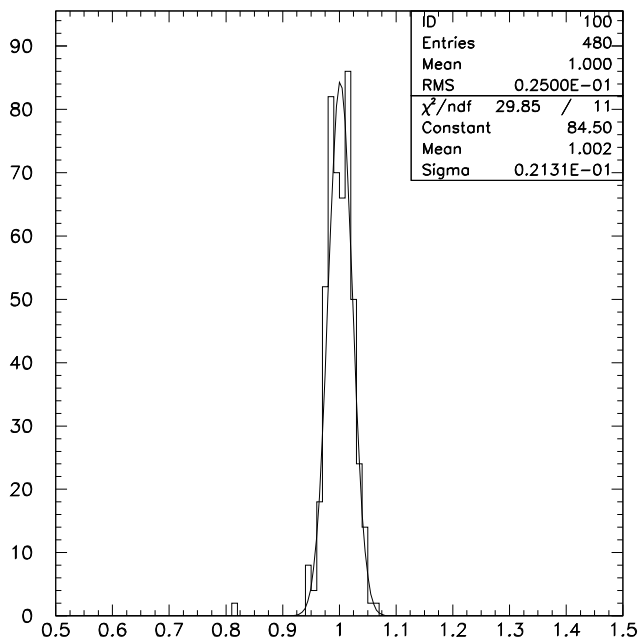


Figure 2: *Mip's peaks ratio for two different periods: March - May and July-August 2004.*

the necessary statistics to determine the peaks of μ 's hadronic energy, HadE, distributions with enough precision per every CHA tower. With a statistics of $\sim 40 \text{ pb}^{-1}$ we find that the tower by tower peak is determined with a precision of $\sim 1.5\%$. The LER's correction factors are derived comparing tower by tower the HadE deposition for Run I and Run II mips:

$$LER = LER^{2003} \times \frac{MIP(RunI)}{MIP('04)},$$

i.e. multiplying the last LER's values (we used during year 2003), measured normalizing the response to Run I Mip's, by the ratio of the MIP peaks between the latest 30 pb^{-1} period of data taken during Jul-Aug 2004 and Run I data.

In Figure 2 we show the stability of the detector plotting the ratio of the muon peaks for two different periods of data taking: March - May and July-August 2004; it can be seen that the CHA calorimeter response did not move within 2%.

2.1 N_2 Laser

The laser system represents a quick tool to follow the trend of the PM's gains. We have continuously acquired laser runs since year 2003 to monitor the gain variations of each photomultiplier. In Figures 3 and 4 we show the comparison of two laser runs taken in march and september 2004; we plot, per every arch and per every tower, the ratio of the mean ADC counts after fitting every tower distribution with a gaussian function. It can be seen that the CHA is stable within $\sim 2\%$ and that the WHA moved a bit more. In Figure 5 we show the trend of the gain variations as measured with laser runs during the last two years.

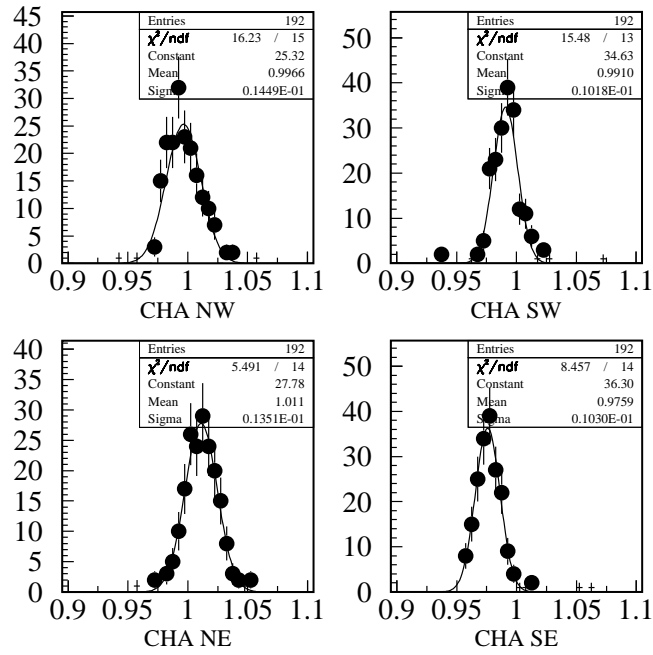


Figure 3: *Laser run. Comparison between two laser runs, for CHA arches.*

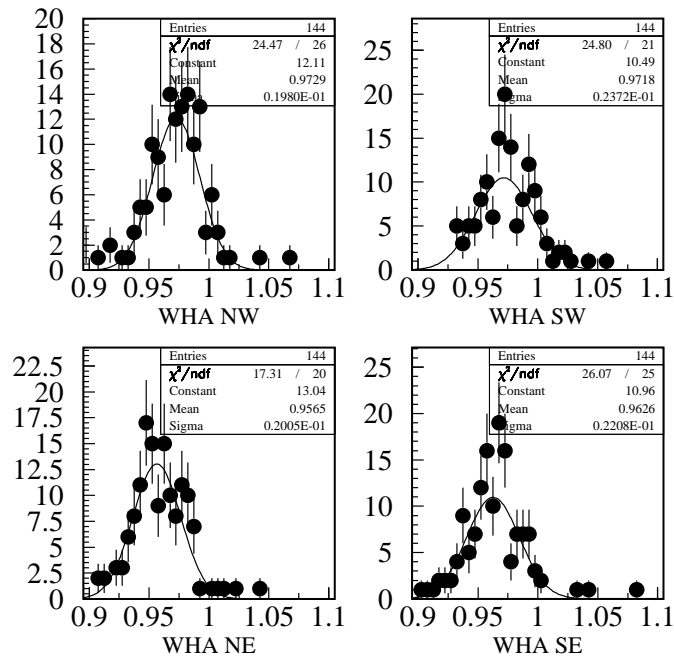


Figure 4: *Laser run. Comparison between two laser runs, for WHA arches.*

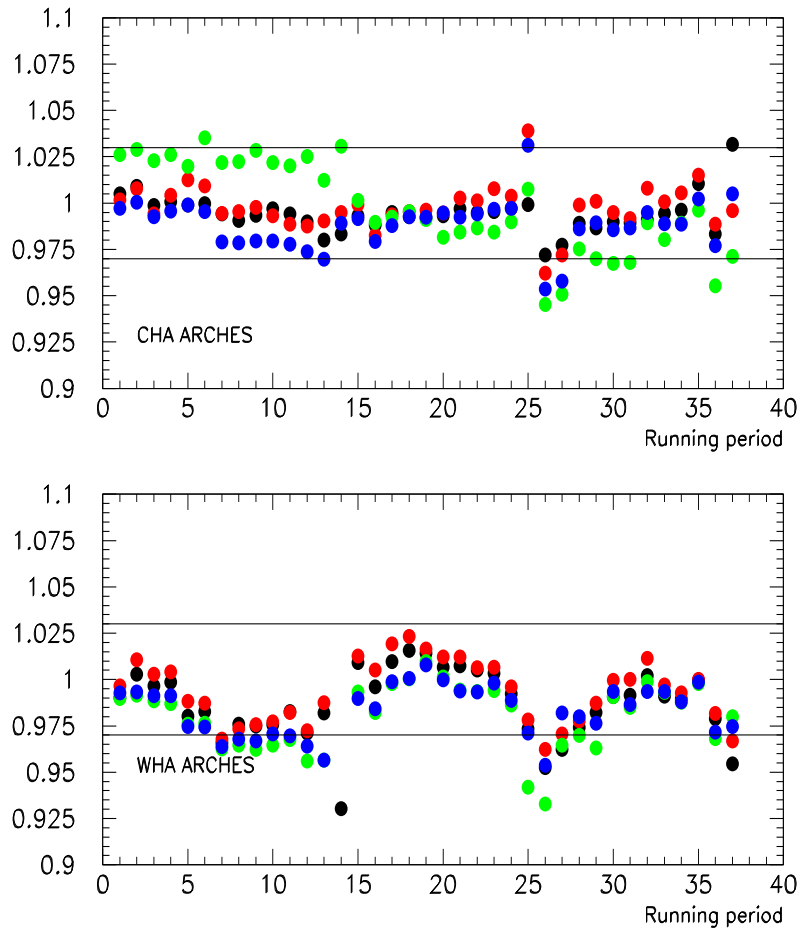


Figure 5: *Laser run. Trend of the gain scale determined using the laser during years 2003/2004.*

3 CAF

The Frascati group is also responsible for developing the CDF Analysis Facility (CAF). The Central CAF system is composed of ~ 600 computing nodes used for user's analysis. It has been developed a simple-to-use graphical interface that allows the submission of jobs from any desktop also outside Fermilab; the output of the jobs is then written on a central disk's pool and can be retrieved at the user's will. This interface also provides the user with a *quasi*-interactive access to the running job.

The Fermilab CAF is not the only user batch pool available at CDF. Several contributing institutions (including INFN) are building their own pools and are using the CAF infrastructure.

The initial *production* version of the CAF was based on the FBSNG batch manager. However, the FBSNG product is not supported anymore, so the CAF software needed to be adapted to a different batch system, and Condor was selected for this task. The transition started in autumn 2003 and by spring of 2004, a first production system was released. As of autumn 2004, the complete FNAL CAF is based on Condor.

In the summer of 2004, CondorCAF was installed also at San Diego Supercomputing Center. In autumn 2004, the CNAF dCAF was also converted to CondorCAF.

During the last months of 2004, the Frascati group has also started the development of a CondorCAF version that can exploit Grid resources, using Condor glide-ins. The work was carried on in conjunction with the CNAF team.

Talks 2004

1. CDF Collaboration, “Globally Distributed User Analysis Computing at CDF” - CHEP 2004.

Publications 2004

1. CDFNOTE 6891: Energy Scale Calibration of Central Hadron Calorimeters.
2. D. Acosta *et al.* [CDF Collaboration], “Measurement of the J/psi meson and b-hadron production cross sections in p anti-p collisions at $s^{*(1/2)} = 1.96\text{-TeV}$,” arXiv:hep-ex/0412071.
3. D. Acosta *et al.* [CDF Collaboration], “Analysis of decay-time dependence of angular distributions in $B/s0 \rightarrow J/\psi \text{ Phi}$ and $B/d0 \rightarrow J/\psi \text{ K}^*0$ decays and measurement of the lifetime difference between B/s mass eigenstates,” arXiv:hep-ex/0412057.
4. D. Acosta *et al.* [CDF Collaboration], “Measurement of the cross section for prompt diphoton production in p anti-p collisions at $s^{*(1/2)} = 1.96\text{-TeV}$,” arXiv:hep-ex/0412050.
5. D. Acosta *et al.* [CDF Collaboration], “Search for anomalous kinematics in t anti-t dilepton events at CDF II,” arXiv:hep-ex/0412042.
6. D. Acosta *et al.* [CDF Collaboration], “Measurements of bottom anti-bottom azimuthal production correlations in proton antiproton collisions at $s^{*(1/2)} = 1.8\text{-TeV}$,” arXiv:hep-ex/0412006.
7. D. Acosta *et al.* [CDF Collaboration], “Measurement of the W boson polarization in top decay at CDF at $s^{*(1/2)} = 1.8\text{-TeV}$,” arXiv:hep-ex/0411070.
8. D. Acosta *et al.* [CDF Collaboration], “Measurement of the forward-backward charge asymmetry of electron positron pairs in p anti-p collisions at $s^{*(1/2)} = 1.96\text{-TeV}$,” arXiv:hep-ex/0411059.
9. D. Acosta *et al.* [CDF Collaboration], “Measurement of charged particle multiplicities in gluon and quark jets in proton anti-proton collisions at $s^{*(1/2)} = 1.8\text{-TeV}$,” FERMILAB-PUB-04-113-E.
10. D. Acosta *et al.* [CDF Collaboration], “Search for scalar leptoquark pairs decaying to nu anti-nu q anti-q in p anti-p collisions at $s^{*(1/2)} = 1.96\text{-TeV}$,” arXiv:hep-ex/0410076.
11. D. Acosta *et al.* [CDF Collaboration], “Search for electroweak single top quark production in p anti-p collisions at $s^{*(1/2)} = 1.96\text{-TeV}$,” arXiv:hep-ex/0410058.
12. D. Acosta *et al.* [CDF Collaboration], “Search for anomalous production of diphoton events with missing transverse energy at CDF and limits on gauge-mediated supersymmetry-breaking models,” arXiv:hep-ex/0410053.
13. D. Acosta *et al.* [CDF Collaboration], “Measurement of the t anti-t production cross section in p anti-p collisions at $s^{*(1/2)} = 1.96\text{-TeV}$ using lepton + jets events with secondary vertex b-tagging,” arXiv:hep-ex/0410041.
14. D. Acosta *et al.*, “Comparison of three-jet events in p anti-p collisions at $s^{*(1/2)} = 1.8\text{-TeV}$ to predictions from a next-to-leading order QCD calculation,” arXiv:hep-ex/0410018.
15. D. Acosta *et al.* [CDF Collaboration], “Measurement of partial widths and search for direct CP violation in D0 meson decays to $K^- K^+$ and $\pi^- \pi^+$,” FERMILAB-PUB-04-148-E.

16. D. Acosta *et al.*, “Search for excited and exotic electrons in the $e \gamma$ decay channel in p anti- p collisions at $s^{**}(1/2) = 1.96\text{-TeV}$,” arXiv:hep-ex/0410013.
17. D. Acosta *et al.* [CDF II Collaboration], “Measurement of $W \gamma$ and $Z \gamma$ production in p anti- p collisions at $s^{**}(1/2) = 1.96\text{-TeV}$,” Phys. Rev. Lett. **94**, 041803 (2005).
18. D. Acosta *et al.* [CDF-II Collaboration], “Measurement of the t anti- t production cross section in p anti- p collisions at $s^{**}(1/2) = 1.96\text{-TeV}$ using kinematic fitting of b -tagged lepton + jet events,” arXiv:hep-ex/0409029.
19. D. Acosta *et al.* [CDF II Collaboration], “First measurements of inclusive W and Z cross sections from Run II of the Tevatron collider,” arXiv:hep-ex/0406078.
20. D. Acosta *et al.* [CDF Collaboration], “Search for doubly-charged Higgs bosons decaying to dileptons in p anti- p collisions at $s^{**}(1/2) = 1.96\text{-TeV}$,” Phys. Rev. Lett. **93**, 221802 (2004) [arXiv:hep-ex/0406073].
21. D. Acosta *et al.* [CDF Collaboration], “Inclusive search for anomalous production of high- $p(T)$ like-sign lepton pairs in p anti- p collisions at $s^{**}(1/2) = 1.8\text{-TeV}$,” Phys. Rev. Lett. **93**, 061802 (2004) [arXiv:hep-ex/0405063].
22. D. Acosta *et al.* [CDF Collaboration], “Measurement of the t anti- t production cross section in p anti- p collisions at $s^{**}(1/2) = 1.96\text{-TeV}$ using dilepton events,” Phys. Rev. Lett. **93**, 142001 (2004) [arXiv:hep-ex/0404036].
23. D. Acosta *et al.* [CDF Collaboration], “Direct photon cross section with conversions at CDF,” Phys. Rev. D **70**, 074008 (2004).
24. D. Acosta *et al.* [CDF Collaboration], “The underlying event in hard interactions at the Tevatron anti- p p collider,” Phys. Rev. D **70**, 072002 (2004).
25. D. Acosta *et al.* [CDF Collaboration], “Optimized search for single top quark production at the Fermilab Tevatron,” Phys. Rev. D **69**, 052003 (2004).
26. D. Acosta *et al.* [CDF Collaboration], “Search for $B/s_0 \rightarrow \mu^+ \mu^-$ and $B/d_0 \rightarrow \mu^+ \mu^-$ decays in p anti- p collisions at $s^{**}(1/2) = 1.96\text{-TeV}$,” Phys. Rev. Lett. **93**, 032001 (2004).

E831

R. Baldini-Ferroli, L. Benussi (Art. 23), M. Bertani,
S. Bianco (Resp.), F.L. Fabbri, S. Pacetti (Bors.)

1 Introduction

FOCUS (Experiment 831 at Fermilab, www.focus.fnal.gov) studies photoproduction and decays of charm mesons and baryons at Fermilab. In FOCUS, a forward multi-particle spectrometer is used to measure the interactions of high energy photons on a segmented BeO target. The FOCUS detector is a large aperture, fixed-target spectrometer with excellent vertexing, particle identification, and reconstruction capabilities for photons and π^0 's. FOCUS is a considerably upgraded version of a previous experiment, E687, and it amply surpassed the goal of collecting ten times the E687 sample of fully reconstructed charm decays, i.e. a sample of over 1 million fully reconstructed charm particles in the three major decay modes: $D^0 \rightarrow K^-\pi^+$, $K^-\pi^+\pi^-\pi^+$ and $D^+ \rightarrow K^-\pi^+\pi^+$. The FOCUS Italian groups (Milano, Pavia and Frascati) hold full responsibility for the μ -strip detector, the Hadron calorimetry, and the outer em calorimetry respectively, and coordinate about half of the software-related projects. The Frascati group also coordinates the calorimetry working group, and is responsible for the first level selection process in physics analyses utilizing em calorimetry.

2 Activity during year 2004

The activity of the Frascati FOCUS group in 2004 was concentrated on the data analysis and presentation of results at conferences. The data analysis studies of the group were centered on spectroscopy. Along with the traditional ensemble of studies on the spectroscopy of orbitally and radially excited charm mesons, a new line of research was opened, regarding the spectroscopy of light quark mesons diffractively photoproduced.

Heavy Quark Symmetry and Heavy Quark Effective Theory predict a rich spectrum for the excited charm mesons. In 2004 FOCUS progressed with the analysis carried on by the Frascati group on the precise new measurements of D_2^* and $D_1(j_q = 3/2)$ masses and widths (with errors less than or equal to PDG2003 averages). Light quark diffractive physics is a surprise for a heavy quark experiment. Thanks to a dedicated trigger FOCUS has collected a very significant sample of diffractive events, thus starting studies of interest in hadronic physics and predictions of χ QCD. During 2003, the Frascati group published a follow-up study of the evidence found in 2001 for a narrow dip structure in diffractive photoproduction of the 6π final state. When interpreted as a new resonance interfering with the diffractive continuum, the structure has $1.911 \pm 0.004 \text{ GeV}/c^2$ mass and $29 \pm 11 \text{ MeV}/c^2$ width.

In 2004 the search for a confirmation signal in FOCUS data, at a mass and width compatible with the E687 published result, was pursued and results confirmed. Publication is in progress. Work also progressed on the study of diffractively photoproduced $\phi\eta$, $\phi\eta'$, ϕf_0 events, studied the q^2 evolution, and investigated a relationship via dispersion relations to the debated value of the branching ratio $\Gamma(\phi \rightarrow f_0\gamma)$.

3 Outlook

The activity in 2005 will be focussed in finalizing the ongoing analysis of the $D^*\pi$ final state, and in searching for radial excitations, including channels with γ and π^0 in the final state. In the light

quark sector, we plan to finalize the study to seek confirmation of the six pion structure and to finalize the study f_0 production and $\eta - \eta'$ mixing from our diffractive sample.

4 Conference Talks in 2004

1. S. Bianco, “Hot Topics in Charm Physics”, invited review talk given at the Second PANDA Workshop, Frascati (2004), preprint LNF-04/15(P).
2. S. Bianco (on behalf of the FOCUS Coll.) “New Focus Results On Charm Physics”, presented at La Thuile 2004, preprint LNF-04/14(P).
3. L. Benussi (on behalf of the FOCUS Coll.) “Focus Measurements of Masses And Widths of Excited Charm Mesons D_2^* And Evidence for Broad States”, presented at MESON04, Cracow, preprint LNF-04/13(P).

References

1. J. M. Link *et al.* [FOCUS Collaboration], arXiv:hep-ex/0412034.
2. S. Bianco [FOCUS Collaboration], “New charm results from FOCUS,” arXiv:hep-ex/0412003.
3. J. M. Link *et al.* [FOCUS Collaboration], arXiv:hep-ex/0411031.
4. J. M. Link *et al.* [FOCUS Collaboration], Phys. Lett. **B607**, 59 (2005) [arXiv:hep-ex/0410077].
5. J. M. Link *et al.* [FOCUS Collaboration], Phys. Lett. **B607**, 51 (2005) [arXiv:hep-ex/0410068].
6. J. M. Link *et al.* [FOCUS Collaboration], Phys. Lett. **B607**, 67 (2005) [arXiv:hep-ex/0410067].
7. J. M. Link *et al.* [FOCUS Collaboration], arXiv:hep-ex/0410037.
8. J. M. Link *et al.* [FOCUS Collaboration], Phys. Lett. **B601**, 10 (2004) [arXiv:hep-ex/0407014].
9. J. M. Link *et al.* [FOCUS Collaboration], Phys. Lett. **B598**, 33 (2004) [arXiv:hep-ex/0406060].
10. J. M. Link *et al.* [FOCUS Collaboration], Phys. Lett. **B586**, 21 (2004) [arXiv:hep-ex/0401019].
11. J. M. Link *et al.* [FOCUS Collaboration], Phys. Lett. **B586**, 183 (2004) [arXiv:hep-ex/0401001].

KLOE

The KLOE-LNF Collaboration

A. Antonelli, M. Antonelli, G. Bencivenni, S. Bertolucci, C. Bloise, F. Bossi,
P. Campana (Resp.), G. Capon, P. Ciambrone, E. DeLucia (Art. 23), S. Dell’Agnello,
P. DeSimone, M. Dreucci, G. Felici, M.C. Ferrer, A. Franceschi, G. Finocchiaro,
C. Forti, C. Gatti, S. Giovannella, G. Lanfranchi, J. Lee-Franzini,
M. Martini (Dott.), S. Miscetti, M. Moulson, F. Murtas, M. Palutan, V. Patera* (Ass.),
P. Santangelo, B. Sciascia (Art. 23), A. Sciubba* (Ass.), I. Sfiligoi, T. Spadaro, G. Venanzoni
(* Also at Dipartimento di Energetica, “La Sapienza” University, Rome)

The KLOE-LNF Technical Staff

M. Anelli, A. Balla, G. Fortugno, G. Paoluzzi, G. Papalino, R. Rosellini, M. Santoni

1 The KLOE data taking

In May 2004 Kloe resumed the data taking and since then collected up to the end of the year 730 pb^{-1} to be added to the 400 pb^{-1} acquired in 2001 and 2002. The machine luminosity passed in 2004 the 100 $\mu b^{-1}s^{-1}$ limit and peak luminosities of $1.2 \cdot 10^{32} cm^{-2}s^{-1}$ were often attained. Background conditions have been very variable, on the high side until September and gradually better afterwards. The daily average record was 8 pb^{-1} and the daily average over the run was 3.2 $pb^{-1}day^{-1}$.

All data taken in 2004 has been processed through the reconstruction programs.

The analysis criteria and tools have been refined and in particular great care has been given to the Monte Carlo program in order to simulate the detector behavior as accurately as possible, including also the effects of machine background. The analyses of the 2001/02 data have been carried largely to completion. As reported at the summer conferences, especially at ICHEP2004 in Beijing, KLOE results are of exceptional interest in many fields of particle physics:

- 1) The resolution of a possible problem with unitarity of the CKM matrix, by the correct determination of the semileptonic branching ratios of neutral and charged kaons, new precise measurements of the charged kaons and of KL mesons;
- 2) The resolution of an unsatisfactory question in deriving the hadronic corrections to the muon anomaly. KLOE confirms the results on $\sigma(e^+e^- \rightarrow \pi\pi)$ and the disagreement with τ data;
- 3) The best limit on the CP-violating decay $K_S \rightarrow \pi^0\pi^0\pi^0$;
- 4) The precision tests of C-invariance in eta decays;
- 5) The continued study of scalar and pseudo scalars as far as their structure and their mixing are concerned.

2 Neutral kaon analysis

Data taken during years 2001 and 2002 for a total integrated luminosity of $\sim 400 pb^{-1}$ have been studied in depth. The aim was twofold: to update measurements previously published, based on analysis of $\sim 20 pb^{-1}$ of data taken in year 2000; to complete new studies, some of which are affordable only now, from the statistical point of view.

Many measurements have been completed in 2004 and are nearly ready for publication. In the following, we summarize the status of these measurements at the end of the year and provide

perspectives on analyses that will be completed in 2005.

2.1 Measurement of the ratio $\text{BR}(K_S \rightarrow \pi^+\pi^-(\gamma))/\text{BR}(K_S \rightarrow \pi^0\pi^0)$

The physics motivation of this analysis is twofold: from one side, this quantity directly enters in the double ratio used to measure the direct CP violation parameter $\Re(\epsilon'/\epsilon)$; besides, it can be used to extract the π - π phase shift difference for transitions with isospin 0 and 2 at $\sqrt{s} = m_\pi$ ($\delta_0 - \delta_2$) and thus to clarify the discrepancy of this quantity as extracted from kaon decays with the value obtained from π - π scattering data.

The published result had a 0.7% total accuracy, dominated by systematic uncertainties. The goal of the re-analysis is to push the error down to the level of 0.1-0.2% and to complement the analysis with the study of the photon spectrum in the decay $K_S \rightarrow \pi^+\pi^-\gamma$, sensitive to terms of $\mathcal{O}(p^6)$ in the chiral perturbation theory (χ Pt) expansion.

At the end of 2004, the status of the analysis is advanced; it is expected to be completed in the first months of 2005.

2.2 Analysis of the decay $K_S \rightarrow \pi e \nu$

The measurement of the kaon semileptonic decay widths provides several tests of many fundamental aspects of the standard model, SM. With the present knowledge of $|V_{ud}|$ and the value of $|V_{us}|$ extracted from the semileptonic decay widths of the K_S and K_L , a unitarity test to better than 1% can be performed.

Besides, the knowledge of both the K_L and the K_S semileptonic decay branching ratios and lifetimes allows the validity of the $\Delta S = \Delta Q$ rule to be tested through the quantity

$$\text{Re}(x_+) = \frac{1}{2} \times \frac{\text{BR}(K_S \rightarrow \pi e \nu)/\tau_S - \text{BR}(K_L \rightarrow \pi e \nu)/\tau_L}{\text{BR}(K_S \rightarrow \pi e \nu)/\tau_S + \text{BR}(K_L \rightarrow \pi e \nu)/\tau_L}.$$

In the SM, $\text{Re}(x_+)$ is expected to be of the order of $G_F m_\pi^2 \sim 10^{-7}$. At present, the most precise test of the $\Delta S = \Delta Q$ rule finds $\text{Re}(x_+)$ to be compatible with zero with an error of 6×10^{-3} ¹⁾.

Finally, discrete symmetries are tested through the measurement of the charge asymmetries for K_L and K_S decays, $A_{L,S}$, defined as

$$A_{L,S} = \frac{\Gamma(K_{L,S} \rightarrow \pi^- e^+ \nu) - \Gamma(K_{L,S} \rightarrow \pi^+ e^- \bar{\nu})}{\Gamma(K_{L,S} \rightarrow \pi^- e^+ \nu) + \Gamma(K_{L,S} \rightarrow \pi^+ e^- \bar{\nu})}.$$

If CPT invariance holds, each of the two charge asymmetries are expected to be equal to $2 \times \text{Re}(\epsilon) \simeq 3 \times 10^{-3}$, where ϵ is the parameter describing CP violation in the $K^0 - \bar{K}^0$ mass matrix. A difference between A_S and A_L signals CPT violation either in the mass matrix, or in the decay amplitudes. The value of A_L is known at present with a precision of 10^{-4} ^{2, 3)}, while A_S has never yet been measured.

From the analysis of the 2001-2002 data set, the following preliminary results have been obtained and presented at the ICHEP 2004 Conference in Beijing ⁴⁾. For the branching ratios:

$$\begin{aligned} \text{BR}(K_S \rightarrow \pi^- e^+ \nu) &= (3.54 \pm 0.05_{\text{stat}} \pm 0.05_{\text{syst}}) \times 10^{-4}, \\ \text{BR}(K_S \rightarrow \pi^+ e^- \bar{\nu}) &= (3.54 \pm 0.05_{\text{stat}} \pm 0.04_{\text{syst}}) \times 10^{-4}, \\ \text{BR}(K_S \rightarrow \pi^\pm e^\mp \bar{\nu}(\nu)) &= (7.09 \pm 0.07_{\text{stat}} \pm 0.08_{\text{syst}}) \times 10^{-4}. \end{aligned}$$

From the last result, and using the PDG-fit result of the K_S lifetime, $\tau_S = (89.58 \pm 0.06)$ ps ⁵⁾, we can extract the parameter $\text{Re}(x_+)$. The result depends on the value of the K_L BR and lifetime:

using the BR from PDG-fit and τ_L averaged by PDG, the result is $\sim 3\sigma$ away from zero; using the BR from a recent measurement by KTeV collaboration ⁶⁾ and τ_L averaged by PDG, we get a value compatible with zero; using BR and lifetime from preliminary measurements by KLOE ⁷⁾, the result is $\sim 1.3\sigma$ from zero.

The charge asymmetry is also obtained:

$$A_S = (-2 \pm 9_{\text{stat}} \pm 6_{\text{syst}}) \times 10^{-3}.$$

This result is compatible with that for K_L semileptonic decays and with the expectation obtained assuming CPT symmetry, $A_S = 2\text{Re}(\epsilon)$.

The method used to extract the product $f_+^{K^0} \times V_{\text{us}}$ of the vector form factor at zero momentum transfer and the CKM element V_{us} from the measurement of $\text{BR}(K_S \rightarrow \pi e \nu)$ and from the K_S lifetime is described in detail in the contribution to the ICHEP 2004 conference ⁴⁾. We obtain:

$$f_+^{K^0 \pi^-}(0) \times V_{\text{us}} = 0.2171 \pm 0.0017.$$

Using $V_{\text{ud}} = 0.9740 \pm 0.0005$ from ⁸⁾ and $f_+^{K^0 \pi^-}(0) = 0.961 \pm 0.008$ from ⁹⁾, also in agreement with a recent lattice calculation ¹⁰⁾, the unitarity band is shown to be in agreement with our preliminary result: $f_+^{K^0 \pi^-}(0) \times V_{\text{us}} = 0.2177 \pm 0.0028$.

2.3 Analysis of the decay $K_S \rightarrow \pi \mu \nu$

The physics motivations for this analysis are exactly the same discussed in the previous section. Moreover, no direct measurement exists of this BR. The background rejection factor needed is higher than that for the $\pi e \nu$ selection: since the background is dominated by early decays in flight of $\pi \rightarrow \mu \nu$, particle identification techniques are less effective in this case. Therefore, a harder rejection by means of kinematic variables has been applied, giving a satisfactory separation of signal from the background. From the analysis of 2001–2002 data, a fractional statistical error of $\sim 3\%$ can be obtained for each charge state. This analysis is expected to be completed by the end of 2005.

2.4 Measurement of the main K_L branching ratios

There are no good measurements of the absolute value of the main K_L branching fractions; at present, the PDG “fit” values for this branching ratio have 0.5–2% relative errors, and are obtained from various K_L branching ratio and rate measurements ⁵⁾. A recent analysis from KTeV ⁶⁾ of the relative K_L main branching fractions has shown discrepancies with respect to the PDG values up to 8% depending on the channel.

Knowledge of the K_L lifetime τ_L is very important not only for the determination of V_{us} but it is also necessary for the absolute branching fraction measurement. τ_L can be obtained from the K_L proper time distribution and also by measuring all K_L decay branching ratios in a given fiducial volume, FV, by requiring they add up to 1.

Preliminary results were presented in July 2004 at the ICHEP conference in Beijing ⁷⁾. The results presented below were obtained by the end of 2004 and first presented at La Thuile in February 2005.

A total of about 13×10^6 tagged K_L events are used for the measurement of the branching fractions. Almost twice as many additional events provide calibration. The fit to the distribution of the difference $\Delta_{\mu\pi}$ of the missing energy and momentum in the $\pi\text{--}\mu$ hypothesis is used to identify the charged modes. Data is fit to a linear combination of Monte Carlo distributions for $K_L \rightarrow \pi^\pm e^\mp \nu$, $K_L \rightarrow \pi^\pm \mu^\mp \nu$ and $K_L \rightarrow \pi^+ \pi^- \pi^0$, as shown in the left panel of figure 1.

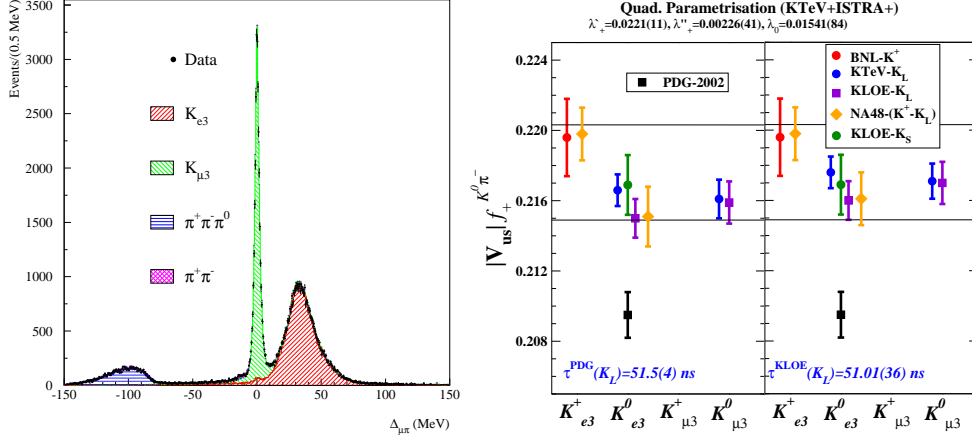


Figure 1: Left: distribution for data and Monte Carlo of the variable $\Delta_{\mu\pi}$. The contributions from different channels is also given. Right: $V_{us} \times f_+^{K^0}(0)$ from semileptonic decays of K_S and K_L mesons.

The sum of all measured branching fractions plus the PDG value for rare decays, 0.0036, is $1.0068 \pm 0.0046 \pm 0.0061$. This result, as remarked earlier, depends on K_L lifetime; by renormalizing the sum to 1.0, we eliminate systematics arising from uncertainty on the K_L lifetime, and obtain:

$$\begin{aligned}
 \tau_L &= 51.01 \pm 0.08_{stat} \pm 0.35_{syst} \text{ ns}, \\
 \text{BR}(K_L \rightarrow \pi^\pm e^\mp \nu) &= 0.4007 \pm 0.0006_{stat} \pm 0.0020_{syst}, \\
 \text{BR}(K_L \rightarrow \pi^\pm \mu^\mp \nu) &= 0.2698 \pm 0.0006_{stat} \pm 0.0015_{syst}, \\
 \text{BR}(K_L \rightarrow \pi^0 \pi^0 \pi^0) &= 0.1997 \pm 0.0003_{stat} \pm 0.0023_{syst}, \\
 \text{BR}(K_L \rightarrow \pi^+ \pi^- \pi^0) &= 0.1263 \pm 0.0004_{stat} \pm 0.0015_{syst}.
 \end{aligned}$$

The method used to extract the product $f_+^{K^0} \times V_{us}$ from the measurement of the BR for $\pi^\pm e^\mp \nu K_{\mu 3}$ is discussed in detail in ⁽⁷⁾. The results are:

$$\begin{aligned}
 f_+^{K^0} \times V_{us} &= 0.2160 \pm 0.0011 \text{ from } K_{e3}, \\
 f_+^{K^0} \times V_{us} &= 0.2170 \pm 0.0012 \text{ from } K_{\mu 3}.
 \end{aligned}$$

The right panel of figure 1 shows the value of the product $V_{us} \times f_+^{K^0}(0)$ as obtained from all sources, as well as the recent results reported by the KTeV collaboration. All of the new results are compatible with unitarity.

2.5 Measurement of the K_L lifetime

In figure 2 we show the K_L proper time distribution obtained with $\sim 15 \times 10^6$ $K_L \rightarrow \pi^0 \pi^0 \pi^0$ decays. The distribution is fitted with an exponential inside the FV, ranging from 50 to 160 cm. The position of the K_L decay vertex is reconstructed, using the arrival times of the photons measured by the calorimeter, on the K_L flight direction given by the accompanying $K_S \rightarrow \pi^+ \pi^-$ decay. The spatial resolution for this “neutral vertex” technique is of the order of 2 cm. The result obtained is compatible with that presented in the previous section:

$$\tau_L = 50.87 \pm 0.15_{stat} \pm 0.26_{syst} \text{ ns}.$$

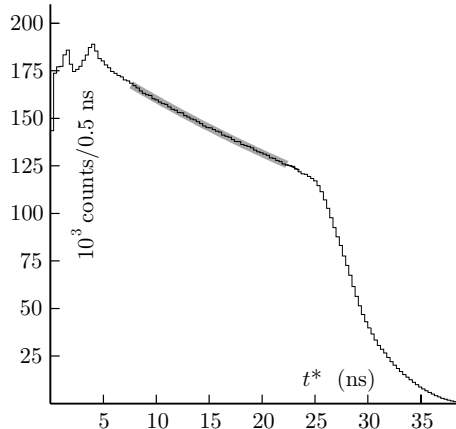


Figure 2: K_L proper time distribution. The interval used in the fit is shown shaded.

2.6 Measurement of the BR for the decay $K_L \rightarrow \pi^+\pi^-$

A measurement of the *absolute* BR for this decay is aimed at shedding light on the unclear experimental picture for this quantity: the value averaged by PDG ⁵⁾ is different at a $3\text{-}\sigma$ level with that coming from a recent precise KTeV measurement ¹¹⁾. Moreover, used together with the ratio of $K_S \rightarrow \pi\pi$ BR's and the *absolute* BR for $K_L \rightarrow \pi^0\pi^0$, it can be exploited to get a value for the double ratio, independent from the measurements by KTeV and NA48.

The preliminary result of this quantity has an accuracy comparable to that of the most precise direct measurement so far. The study of the systematics is under completion; the analysis is expected to be finalized by the end of 2005.

2.7 Measurement of the branching ratio for the decay $K_S \rightarrow \pi^0\pi^0\pi^0$

The decay $K_S \rightarrow \pi^0\pi^0\pi^0$ is a pure CP violating process. The related CP violation parameter, η_{000} is defined as the ratio of K_S and K_L decay amplitude. In the SM, this is expected to be similar in magnitude to the CP violation parameter for the $\pi^0\pi^0$ final state, η_{00} . The expected value for $\text{BR}(K_S \rightarrow \pi^0\pi^0\pi^0)$ in the SM is $\sim 2 \times 10^{-9}$, making a direct observation impossible, with the present data taking.

Details on the analysis had been presented at the ICHEP 2004 International Conference ¹²⁾. Exploiting the K_S -tagged beam from the identification of the K_L interactions in the calorimeter, we selected a total of 2 candidate events, with a background expected from the analysis of the simulation (MC) of $3.1 \pm 1.1_{\text{MCstat}} \pm 0.5_{\text{syst}}$. We finally derive the upper limit:

$$\text{BR}(K_S \rightarrow \pi^0\pi^0\pi^0) \leq 1.2 \times 10^{-7} \text{ at } 90\% \text{ of CL.}$$

This improves by a factor of 7 the most stringent limit in the literature. we expect to reach a sensitivity of 10^{-8} for the BR from the analysis of 2004 data.

2.8 Measurement of the branching ratio for the decay $K_S \rightarrow \pi^+\pi^-\pi^0$

The BR for this decay is known at 30% of accuracy from interferometry techniques; the value is $\sim 3 \times 10^{-7}$ ⁵⁾. With 410 pb^{-1} of integrated luminosity, 4 events are expected to be observed with the present selection, which only uses the K_L -crash tag. Using the statistics collected in the

current data taking, which presumably will amount to a total of 2 additional fb⁻¹, ~ 20 events will be observed, thus allowing a measurement of the BR for this channel that is more precise than the world average. The analysis of the 2001-2002 data is in an advanced state and it is expected to be finalized by the end of 2005.

2.9 Study of the interference pattern for $\pi^+\pi^-\pi^+\pi^-$ final states

The kaon pair from the decay $\phi \rightarrow K^0\bar{K}^0$ is in a quantum-mechanical coherent superposition. The study of distribution of the difference of proper times for the decay to $\pi^+\pi^-$ final states gives information on the K_L-K_S mass difference and allows to implement a test for the quantum mechanics, QM, itself. Admitted violations from the QM prediction are described by a decoherence parameter, ζ . The present knowledge of this quantity is established by an analysis of CPLEAR data ¹³⁾: ζ is compatible with zero at the level of 10^{-2} , both in the $K_S K_L$ and in the $K_L \bar{K}^0$ basis. The preliminary results from the analysis of 2001-2002 data show no QM violation, or ζ compatible with zero with a 3×10^{-2} (2×10^{-7}) accuracy in the $K_S K_L$ ($K^0 \bar{K}^0$) basis.

3 Charged Kaons

3.1 Data reconstruction and Monte Carlo

The year 2004 has been devoted to the analysis of the data acquired during the 2001-2002 data taking, to the generation of a new Monte Carlo sample, and to the production of DST for both Monte Carlo and data.

The main physics issue addressed by the study of charged kaon decays is the extraction of the CKM matrix element V_{us} , both through the measurement of the semileptonic and $K^\pm \rightarrow \mu^\pm \nu$ widths, via the methods discussed in ¹⁴⁾ and ¹⁵⁾, respectively. Experimental inputs to the determination of V_{us} are, among others, the value of the partial decay width of the decays $K^\pm \rightarrow \pi^0 e^\pm \nu$, $K^\pm \rightarrow \pi^0 \mu^\pm \nu$, and $K^\pm \rightarrow \mu^\pm \nu$, and the value of the charged kaon lifetime, τ_{K^\pm} . In the last year, a large effort has been taken to complete the measurement of all these quantities. In 2004 all the DST's relative to the entire 2001-2002 data set, needed for the analysis of charged kaons, have been produced. For what concern the Monte Carlo, the simulation of 2001-2002 data for the K^+K^- events were produced in 2003 with a scale 1:5 with respect to integrated luminosity (*alphis* production). During august 2004 a new Monte Carlo sample has been generated and reconstructed, which simulates with a 1:1 scale the K^+K^- events, on the 450 pb⁻¹ acquired during years 2001 and 2002 (*kpm04* production).

3.2 Study of the charged kaon semileptonic decay

The decays $K^\pm \rightarrow \pi^0 e^\pm \nu$ and $K^\pm \rightarrow \pi^0 \mu^\pm \nu$ are particularly relevant for the extraction of V_{us} ¹⁴⁾. The very clean signature of the decays $K^\pm \rightarrow \pi^\pm \pi^0$ and $K^\pm \rightarrow \mu^\pm \nu$ is exploited to tag the charged kaons events. For the first tag, the π^0 connected to the kaon decay vertex is asked to satisfy the calorimeter trigger requirements, while for the second tag these requirements have to be fulfilled by the muon itself. The use of two tags allow for four independent measurement (2 tags \times 2 charge) of the two branching ratios.

The signal sample of $K_{\ell 3}^\pm$ events is selected by asking for a decay vertex in the drift chamber and one π^0 in the electromagnetic calorimeter connected to the same vertex. The two body decays are removed using kinematical cuts in the K^\pm center of mass. The difference of the time of flight of the lepton and of the π^0 has been used to separate muons, electrons, and residual charged pions in the sample, by means of the distribution of the squared mass of the lepton (figure 3, right panel). Most of the selection efficiencies have been evaluated directly from data using control samples and the effect of radiative K_{l3} decays have been accounted for, using an accurate Monte Carlo

simulation of the radiation in the Monte Carlo ¹⁶⁾. The statistical accuracy of the measurements range from 0.4% to 0.9% depending on the tag and the signal type. The systematic are under study.

3.3 Study of the charged kaon lifetime

Looking at the PDG ¹⁷⁾ fit of the charged kaon lifetime, some discrepancies between “in-flight” and “at-rest” measurements can be found. Moreover, there are some differences between the various “at-rest” measurements obtained using different materials to stop the kaons. The new high-statistics measurement by KLOE could clarify this situation.

A pure sample of kaons of one charge has been obtained by tagging a coincident $K^\pm \rightarrow \mu^\pm \nu$ decay of the kaons with opposite charge. Two independent methods to measure the charged kaon lifetime have been developed. The first one relies on drift chamber information only and evaluates the K^\pm proper lifetime stepping along the charged kaon track up to the decay vertex, taking into account the energy losses in the gas mixture of the drift chamber (10% *iso*C₄H₁₀-90%He)

In the second method the kaon track of the tagging side is extrapolated to the signal hemisphere and the time measurements of the two photons from the π^0 decay are used to evaluate the time of flight of the kaon.

The precision reached for both measurement is comparable to the measurement in literature. The efficiencies of both selections have been evaluated on data, while the systematics of the measurements are under study.

3.4 Study of two-body decays of charged kaons

The $K^\pm \rightarrow \mu^\pm \nu$ is the main decay channel of the charged kaon. Its absolute branching ratio has been measured only once in the seventies by Chiang without a clear prescription for the treatment of the photon coming from the parent decay $K^+ \rightarrow \mu \nu \gamma$. Following Marciano ¹⁵⁾, combining the ratio of experimental kaon and pion decay widths $\Gamma(K \rightarrow \mu \nu(\gamma))/\Gamma(\pi \rightarrow \mu \nu(\gamma))$, with a recent lattice gauge theory calculation of f_K/f_π , provides a precise value of V_{us} .

About 175 pb⁻¹ of the 2002 data taking have been analyzed to measure the branching ratio of the $K^+ \rightarrow \mu \nu(\gamma)$ inclusive decay ¹⁸⁾. A pure sample of positive kaons has been obtained by tagging a coincident two-body decay of negative kaons. For this analysis only events tagged by a $K^- \rightarrow \mu^- \nu$ decay in which the muon satisfies by itself the requirements of the calorimeter trigger, have been used. The sharp peak at 235 MeV in the distribution of the momentum of the secondary track in the kaon reference frame, is the clear signature of the $K^+ \rightarrow \mu^+ \nu$ decay, which is used to select the signal sample. The residual background in this sample is represented by the decays with a π^0 in the final state. A background spectrum has been determined looking for a π^0 from the kaon decay vertex, and has been subtracted from the selected $K^+ \rightarrow \mu^+ \nu$ sample. The efficiency of the selection has been evaluated on a sample selected using only the calorimeter information. The statistical error of the measurement is at the 0.1% level while the systematics is going to be finalized.

Also the decay $K^+ \rightarrow \pi^+ \pi^0$ is under study. The measurement of the absolute branching ratio has been performed selecting events tagged by a $K^- \rightarrow \mu^- \nu$ decay and fitting the momentum distribution of the secondary track in the kaon rest frame. The signature of the $K^+ \rightarrow \pi^+ \pi^0$ decay is the narrow peak at 205 MeV. The $K^+ \rightarrow \mu^+ \nu$ background contributions under the peak have been evaluated on data using the independent calorimeter information, while the K_{l3}^+ distribution comes from the Monte Carlo simulation. The reconstruction efficiency of the tracker has been evaluated on data using the calorimeter information. The systematic and background sources and their impact on the measurements are under study.

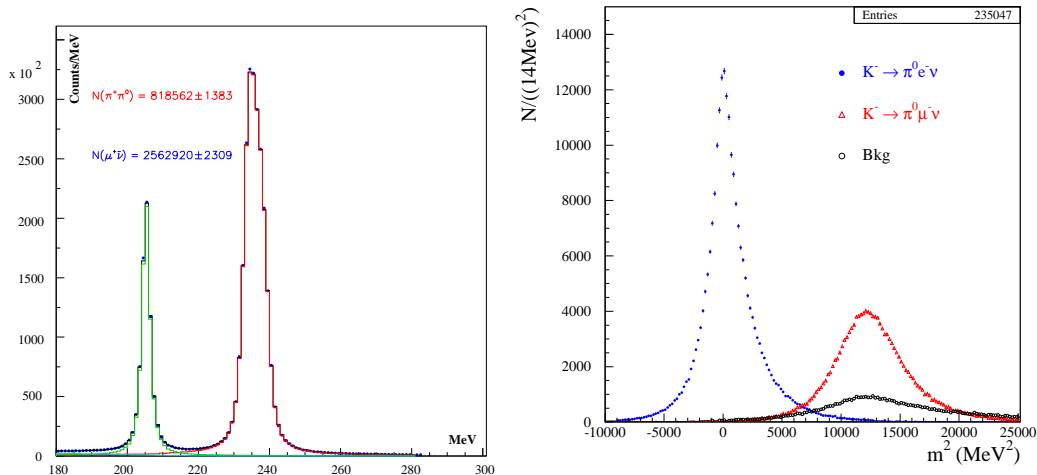


Figure 3: **Left:** Distribution of the momentum of the secondary track in the charged kaon reference frame. **Right:** The m^2 distribution for $K^\pm \rightarrow \pi^0 e^\pm \nu$, $K^\pm \rightarrow \pi^0 \mu^\pm \nu$ and background, at the end of the selection of K_{l3}^\pm decays.

3.5 Measurement of the branching ratio for the decay $K^\pm \rightarrow \pi^\pm \pi^0 \pi^0$

Recently there has been a renewed interest in the three pion decays of charged kaon. Because of the small energy available in the reaction, $k \rightarrow 3\pi$ is an ideal process where to apply the notion of the Goldstone-boson nature of the pseudoscalar mesons, by testing the prediction obtained from the chiral lagrangian realization of the $\Delta S = 1$ weak interaction.

The absolute branching ratio $\text{BR}(K^\pm \rightarrow \pi^\pm \pi^0 \pi^0)$ has been measured, using 187 pb^{-1} of data for the counting; the rest of the acquired statistics has been used for the determination of the signal efficiency and for other systematic studies. The result $\text{BR}(K^\pm \rightarrow \pi^\pm \pi^0 \pi^0) = (1.763 \pm 0.013_{stat} \pm 0.022_{syst}) \times 10^{-2}$ has been published¹⁹⁾. The dalitz plot parameters g , h , and k have also been measured, obtaining preliminary values significantly more precise than those reported in the literature.

Besides the measurement of the ratio $\text{BR}(K^\pm \rightarrow \pi^0 \pi^0 e^\pm \nu) / \text{BR}(K^\pm \rightarrow \pi^\pm \pi^0 \pi^0)$ is under study. Given the good precision of the value of $\text{BR}(K^\pm \rightarrow \pi^\pm \pi^0 \pi^0)$, the measurement of this ratio allows a new estimation of $\text{BR}(K^\pm \rightarrow \pi^0 \pi^0 e^\pm \nu)$. The study of the decay $K^\pm \rightarrow \pi^0 \pi^0 e^\pm \nu$ is important to extract information on the low-energy $\pi\pi$ interaction²⁰⁾.

4 ϕ decays and not resonant processes

4.1 Pseudoscalar mesons

DAΦNE, through the radiative decay $\phi \rightarrow \eta\gamma$, is a high luminosity and clean η factory. The total KLOE integrated luminosity ($\sim 1 \text{ fb}^{-1}$) corresponds to $\sim 4 \times 10^7$ η mesons produced and the monochromatic radiative photon (373 MeV) can be used to tag the η .

The 450 pb^{-1} of the 2001/2002 data taking have been reconstructed and used to perform a complete study of the dynamic of the $\eta \rightarrow \pi^+ \pi^- \pi^0$ and $\eta \rightarrow \pi^0 \pi^0 \pi^0$ decays through a Dalitz plot analysis.²¹⁾

Another interesting and rare η decay is $\eta \rightarrow \pi^0 \gamma \gamma$, whose branching ratio (BR) can be predicted using Chiral Perturbation Theory (ChPT). All previous measurements were done at hadron machines, using mainly $\pi^- p \rightarrow \eta n$. The value of the BR has decreased of three order of magnitude in the last 40 years, due to the improved separation of the $\eta \rightarrow \pi^0 \pi^0 \pi^0$ background. KLOE performs this measurement in a clean environment, with different background topologies and experimental systematics. The preliminary results obtained fitting the η invariant mass spectrum (Fig. 4) gives a BR in agreement with $\mathcal{O}(p^6)$ ChPT calculations, with a statistical error which is three times smaller than the best previous measurement.

Furthermore, the C violating decay $\eta \rightarrow \gamma \gamma \gamma$ and the P/CP violating decay $\eta \rightarrow \pi^+ \pi^-$ have been searched for. ^{23, 24)} For both decays the KLOE sensitivity significantly improves the previous experiments. The measured upper limits at 90% C.L. are:

$$\text{BR}(\eta \rightarrow \gamma \gamma \gamma) \leq 1.6 \times 10^{-5} \quad \text{and} \quad \text{BR}(\eta \rightarrow \pi^+ \pi^-) < 1.3 \times 10^{-5}.$$

The ratio $R = \frac{\text{BR}(\phi \rightarrow \eta' \gamma)}{\text{BR}(\phi \rightarrow \eta \gamma)}$ have been measured using for the η' the two charged and three neutral pions final state. No background with a similar topology is expected in KLOE. By normalizing to the number of $\eta \rightarrow \pi^0 \pi^0 \pi^0$ decays, we obtain the preliminary result ²¹⁾ $R = (4.9 \pm 0.1_{\text{stat}} \pm 0.2_{\text{syst}}) \times 10^{-3}$, which significantly improves our previous measurement. ²²⁾

4.2 Scalar mesons

A complete study of the radiative decay of the ϕ to the scalar mesons $f_0(980)$ and $a_0(980)$ is in progress involving the decays $f_0 \rightarrow \pi^+ \pi^- / \pi^0 \pi^0$ and $a_0 \rightarrow \eta \pi^0$, with $\eta \rightarrow \gamma \gamma$ and $\eta \rightarrow \pi^+ \pi^- \pi^0$. Since the mass spectra are sensitive to the nature of such mesons, which is still unclear, the data are compared with several models based on different approaches, considering also the interference with the backgrounds. For the $\pi^+ \pi^- \gamma$ final state there is a huge irreducible background due to initial state radiation (ISR) and final state radiation (FSR) (Fig. 5.left). A forward-backward asymmetry $A = \frac{N^+(\theta > 90^\circ) - N^+(\theta < 90^\circ)}{N^+(\theta > 90^\circ) + N^+(\theta < 90^\circ)}$ is expected due to the interference of FSR and ISR. ²⁵⁾ Fig. 5.right shows this asymmetry as a function of $M_{\pi\pi}$, compared with the theoretical prediction. A clear deviation is observed in the f_0 region and in the mass range below 700 MeV.

4.3 $e^+e^- \rightarrow \pi^+ \pi^- \gamma$

With the method of radiative return, the cross section of the process $e^+e^- \rightarrow \pi^+ \pi^-$ has been obtained in the center of mass energy range $0.35 < s_\pi < 0.95 \text{ GeV}^2$. This allow to get an estimate of the hadronic contribution to the muon anomaly with a very good accuracy. The resulting value is: ²⁷⁾

$$a_\mu^{\pi\pi}(0.35, 0.95) = (388.7 \pm 0.8_{\text{stat}} \pm 3.5_{\text{syst}} \pm 3.5_{\text{th}}) \times 10^{-10}. \quad (1)$$

This measurement confirms the discrepancy between the a_μ evaluation obtained using e^+e^- and τ data, ^{28, 29)} and the 2.7 standard deviation difference with the experimental measurement of a_μ . ³⁰⁾

Future improvement are expected from this measurement both from the experimental and theoretical point of view, by using data with more stable background conditions and improved Montecarlo generators which are expected to be available in the near future.

4.4 Leptonic widths

Using the $e^+e^- \rightarrow e^+e^-$ and $e^+e^- \rightarrow \mu^+\mu^-$ data from the 2002 energy scan, the ϕ meson leptonic widths Γ_{ee} , $\sqrt{\Gamma_{ee}\Gamma_{\mu\mu}}$ have been measured. ²⁶⁾ The results are compatible with $\Gamma_{ee} = \Gamma_{\mu\mu}$,

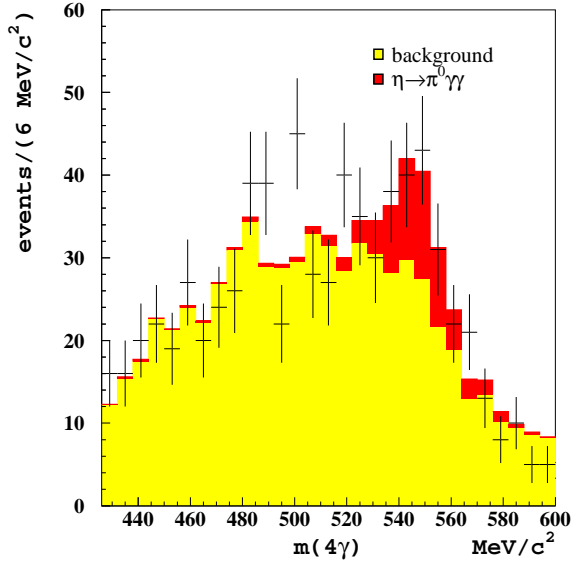


Figure 4: $\eta \rightarrow \pi^0 \gamma \gamma$: η invariant mass obtained with 2001-2002 data (+). In yellow and red the expected quantity of background and signal after a fit to the mass shape are shown.

providing a precise test of lepton universality. Combining the two measurements, the leptonic width turns to be: $\Gamma_{ll} = (1.320 \pm 0.017_{\text{stat}} \pm 0.015_{\text{syst}})$ keV.

4.5 $e^+e^- \rightarrow \omega \pi^0$

The cross section of the process $e^+e^- \rightarrow \omega \pi^0$ in the region around the ϕ resonance energy has been measured and the analysis is in progress to extract the $\phi \rightarrow \omega \pi^0$ branching ratio that shows up as an interference pattern in the cross section as a function of the center of mass energy.

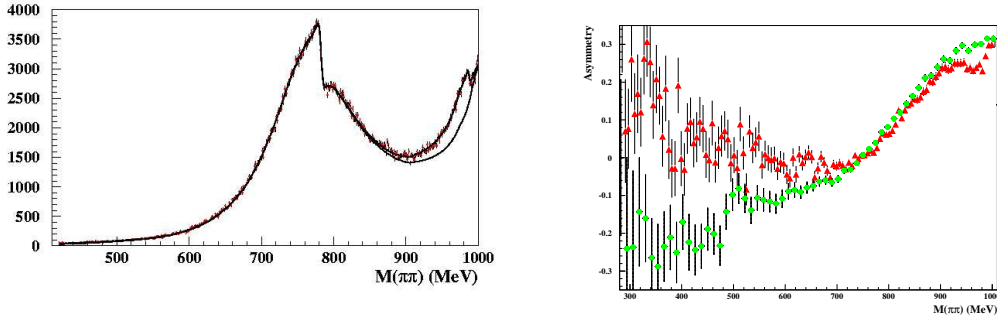


Figure 5: Left: invariant mass of $\pi^+ \pi^-$ for $\pi^+ \pi^- \gamma$ events. The upper/lower curves are the results of the fit and the contribution of ISR+FSR+ $\rho\pi$ respectively. Right: Forward-backward asymmetry as a function of $M_{\pi\pi}$. Experimental data are reported in red while green dots are the Montecarlo expectations based on FRS and ISR.

5 KLOE papers in 2004

- A. Aloisio *et al.*, “Measurement of the branching ratio for the decay $K^\pm \rightarrow \pi^\pm \pi^0 \pi^0$ with the KLOE detector”, Phys.Lett. **B597** (2) 139-144 (2004).
- A. Aloisio *et al.*, “Upper limit on the $\eta \rightarrow 3\gamma$ branching ratio with the KLOE detector”, Phys.Lett. **B591** (1-2) 49-54 (2004).
- A. Aloisio *et al.*, “The hadronic cross section measurement at KLOE”, Nucl.Phys.**B** Proc.Suppl. **131**, 75-81 (2004).
- A. Aloisio *et al.*, “Measurement of the phi meson radiative decays into scalar and pseudoscalar mesons with the KLOE detector”, Nucl.Phys.**B** Proc.Suppl. **126**, 199-203 (2004).
- A. Aloisio *et al.*, “Measurement of the $e(+)\bar{e}(-)$ hadronic cross section at DAFNE via radiative return”, Nucl.Phys.**B** proc.Suppl. **126**, 335-340 (2004).
- A. Aloisio *et al.*, “Measurement of the branching ratio for the decay $K_S \rightarrow \pi^\pm e^\mp \bar{\nu}(\nu)$ with the KLOE Detector”, contributed paper to the 32nd International Conference on High Energy Physics ICHEP, 16-22 August 2004, Beijing, China, paper number 8-0811.
- A. Aloisio *et al.*, “Preliminary measurement of the Dominant K_L Absolute Branching ratios, the K_L Lifetime, and V_{us} with the KLOE Detector”, contributed paper to the 32nd International Conference on High Energy Physics ICHEP, 16-22 August 2004, Beijing, China, paper number 8-0813.
- A. Aloisio *et al.*, “A direct search for $K_S \rightarrow 3\pi^0$ with the KLOE Detector at DAFNE”, contributed paper to the 32nd International Conference on High Energy Physics ICHEP, 16-22 August 2004, Beijing, China, paper number 8-0811.

6 Talks by LNF authors in 2004

- M. Antonelli, “Results from KLOE”, 12 Feb 2004, Euridice meeting, Vienna.
- T. Spadaro, “Recent results from KLOE at DAFNE”, 29 Feb 2004, Les rencontres de Physique de la vallee d’aoste, La Thuile.
- S. Miscetti, “Highlights from the KLOE experiment at DAFNE”, 21 Mar 2004, 39th Rencontre de Moriond: Electroweak Interactions and unified Theories, La Thuile.
- T. Spadaro, “Response of the KLOE calorimeter to low energy particles”, 29 Mar 2004, 11th International conference on calorimetry in high energy, Perugia.
- B. Sciascia, “Recent results from KLOE at DAFNE”, 14 Apr 2004, Incontri di fisica delle alte energie IFAE 2004, Torino.
- M. Moulson, “Kaon physics with KLOE”, 13 May 2004, Workshop on future kaon experiments at AGS, Brookhaven.
- E. De Lucia, “Recent results on kaon physics from KLOE”, 12 May 2004, From zero to Z0, Fermilab.
- M. Martini, “A direct search for $K_S \rightarrow 3\pi^0$ at KLOE”, 20 May 2004, LNF spring school.
- A. Antonelli, “Vus from K_0 semileptonic decays at KLOE”, 2 Jun 2004, Heavy quarks and leptons 04, Portorico.
- G. Lanfranchi, “Recent results from KLOE at DAFNE”, 8 Jun 2004, Meson 2004, Crakow.
- M. Martini, “A direct search for $K_S \rightarrow 3\pi^0$ at KLOE”, 7 Jun 2004, DAFNE 2004.
- M. Antonelli, “Vus and rare KS decays from KLOE”, 5 Aug 2004, VietNam 2004.

- P. de Simone, “Recent results from KLOE at DAFNE”, 30 Aug 2004, Hadron structure 2004, Smolenice Castle.
- V. Patera, “Rare kaon decays and CP, TCP violation”, 16 Aug 2004, ICHEP04, Beijing.
- M. Antonelli, “Vus and rare KS decays from KLOE”, 16 Aug 2004, ICHEP04, Beijing.
- G. Venanzoni, “The hadronic cross section measurement at KLOE”. 16 Aug 2004, ICHEP04, Beijing.
- S. Giovannella, “Status of $f^0 \rightarrow \pi^0\pi^0$ at KLOE”, 1 Sep 2004, Euridice meeting, Barcelona.
- S. Dell’Agnello, “Physics results of KLOE at DAFNE”, 24 Sep 2004, SIF 2004, Brescia.
- F. Bossi, “Other recent kaon decays results”, 8 Oct 2004, FPCP, Daegu, Korea.

References

1. A. Angelopoulos, *et al.*, Phys. Lett. **B444** (1998) 38.
2. A. Alavi-Harati, *et al.*, Phys. Rev. Lett. **88** (2002) 181601, hep-ex/0202016.
3. R. Wanke, New Results on Kaon Decays from NA48, in: Proceedings of the 38th Rencontres de Moriond on Electroweak Interactions and Unified Theories Les Arcs, Savoie, France March 15-22, 2003, 2003, p. 6, hep-ex/0305059.
4. A. Aloisio, *et al.*, Measurement of the branching ratio for the decay $K_S \rightarrow \pi^\pm e^\mp \bar{\nu}(\nu)$ with the KLOE Detector Contributed paper to the 32nd International Conference on High Energy Physics ICHEP, 16-22 August 2004, Beijing, China, paper number 8-0811. <http://ichep04.ihep.ac.cn/papers.htm>
5. S. Eidelman, *et al.*, Review of Particle Physics, Physics Letters **B 592**. <http://pdg.lbl.gov>
6. T. Alexopoulos, *et al.*, hep-ex/0406002 Submitted to Phys.Rev. **D**.
7. A. Aloisio, *et al.*, Preliminary measurement of the Dominant K_L Absolute Branching ratios, the K_L Lifetime, and V_{us} with the KLOE Detector Contributed paper to the 32nd International Conference on High Energy Physics ICHEP, 16-22 August 2004, Beijing, China, paper number 8-0813. <http://ichep04.ihep.ac.cn/papers.htm>
8. A. Czarnecki, W. J. Marciano, A. Sirlin hep-ph/0406324.
9. H. Leutwyler, M. Roos, Z. Phys. **C25** (1984) 91.
10. D. Becirevic, *et al.*, hep-ph/0403217.
11. A. Alavi-Harati, *et al.*, hep-ex/0406002.
12. A. Aloisio, *et al.*, A direct search for $K_S \rightarrow 3\pi^0$ with the KLOE Detector at DAFNE Contributed paper to the 32nd International Conference on High Energy Physics ICHEP, 16-22 August 2004, Beijing, China, paper number 8-0811. <http://ichep04.ihep.ac.cn/papers.htm>
13. R. R. Bertlmann, *et al.*, Phys. Rev. **D 60** (1999) 114032.
14. Among the others: M. Battaglia *et al.*, “The CKM matrix and the unitarity triangle”, hep-ph/0304132.
15. W.J.Marciano, arXiv:hep-ph/0402299. A.Czarnecki, W.J.Marciano, and A.Sirlin, arXiv:hep-ph/0406324.
16. C. Gatti, “MC generators for radiative kaon decays”, KLOE memo 290.
17. Particle Data Group 2004, S. Eidelman *et al.*, Phys. Lett. **B 592** (2004).

18. E. De Lucia and R. Versaci “Measurement of the branching ratio of the $K^+ \rightarrow \mu\nu\gamma$ decay”, KLOE memo 300.
19. the KLOE Collaboration, “Measurement of the branching ratio for the decay $K^\pm \rightarrow \pi^\pm\pi^0\pi^0$ with the KLOE detector”, Phys. Lett. **B 597** (2004) 139–144, hep-ex/0307054.
20. G. Colangelo, M. Knecht, and J. Stern, “Pais-Treiman method $\pi\pi$ phase shifts in K_{e4} decays”, The Second DafΦne Physics Handbook, Edited L. Maiani, G. Pancheri and N. Paver, INFN LNF (1995), 405.
21. The KLOE Collaboration, Proc. of the 32nd International Conference on High Energy Physics (ICHEP04), Beijing, China, 16-22 August 2004.
22. The KLOE Collaboration, Phys. Lett. **B 541** (2002) 45.
23. The KLOE Collaboration, Phys. Lett. **B 591** (2004) 49.
24. The KLOE Collaboration, hep-ex/0411030, accepted by Phys. Lett. **B**.
25. S. Binner, J. H. Kuhn, K. Melnikov, Phys. Lett. **B 459** (1999) 279
26. The KLOE Collaboration, hep-ex/0411082, accepted by Phys. Lett. **B**.
27. The KLOE Collaboration, hep-ex/0407048, accepted by Phys. Lett. **B**.
28. R. Akhmeshin *et al.*, Phys. Lett. **B 527** (2002) 161.
29. M. Davier *et al.*, Eur. Phys. J. **C 27** (2003) 492.
30. H. N. Brown *et al.*, Phys. Rev. Lett. **86** (2001) 2227.

LHCb

M. Alfonsi (Bors.), M. Anelli (Tecn.), G. Bencivenni, C. Bloise, F. Bossi, P. Campana, G. Capon, M. Carletti (Tecn.), P. Ciambrone, P. de Simone, C. Forti, A. Franceschi, G. Lanfranchi, F. Murtas, V. Patera (Ass.), M. Poli Lener (Dott.), R. Rosellini (Tecn.), M. Santoni (Tecn.), A. Saputi (Tecn.), A. Sarti (Dott.), A. Sciubba (Resp. Ass.)

In collaboration with the “Servizio di Automazione”:
U. Denni, M.A. Frani

In collaboration with the “Servizio di Elettronica”:
A. Balla, F. Bertino, G. Corradi,
G. Felici, G. Paoluzzi, G. Papalino

1 Introduction

The LNF group of LHCb operates on the **muon subdetector** with responsibilities on detectors (MWPC and GEM), electronics and mechanics. The detector production started in autumn 2003 and is expected to be completed within three years. The electronics production will start in 2005.

2 Multiwire Proportional Chambers

LHCb-LNF has the responsibility for the construction of $\sim 1/4$ of the MWPCs of the muon detector. Depending on the position inside the detector, there are different chamber dimensions with different readout: anode pads, cathode pads, anode & cathode pads.

We designed, collaborating with the Ferrara group, all the details of 10 different chambers types (with active dimensions ranging from $29 \times 35 \text{ cm}^2$ to $31 \times 151 \text{ cm}^2$). With these characteristics 292 chambers will be assembled and tested in LNF. The same design is applied to the remaining 1170 chambers that will be built in Ferrara, Firenze, CERN and S.Petersbourg.

2.1 Brief description of MWPC

The MWPC chambers of the LHCb muon detector must fulfill stringent requirements on time response: for triggering purpose $\sim 99\%$ minimum efficiency must be exploited in 20 ns. Each chamber is constituted by four layers assembled as two independent bigaps with hardwired-OR of the readout. In each 5 mm gap there are 30 microns gold-plated tungsten wires stretched at about 65 grams with a pitch of 2 mm. The filling mixture is Ar/CO₂/CF₄ (40/40/20).

2.2 Main goals reached in 2004

STATUS OF PRODUCTION

In autumn 2003, we started the production of chambers for the region M3R3 of the Muon System. We have built 56 usable chambers. The chambers needed in the Muon System are 48, the eight additional chambers are spare detectors. Two of them have been tested at CERN PS in October 2003 ¹⁾, one has been tested at the CERN GIF (see below).

In October 2004 we started the production of the M5R3 chambers. At present, we have already assembled 33 chambers. The production is expected to be completed (48 chambers plus 4 spare) in April 2005.

CHAMBER QUALITY CONTROL

All the chambers built are expected to pass successfully three main tests:

- Test of gas tightness: the chamber is inflated at an overpressure of 5 mbar and the pressure drop ΔP is measured as a function of time. The requirement is $\Delta P < 2$ mbar/hour.
- HV training: the chamber is slowly conditioned and is required to reach at least 2.85 kV of high voltage, drawing a negligible dark current.
- Test of gap gain uniformity: the gain fluctuation of each double-gap detector must be compatible with the plateau width measured at test beams (see below).

All the chambers tested up to now (56 M3R3 and 27 M5R3) satisfy the requirements on gas tightness and dark current ($< \text{nA/gap}$ at 2.85 kV).

Uniformity of the gap gain is tested with a 40 mCi ^{137}Cs source. The current drawn by each gap is monitored while the lead case containing the source is moved by means of a mechanical arm over the chamber surface. These measurements allow to check the gain uniformity within each gap and to compare different chambers among them. This system and the control software were designed and realized by the LHCb Rome-1 group.

Since each pair of adjacent gaps is hardware OR-ed into one Front End chip, the four-gap chamber can be considered as a couple of two independent double-gap detectors. For each double-gap of each chamber tested, we measured the spread of the current with respect to the average current of all double-gaps. In order to have the area of all the double-gaps inside the plateau the gap gain disuniformity translated in voltage should be lower than ± 80 V.

In Fig. 1 we plot the current factor, i.e. the current in each double-gap normalised to the average current in all double-gaps. The error bars are obtained from the minimum and the maximum currents. Each double-gap is classified according to:

- Class A: all measurements $I(i)$ are in the range $\langle I \rangle / 1.4 < I(i) < \langle I \rangle \times 1.4$, corresponding to ± 50 V;
- Class B: all measurements $I(i)$ are in the range $\langle I \rangle / 1.7 < I(i) < \langle I \rangle \times 1.7$, corresponding to ± 80 V;
- Class C: requirement B is not satisfied.

A four-gap chamber is then classified as:

- GOOD: at least one double-gap is of class A, the second one is of class A or B;
- RESERVE: both double-gaps are of class B;
- REJECTED: at least one double-gap is of class C.

Over 56 M3R3 chambers, 52 are GOOD and four are RESERVE; over 27 M5R3 chambers, 26 are GOOD and one is a RESERVE.

CHAMBER TEST AT CERN GIF FACILITY

In July 2004 we have tested one M3R3 chamber at the Gamma Irradiation Facility at CERN ²⁾. This was the first test of a chamber equipped with the final front end electronics.

The goal of the test was to study the performance of the detector in presence of a high particle rate produced, at GIF, by the photon flux from the ^{137}Cs source. In particular, we aimed to measure the consequences on chamber performance of the electronics dead-time and of space-charge effect.

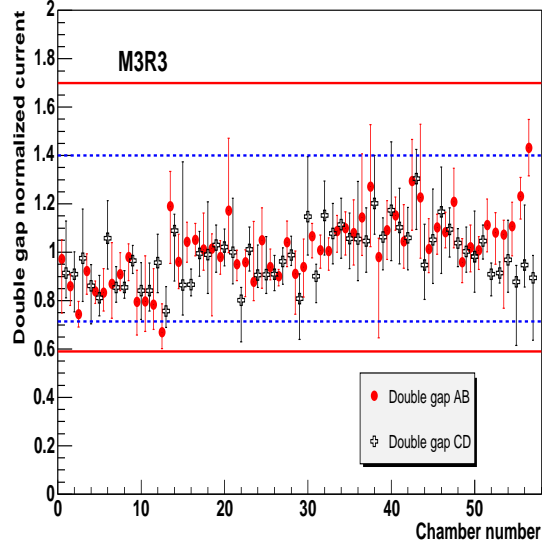


Figure 1: Left: average current in each double-gap of M3R3 chambers, normalised to the average of all double-gaps. The error bars are obtained from the minimum and the maximum currents. Right: same as in Left plot, for M5R3 chambers.

The chamber efficiency and time resolution were measured in presence of the X5 muon beam ($E_\mu \sim 100$ GeV) varying, by means of filters, the intensity of the γ flux reaching the detector.

The requirement fixed in TDR^{3, 4)} is to have for each station working at $> 99\%$ efficiency in 20 ns time window and an average number of pad-hit less than 1.2.

In Fig.(2,left) we show the efficiency of the four-gap detector, as a function of the high voltage, in different background rate conditions. The efficiency measurements obtained with source ON (without filters) have been corrected for the expected efficiency loss due to electronics dead-time. The results are shown in Fig.(2,right): after the correction the two curves (with/without source) are almost superimposed. The four-gap chamber reaches the 99% in 20 ns time window already at 2.55 kV (about 100 V below the working point). We can conclude that up to a γ rate of 10 kHz/cm² (70% of the M2R1 rate/cm²) there is no visible space-charge effect on the efficiency and time performance.

3 Triple GEM detectors for M1R1

For the innermost part (regions R1, $\sim 0.6\text{m}^2$ area) of the first muon station (M1) of the LHCb experiment the LNF group, in collaboration with INFN-Cagliari, proposes a detector based on Gas Electron Multiplier (GEM) technology. The requirements³⁾ for detectors in M1R1 are: a rate capability of ~ 500 kHz/cm²; each station must have an efficiency of $\sim 96\%$ in a 20 ns time window (two independent detector layers per station, logically OR-ed, are foreseen); a cluster size, i.e. the number of adjacent detector pads fired when a track crosses the detector, should not be larger than 1.2, for a 10×25 mm² pad size. In addition the detector must tolerate, without damages or large performance losses, an integrated charge of ~ 0.88 C/cm² in 10 years of operation at a

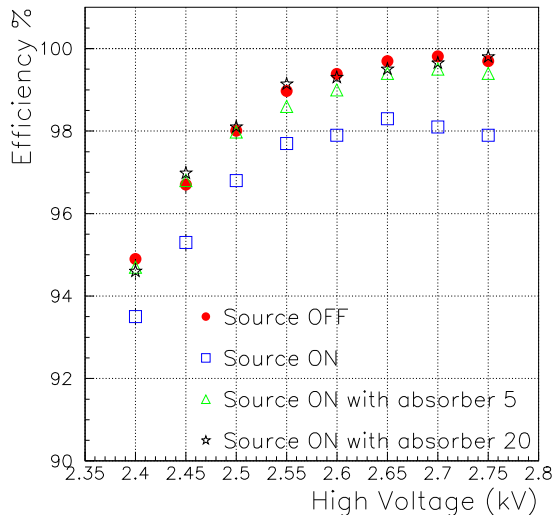


Figure 2: Left: efficiency of the four-gap detector as a function of the high voltage, for several absorption factors of the γ filter. Right: efficiency with source ON (without filter) corrected for the effect of the expected electronics dead-time.

gain of $\sim 6 \times 10^3$ and an average particle flux of 184 kHz/cm^2 , for an average machine luminosity of $2 \times 10^{32} \text{ cm}^{-2} \text{ s}^{-1}$.

The GEM⁵⁾ consists of a thin ($50 \mu\text{m}$) kapton foil, copper clad on each side, chemically perforated by a high density of holes having bi-conical structure, with external (internal) diameter of $70 \mu\text{m}$ ($50 \mu\text{m}$) and a pitch of $140 \mu\text{m}$. In safe condition, gains up to 10^4 are reachable using multiple structures, realized assembling more than one GEM at close distance one to each other.

After a long period of R&D, spent to qualify the GEMs as detectors suitable for the intense and radioactive environment around the beam pipe of LHCb, we chosed to operate the detector with the $\text{Ar}/\text{CO}_2/\text{CF}_4(45/15/40)$ gas mixture with an overall gain of ~ 8000 (see the activity report of the 2003 for details).

In the 2004 the major effort was to finalize the detector and the construction tools design as well as the definition of the chamber quality controls and the preparation of the production site.

The detector mechanics was completely revised in order to fit with the very stringent space requirements in M1R1. The first prototypes of PCB panels, realized with honeycomb, have been built (Fig. 3): their planarity, measured with a 3D-machine, comes out to be better than $50 \mu\text{m}$.

The whole assembly procedure has been defined in each single step:

- GEM foils are preliminary tested with high voltage in order to check their quality. The test, for each of the six sectors in which the foil is divided, is performed in a gas tight box, Fig. 4, flushed with nitrogen in order to reduce the relative humidity at less than 5%. The voltage to each sector is applied through a $500 \text{ M}\Omega$ limiting resistor to avoid GEM damages in case of discharges. The acceptance requirements is a maximum leakage current $< 1 \text{ nA}$ (on each sector) at 600 V .
- Frames, made of FR4, are visual inspected and broken fibers carefully removed. Frames and

all the FR4 components are then cleaned in a ultrasonic bath, Fig. 5, and successively dried in a oven at 80°C for 12 hours.

- GEM foils that pass the HV test, are stretched with a specific tool (Fig. 6). The GEM foil is clamped with jaws equipped with plastic O-ring. The mechanical tension (18 kg/jaw, two jaws per side) applied at the edge of the foil is monitored with gauge-meters. Then the frame is glued on the stretched GEM foil using the Araldite 2012: good electrical behaviour, suitable handling properties (work life: 5min, curing time: 2 h) and aging tested by us during the Casaccia test ⁶). For each chamber three GEM foil are framed (with frames thick 1,2 and 3 mm) following the above procedure, Fig. 7.
- The three framed GEMs are glued with the right sequence (3 mm frame, then 1 mm and 2 mm) on the top of the cathode PCB, Fig. 8. The chamber is finally closed gluing the last 1 mm (bare) frame and the pad PCB. This assembly operation is performed on a machined Al-alloy reference plane equipped with four reference pins. On the top of the whole sandwich a load of 80 kg is uniformly applied for 24h, as required for epoxy polimerization (Araldite AY103 + HD991 hardener).
- The chamber is then completed with the final soldering of the GEM HV connections to the cathode, and with the mounting of the gas connectors and tubes and the external faraday cage.

All construction operations are performed in the class 1000 clean room equipped for the construction of the detectors, Fig. 9.

The gas tightness of the chamber is tested inflating it with an overpressure of ~ 5 mbar. The gas leak rate is obtained by the comparison of the differential pressure drop of the chamber with the result of the same measurement performed in parallel on a chamber with negligible gas leak: less than 1mbar/day (so called reference chamber). A gas leak of the order of a few mbar/day, Fig. 10, has been achieved, corresponding with a humidity level in the gas mixture (supply to the chamber in open mode, with a flow rate of 80 cc/min) of the order of 50 ppm per volume.

The gain uniformity of the chamber is performed with an X-ray gun facility, Fig. 11. The current signal induced on each pad (192 pads per chamber), is read-out with a 1 nA sensitivity current-meter and corrected for T and p variations. The water content and temperature of the gas mixture are monitored with the same probe mounted at the gas line outlet. The atmospheric pressure is monitored outside the gas line with a stand-alone probe. The chamber is mounted on an X-Y plane moved with computer controlled step-motors and the measurement is done automatically and takes about 12 hours. The measured gain uniformity Fig. 12 was better than 10% (6% excluding edge effects due to the finite diameter of the X-ray collimator, ~ 5 mm).

The global performances of the chamber have been finally measured at the T11-PS at CERN.

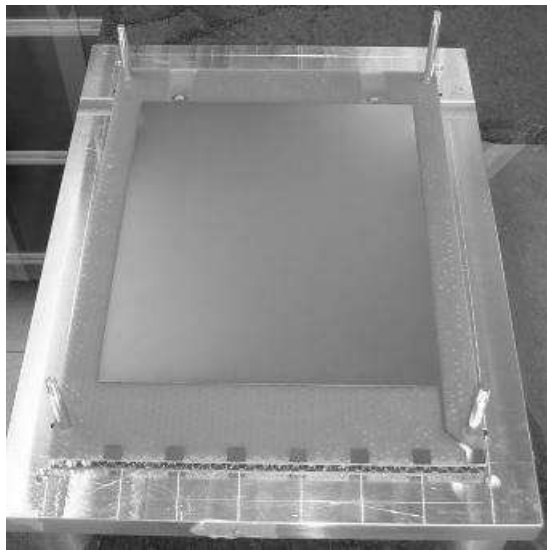


Figure 3: Prototype of the cathode PCB panel realized with honeycomb.

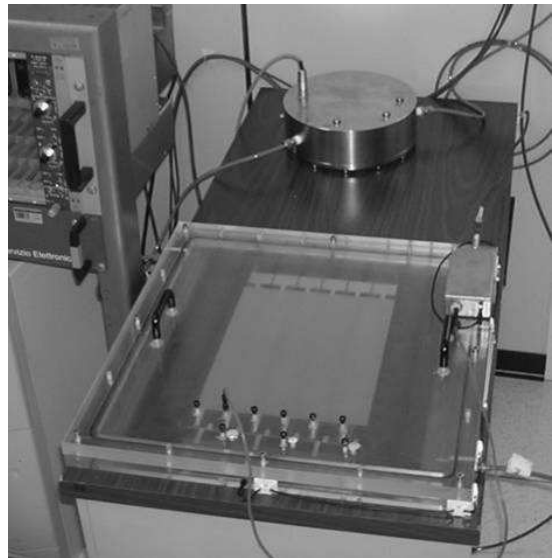


Figure 4: The gas tight plexiglass box used for the HV test of GEM foils.

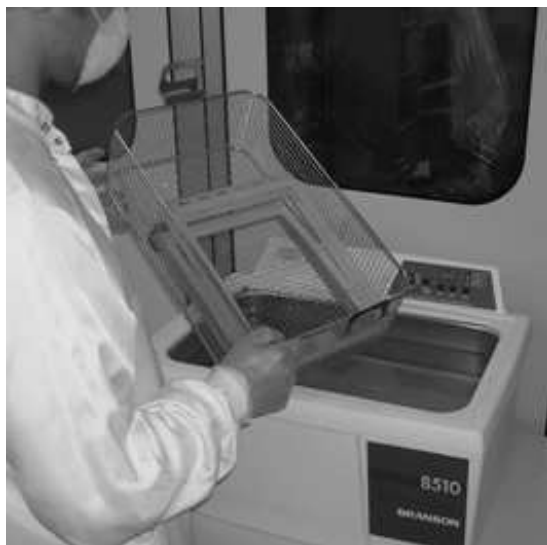


Figure 5: The ultrasonic bath used for the cleaning of frames and FR4 components.

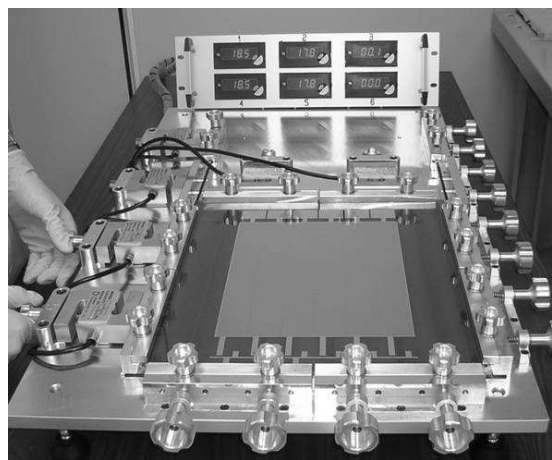


Figure 6: The GEM foil under stretching. The connections to the six sectors are visible.



Figure 7: The assembly of the framed GEM foils on top of the cathode PCB panel.

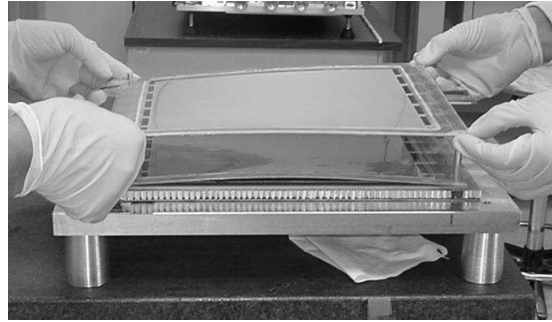


Figure 8: The framed GEMs are assembled on the cathode PCB with the right sequence (3mm, 1 mm, 2mm), facilitating with the reference pins.



Figure 9: View of the class 1000 clean room.

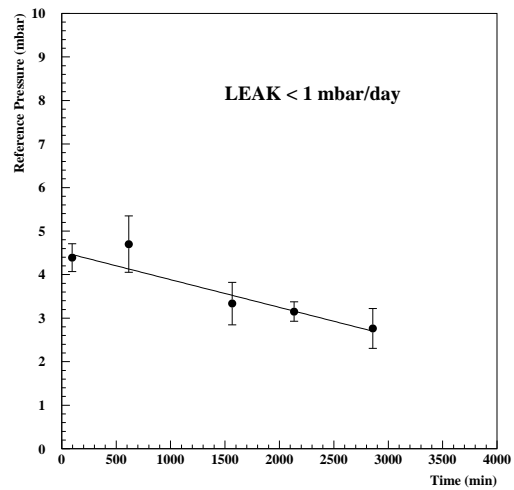


Figure 10: Measurement of the gas leak rate of a prototype chamber.

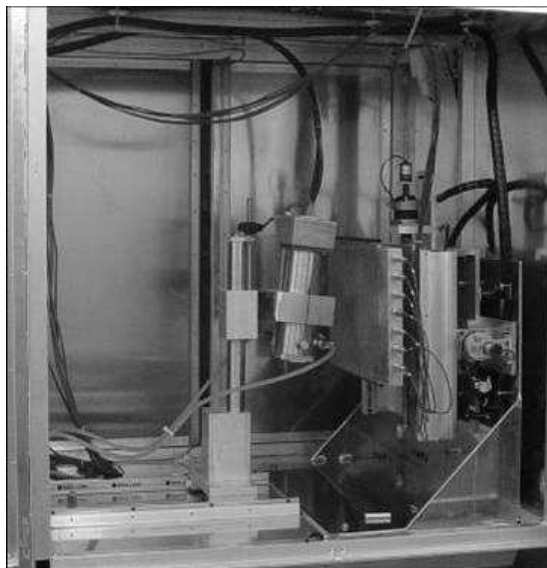


Figure 11: Picture of the X-ray gun facility used for the gain uniformity of the chambers.

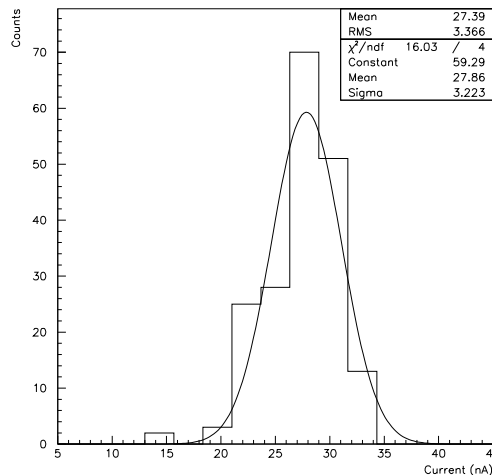


Figure 12: Distribution of the currents induced on the 192 pads of a chamber. The measurement show a gain uniformity better than 10%.

4 Electronics

The LHCb muon trigger architecture relies on 1248 *Trigger Sectors* (TS) built by the first stage of the front-end electronic chain. About 122,112 physical channels are firstly merged to generate about 26,000 logical channels both in the chamber front-end and in the *Intermediate Boards* (IB) system.

The IB system is used to merge part of the physical channels and is made of 176 boards. Each IB board can manage up to 192 LVDS input signals and 60 LVDS output signals. To minimize the number of boards (because the chamber/TS geometries we have 5 different IB I/O configurations) the logic functions have been implemented using programmable devices. That choice allowed us to design a single PCB to fit the whole detector geometry. The use of anti-fuse technology for programmable devices (we have used ACTEL devices) gives also an intrinsic robustness in moderate radiation environment (like the levels foreseen near the LHCb detector).

In the *Off Detector Electronics* (ODE) boards, the logical channels are then synchronized to the bunch crossing, arranged to implement the required TS, and, finally sent to the Level-0 (L0) trigger logic through 1248 optical links at 1.6 Gbit/s. The ODE board also provides a measure of signal arrival times with 1.5 ns time resolution and implements L0-pipelines, DAQ interface via a 1,6 Gbit/s optical link and ECS interface. Because the huge number of input channels per boards (192 LVDS) and the very strict requirements on timing performances for optical link connections (less than 100 ps peak to peak on clock jitter) the design of this board has been very challenging. To fully instrument the muon detector 148 ODE boards will be used.

A big effort was devoted to match the skew requirements, due to the huge number of I/O managed by the board. IB and ODE system use a passive *Transition Board* (TB) to arrange the different topologies of input logical channels and are hosted in a mechanical standard 7U VME crate with custom backplane. The backplane allows to interconnect IB and TB boards and to distribute low voltage (+2.5V and +3.3V) to the IB boards. The crate can hold up to 21 boards. Both IB and ODE systems are localized close to the detector to minimize the cables length, then

the boards must be implemented using radiation tolerant components.

During 2004 two fundamental tests were successfully performed: a full chain electronic test (including IB and ODE) with a fully instrumented chamber and the high speed data transmission from ODE to the L0 trigger and DAQ optical receivers. To measure the performance of the high speed serial links implemented on the ODE a dedicate instrumentation was provided that will be also used to qualify the final production.

Critical components (anti-fuse and flash based FPGA) were qualified under radiation at Louvain La Neuve irradiation facility with 70 MeV proton beam at a maximum fluence of 6×10^{11} p/cm².

The TB PCB have been produced in 2004 and are now being assembled. IB design and final prototype are ready; Actel FPGA are being re-designed to minimize skew effects. IB production will start and finish in 2005; ODE production will start in 2005 and will finish in 2006.

Besides the IB and ODE system the LNF group is also in charge for the low voltage system layout and for the on-chamber low voltage generation. Both projects have been finalized during 2004. However, due to the required radiation and magnetic field tolerances, the choice of the low voltage power supply is a general LHC community task. Given the positive answer of first prototypes, the production of the low voltage distribution boards on-chamber will start at the beginning of next year.

5 Chamber supporting structure

LHCb-LNF has the responsibility for the construction of the ten movable walls that will support the chambers in between the iron absorbers of the muon filter. The project was reviewed to reduce the overall cost of the mechanical structure. In particular, the old corrugated aluminium sandwich has been replaced by aluminium honeycomb panels with the drawback of an increased reliability of the structure. Detailed studies were performed on the mechanical characteristics of the raw material and of the components that will be used to assemble large walls starting from 2 m height honeycomb panels.

The re-drawing process finished and an integration review was done at CERN on the subject. Still some decision has to be taken about the procedure to align the chambers on the walls. Tendering process already started; the walls installation is foreseen for the end of 2005.

The chambers will be positioned on the wall over aluminium supports that will be attached to the wall by means of glue and rivets. A few kind of different supports were drawn to avoid interference during the opening and closing of the walls.

Each chamber is fixed to the support lying on two feet that allow positioning and blocking by means of screws and spacers. The final drawing is now being finalized after several iterations that considered the insertion of low voltage and high voltage connectors, filters on cables inside the foot.

The four corners of each chamber are then closed by a thin brass Faraday cage with several holes to allow the insertion of signal, controls and low voltage connectors on the front end boards.

After the successful electronic test given on a first prototype, the final drawings are being produced for all the WPC and GEM detectors.

In the meanwhile it is going on, together with the CERN group, the optimization of the dimensions and the positioning of the racks for the electronics and of the platforms around the detector since they must both move together with the supporting structure without interfere with some elements of the cryogenics and the RICH and the PS detectors. The adopted solution sees a unique structure per side that will move together the walls of stations M2 to M5. The electronics of station M1 will be housed in the tunnel under the RICH.

On M1 mechanical constraints for the routing of the cables (for signals, power supply and

pulse and control signals), and the gas piping and air cooling are more stringent; system integration is under continuous and progressing study.

6 List of Conference Talks by LNF Authors in Year 2004

- “Systems for the MWPC test at the LNF production site”, Poster presented at the IEEE 2004 (Rome, Italy, October 16-22, 2004), and submitted to Transaction on Nuclear Science.
- “Time Resolution and aging properties of the MWPCs for the LHCb Muon System”, presented by G. Lanfranchi at the Vienna Conference on Instrumentation 2004, Vienna, Austria, February 16-21,2004; Nucl. Instrum. Meth. **A535** (2004) 221.

The results of the R&D on triple-GEM detectors have been presented at the following conferences:

- “Fast triggering of high-rate charged particles with a triple-GEM detector”, Poster presented at the Vienna Conference on Instrumentation 2004, Vienna, Austria, February 16-21,2004.
- “Aging measurements on triple-GEM detectors operated with CF_4 -based gas mixtures”, presented by M. Alfonsi at the 9th Topical Seminar on Innovativa Particle and radiation Detectors, 23-26 May 2004, Siena, Italy.
- “Studies of etching effects on triple-GEM detectors operated with CF_4 -based gas mixtures”, presented by P. De Simone at the IEEE 2004 (Rome, Italy, October 16-22, 2004).

References

1. M. Anelli *et al.*, “Test of MWPC prototypes for Region 3 of Station 3 of the LHCb muon system”, Public Note LHCb MUON-2004-074.
<http://cdsweb.cern.ch/search.py?recid=793160&ln=en>
2. M. Anelli *et al.*, “Test of a MWPC for the LHCb Muon System at the Gamma Irradiation Facility at CERN”, Public Note LHCb MUON-2005-003.
<http://cdsweb.cern.ch/search.py?recid=815058&ln=en>
3. LHCb Collaboration, “LHCb: muon system technical design report”, CERN LHCC MUON 2001-010, LHCb TDR 4, 28 May 2001.
4. LHCb Collaboration, “LHCb: Addendum to muon system technical design report”, CERN LHCC MUON 2003-002, LHCb TDR 4 Addendum 1, 15 January 2003.
5. F. Sauli, Nucl. Instrum. Meth. **A386** (1997) 531.
6. M. Alfonsi *et al.*, “Studies of etching effects on triple-GEM detectors operated with CF_4 -based gas mixtures”, presented at IEEE conference (Oct 16-22, 2004, Rome) and submitted to Transaction on Nuclear Science.

ICARUS

G. Mannocchi (Ass.), M. Meli (Tecn.), L. Periale (Ass.), P. Picchi (Resp.),
M. Santoni (Tecn.), G. Satta (Ass.), G. Trincherro (Ass.)

1 Introduction

The year 2004 marked a very important step in the successful development of the ICARUS experiment with the first two 300 ton semi-modules finally installed at LNGS (see fig.1). During this period the *R&D* activity of the LNF group was devoted to the improvement of aspects of the ICARUS detector not yet fully matured. During the year 2005 we intend to continue the *R&D* on the two-phase (gas and liquid) Argon detector with the goal of WIMP's search.



Figure 1: *The first T300 ICARUS module entering Hall B at LNGS.*

2 Activity 2004

2.1 Liquid Argon *R&D*

Energy measurement and resolution in LAr highly improved with the simultaneous collection of ionization charge and scintillation light, being the two phenomena strongly correlated (through electron-ion recombination) and dependent on dE/dx .

We investigated how the addition of photo-dopant in LAr could be exploited to transform the scintillation VUV light into charge, thus linearizing the ionization collection response over a very

wide energy range (from few keV to several GeV). We also investigated the possibility to exploit the residual IR light (read through LAAPD) as a T=0 system for the LAr-TPC.

2.2 CsI photo-cathodes

We have demonstrated that gaseous detectors with CsI photo-cathodes can operate perfectly well at cryogenic temperatures up to 87K. In several tests the primary scintillation light from noble gases and liquids was detected simultaneously with a vacuum PM and gaseous detector with CsI photo-cathode and we observed that the last one had higher overall sensitivity and almost zero noise.

We also demonstrated that hole-type structures combined with CsI photo-cathodes could operate in pure noble gases at cryogenic temperatures. These preliminary results may open avenues for many applications of gaseous detectors with CsI photo-cathodes (let's call them "gaseous PM") including noble liquid TPC's such as WIMP detectors of ICARUS.

However, before implementing this new technique in real experiments, long-term tests are necessary to verify the time stability of this detectors. We believe that this could be done, in the near future, relatively fast and in a cost effective way with existing cryogenic equipments especially foreseen for these tests.

2.3 Liquid Argon TPC in Magnetic Field

Aim of this test is the discrimination of particle charge in LArTPC. The test, in preparation, is based on the 50 liters LArTPC and exploits coils and iron yokes available at CERN. In a first phase we intend to apply field up to 0.4 Tesla, just enough to compensate for multiple scattering effects. Such a value should allow to discriminate the charge of cosmic rays stopping muons in the 40 cm drift of the 50 liter LArTPC.

This 50 liter LArTPC has also been used for tests on the ICARUS DAQ (data compression) and on the new ICARUS trigger system boards.

3 Activity 2005

We will continue the activity of 2004 with the aim of demonstrating the possibility of implementing the results of our successful *R&D* in actual experiments.

References

1. S. Amoruso *et al.*, Nucl. Instr. and Meth. **A 516** (2004) 6879.
2. M. Antonello *et al.*, Nucl. Instr. and Meth. **A 516** (2004) 348363.
3. S. Amoruso *et al.*, Nucl. Instr. and Meth. **A 523** (2004) 275286.
4. S. Ameri *et al.*, Nucl. Instr. and Meth. **A 527** (2004) 329410.
5. L. Periale *et al.*, Nucl. Instr. and Meth. **A 533** (2004) 154158.

LARES

S. Dell’Agnello (Resp.), G. Delle Monache, M. A. Franceschi, A. Paolozzi (Ass.)

LARES is a satellite laser-ranging (SLR) experiment. This category of satellites carry on board numerous Cube Corner Reflectors (CCRs), which are used for tracking (“ranging”) their positions along their orbits. CCRs are special mirrors which always reflect an incoming light beam back in the direction it came from. The satellite ranging is achieved by shining from Earth multiple laser beams (each associated with a telescope for aiming at the satellite) managed by the International Laser Ranging Service (ILRS). The reflected laser beam is also observed with the telescope, providing a measurement of the round-trip distance between Earth and the satellite. A number of ranging experiments during the past three decades have provided important geodesy measurements, including the Earth Gravity Model (EGM) and its time variations.

The ancestor of the SLR technique was the Lunar Ranging RetroReflector (LRRR) Experiment deployed by the Apollo 11, 14 and 15 missions to the Moon (a similar device was on board of the Soviet Union *Lunokhod 2* lunar rover, in 1973). This is the only Apollo experiment that is still returning data from the Moon ¹⁾. The laser beam has a 7 Km diameter when it reaches the Moon and about 20 Km back to Earth. The Moon distance has been determined with an accuracy of 3 cm (the average Earth-Moon distance is 384,400 kilometers). The LRRR experiment improved the knowledge of ¹⁾: 1) the Moon’s orbit; 2) the rate at which the Moon is receding from Earth (currently 3.8 cm/yr); 3) variations in the rotation of the Moon; 4) changes of the Earth’s rotation rate; 5) the precession of the Earth spin axis (18.6-yr “nutation”). In addition, the LRRR data have been used to measure the De Sitter or “geodetic precession” ²⁾ predicted by GR to an accuracy of 0.35%. This shift arises from the effect of the gravitational field on the velocity of an orbiting gyroscope ³⁾.

GR also predicts that a rotating central body like Earth will drag the local space-time around it (*frame dragging*). This effect, predicted by Lense and Thirring (LT) in 1918, will cause the precession of the *node* of an artificial satellite of the Earth (the node, or nodal line, is the intersection of the Earth equatorial plane with the satellite orbit; see Fig. 1). Note that the LT precession is fundamentally different from the De Sitter precession: while the latter is basically due to the mass of the central non-rotating body, the former is a genuine rotation effect: currents of mass generate additional space-time curvature. This phenomenon is called gravitomagnetism for its close formal analogy with magnetism in electrodynamics ³⁾. The LT effect has been observed for the first time in 1998 ⁴⁾ using two laser-ranged satellites: LAGEOS (LAsER GEODynamics Satellite) (NASA), launched in 1976 with a Delta-2 rocket and LAGEOS II (NASA-ASI) launched in 1992 with the Space Shuttle. The LAGEOS orbits have a semi-major axis of about 12,000 Km and their LT node shift is just 33 mas/yr (mas = millisecond of arc), that is, 1.9 meter/yr ! With laser-ranging the LAGEOS position can be tracked with a mm-level accuracy and their orbits reconstructed with cm-level instrumental uncertainty. The measured value is in agreement with GR, with an error much larger than the ranging resolution, due to two non-gravitational perturbations (NGP): (1) the deviation of the EGM from the perfect $1/r$ behavior and (2) the thermal thrusts (TTs) that the satellites receive along their orbits. TTs have three basic sources: (i) the direct solar radiation pressure, (ii) the pressure from the solar radiation reflected by Earth (Earth UV albedo) and (iii) the IR radiation from Earth (Yarkovski-Rubincam effect, which dominates the error on LT).

The 2002 GRACE EGM and a re-analysys of the LAGEOS I/II data (Fig. 1, allowed a decrease of the LT uncertainty to $\sigma_{LT} \sim 10\%$. The 1998 result, based on older EMGs (JGM-3 and

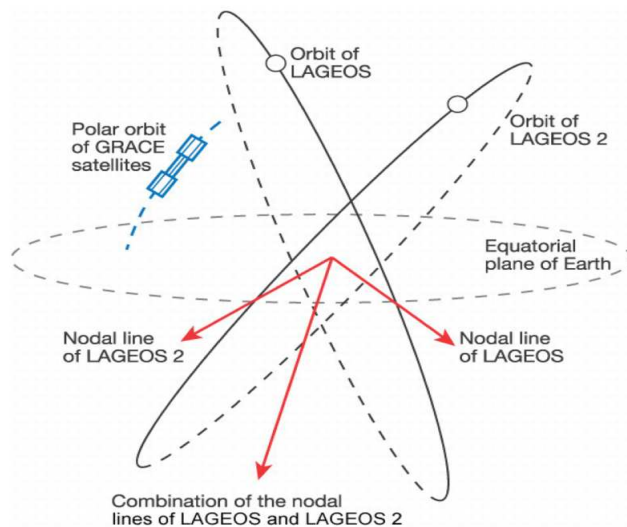


Figure 1: The LAGEOS orbits and nodal lines. The orbit of the two GRACE satellites.

EGM96), is considered to have $\sigma_{LT} \sim 20 - 40\%$ (and “not easy to be confidently assessed”³⁾).

A modern and improved version of the LAGEOS, called LARES/Weber-Sat, is being designed by a Collaboration of Italian and US Universities, the ILRS, INFN-LNF and INFN-Lecce. LARES (LAsER RELativity experiments) will measure LT at $\sigma_{LT} \leq 1\%$, taking advantage of the recent high-accuracy EGMs and exploiting a thorough geometrical, mechanical and thermal characterization of the satellite and, possibly, a new design to reduce TTs. The LNF group has been funded by INFN GR II to perform an R&D work to find a suited satellite structure to strongly suppress TTs and to estimate the residual TTs accurately. An additional physics goal of LARES is the improvement of the limits on the violation of the Einstein Equivalence Principle.

A strong suppressions of the TTs, which are nowadays the limiting NGP, opens the way to studying effects due to new physics on the orbital elements of LARES. For this purpose, perigee shifts are among the most sensitive observables. For example, a recent string-inspired brane model⁵⁾ might imply perigee shifts observable after 5 years of ranging data with LARES, if TTs are kept under control. This possibility is currently under study. Measuring such an effect for the Moon with Lunar ranging data requires at least a 20-fold improvement of ranging resolution⁵⁾ and is greatly complicated by the difficulty of knowing the Moon center of mass, while knowledge of the center of mass is extremely simplified for a spherical artificial satellite like LARES. Models like⁵⁾ are on a less firm theoretical ground than GR, but they are still very interesting, also because superstring theories are hoped to offer a way to the quantization of gravity.

References

1. [HTTP://www.lpi.usra.edu/expmoon/Apollo11/A11_Experiments_LRRR.html](http://www.lpi.usra.edu/expmoon/Apollo11/A11_Experiments_LRRR.html).
2. I. I. Shapiro, R. D. Reasenberg, J. F. Chandler, R. W. Babcock, Phys. Rev. Lett. **61**, 2643-2646 (1988).
3. I. Ciufolini, E. C. Pavlis, Nature, Vol 431, 21 October 2004. Ciufolini I. & Wheeler J. A., “Gravitation and Inertia” (Princeton Univ. Press, Princeton, NJ, 1995).
4. I. Ciufolini, E. C. Pavlis, F. Chieppa, E. Fernandes-Vieira, J. Perez-Mercader, Science, Vol 279, 27 March 1998.
5. G. Dvali, A. Gruzinov, and M. Zaldarriaga, Phys. Rev. D **68**, 024012 (2003).

NEMO

M. Cordelli, H. Roberto (Ass.), A. Martini, L. Trasatti (Resp.)

1 Activity

The NEMO project (construction of a kilometer cube detector for neutrino astronomy) has continued studying the properties of possible sites in the Mediterranean sea, and produced several instruments to study the marine depths. During the year 2004 the group has been preparing for the pilot project, NEMO Phase 1, which is proceeding toward the construction of two towers at the Catania Test Site.

The experiment includes groups from: INFN Bari, Bologna, Catania, Genova, LNF, LNS, Messina, Roma1.

The LNF group has completed a thorough revision of the project of NERONE, an instrument to measure with great accuracy the water transparency using measurements performed at several distances from the source. The alignment system in particular has been redesigned and tested. We are planning a series of deployments starting in the spring 2005. The group has also become involved in the console development for the NEMO Phase 1 project.

OPERA

F. Bersani Greggio (Ass.), C. Di Troia (Dott.),
B. Dulach, G. Felici, A. Franceschi, F. Grianti (Ass.), A. Gambarara (Tecn.),
A. Mengucci (Tecn.), T. Napolitano, A. Paoloni (Ass. Ric.), M. Spinetti (Resp.),
L. Terminiello (Ass.), F. Terranova, M. Ventura (Tecn.), L. Votano

in collaboration with

LNF-SEA: A. Balla, G. Corradi, U. Denni, A. Frani, G. Paoluzzi, G. Papalino
LNF-SPAS: A. Cecchetti, D. Orecchini
LNF-SSCR: G. Catitti, E. Iacuessa, A. Tiburzi
LNF Divisione acceleratori: M. Incurvati, L. Pellegrino, C. Sanelli

1 The experiment

The aim of the OPERA experiment ¹⁾ is the observation of $\nu_\mu \rightarrow \nu_\tau$ oscillations in the parameter region indicated by Super-Kamiokande as the explanation of the zenith dependence of the atmospheric neutrino deficit. OPERA is a long baseline experiment to be located at the Gran Sasso Laboratory (LNGS) in the CNGS neutrino beam from the CERN SPS. The detector design is based on a massive lead/nuclear emulsion target. The target is made up of emulsion sheets interleaved with 1mm lead plates and packed into removable “bricks” (56 plates per brick). The bricks are located in a vertical support structure making up a “wall”. Nuclear emulsions are used as high resolution tracking devices, for the direct observation of the decay of the τ leptons produced in ν_τ charged current interactions. Electronic detectors, positioned after each wall, locate the events in the emulsions. They are made up of extruded plastic scintillator strips read out by wavelength-shifting fibers coupled with photodetectors at both ends. Magnetised iron spectrometers measure charge and momentum of muons. Each spectrometer consists of a dipolar magnet made of two iron walls interleaved with pairs of precision trackers. The particle trajectories are measured by these trackers, consisting of vertical drift tube planes. Resistive Plate Chambers (RPC) with inclined strips, called XPC, are combined with the precision trackers to provide unambiguous track reconstruction in space. Moreover, planes of RPCs (Inner Tracker) are inserted between the magnet iron plates. They allow a coarse tracking inside the magnet to identify muons and ease track matching between the precision trackers. They also provide a measurement of the tail of the hadronic energy leaking from the target and of the range of muons which stop in the iron. A block of 31 walls+scintillator planes, followed by one magnetic spectrometer constitutes a “super-module”. OPERA is made up of two supermodules located in the Hall C of LNGS (see Fig. 1). The total number of bricks amounts to 206,336 resulting in a target mass of 1766 tons. The discovery potential of OPERA originates from the observation of a ν_τ signal with very low background level. The direct observation of $\nu_\mu \rightarrow \nu_\tau$ appearance will constitute a milestone in the study of neutrino oscillations. Moreover, OPERA has some sensitivity to the sub-dominant $\nu_\mu \leftrightarrow \nu_e$ oscillations in the region indicated by the atmospheric neutrino experiments. It has been shown ²⁾ that the CNGS beam optimized for ν_τ appearance, will improve significantly (about a factor of five for ICARUS and OPERA combined, a factor of three for OPERA alone) the current limit of CHOOZ and explore most of the region $\sin^2 2\theta_{13} \simeq \mathcal{O}(10^{-2})$. Opera is an international collaboration (Belgium, China, Croatia, France, Germany, Israel, Italy, Japan, Russia, Switzerland, and Turkey) and the INFN groups involved are Bari, Bologna, LNF (Frascati), LNGS (Gran Sasso), Naples, Padova, Rome and Salerno.



Figure 1: 3D view of OPERA.

2 Overview of the OPERA activities in 2004

Several important milestones have been achieved in 2004. The first magnetic spectrometer has been installed in Hall C and the second will be completed in spring 2005. In the meantime, the first part of the general support structure has been mounted together with the first wall and scintillator plane. The BAM project has completed the prototyping phase with manual/semiautomatic tools and the actual construction has started in firm site. The underground BAM site is in preparation and will be delivered by spring 2005. Several scanning systems in Europe have reached the nominal speed of $20 \text{ cm}^2/\text{h}$ and the commissioning of the S-UTS in Japan will start at beginning of 2005. The first bunch of nuclear emulsions has reached LNGS after production at Fuji and refreshing in a Japanese underground mine. They are currently stored in the Hall B of the Gran Sasso labs.

3 Activities in Frascati

The Frascati group is responsible for the design and construction of the dipolar magnets and the general support structure for the subdetectors. It shares responsibility with INFN Padova and LNGS for the construction and installation of the bakelite RPC planes (Inner Tracker). Frascati and Naples also designed and prototyped the wall support structure housing the lead/emulsion bricks. Moreover, the group contributes to software development and to the analyses aimed at assessing the performance of the experiment after the completion of the CNGS programme. Finally, since 2002 LNF is involved in the construction of the Brick Assembly Machine (BAM).



Figure 2: The support structure in the factory before transportation at LNGS.

3.1 OPERA general layout

The overall support structure for the OPERA subdetectors has been designed by LNF-SPAS in collaboration with external firms. It has been re-optimized in 2002 for the two-spectrometer design ³⁾ and finalized at the beginning of 2003. The studies included risk analysis and full seismic response. Tendering and ordering for the support structure have been carried out in 2003 while mass production has started in 2004 (Fig. 2). The installation of the mechanical structure started after the completion of the first spectrometer (see below). By august 2004 (see Fig.3) the upper and lower support rails together with the dumping structure have been mounted and aligned. After this operation most of the activities in the underground hall were halted to allow for the safety works in Hall C. These modifications of the LNGS infrastructures have been planned by the Commissioner appointed by the Italian government (July 2003) with the task of ensuring LNGS to be compliant with safety and environmental rules. The installation of the second magnet was resumed in autumn 2004 and completion is planned in spring 2005. As for 2003, LNF-SPAS follows closely the installation procedure at LNGS; together with LNGS staff, it coordinates material transportation and logistics and validates the installation operations done by the external firms operating in the underground hall. It is also in charge of the geometrical survey of the hall and the positioning of the main marks fixing the absolute reference system for the location of the OPERA subdetectors.

3.2 Magnets

The mass production of the iron for both spectrometers has been carried out in 2003. A detailed assessment of its magnetic and mechanical properties was completed in 2004 in collaboration with the suppliers, LNF-SPAS and CERN technical staff and it is summarized in ⁴⁾. The installation of the lower return yokes and coils of the magnet started in 2003 while the first slab was mounted at the end of 2003. The installation of the iron slabs and the active detectors has run in parallel



Figure 3: The upper structure between the first spectrometer and the dumping support (Oct 2004).

(see next section) and was completed in May 2004. Thereafter, the upper return yoke, the coil and the corresponding cooling system has been mounted (Fig. 4). Similarly, the devices for field monitoring (pickup coils and Hall probes) have been installed. The construction of the second spectrometer started after the completion of the Commissioner's works near the OPERA area. By December 2004 about 1/3 of the slabs for the second spectrometer has been successfully mounted. The water cooling system for the spectrometer is rather complex because it needs to be operated in standalone mode until the water circulating system of LNGS is fully re-activated. The latter has been halted just after the Borexino accident of August 2002³⁾; moreover, the OPERA system supplies users that need independent circuits with different water type specifications. This system has been designed at the end of 2004 in collaboration with LNF-Div.Acc (Fluid System Group) and LNGS. Similarly, the specifications for the high current power supplies driving the magnet coils have been finalized in collaboration with LNF-Div.Acc. (Magnet and Power supply Group) and LNGS and are based on the results obtained during the prototyping phase of the spectrometer^{3, 5, 6)}. The tender for the power supplies has been completed in spring 2004 and the devices are under construction at firm site. LNF-Div.Acc. is following up the production phase and validates the solution proposed by the supplier before the implementation of the executive drawing.

3.3 Inner trackers

The mass production of the Resistive Plate Chambers has been nearly (> 90%) completed in 2004. During the simultaneous installation of the magnet slabs and the RPCs, several checks have been performed underground. They include gas tightness tests of the detectors and electric tests of the pickup strips. The validation of the installed detectors is performed with pure nitrogen, by operating the RPCs at 6.5 kV. At this voltage nitrogen acts as an insulator between the RPC electrodes and the presence of discharges in the HV system can be tested. The space between the active detectors and the iron slabs is filled with non flammable polyester fiber. An excessive pressure

produced by the polyester fiber is evidenced by an increase of the current after the slab installation; in such a case, the slabs are dismantled and the thickness of the filling material is reduced.

Before installation, extensive quality tests have been carried out at the LNGS external laboratory ³⁾. The large number of tested RPCs (>1000), allowed a detailed assessment of the main detector parameters ⁷⁾. In particular, it has been demonstrated that the ohmic current, the operating current and the intrinsic noisiness decrease with the electrode resistivity. Long term operation tests have been performed on six RPCs rejected by the quality control (QC) tests because of the high intrinsic noise. After more than three months of operation at cosmic ray fluxes, equivalent to 5 years of operation underground, the detectors show stable currents (lower than $1 \mu\text{A}$) and counting rates (around 300 Hz/m^2), with no efficiency loss. About 5% of the RPCs installed on the first spectrometer has also been tested with the gas mixture $\text{Ar}/\text{C}_2\text{H}_2\text{F}_4/\text{iso}-\text{C}_4\text{H}_{10}/\text{SF}_6 = 75.4/20/4/0.6$, similar to the one that will be used during the OPERA data taking. The counting rates don't show a plateau as a function of the voltage, therefore a nominal operating voltage of 5.6 kV has been estimated from measurement performed at cosmic ray fluxes in the external Gran Sasso laboratory. The counting rates and currents measured at the operating voltage are shown in figure 5. Typical counting rate values are below 10 Hz/m^2 . Measured currents are of the order of few hundreds nA, lower with respect to those measured in the QC tests, with some exception due to the ohmic current increase in presence of wet gas flushing.

The tasks concerning the design and construction of the RPC electronics are shared among LNF-SEA (strip boards, current monitoring, timing boards), Padova (front-end boards) and Napoli



Figure 4: The first OPERA magnet at Gran Sasso.

(controller boards interfaced to DAQ) and coordinated by LNF-SEA. During 2004, the high voltage splitters with embedded nanoamperometers have been produced and tested. The timing board design has been finalized according to the results of cosmic ray tests performed at LNF on small size RPCs operated with the OPERA gas mixture.

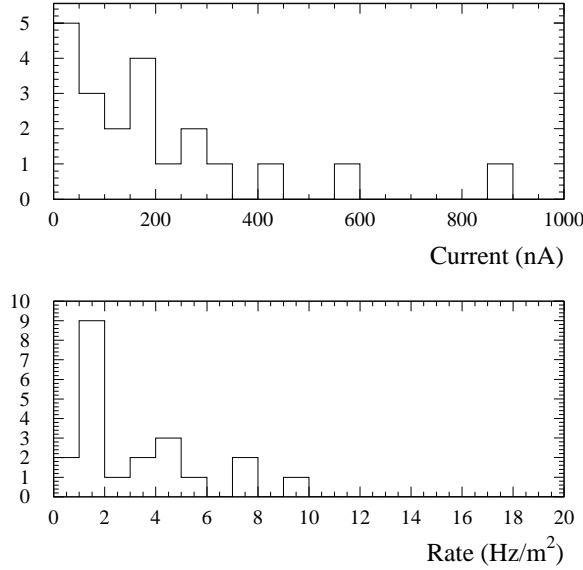


Figure 5: Operating currents and counting rates measured underground on several installed RPCs.

3.4 Wall support structure

The wall support structure is made of thin stainless steel vertical bands welded to light horizontal trays where the bricks are positioned with a precision of one millimeter. The structure is suspended through rods and joints from the general support structure and tensioned from the bottom through a spring system. During 2004 the production cycle has been finalized by LNF-SSCR and the external firm in charge of the mass production (see Fig.6). Moreover a quality control system was set up to provide feedback during the production phase and allow optimization of the machine operations. Since the end of the year, the production cycle has been running well within specifications with a production rate of about 1.2 walls per week. Particular care has been put into the development of the alignment system in the underground hall. It is based on photogrammetry complemented by laser trackers and it has been commissioned by LNGS in collaboration with Lyon and CERN technical staff. In the meanwhile, the top and bottom rails of the first supermodule have been installed and aligned in Hall C. All insertion tools were commissioned by Nov 2004 and the first wall was delivered in Gran Sasso in October 2004. Such a wall has been installed and aligned in December by LNF-SSCR and LNGS.



Figure 6: Production of an OPERA wall.

3.5 Brick Assembly Machine

LNF has played an important role in the identification of the mechanical packaging as a robust alternative solution to vacuum packaging of the OPERA bricks. The former has been endorsed as the final solution for the design of the BAM in spring 2004; the size and thickness of all pile components has been fixed in September 2004. In the new brick configuration, pressure is maintained by the mechanical structure and high resistance scotch tapes while Al tapes guarantee light tightness. Systematic tests on the pressure exerted for various configurations and the resulting planarity have been carried out at LNF. Finally, the new bricks have been successfully validated through testbeams at CERN in winter 2004.

3.6 Software and analysis

As for 2003, LNF contributed to the simulation of the magnetic spectrometers, the embedding of the magnetic field maps and the development of reconstruction algorithms for charged particles in the new offline framework for OPERA. A topic that has been recently investigated at LNF is the monitoring of the CNGS beams through the identifications of muons emerging from the rock in coincidence with the CNGS spill. This channel offers the opportunity to tag in real-time (i.e. employing only the electronic detectors of OPERA) misalignments and time variations both during the commissioning phase of CNGS and during data taking.

References

1. M. Guler *et al.*, OPERA Proposal, CERN/SPSC 2000-028, SPSC/P318, LNGS P25/2000.
2. M. Komatsu, P. Migliozzi, F. Terranova, J. Phys. G **29** (2003) 443;
P. Migliozzi, F. Terranova, Phys. Lett. B **563** (2003) 73.

3. See “LNF 2002 Annual Report”, S.Dell’Agnello ed., LNF-03/10 (IR), p.59; “LNF 2003 Annual Report”, S.Dell’Agnello ed., LNF-04/08 (IR), p.64.
4. A. Cecchetti, B. Dulach, D. Orecchini, G. Peiro, F. Terranova, “Chemical and Magnetic Characterization of the Steels for the Opera Spectrometers”, LNF-04/28(IR) and OPERA note, 2004.
5. G. Di Iorio et al., “Measurements of the Magnetic Field in the Prototype of the OPERA Spectrometer”, OPERA note, LNF-01/028.
6. M. Incurvati, F. Terranova, Nucl. Instr. Meth. A **500** (2003) 442.
7. E. Carrara, A. Mengucci, A. Paoloni, M. Ventura, “Electrical tests on OPERA RPCs”, OPERA note, 2004.

Conference talks by LNF authors

8. A. Paoloni et al., “The OPERA Spectrometers RPC System”, talk at the 2004 Nuclear Science Symposium and Medical Imaging Conference (IEEE NSS/MIC), October 16-22, 2004, Rome, Italy.
9. C. Di Troia et al., “Monitoraggio del fascio CNGS tramite i muoni rivelati da OPERA”, talk at the 90th Congresso Nazionale della Società Italiana di Fisica, September 20-25, 2004, Brescia, Italy.

Publications by LNF authors

10. G. Barichello *et al.*, Nucl. Instrum. Meth. A **533** (2004) 42.
11. M. Ambrosio *et al.*, Nucl. Instrum. Meth. A **533** (2004) 173.
12. A. Bergnoli *et al.*, Nucl. Instrum. Meth. A **533** (2004) 203.
13. R. Brugnera *et al.*, Nucl. Instrum. Meth. A **533** (2004) 221.
14. M. Ambrosio *et al.*, IEEE Trans. Nucl. Sci. **51** (2004) 975.
15. P. Migliozzi, F. Terranova, Eur. Phys. J. C **33** (2004) S846.

PVLAS

M. Bregant¹, G. Cantatore¹, S. Carusotto⁴, R. Cimino (Resp)⁶,
 F. Della Valle¹, G. Di Domenico², U. Gastaldi³, M. Karuza¹, E. Milotti⁵,
 E. Polacco⁴, G. Ruoso³, E. Zavattini¹, G. Zavattini²,

- 1) Dipartimento di Fisica and INFN, Trieste; 2) Dipartimento di Fisica and INFN, Ferrara;
 3) INFN, Laboratori Nazionali di Legnaro; 4) Dipartimento di Fisica and INFN, Pisa;
 5) Università di Udine and INFN Trieste; 6) INFN, Laboratori Nazionali di Frascati.

The PVLAS collaboration is conducting experimental studies of vacuum magnetic birefringence and dichroism by operating a high-sensitivity ($10^{-7} 1/\sqrt{\text{Hz}}$) optical ellipsometer, located at the INFN Legnaro National Laboratory, Legnaro, Italy. This instrument is capable of detecting, using the heterodyne technique, both ellipticities and rotations in an independent way, down to levels below 10^{-8} rad, for about one hour of data taking time. Contributions to vacuum magnetic birefringence and dichroism could come from photon-photon scattering processes predicted by QED or from the existence of light scalar/pseudoscalar particles coupled to two photons. Figure 1 shows a schematic drawing of the PVLAS apparatus. The interaction region, where a 1064 nm linearly polarized laser beam interacts with an external transverse magnetic field, is contained within the bore of a superconducting, 1 m long, dipole magnet normally operated at field of 5.5 T. The magnet is enclosed in a warm-bore rotating cryostat which keeps the magnet at liquid He temperatures (4.2 K). Detection strategy is based a high finesse ($\sim 10^5$), 6.4 m long Fabry-Perot (FP) cavity formed by mirrors M1 and M2. The resonator provides amplification of the optical path in the interaction region, while rotation of the magnet-cryostat assembly results in a time-varying signal which beats with a carrier signal introduced by an ellipticity modulator (PM) and allows heterodyne detection. Furthermore, by inserting or removing from the light path, before the PM, a properly aligned quarter-wave plate (QWP), the ellipsometer can be configured for detecting rotations or ellipticities generated in the interaction region. The signal generated from the photodiode is demodulated at the carrier frequency and Fourier analysed to obtain amplitude and phase of the relevant physical quantities. In the resulting amplitude spectrum, the signal to be measured should appear at twice the magnet rotation frequency. The phase of a physical signal is determined by the initial position of the polarization. During 2004, the Cotton-Mouton effect

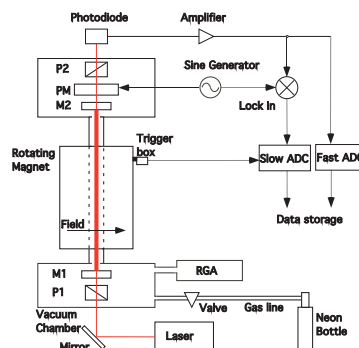


Figure 1: *Schematic layout of the PVLAS experimental apparatus.*

in Xenon, Krypton ¹⁾, Ne ²⁾ and Nitrogen has been measured. Figure 2a) shows a demodulated amplitude spectrum of the photodiode signal with 8 mbar of Ne in the interaction region and $B = 4.53$ T. The ellipticity peak at twice the magnet rotation frequency is due to the Cotton-Mouton of Ne ²⁾. Its phase has the correct value given the geometry of the set-up.

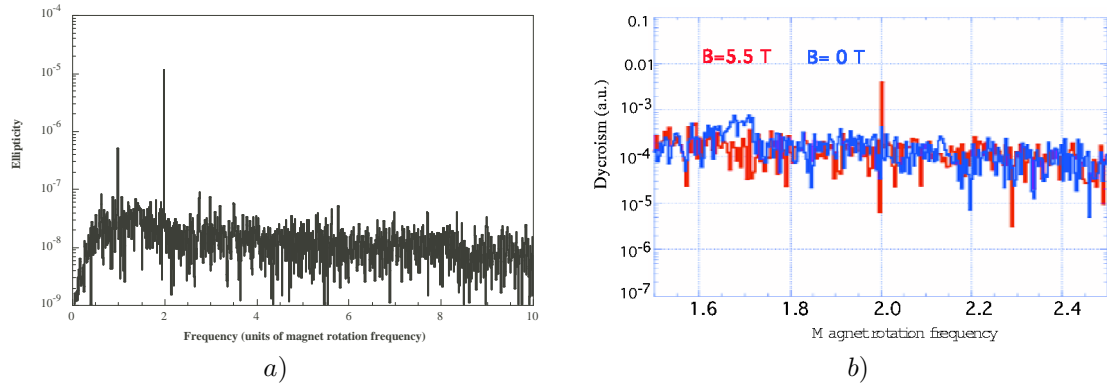


Figure 2. Demodulated amplitude spectra of the photodiode signal with a) 8 mbar of Ne and $B = 4.53$ T; b) vacuum with (red line) and without (blue line) magnetic field (see text).

Following the checks of the apparatus with gases, data runs have been mostly devoted to rotation measurements in vacuum ($P \sim 10^{-8}$ mbar). Figure 2 b) shows two superimposed typical amplitude spectra of the rotation signal in vacuum with $B = 5.5$ T and $B = 0$. Notice the peak, visible well above the background, at twice the magnet rotation frequency present in the $B = 5.5$ T spectrum which disappears when $B = 0$. Noise backgrounds are comparable. Signal peaks such as the one shown in Figure 2 b) have been consistently observed in all vacuum data runs with B different from zero. Diagnostic tests have shown that the signal corresponds to a true optical rotation generated within the Fabry-Perot cavity. If not coming from an instrumental effect, rotation in vacuum of the polarisation plane of incident light could be due to a dichroism resulting from selective absorption of photons polarised parallel to the magnetic field. An absorption of this kind could be explained by a model where a light, neutral, pseudoscalar boson coupled to two photons is produced in the interaction region ³⁾. Future short term plans include a change in the laser wavelength from 1064 nm to 532 nm. This change, in addition to the practical advantages of operating with visible light, will allow a check of the energy dependence of the signal.

References

1. PVLAS collab., “Measurement of the Cotton-Mouton effect in Krypton and Xenon at 1064 nm with the PVLAS apparatus”, Chemical Physics Letters Vol 392/1-3 pp 276-280.
2. PVLAS collab., “A precise measurement of the Cotton-Mouton effect in neon”, submitted to Chemical Physics Letters.
3. PVLAS collab., “PVLAS results on Laser production of Axion-like Dark matter Candidate Particles”, presented at IDM 2004.

RAP

S. Bertolucci, B. Buonomo (Bors.), G.O. Delle Monache, G. Ceccarelli (Tecn.),
R. Ceccarelli (Tecn.), M. De Giorgi (Tecn.), D. Di Gioacchino, V. Fafone, C. Ligi (Art.23),
R. Lenci (Tecn.), A. Marini (Resp. Naz.), G. Mazzitelli, G. Modestino, S. Panella (Laur.),
G. Pizzella (Ass. Ric.), L. Quintieri (Art.23), S.Roccella (Dott.), F. Ronga (Resp.),
P. Tripodi (Osp.) and P. Valente (Art.23)

1 Aim of the experiment

The primary scope of the experiment RAP is to measure the longitudinal vibrations of an aluminum cylindrical test mass, impinged by the electrons provided by the DAΦNE Beam Test Facility (BTF), in order to investigate if a higher efficiency mechanism for the particle energy loss conversion into mechanical energy takes place when the bar is in the superconducting state.

To some extent the motivation of the experiment and the set up components (*viz.* the beam, the test mass, the suspension system, the cryogenic and vacuum system, the mechanical structure hosting the cryostat, the readout and the data acquisition system) were reviewed in the 2003 Edition of the LNF Activity Report and in the papers listed in the bibliography.

INFN and Physics Department Università di Roma Tor Vergata and Kamerlingh Onnes Laboratory, Leiden University (The Netherlands) are participating institutions to the experiment.

2 Activities in the year 2004

Cryogenic tests and physics runs down to the liquid He temperature (4.2 K) took place in the year 2004, according to the temporal planning of the experiment. Unfortunately, on February a severe cryostat failure occurred due to a fissure in the welding that seals the nitrogen dewar. The cryostat was fixed on May and the complete detector was put on the BTF beam line shortly after. During the period May, 26th - June, 17th the bar was cooled down to 4.2 K and simultaneously was exposed to the BTF electron beam with the DAQ collecting data at different temperatures.

The maximum amplitude of the first longitudinal mode of oscillation of the bar, B_m is related to measured values according to the relation: $B_m = V_m/(G\lambda)$, where V_m is the maximum amplitude of the component of the signal at the frequency corresponding to the first longitudinal mode, G is the gain of the piezoelectric transducer chain and λ is the electro-mechanical conversion factor of the transducer, measured before each run exploiting a self-calibration procedure based on the injection in the chain of a known sinusoidal waveform.

According to the thermo-acoustic model the maximum amplitude B_{th} of the first longitudinal mode of oscillation can be written as $B_{th} = (2/\pi)(\alpha L/(c_V M))NW_e$ for our transducer configuration and beam impact point. Here α is the linear thermal expansion coefficient, L and M are respectively the mass and the length of the cylinder, c_V is the specific heat, N is the number of the impinging electrons measured by the BTF monitoring system and W_e is the energy released to the bar by a single electron, determined by a complete Montecarlo simulation program.

The correlations in Fig. 1 among B_m and B_{th} at different temperatures indicate a good agreement, in a wide temperature range, between the expectations of the thermo-acoustic model and the measurements we have performed.

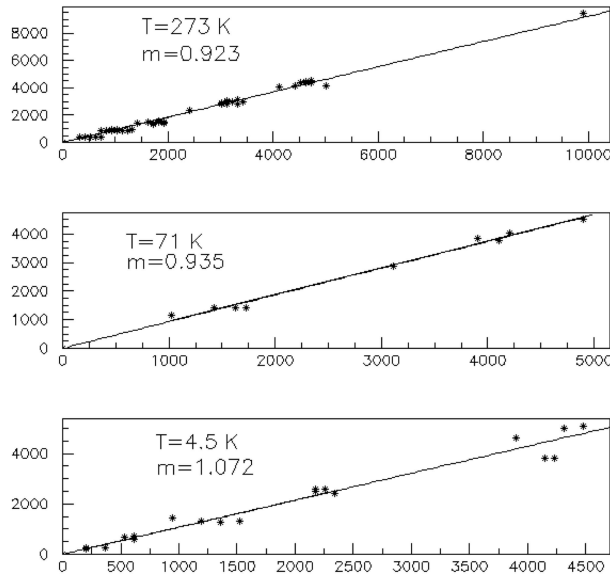


Figure 1: Measured amplitudes [fm] of induced vibrations, B_m (vertical), versus the expected ones, B_{th} (horizontal), for various beam intensities at different temperatures.

3 Activities in the year 2005

The dilution refrigerator will be tested as soon as this component will be made available to the group. After this step, the execution of first measurements at $T < 1$ K is planned by the end of the year.

4 List of Conference Talks by LNF Authors in the Year 2004

1. C. Ligi, RAP Collaboration: RAP - Acoustic Detection of Particles: First Results at 4.2 K, 19th European Cosmic Rays Symposium, Florence, Italy.
2. L. Quintieri, RAP Collaboration: RAP-Rivelazione Acustica di Particelle- Present Status and First Results, LXXXX Congresso Nazionale SIF, Brescia, Italy.

References

1. S. Bertolucci *et al.*, *Class. Quant. Grav.* **21**, S1197 (2004).
2. S. Bertolucci *et al.*, *Nucl. Instrum. Meth. A* **520**, 205 (2004).
3. P. Valente *et al.*, *Nucl. Instrum. Meth. A* **518**, 261 (2004).

ROG

D. Babusci, F. Campolungo (Tecn.), V. Fafone, G. Giordano, M. Iannarelli (Tecn.),
R. Lenci (Tecn.), A. Marini, G. Modestino, G.P. Murtas, G. Pizzella (Resp. Ass.),
L. Quintieri, F. Ronga (Resp.), E. Turri (Tecn.)

Collaboration with: Roma 1 La Sapienza, Roma 2 Tor Vergata, Leiden University

1 Introduction

The ROG group is currently operating two cryogenic gravitational wave (GW) bar detectors: EXPLORER (at CERN) and NAUTILUS (in Frascati). The main goal of this search is the direct detection of the GW's that could be emitted by astrophysical sources (such as Supernova or Coalescent Binaries). Such detection could be of enormous interest for general relativity and for astrophysics.

Cryogenic resonant-mass detectors were conceived in the '70s with the aim of improving the sensitivity of room temperature Weber detectors by many orders of magnitude, by reducing the temperature of the bar to or below liquid helium temperature (4.2 K) and employing superconducting electronic devices in the readout system.

The principle of operation of resonant-mass detectors is based on the assumption that any vibrational mode of a resonant body that has a mass quadrupole moment, such as the fundamental longitudinal mode of a cylindrical antenna, can be excited by a GW with non zero energy spectral density at the mode eigenfrequency. The mechanical oscillation induced in the antenna by interaction with the GW is transformed into an electrical signal by a motion or strain transducer and then amplified by an electrical amplifier. Unavoidably, Brownian motion noise associated with dissipation in the antenna and the transducer, and electronic noise from the amplifier, limit the sensitivity of the detector.

The sum at the output of the contributions due to the Brownian noise and to the electronic noise gives the total detector noise. This can be referred to the input of the detector (as if it was a GW spectral density) and is usually indicated as $S_h(f)$. This function has a resonant behaviour and can be characterized by its value at the detector resonance frequency f_0 and by its half height width. $S_h(f_0)$ can be written as:

$$S_h(f_0) = \frac{\pi}{8} \frac{KT}{MQL^2} \frac{1}{f_0^3}, \quad (1)$$

where T is the antenna temperature, M is the mass of the antenna, Q is the quality factor of the mode. The half height width of this function gives the bandwidth of a resonant detector. The bandwidth of a resonant detector depends from the mechanical parameters of the detector and from the characteristic of the electronic amplifier and can be written as:

$$\Delta f = \frac{4f_0}{Q} \frac{T}{T_{eff}}, \quad (2)$$

where T_{eff} is the noise temperature when the data are filtered to have the maximum signal to noise ratio in the case of delta-like signals (like those expected from supernova). T_{eff} decreases as the noise temperature of the amplifier decreases and as the transducer efficiency increases.

These relations characterize completely the sensitivity of a resonant-mass detector. For instance, the minimum detectable (SNR=1) GW amplitude for a short burst signal lasting for a time τ_g can be written as:

$$h_0 = \frac{2}{\tau_g} \sqrt{\frac{S_h(f_0)}{2\pi\Delta f}}. \quad (3)$$

During these years, experimentalists devoted a continuous effort to improve the antenna sensitivity. All the upgrades are mainly devoted to:

- increase the duty cycle and lower the background noise, by upgrading the cryogenics to minimize maintenance stops and to ensure more stable operating temperature, and by acting on the vibration attenuation system, including the thermal links between refrigerating stages and the electromechanical sensitive components.
- improve the sensitivity and the useful bandwidth, by acting on the readout components. These efforts promise to be successful, as recently shown by EXPLORER and NAUTILUS where upgraded transducers, more strongly coupled to the bar, and less noisy single stage SQUID amplifiers have been used. Even better results are expected very soon with the development of double stage SQUID amplifiers, with energy resolution of less than 100 quanta, and of a high Q superconducting LC coupling circuit, resonating at the bar frequency. This activity is currently in progress at LNF in collaboration with the IFN-CNR (Istituto di Fotonica e Nanotecnologie) in Rome.

2 NAUTILUS and EXPLORER

The ultra-cryogenic detector NAUTILUS ¹⁾ is operating at the Frascati INFN National Laboratory since December 1995. It consists of an Al5056 cylindrical bar, 2300 kg in weight and 3 meters in length, cooled to a temperature of 0.1 K by means of a dilution refrigerator, and equipped with a resonant capacitive transducer and a dc SQUID amplifier. The two characteristic resonance frequencies, due to the coupling of the antenna and the transducer are about 926 and 941 Hz. NAUTILUS is equipped with a cosmic ray detector.

The present data taking started in 2003, with a new bar tuned at 935 Hz, where a pulsar, remnant of the SN1987A, is supposed to emit GW ²⁾, a new readout chain (the same as for EXPLORER), plus a new suspension cable, to provide a more stable position setting. At present, the temperature of the bar is 3.5 K. The resulting strain noise (the minimum detectable spectral density) is $\tilde{h} \equiv \sqrt{S_h} \simeq 2 \cdot 10^{-21} / \sqrt{\text{Hz}}$ around 935 Hz, and $\tilde{h} \leq 10^{-20} / \sqrt{\text{Hz}}$ over about 30 Hz (see Figure 1). The noise temperature is 2 mK, corresponding to an adimensional amplitude of GW bursts $h = 3.5 \cdot 10^{-19}$ ³⁾. Better results in terms of sensitivity are expected when the system will be cooled down to 0.1 K. The duty cycle is now very high (about 90%), mainly limited by the cryogenic maintenance operations. The high duty cycle and the stationary behaviour are very important to collect the data needed to further investigate the coincidence excess between EXPLORER and NAUTILUS ^{4, 5)} found in the 2001 data.

The EXPLORER antenna is located at CERN and is very similar to NAUTILUS, but can operate down to 2.6 Kelvin. The present data taking started in February 2004. The duty cycle is very high (of the order of 90%) and the noise temperature of the order of 2 mK ³⁾, with a strain sensitivity $\tilde{h} \simeq 3 \cdot 10^{-21} / \sqrt{\text{Hz}}$ around the two resonances at 904 Hz and 927 Hz, and $\tilde{h} \leq 10^{-20} / \sqrt{\text{Hz}}$ over about 30 Hz.

Also EXPLORER is equipped with a cosmic ray detector. Thanks to the larger bandwidth obtained with the read-out installed in 2001 on EXPLORER and in 2003 on NAUTILUS, a good time resolution (less than 10 ms) in the determination of the events due to the passage of cosmic rays has been reached (see Figure 2).

The LNF group has major responsibilities in the maintenance and running of NAUTILUS (including the production of liquid helium), in the maintenance, building and running of the cosmic ray detectors, in the development of a new nearly quantum limited signal read-out, in the data acquisition and in many items of data analysis.

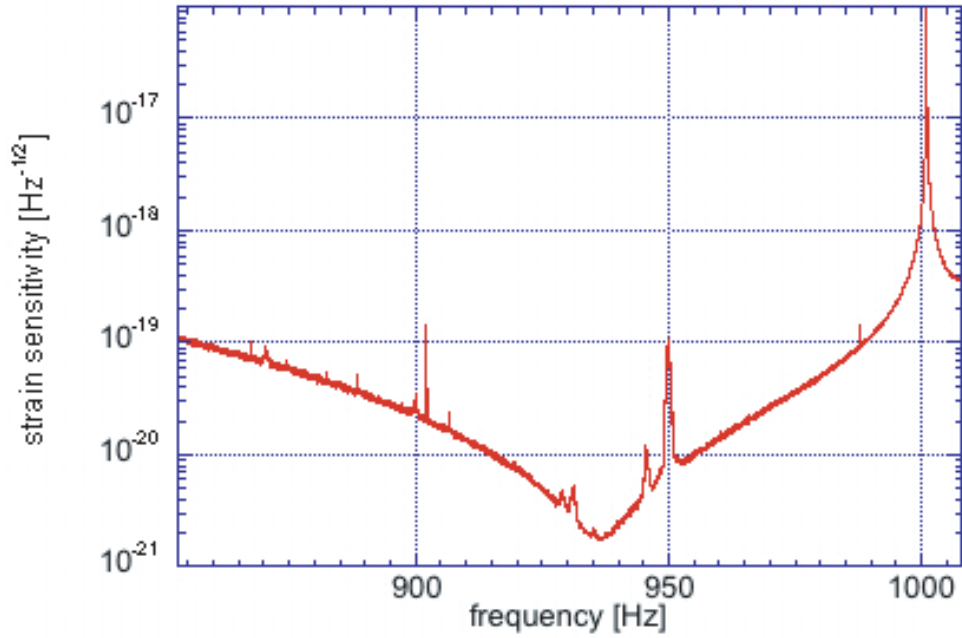


Figure 1: Experimental strain sensitivity of NAUTILUS in 2004, with the bar cooled at 3.5 K. The detector performances are very stationary, resulting in a duty cycle of about 90%.

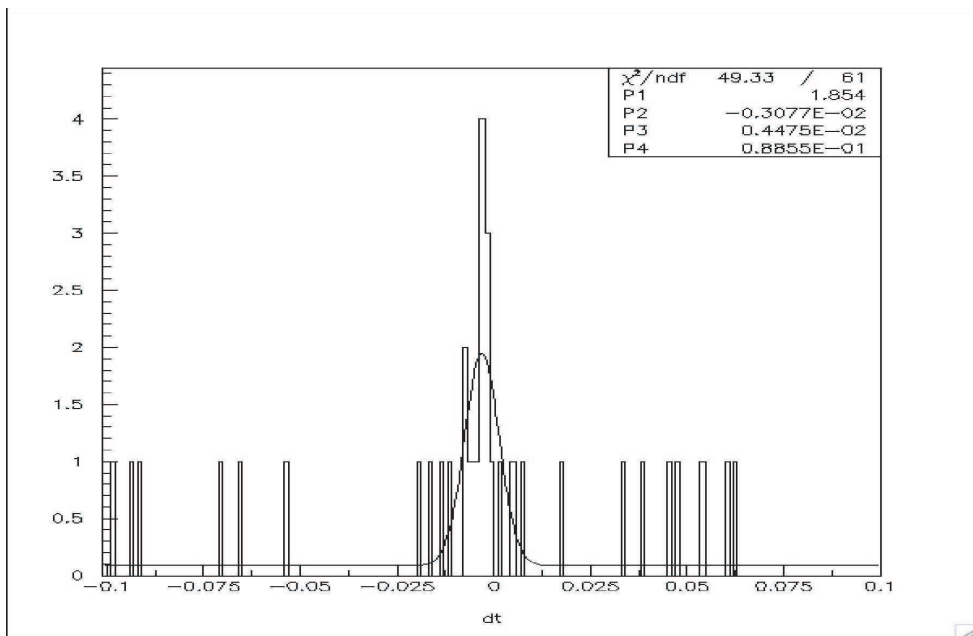


Figure 2: Experimental distribution of cosmic ray arrival times as measured from the EXPLORER events. The standard deviation derived from the fit is 4 ms.

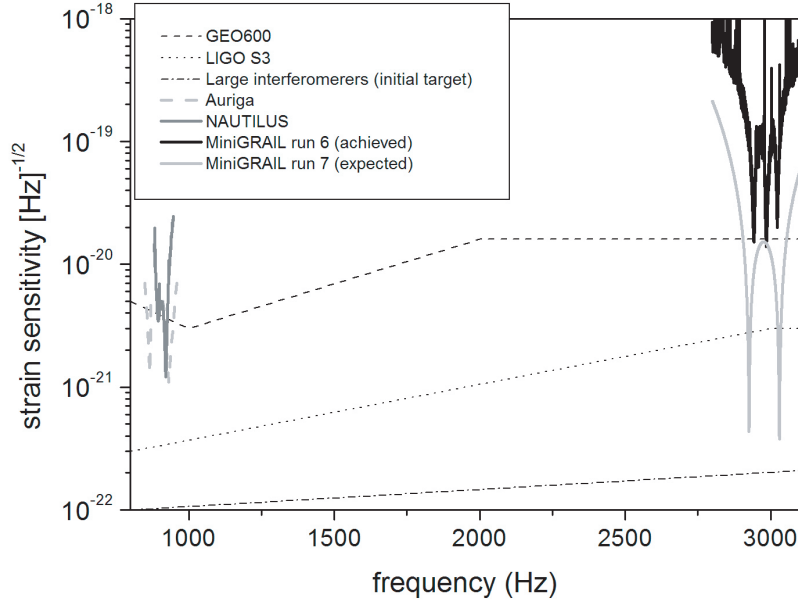


Figure 3: Experimental strain sensitivity of MiniGRAIL during the first run in 2004, with the sphere cooled at 4 K. The expected curve of the next run, planned by the end of 2005, is also shown.

3 Advanced detectors

The LNF group is involved in the development of resonant-mass detectors of spherical shape. A single sphere is capable of detecting GW from all directions and polarizations and is capable of determining the direction information and tensorial character of the incident wave. A sphere will have a larger mass than the present bars (with the same resonance frequency), turning into an increased cross section and improved sensitivity. Omnidirectionality and source direction finding capability make a spherical detector a unique instrument for GW astronomy with respect to all present detectors. At present, two small spheres (about 1 ton) are being developed: one in Brasil and one (MiniGRAIL) in Holland. The ROG group is collaborating with the Leiden University group for the development of MiniGRAIL, mainly on new read-out chains, the data acquisition and the effect of cosmic rays. After a cryogenic run, when MiniGRAIL was cooled down to 79 mK⁶⁾, in 2004 MiniGRAIL operated for the first time with three read-out transducers (in the final configuration, 6 transducers will be necessary, to completely reconstruct all the features of the impinging GW). The high Q superconducting transformers were realized and tested at LNF. For the first time the brownian noise of a spherical detector at low temperature was measured⁷⁾. The resulting strain sensitivity is shown in Figure 3, compared with the sensitivity curves of the other GW detectors. A new run with an upgraded read-out is foreseen by the end of 2005.

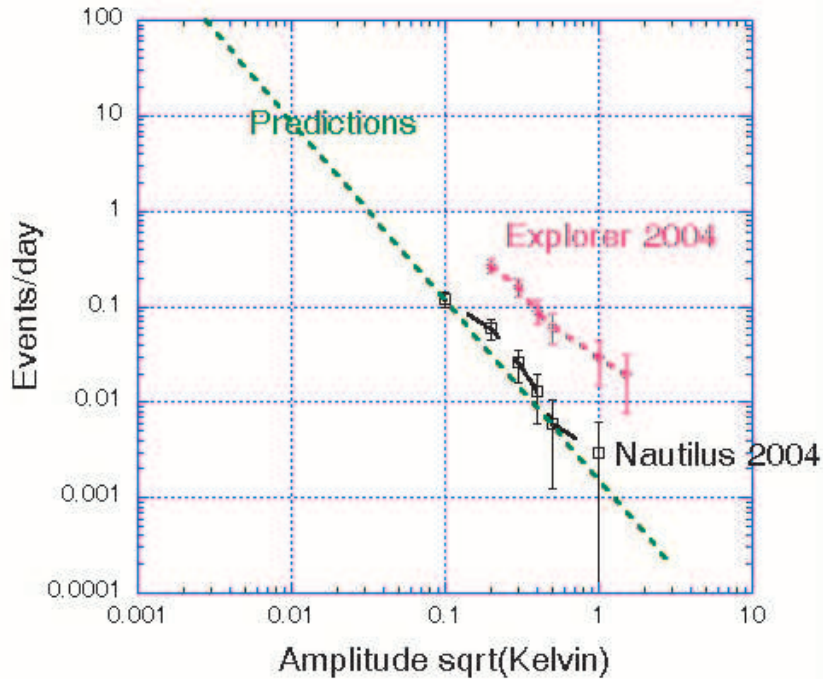


Figure 4: Integral distribution of the events recorded by NAUTILUS and EXPLORER in coincidence with cosmic rays. The x axis is the amplitude of the events. In EXPLORER a rate higher than the theoretical predictions is found.

4 Main data analysis results obtained in 2004

The main analyses using the NAUTILUS and EXPLORER data, just published or in progress, are the following:

- Search for coincidences between resonant bar detectors. The analysis of the EXPLORER-NAUTILUS data is in progress to further investigate the coincidence excess found in the 2001 data ⁸⁾.

- Search for coincidences with gamma ray bursts ⁹⁾. Data collected by EXPLORER and NAUTILUS, between 1991 and 1999, have been correlated with the GRB events. The analysis excludes the presence of a signal of amplitude $h \geq 5.4 \cdot 10^{-19}$, if we allow a time delay between GW burst and GRB within 10 s.

- Further study of excitation of NAUTILUS and EXPLORER due to the passage of cosmic rays. We report in Figure 4 the results of the 2004 analysis. In EXPLORER we have observed a rate higher than expected. We had already observed such an excess in NAUTILUS, but this anomalous behaviour seemed to be related with the superconducting state of the bar: the excess appeared only when the bar was below 1 K. The 2004 events suggest that superconductivity is not, or not the only explanation of our observation.

5 List of Conference Talks by LNF Authors in Year 2004

1. G. Pizzella, “Coincidences between the Gravitational Wave detectors EXPLORER and NAUTILUS”, Vulcano Workshop, 24th-29th May, 2004.
2. L. Quintieri, “Rapporto sullo stato dei rivelatori di onde gravitazionali Nautilus ed Explorer”, XC Congresso Nazionale SIF, September 2004, Brescia.

References

1. P. Astone *et al.*, (ROG Collaboration), “The gravitational wave detector NAUTILUS operating at $T = 0.1$ K”, *Astropart. Phys.* **7**, 231 (1997).
2. J. Middleditch *et al.*, *New Astronomy* **5**, 243 (2000).
3. V. Fafone, “Resonant-mass detectors: status and perspectives”, *Class. Quantum Grav.* **21** (5), S377-S383 (2004).
4. P. Astone *et al.*, (ROG Collaboration), “Study of the coincidences between the gravitational wave detectors EXPLORER and NAUTILUS in 2001”, *Class. Quantum Grav.* **19**, 5449 (2002).
5. P. Astone *et al.*, (ROG Collaboration), “Comments on the 2001 run of the EXPLORER/NAUTILUS gravitational wave experiment”, *Class. Quantum Grav.* **20**, S785 (2003).
6. A. de Waard, L. Gottardi, M. Bassan, E. Coccia, V. Fafone, J. Flokstra, A. Karbalai-Sadegh, Y. Minenkov, A. Moleti, G.V. Pallottino, M. Podt, B.J. Pors, W. Reincke, A. Rocchi, A. Shumack, S. Srinivas, M. Visco, G. Frossati, “Cooling down MiniGRAIL to milli-Kelvin temperatures”, *Class. Quantum Grav.* **21** (5), S465-S471 (2004).
7. A. de Waard, Y. Benzaim, G. Frossati, L. Gottardi, H. van der Mark, J. Flokstra, M. Podt, M. Bassan, Y. Minenkov, A. Moleti, A. Rocchi, V. Fafone, G.V. Pallottino, “MiniGRAIL, progress report 2004”, *Class. Quantum Grav.*, in press.
8. G. Pizzella, “Coincidences between the Gravitational Wave detectors EXPLORER and NAUTILUS”, in: *Proc. of Vulcano Workshop 2004*.
9. P. Astone, D. Babusci, M. Bassan, P. Bonifazi, P. Carelli, E. Coccia, C. Cosmelli, S. D’Antonio, V. Fafone, G. Giordano, A. Marini, Y. Miennkov, I. Modena, G. Modestino, A. Moleti, G.V. Pallottino, G. Pizzella, L. Quintieri, A. Rocchi, F. Ronga, R. Terenzi, G. Torrioli, M. Visco, “Searching for counterpart of gamma-ray bursts with resonant gravitational wave detectors”, *Class. Quantum Grav.* **21** (5), S759-S764 (2004).

VIRGO

D. Babusci, G. Giordano (Resp.), M. Iannarelli (Tecn.), E. Turri (Tecn.)

1 Introduction

Virgo is a collaboration between Italy (INFN) and France (CNRS) for the construction of an interferometric detector of gravitational waves (GW). The participating laboratories are: LAPP-Annecy, IPN-Lyon, OCA-Nice, LAL-Orsay and ESPCI-Paris for CNRS and Firenze/Urbino, Frascati, Napoli, Perugia, Pisa, Roma for INFN.

The aimed sensitivity should allow to detect, in the frequency range between a few Hz and a few kHz, GW emitted by coalescing binary compact stars, gravitational collapses, spinning neutron stars, or constituting the stochastic GW background.

Virgo will be a recycled (power enhancement factor $\simeq 50$) Michelson interferometer, having in each arm a 3 km Fabry-Perot cavity with finesse of 50. The interferometer (ITF) will be illuminated by a 25 W Nd:YAG laser ($\lambda = 1.064 \mu m$), stabilized through a monolithic reference cavity and filtered by a high-finesse triangular mode cleaner of 144 m length.

The construction of the 3 km arms full ITF was completed in June 2003. The optical path is completely under vacuum and all the optical components are suspended in vacuum by anti-seismic Super Attenuators able to reduce the seismic noise of more than a factor 10^{12} above a few Hz.

2 Responsibility of the Frascati Group

The Frascati group has the responsibility of the “linear alignment”, that is the system providing the informations about the misalignment of the ITF mirrors during the standard operation of Virgo. It will employ 8 quadrant photodiodes (QPHD) placed on the beams emerging from the ITF; demodulating the up-down and left-right differences, the misalignments status will be derived.

3 Activity in 2004

All the electronic components of our system (quadrant photodiode front-end electronics, demodulation modules, reference signals shifters and splitters) have been successfully installed.

The large lenses that receive the beam transmitted by the FPs end mirrors have been replaced by a doublet in order to reduce the aberrations introduced in the beam shape.

Remotely controlled laser shutters have been built and installed in front of each of our quadrant photodiodes.

The commissioning of the full Virgo ITF has proceeded through three main steps:

- commissioning of a single Fabry-Perot (FP);
- recombination of the two FPs (not recycled Michelson);
- recycled Michelson (final configuration).

The first phase, began in July 2003 on the North-arm FP, was then extended to the West-arm FP, and was successfully completed at the beginning of 2004. The second phase is practically

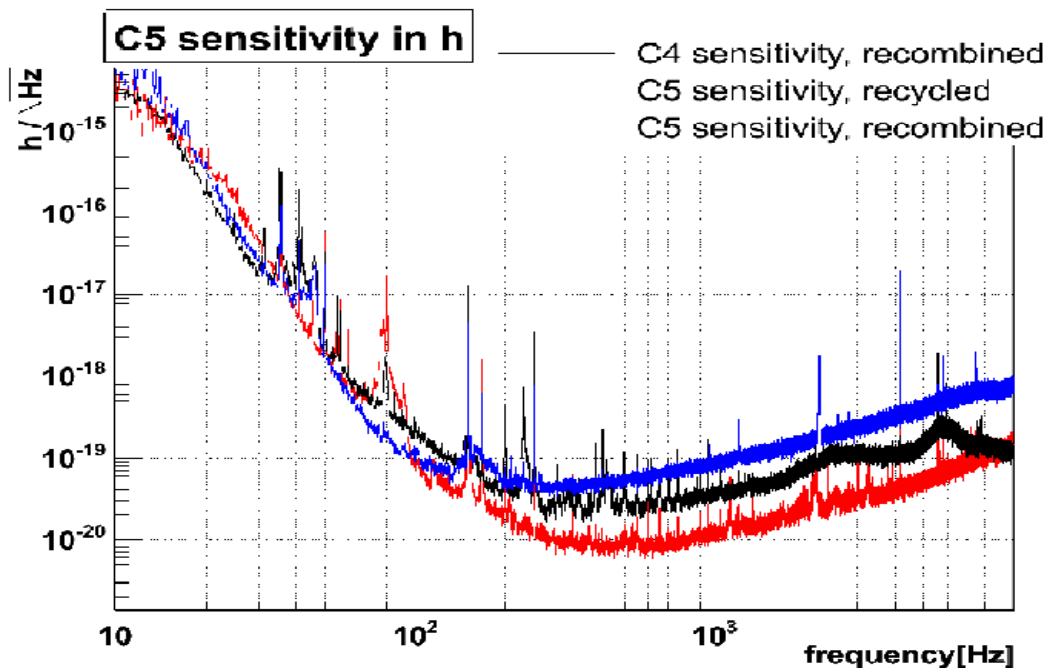


Figure 1: *Sensitivity during the engineering runs C₄ and C₅.*

completed including the full integration of the linear alignment system. We are currently working in the third, and final, phase of the commissioning.

During 2004 four engineering runs have been performed:

- C2 - with North and West arms locked separately;
- C3 - North cavity locked with second stage frequency stabilization and automatic alignment;
- C4 - ITF in recombined mode including automatic alignment;
- C5 - ITF in recombine and recycled mode.

The sensitivities achieved in the last two runs are shown in fig. 1.

4 Activity in 2005

Participation to the scientific runs and to data analysis activities.

5 Publications

1. F. Acernese *et al.*, *Astropart. Phys.* **20**, 617 (2004).
2. F. Acernese *et al.*, *Astropart. Phys.* **20**, 629 (2004).
3. F. Acernese *et al.*, *Astropart. Phys.* **21**, 1 (2004).
4. F. Acernese *et al.*, *Astropart. Phys.* **21**, 465 (2004).

WIZARD

S. Bartalucci, G. Basini, F. Bongiorno (Ass.), L. Bongiorno (Ass. Ric.),
G. Mazzenga (Tecn.), M. Ricci (Resp.)

Participant Institutions:

ITALY: INFN Bari, LNF, Firenze, Napoli, Roma2, Trieste;
CNR Ist. Fisica Applicata “Nello Carrara” Firenze;
ASI (Italian Space agency);
Electronic Engineering Department, University of Roma 2 “Tor Vergata”;
RUSSIA: MePhi Moscow;
FIAN Lebedev Moscow;
IOFFE St Petersburg;
TsSKB-Progress Samara;
SWEDEN: KTH Stockholm;
GERMANY: Siegen University;
USA: NASA Goddard Space Flight Center;
New Mexico State University.

1 Experimental Program and Scientific Objectives

The WIZARD experimental program is devoted to the extensive study of cosmic ray spectra (particles, antiparticles, isotopes, abundances and search for antimatter) in several energy ranges achievable through different instruments on board stratospheric balloons and long duration satellite missions. WIZARD is an International Collaboration between several Universities and Research Institutions from Russia, Sweden, Germany, USA together with the Space Agencies NASA, RSA (Russia), SNSB (Sweden), DLR (Germany) and ASI. The experimental activities have been and are carried out through three main programs:

- Balloon flights;
- Satellite missions NINA-1 and NINA-2;
- Satellite mission PAMELA.

We refer to previous editions of this report for the description of the activities related to the balloon flights and to the two NINA missions.

1.1 The satellite mission PAMELA

PAMELA is a cosmic ray space experiment that will be installed on board a Russian satellite (Resurs-DK1) whose launch is foreseen in fall 2005 from the cosmodrome of Baikonur, Kazakhstan, by a Soyuz TM2 rocket. The satellite will fly for at least 3 years in a low altitude, elliptic orbit (300-600 km) with an inclination of 70.4 degrees. The PAMELA telescope consists of a magnetic spectrometer including a permanent magnet coupled to a silicon tracker, a Transition Radiation Detector, an imaging silicon-tungsten calorimeter, a time-of-flight system, an anticoincidence detector, a shower tail catcher scintillator and a neutron detector ^{1, 2}). A sketch of the PAMELA instrument is shown in fig.1.

The total height of PAMELA is 120 cm, the mass is 440 kg, the power consumption is 385 W and the geometrical factor is 20.5 cm² sr.

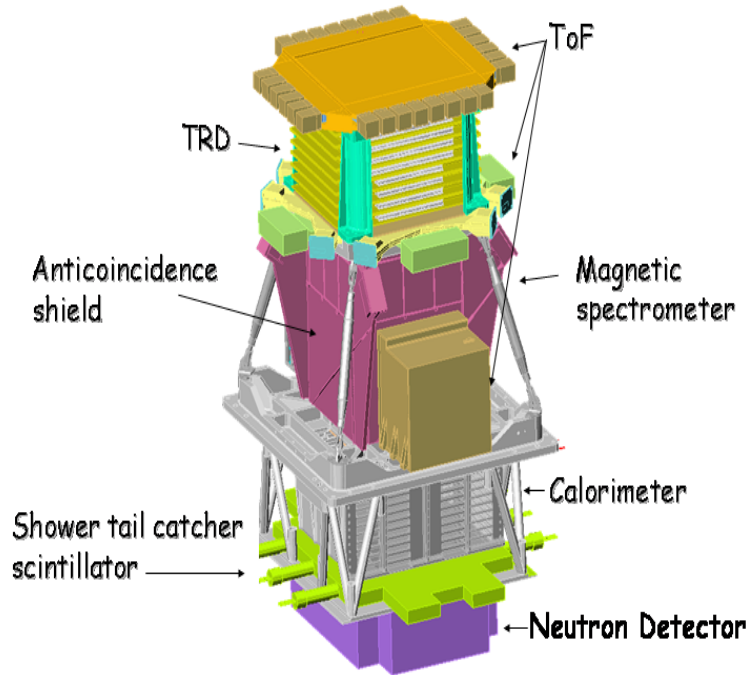


Figure 1: The PAMELA telescope and its main detectors.

The observational objectives of the PAMELA experiment are to measure the spectra of antiprotons, positrons and nuclei in a wide range of energies, to search for antimatter and for indirect signatures of dark matter and to study the cosmic ray fluxes over a portion of the solar cycle.

The main scientific goals can be schematically listed as the following:

- a) measurement of the antiproton spectrum in the energy range 80 MeV-190 GeV;
- b) measurement of the positron spectrum in the energy range 50 MeV-270 GeV;
- c) search for antinuclei with a sensitivity of $\sim 3 \times 10^{-8}$ in the \overline{He}/He ratio;
- d) measurement of nuclei spectra (He, Be, C) at energies up to 700 GeV/n;
- e) measurement of the electron spectrum in the energy range 50 MeV-2 TeV.

In addition, the PAMELA experiment will be able to measure the light nuclear component of cosmic rays and investigate phenomena connected with Solar and Earth physics.

Activity in the year 2004 has covered the following items:

- Integration and compatibility tests (power, telecommands, data transmission, magnetic) of the Technological/Engineering Model (TM) at TsSKB Progress plant (Samara, Russia).
- Integration and tests of the PAMELA Flight Model (FM) in Roma 2 clean rooms.
- Completion and tests of flight CPU.
- Specifications of the PAMELA downlink system.
- Development of control and command software and of general instrument Monte Carlo simulation (GPAMELA).

2 Activity of the LNF group during year 2004

The LNF WIZARD group has been fully involved in all the previous balloon and present satellite programs.

After completing the beam test campaign at CERN in 2003, during the year 2004 the activity for the PAMELA experiment has been carried on as follows:

- Responsibility of the Mechanical Ground Support Equipment (MGSE) for the assembly and integration of the whole apparatus.
- Preparation, assembly and tests of the Technological/Engineering Model.
- Preparation, assembly and tests of the Flight Model.
- Completion and equipment of the transport container for the Flight Model.

3 Planned activity in 2005

- Completion of PAMELA Flight Model, integration and ground tests with cosmoics.
- Establishment of the PAMELA data network and Data Center.
- Shipment and delivery of Flight Model to TsSKB Progress plant (Samara, Russia).
- Tests and integration with spacecraft Resurs DK1.
- Pre-launch readiness tests and launch from Baikonur space center (Kazakhstan).
- Data taking: first phase and establishment of downlink procedures.

4 List of Publications in 2004

1. M.Boezio *et al.*, "PAMELA: A satellite experiment for antiparticles measurement in cosmic rays"; IEE Trans. Nucl. Sci. **51**, (2004) 854.
2. M. Boezio *et al.*, "The Space Experiment PAMELA"; Nucl. Phys. B (Proc. Suppl.) **134**, (2004) 39.
3. R. Sparvoli *et al.*, "Qualification tests of the space telescope PAMELA"; Nucl. Phys. B (Proc. Suppl.) **134**, (2004) 69.

References

1. M. Simon for the PAMELA collaboration: "Status of the PAMELA experiment ", Proc. 28th International Cosmic Ray Conference (Tsukuba, Japan, 2003) **OG 1.5** p.2117.
2. O. Adriani *et al.* "The PAMELA experiment on satellite and its capability in cosmic ray measurements", NIM **A478** (2002) 114.

AIACE

E. De Sanctis (Dir.), M. Mirazita (Ass. Ric.), A. Orlandi (Tech.), W. Pesci (Tech.),
E. Polli, F. Ronchetti (Ass. Ric.), P. Rossi (Resp. Naz.), A. Viticchié (Tech.)

1 Introduction

AIACE stands for Attività Italiana A CEbaf. It is the collaboration of the INFN groups of Frascati and Genova which participate into the physics program carried in the Hall B at the 6 GeV Continuous Electron Beam Accelerator Facility (CEBAF) at the Jefferson Laboratory (JLab). The Hall B collaboration counts about 140 physicists from 35 Institutions from seven Countries.

The scientific program of Hall B, which is equipped with the CLAS detector ¹⁾, is the precision study of the structure of the nucleon and the nature of the strong interaction.

This scientific program can be summarized in the following main topics: search for exotic mesons and baryons, dynamics of the strong interactions, spin structure functions in the resonance region, nucleon tomography, baryon resonances.

In the period covered by this report the Frascati group has carried out:

- the publication on Physical Review Letters and Physical Review C of two papers on the deuteron photodisintegration cross section between 0.5 and 3.0 GeV.
- The data analysis of the reaction $\gamma d \rightarrow \Theta^+ \Lambda$ for the search of the pentaquark Θ^+ using old CLAS data with small statistics and the write-up of an internal CLAS-ANALYSIS-NOTE.
- The data taking of high statistics runs on deuteron and proton target (g10 and g11 runs) for the search of the pentaquark baryon states.
- The start-up of the data analysis for the search of the pentaquark baryon state Θ^+ in the reaction channel $\gamma d \rightarrow \Theta^+ \Lambda$ using the g10 data.
- The start-up of the paper “ Θ^+ production in exclusive reactions $\gamma p \rightarrow \bar{K}^0 \Theta^+$ and $\gamma p \rightarrow K^{*0} \Theta^+$ within the Quark-Gluon Strings Model”.
- The construction and commissioning of the new start counter for CLAS.
- The elaboration of a Letter of Intent to measure the nucleon form factor in the time-like region with DAΦNE.

2 Onset of asymptotic scaling in exclusive photoreactions

2.1 Deuteron photodisintegration (Experiment E93-017): Quantum Chromodynamics (QCD) has been successfully applied in describing the structure and production of hadrons at high energies where perturbation theory can be used. There one can derive QCD scaling laws for the cross sections and hadronic helicity conservation laws. However, nuclear reactions have been conventionally described in terms of baryons and mesons rather than quarks and gluons. It is therefore interesting and important to know in which energy region the transition from hadronic picture to quark-gluon picture takes place. This is why major efforts in nuclear physics have been devoted to looking for qualitatively new phenomena which arise from the underlying quark degrees-of-freedom, and which cannot be modeled using meson field theories.

Deuteron photodisintegration at high energies is especially suited for this study, because a

relatively large amount of momentum is transferred to the nucleons for a relatively low incident photon energy. One possible signature for the transition from nucleon-meson to quark-gluon degrees of freedom is the scaling of reaction cross sections above some incident photon energy. In particular, simple Constituent Counting Rules (CCR) ²⁾ predict an asymptotic s^{-11} dependence of $d\sigma/dt$ of the process at all proton angles. Here s and t are the invariant Mandelstam variables.

To give a clearer answer to this important question, the CLAS experiment E93-017 at Jefferson Lab performed an extensive measurement of the deuteron photodisintegration cross section between 0.5 and 3.0 GeV and over an almost complete proton angular range ($\vartheta_p^{CM} = 10^\circ\text{--}160^\circ$). These recent, extensive cross section data ³⁾ (together with all previous data) offered the unique opportunity for a detailed study of the energy dependence of the $d(\gamma, p)n$ differential cross section at fixed angles to looking for the onset of cross section scaling at some incident photon energy.

The obtained results show that the s^{-11} scaling has been reached for proton transverse momentum above about 1.1 GeV/c. This is shown in Fig. 1 where all cross section data, multiplied by s^{11} , from all the high-energy $\gamma d \rightarrow pn$ experiments ^{3, 4, 5, 6, 7)} at fixed proton angle between 50° and 130° and $P_T \geq 1.1$ GeV/c have been fit to s^{-11} . The fits are limited to these angles, because at $\vartheta_p^{CM} = 35^\circ, 45^\circ, 135^\circ$, and 145° there are not enough data above $P_T = 1.1$ GeV/c to make a reliable fit. The χ_ν^2 of the fits are given in the plots. The vertical arrows indicate the s value corresponding to $P_T = 1.1$ GeV/c. It is worth noticing that for $\vartheta_p^{CM} = 35^\circ$ the last three points show a clear flat behaviour well consistent with an s^{-11} -dependence. For all but two of the fits, $\chi_\nu^2 \leq 1.34$. This shows that the s^{-11} dependence of the cross section is established for $P_T \geq 1.1$ GeV/c. This is a necessary condition for the transition to the QCD scaling.

2.2 Single pion photoproduction: Single pion photoproduction reactions are essential probes of the transition from meson-nucleon degrees of freedom to quark-gluon degrees of freedom in exclusive processes. The cross sections of these processes are also advantageous, for investigation of the oscillatory behavior around the quark counting prediction, since they decrease relatively slower with energy (s^{-7}) compared with other photon-induced processes. Recent data from JLab Hall A show dramatic change in the scaled differential crosssection from the $\gamma n \rightarrow \pi^- p$ and $\gamma p \rightarrow \pi^+ n$ processes in the c.m. energy between 1.8 GeV to about 2.4 GeV and for $\theta_{CM} = 90^\circ$. The AIACE group has started the analysis of the g10 data on the $\gamma n \rightarrow \pi^- p$ to investigate this behavior in much finer photon energy bins and for a wide angular range. Furthermore, the angular dependence of the scaling behavior for this process will also be studied in detail.

3 Search of the pentaquark baryon state Θ^+

All the well-established particles can be categorized using the constituent quark model which describes light mesons as bound states of $q\bar{q}$ pairs, and baryons as bound 3-quarks states. On the other hand, QCD does not prevent more complicated internal structures of mesons and baryons like for example 5-quarks ($qqqq\bar{q}$) states, where the \bar{q} has different flavor than the others quarks. These states, with quark content other than $q\bar{q}$ or qqq are termed as *exotics*.

Although the lack of clear experimental evidence of exotic particles for decades, theoretical work on this subject was continued and in 1997 Diakonov, Petrov and Polyakov ⁸⁾, in the framework of the Chiral Quark Soliton Model, predicted an antidecuplet of 5-quarks baryons, with spin and parity $J^\pi = 1/2^+$. The lowest mass member is an isosinglet state, dubbed Θ^+ , with quark configuration ($uudd\bar{s}$) giving $S=+1$, with mass ~ 1.54 GeV and width of around 15 MeV.

Experimental evidence for a $S=+1$ baryon resonance with mass 1.54 GeV and width less than 25 MeV has been reported for the first time by the LEPS Collaboration at SPring-8 ⁹⁾ in the photoproduction on neutron bound in a carbon target. Immediately after, several other

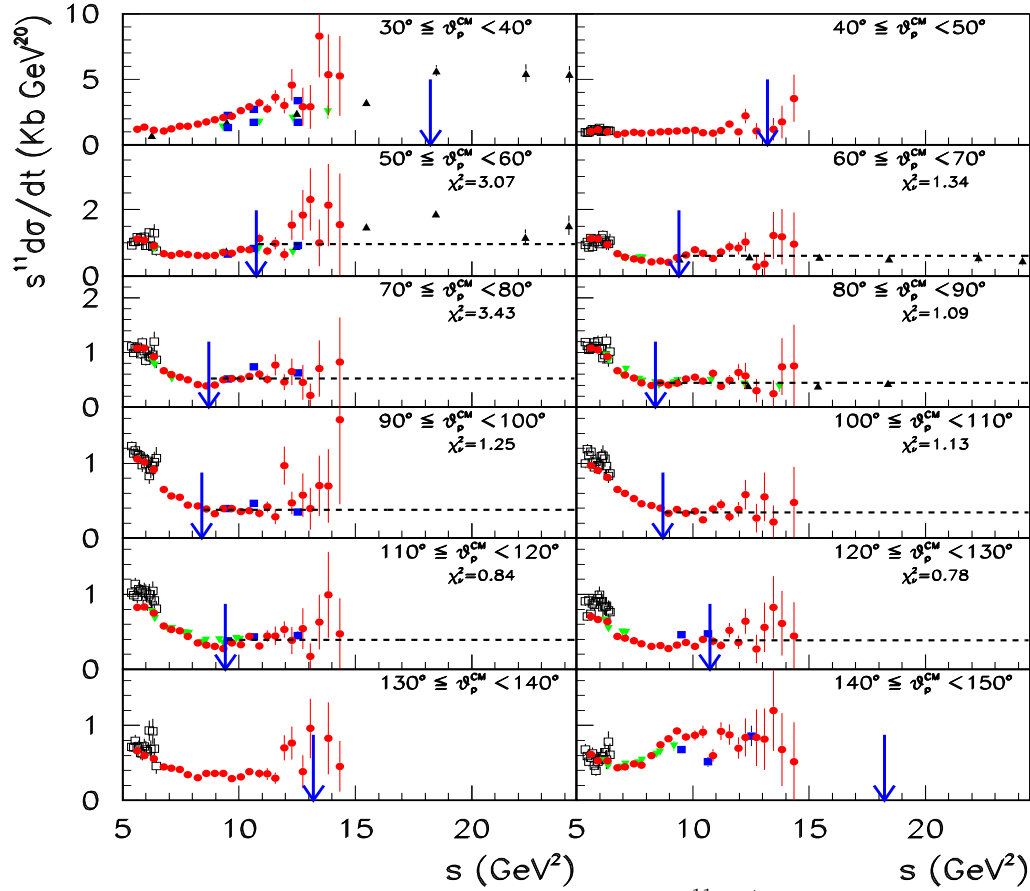


Figure 1: Deuteron photodisintegration cross section, $s^{11}d\sigma/dt$, as a function of s for the given proton scattering angles. Dashed lines are the fits of the data to s^{-11} for $P_T \geq 1.1$ GeV/c. The vertical arrows indicate the s value corresponding to $P_T = 1.1$ GeV/c. Fits are not shown for $\vartheta_p^{CM} = 35^\circ, 45^\circ, 135^\circ$, and 145° where there are not enough data above 1.1 GeV/c. Data are from CLAS ³⁾ (full/red circles), Mainz ⁴⁾ (open/black squares), SLAC ⁵⁾ (full-down/green triangles), JLab Hall C ⁶⁾ (full-up/black triangles) and JLab Hall A ⁷⁾ (full/blue squares).

experimental groups analyzing previously obtained data, have found this exotic baryon in both his decaying channels $\Theta^+ \rightarrow pK^0$ and nK^+ ¹⁰⁾.

The reported masses in some cases vary by more than the uncertainties given for the individual experiments, ranging from 1522 to 1555 MeV, with the masses obtained from processes involving nK^+ signals in the initial or final states giving on average 10-15 MeV higher values than those in the pK^0 channel. The observed width (FWHM) are comprised between (10 – 30) MeV, but in all cases they are dominated by the experimental resolution.

The relatively small statistical significance in every measurement, possibly explained by the fact that all the results come from the analysis of data taken for other purposes, and the discrepancy in mass determination, are not the only problems to face to overcome the reticence to accept the existence of the pentaquark. In fact, a major problem frequently mentioned, is that several experiments at high statistic and high energies reported negative results in searches for the Θ^+ ¹¹⁾. However the different kinematical and experimental conditions between the low energy exclusive experiments and the high energy semi-inclusive experiments do not allow a direct comparison so

that the null results do not prove that the positive ones are wrong.

To find a definite answer to the question of existence of the Θ^+ and of the other 5-quark baryons and, if they do exist, to determinate their intrinsic properties (mass, width, spin, parity) and the reaction mechanism for their production, a broad experimental programs has been approved in the Hall B. The new dedicated experiments, whose main features are summarized in Table 1, aim to improve the statistical accuracy of the measurements by at least one order of magnitude.

Table 1: Summary table of the new dedicated experiments in Hall B at JLab for the search of exotics baryons.

EXP.	SEARCH	TARGET	RUNNING PERIOD	E (GeV)
E03-113 (<i>g10</i>)	Θ^+	LD_2	3/13 - 5/16/04	$E_\gamma = 0.8 - 3.6$
E04-021 (<i>g11</i>)	$\Theta^+, \Theta^{+*}, \Theta^{++}$	LH_2	5/22 - 7/25/04	$E_\gamma = 0.8 - 3.8$
E04-010 (<i>eg3</i>)	Ξ_5	LD_2	11/20/04 - 1/31/05	$E_{e^-} = 5.7$
E04-017 (<i>super g</i>)	Θ^+, Ξ_5	LH_2	2 nd half 2005	$E_\gamma = 1.5 - 5.4$

The Frascati Aiace group is deeply involved in this program: two new approved proposals are signed by the members of the group which also participated to the construction of the new Start Counter of the CLAS detector, necessary to run the new experiments at higher rates. Moreover they served as run coordinators during the data taking of both g10 and g11 runs and they are looking at the Θ^+ signal in the reaction channel $\gamma d \rightarrow \Theta^+ \Lambda(1115)$ in the new data on deuteron. The analysis of the same channel has been also undertaken using old CLAS data with small statistics and an internal CLAS-ANALYSIS-NOTE has been released. Finally, the group is working with a theoretical group from ITEP for the description of the Θ^+ production in exclusive reactions $\gamma p \rightarrow \bar{K}^0 \Theta^+$ and $\gamma p \rightarrow \bar{K}^{*0} \Theta^+$ within the Quark-Gluon Strings Model.

4 Nucleon form factor in the time-like region

The possibility to fully measure nucleon form factors in the time-like region in the proposed high energy upgrade of DAΦNE machine is under investigation within the AIACE group. Differential $e^+e^- \rightarrow p\bar{p}$ and $e^+e^- \rightarrow n\bar{n}$ cross section should be measured, in order to extract the moduli of proton and neutron form factors. The relative phase between electric and magnetic form factors (never measured yet) can be obtained by measuring the polarization of the outgoing nucleon in the normal direction to the scattering plane. The elaboration of a Letter of Intent is underway and will be released soon.

5 List of Publications

1. R. Niyazov *et al.* and CLAS collaboration, “Two-Nucleon Momentum Distributions Measured in $3\text{He}(e,e'pp)n$ ”, Phys. Rev. Lett. **92**, (2004), 052303.
2. J.W.C. McNabb *et al.* and CLAS collaboration, “Hyperon Photoproduction in the Nucleon Resonance Region”, Phys. Rev. **C69**, (2004), 042201.
3. K. McCormick *et al.* and CLAS collaboration, “Tensor polarization of the ϕ meson photo-produced at high t ”, Phys. Rev. **C69**, (2004), 032203.
4. H. Avakian *et al.* and CLAS collaboration, “Measurement of Beam-Spin Asymmetries for π^+ Electroproduction above the Baryon Resonance Region”, Phys. Rev. **D69**, (2004), 112004.

5. V. Kubarovsky *et al.* and CLAS collaboration, “Observation of an Exotic Baryon with $S=+1$ in Photoproduction from Proton”, *Phys. Rev. Lett.* **92**, (2004), 032001.
6. V.Yu Grishina, L.A. Kondratyuk, W. Cassing, E. De Sanctis, M. Mirazita, F. Ronchetti, P. Rossi, “Forward-backward angle asymmetry and polarization observables in high-energy deuteron photodisintegration”, *Eur. Phys. Jour.* **A 19**, (2004), 117.
7. M. Mirazita, F. Ronchetti, P. Rossi *et al.* and CLAS collaboration, “Complete Angular Distribution Measurements of Two-Body Deuteron Photodisintegration between 0.5 and 3 GeV”, *Phys. Rev.* **C70**, (2004), 014005.
8. A. V. Stavinsky *et al.* and CLAS collaboration, “Proton Source Size Measurements in the $eA \rightarrow e'ppX$ Reaction”, *Phys. Rev. Lett.* **93**, (2004), 192301.
9. D. Protopopescu *et al.* and CLAS collaboration, “Survey of $A_{LT'}$ Asymmetries in Semi-Exclusive Electron Scattering on He4 and C12”, Accepted in *Nucl. Phys.*; nuc-ex/0405021.
10. K. Joo *et al.* and CLAS collaboration, “Measurement of the polarized structure function $\sigma_{LT'}$ for $p(\vec{e}, e'\pi^+)n$ in the Δ resonance region”, *Phys. Rev.* **C70**, (2004), 042201.
11. S. Nicolai *et al.* and CLAS collaboration, “Complete Measurements of Three-Body Photodisintegration of ^3He for Photon Energies between 0.35 and 1.55 GeV”, *Phys. Rev.* **C70**, (2004), 064003.
12. P. Rossi *et al.* and CLAS collaboration, “Onset of asymptotic scaling in deuteron photodisintegration”, *Phys. Rev. Lett.* **94**, (2005), 012301; hep-ph/0405207.
13. J. Price *et al.* and CLAS collaboration, “Exclusive Photoproduction of the Cascade (Ξ) Hyperons”, Submitted to *Phys. Rev. C*; nucl-ex/0409030.

6 Presentation at Conferences

1. Marco Mirazita, *Experimental evidence of an exotic $S = +1$ baryon*. Invited talk at the “Xlii International Winter Meeting On Nuclear Physics” - Bormio (Italy), January 25-February 1, 2004.
2. Federico Ronchetti, *AIACE, HERMES and PANDA: Status and Perspectives*, Invited talk at “Iii Workshop Sulle Problematiche Di Calcolo E Reti Nell’infni” - Cagliari (Italy), May 24-28 2004.
3. Patrizia Rossi, *Experimental search for pentaquark*. Invited talk at the “International Nuclear Physics Conference -INPC2004” - Goteborg (Sweden) June 27- July 2 2004.
4. Patrizia Rossi, *Onset of Asymptotic Scaling in Deuteron Photodisintegration*. Contributed talk at the “International Nuclear Physics Conference -Inpc2004” - Goteborg (Sweden) June 27- July 2 2004.
5. Patrizia Rossi, *Pentaquark search at JLab.*, Invited talk at the “Advanced Studies Institute - Symmetries And Spin” - Prague (Czech Republic) July 5-10 2004.
6. Marco Mirazita, *Onset of Asymptotic Scaling in Deuteron Photodisintegration*. Contributed talk at the “19 European Few-Body Conference” - Groninger (Netherlands) August 23-27 2004.

7. Marco Mirazita, *Experimental evidence of an exotic $S = +1$ baryon*. Invited talk at the “XC Congresso SIF” - Brescia (Italy), September 20-26, 2004.
8. Marco Mirazita, *Onset of Asymptotic Scaling in Deuteron Photodisintegration*. Contributed talk at the “XC Congresso SIF” - Brescia (Italy), September 20-26, 2004.
9. Patrizia Rossi, *Ricerca sperimentale della Θ^+ nella reazione $\gamma d \rightarrow \Theta^+ \Lambda$ con CLAS*. Contributed talk at the “XC Congresso SIF” - Brescia (Italy), September 20-26, 2004.
10. Patrizia Rossi, *The experimental search for the Θ^+ in the $\gamma d \rightarrow \Theta^+ \Lambda$ reaction with Clas*. Contributed talk at “Baryon04” - Palaiseau (France) October 25-29 2004.

References

1. B. Mecking *et al.*, Nucl. Instr. and Meth. **A503/3**, (2003) 513.
2. V. Matveev *et al.*, Lett. Nuovo Cimento **7**, (1973) 719; S. L. Brodsky, G. L. Farrar, Phys. Rev. Lett. **31**, (1973) 1153.
3. M. Mirazita *et al.*, Phys. Rev. C **70**, (2004) 014005.
4. R. Crawford *et al.*, Nucl. Phys. A **603**, (1996) 303.
5. J. Napolitano *et al.*, Phys. Rev. Lett. **61**, (1988) 2530; S. J. Freedman *et al.*, Phys. Rev. C **48**, (1993) 1864; J. E. Belz *et al.*, Phys. Rev. Lett. **74**, (1995) 646.
6. C. Bochna *et al.*, Phys. Rev. Lett. **81**, (1998) 4576; E. C. Schulte *et al.*, Phys. Rev. Lett. **87**, (2001) 102302-1.
7. E. C. Schulte *et al.*, Phys. Rev. C **66**, (2002) 042201R.
8. D. Diakonov, V. Petrov, M.V. Polyakov, Z. Phys. A359, (1997) 305.
9. T. Nakano *et al.*, Phys. Rev. Lett. **91**, (2003) 012002; hep-ex/0301020.
10. V. Barmin *et al.*, Phys. Atom. Nucl. **66**, (2003) 1715; S. Stepanyan *et al.*, Phys. Rev. Lett. **91**, (2003) 252001; V. Koubarovsky *et al.*, Phys. Rev. Lett. **92**, (2004) 032001; *ibidem* **92** (2004) 049902(E); J. Barth *et al.*, Phys. Lett. B572, (2003) 127; A. Airapetian *et al.*, Phys. Lett. B585, (2004) 213; A.E. Asratyan, A.G. Dolgolenko, M.A. Kubantsev, Phys. Atom. Nucl. **67**, (2004) 682; Yad. Fiz. **67**, (2004) 704; A. Aleev *et al.*, hep-ex/0401024; M. Abdel-Bary *et al.*, Phys. Lett. B595, (2004) 127; S. Chekanov *et al.*, Phys. Lett. B591, (2004) 7.
11. J.Z. Bai *et al.*, hep-ex/0402012; K.T. Knoepfle *et al.*, hep-ex/0403020; M.I. Adamovich *et al.*, hep-ex/0405042; C. Pinkeburg hep-ex/0404001; BABAR, hep-ex/0408064; Yu.M. Antipov *et al.*, hep-ex/0407026; S. Schaet *et al.*, Phys. Lett. B **599**, (2004) 1; CDF, E690, LEP, Focus, HyperCP (QNP2004 conference presentation, still unpublished).

FINUDA

L. Benussi (Art. 23), M. Bertani, S. Bianco, M. A. Caponero (Ass.), F. L. Fabbri, P. Gianotti (Resp.), M. Giardoni, V. Lucherini, E. Pace, M. Pallotta, S. Tomassini (Art. 23), L. Passamonti (Tecn.), D. Pierluigi (Art. 15), F. Pompili (Art. 23), A. Russo (Art. 15)

1 Introduction

FINUDA (FISica NUCleare a DAΦNE) is an experiment devoted to hypernuclear physics studies. Hypernuclei are nuclear systems in which one or more nucleons are replaced by a hyperon. This adds explicit strangeness to the nuclear system allowing to study, in a more general environment, the baryon-baryon interaction.

At FINUDA, hypernuclei are produced via the reaction:

$$K^- + {}^A_Z \rightarrow {}^A_{\Lambda} Z + \pi^- \quad (1)$$

stopping K^- from $\phi(1020)$ decay almost at rest into a thin ($\sim 0.2 \text{ g cm}^{-2}$) target. The spectroscopy of the hypernuclear levels produced is performed by measuring the momentum of the outgoing π^- . Therefore, it is crucial to determine this quantity very precisely. FINUDA has been designed to reach a momentum resolution of 0.4% corresponding to an energy resolution, of the hypernuclear level, of $\sim 840 \text{ keV}$ ($FWHM$). Moreover, the products of the sub-sequent decay of the Λ embedded in the nucleus can be detected by FINUDA, allowing to investigate the decay mechanisms of hypernuclei, a feature never reached by any other experiment.

The FINUDA detector is a large acceptance magnetic spectrometer housed inside a superconducting solenoid (2.7 m length and 2.4 m diameter) providing a field of 1 T. The apparatus can be sub-divided in two distinct areas: the interaction-target region and the outer tracking one. The former, surrounding the DAΦNE beam pipe, consists of a barrel of plastic scintillators, a layer of double-sided silicon microstrips, and the target station, which can house up to 8 different materials. The latter consists of several layers of tracking detectors: a double-sided silicon microstrip array, two layers of planar drift chambers, and six layers of straw tubes. The outermost detector of the whole complex is a second barrel of plastic scintillators, for trigger purposes and neutron detection. The whole FINUDA tracking volume ($\sim 8 \text{ m}^3$) is filled with helium to reduce multiple-Coulomb scattering that is the main factor limiting the momentum resolution.

The FINUDA Collaboration consists of 40 physicists coming from LNF, several INFN sections and universities (Torino, Bari, Trieste, Pavia, Brescia) plus foreign researchers from the TRIUMF laboratory of Vancouver, Canada, the KEK laboratory of Tsukuba, Japan, and the Seoul National University, South Korea.

2 FINUDA activity in 2004

The activity of the LNF FINUDA group during 2004 has been devoted to the continuation of the first round of data taking on DAΦNE. After that, an intense activity of data analysis began in order to produce scientific results.

2.1 Data taking

FINUDA has performed its first data taking from October 2003 up to March 22, 2004. A first sample of data, corresponding to an integrated luminosity of about 50 pb^{-1} , has been collected both for machine and detector calibration purposes. Further 200 pb^{-1} have been acquired and are being used for the scientific analyses.

2.2 Scientific program of the first FINUDA run

For its first data taking FINUDA has mounted the following set of targets: three ^{12}C , two ^6Li , one ^7Li , one ^{27}Al , one ^{51}V . With the two ^6Li targets FINUDA can access light hypernuclear systems; $^6_\Lambda\text{Li}$ is unstable for proton emission and it decays into $^5_\Lambda\text{He} + \text{p}$, or it may transform into $^4_\Lambda\text{He} + \text{p} + \text{n}$, or into $^4_\Lambda\text{H} + \text{p} + \text{p}$ via a Coulomb assisted mechanism. Furthermore, ^6Li data are used to look for neutron rich hypernuclei and deeply bound kaonic systems. $^7_\Lambda\text{Li}$ is the hypernucleus most extensively studied from the γ -spectroscopy point of view by means of Ge detectors, but its decays are not known. FINUDA can therefore complete the knowledge of this system adding the missing information. The choice of installing three ^{12}C targets is motivated by the fact that $^{12}_\Lambda\text{C}$ is the most studied hypernucleus. Therefore, it can be used as a reference system to tune FINUDA detector performance. Furthermore, being the spectrometer characteristics better than those available in previous experiments, some improvements on the resolution of hypernuclear levels and in the knowledge of the decay modes are also expected. ^{27}Al , and ^{51}V targets have been selected to perform a first study of medium-heavy hypernuclei. For $^{27}_\Lambda\text{Al}$ there are old data taken with a very coarse energy resolution (6 MeV *FWHM*). The excitation spectrum of $^{51}_\Lambda\text{V}$ has been measured at KEK (using a different production mechanism) with an energy resolution of 1.65 MeV *FWHM*. The peaks corresponding to *p* and *d* orbits show possible splitting that might be better resolved with the FINUDA higher resolution.

2.3 Data analysis

2.3.1 Hypernuclear spectroscopy

In order to evaluate the capabilities of FINUDA to yield relevant spectroscopic parameters, the analysis started on the best known hypernucleus $^{12}_\Lambda\text{C}$. Nevertheless, hypernuclear peaks are visible in all the target materials, as shown in fig.1.

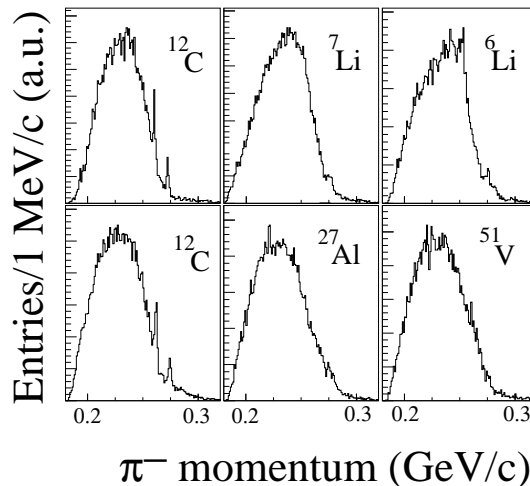


Figure 1: *Inclusive π^- momentum spectra from different nuclear targets.*

2.3.2 Results on $^{12}_\Lambda\text{C}$

In order to obtain the Λ binding energy distribution ($-B_\Lambda$) the contribution of the two nucleon K^- absorption $K^-(NN) \rightarrow \Sigma^- N$ followed by $\Sigma^- \rightarrow n\pi^-$, is subtracted from the π^- momentum

distribution. Fig. 2 displays $-B_\Lambda$ for ${}^{12}_\Lambda\text{C}$. Here the data of only two targets have been summed since the third one showed a slight systematic energy displacement that must be corrected with better detector calibrations. The curve, drawn over the histogram, is the result of the best fit performed using seven gaussians for the hypernuclear states, and a proper function for the residual background. The obtained energy resolution of 1.250 MeV (*FWHM*), already represents an

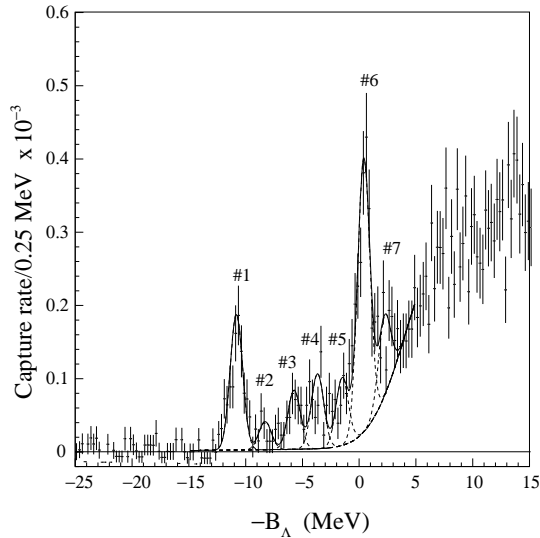


Figure 2: *The hypernuclear levels of ${}^{12}_\Lambda\text{C}$.*

improvement with respect to the best measurement performed by the E369 collaboration at KEK (1.450 MeV). This value is not far from the FINUDA expected one (0.840 MeV), that will be reached as soon as the final alignment of all the sub-detectors will be performed. The spectrum of fig. 2 shows two new peaks: one at $-B_\Lambda = 0.27$ MeV, and a second at $-B_\Lambda = 2.1$ MeV. Moreover, the peaks in the region between $10 \text{ MeV} < -B_\Lambda < -1.0 \text{ MeV}$ are here more clearly resolved than in the previous experiments. Those at lower energy (#2 and #3) are linked to ${}^{11}\text{C}$ core excitation, while the explanation of the others (#4 and the newly observed #5) is puzzling. The capture rates, per stopped K^- , for the seen hypernuclear levels have been determined. In particular, for the ground state, it turns out to be $1.01 \cdot 10^{-3} \pm 0.11 \text{ stat} \pm 0.10 \text{ sys}$, in agreement with previous measurements, and confirming a discrepancy between experiment and theory that forecasts capture rates smaller of a factor from two to three.

2.3.3 Hypernuclear decay

FINUDA can study not only the hypernuclei formation reaction, but also their decays or, more generally, all the processes that follow K^- nucleus interaction. Inside the nucleus, due to the Pauli blocking mechanism, the Λ decay into pion-nucleon pairs is inhibited. This effect increases with nucleon number, and therefore hypernuclei decay via different weak interactions involving four baryons: $\Lambda + N \rightarrow n + N$, N being a neutron or a proton. FINUDA is able to detect both the protons and the neutrons from hypernuclear decay, and hence to measure these reaction channels. This allows to obtain experimental information on weak interaction between four baryons involving strangeness. Fig. 3 shows the momentum spectra of the protons measured in coincidence with negative pions emitted in the region expected for the hypernuclear states. The ability of FINUDA to detect particles produced following K^- interaction allows also to investigate other rare processes.

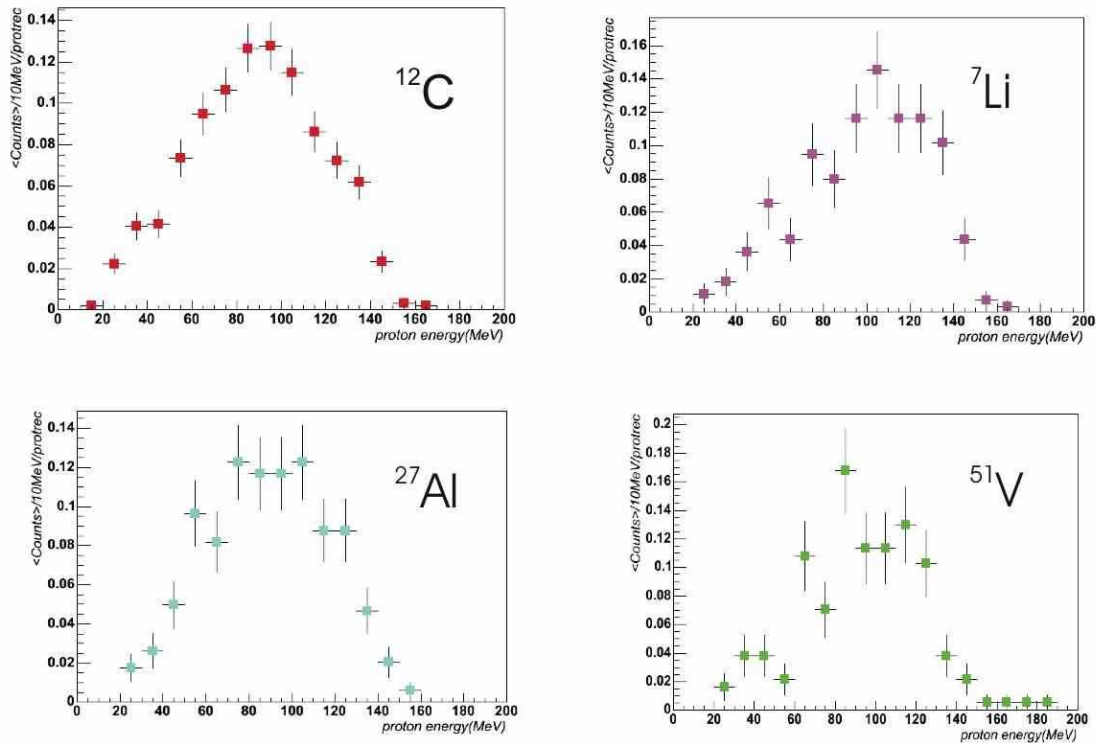


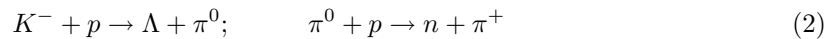
Figure 3: *Momentum spectra of protons, emitted in coincidence with π^- whose momentum lie in the region of hypernuclear levels, for different nuclear targets.*

One of these is shown in fig. 4. Here the rare non mesonic decay of ${}^4_{\Lambda}\text{He}$, formed after K^- capture on the ${}^6\text{Li}$ target, into a dd pair (d being a deuteron) can be seen for the first time.

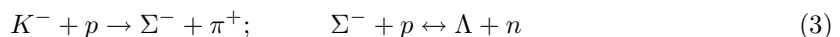
2.3.4 Search for neutron rich hypernuclei

The existence of Λ hypernuclei with a large neutron excess has been predicted but never observed. A Λ in a nucleus can provide an extra binding for the nucleons, and being not affected by the Pauli exclusion principle, a larger number of neutrons can be bounded with respect to ordinary matter. The search of neutron-rich hypernuclei is relevant in order to fill up the chart of nuclei with strangeness $S = -1$, and has relevance in several fields of physics. FINUDA can investigate the existence of neutron-rich hypernuclei through two reactions.

- Double charge exchange:



- Strangeness exchange with Σ - Λ coupling:



Both mechanisms produce in the final state a Λ hypernucleus in which the original (Z, A) nucleus is transformed into a “neutron-enriched” $(Z-2, A)$ system. The neutron enrichment is more significant for light nuclei, and therefore the search for this states is carried out on light targets. A monochromatic π^+ emitted after K^- interaction would be the signature for such events, whose

momentum depends from the formed hypernuclear state. A typical candidate event is shown in fig. 5. Presently, the data are under analysis, and the background contamination, and the systematic effects are under study: with the collected statistics, FINUDA will give new and more stringent upper limits for the existence of light neutron rich hypernuclei.

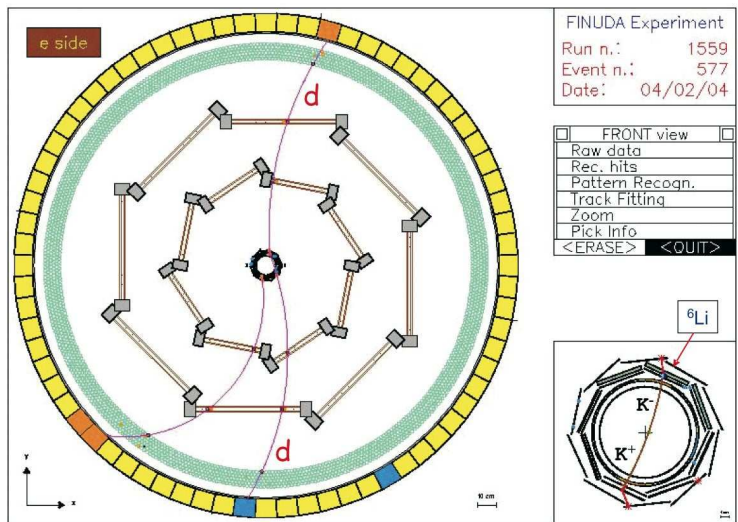


Figure 4: Display of a typical event of the rare decay: ${}^4_{\Lambda}\text{He} \rightarrow dd$. ${}^4_{\Lambda}\text{He}$ s produce following the K^- absorption on a ${}^6\text{Li}$ target. The μ^+ , from the $K_{\mu 2}$ decay of the K^+ stopped in the opposite target, is also visible.

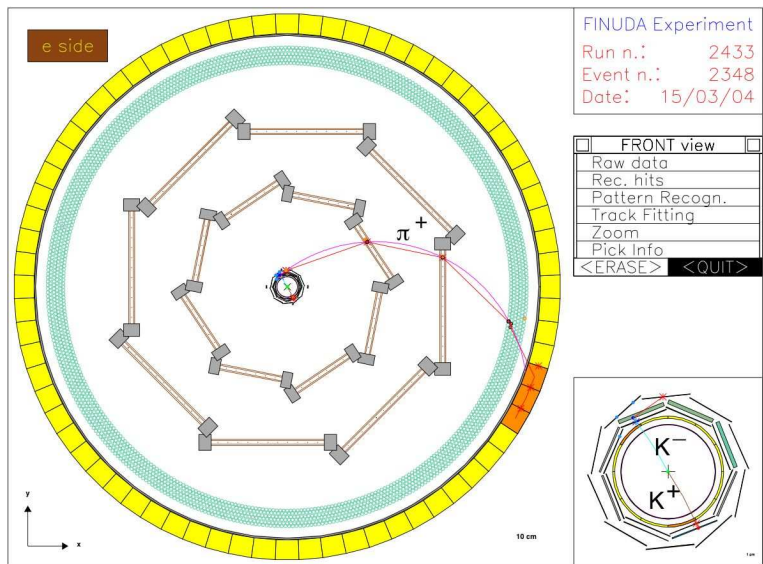


Figure 5: Display of a neutron rich hypernucleus candidate (see text for more details).

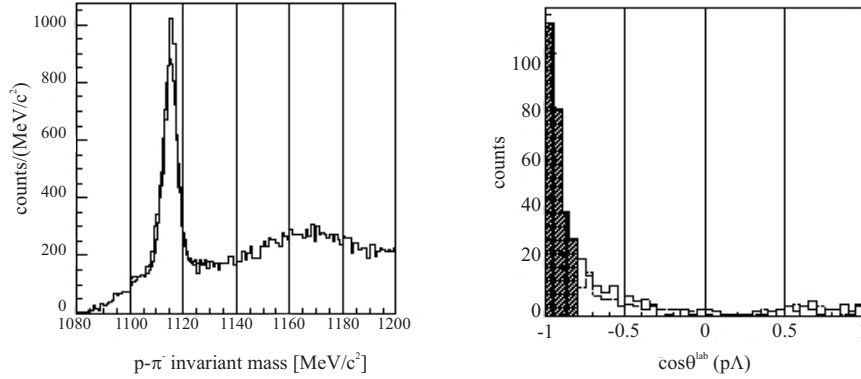


Figure 6: **Left:** Invariant mass $p\pi^-$ of events with a π^- and at least one p in the final state. The Λ is clearly seen. **Right:** Distribution of the opening angle between a Λ and a proton: solid line light targets (${}^6\text{Li}$, ${}^7\text{Li}$, ${}^{12}\text{C}$); dashed line medium heavy targets (${}^{27}\text{Al}$, ${}^{53}\text{V}$). The shadowed area indicates the selection of $\cos\theta \leq -0.8$.

2.3.5 Search for kaon-bound states

In October 2003, during the HYP2003 Conference, hints for the existence of deeply-bound kaonic states in ${}^{16}\text{O}$ and ${}^4\text{He}$ were reported. Soon after, a paper claiming the observation of a tri-baryonic state K^-pn observed in the reactions of stopped K^- with ${}^4\text{He}$ was published. The existence of these systems had been suggested in several theoretical papers, and the reported experimental signatures determined a great excitement in the scientific community. Nevertheless, the above mentioned experimental results have been obtained with the missing-mass method, and hence they are not clear and direct observations of the supposed K-bound states. On the contrary, FINUDA, being able to fully detect all the products of the K^- interaction, is ideally suited to look for these signals by using the direct method of the invariant-mass of the decay particles. In FINUDA, a kaonic bound state like K^-pp would decay via Λp , with the Λ then transforming into $p\pi^-$. The data sample used for this analysis is that with two protons and a π^- in the final state;

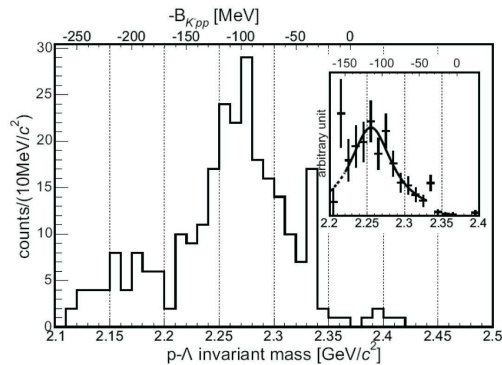


Figure 7: Distribution of the invariant mass of a Λ and a p in back-to-back correlation ($\cos\theta \leq -0.8$) for events from the light targets (${}^6\text{Li}$, ${}^7\text{Li}$, ${}^{12}\text{C}$). The inset shows the same distribution after acceptance correction with the fitting curve superimposed.

the Λ is reconstructed via its decay and finally a p emitted back-to-back with respect to the Λ is requested. The invariant mass of $p\pi^-$ events is plotted in fig. 6 (*Left*); the Λ peak is clearly seen.

Fig. 6 (*Right*) reports the distribution of the angle between the Λ and the proton both for the light (solid line, ${}^6\text{Li}$, ${}^7\text{Li}$ and ${}^{12}\text{C}$) and for the heavier (dashed line, ${}^{27}\text{Al}$ and ${}^{53}\text{V}$) targets. The back to back correlation is more evident for the light target events. For this reason, only the data on light nuclei, with $\cos\theta \leq -0.8$, have been used for the further analysis (shadowed region of fig.6 (*Left*)). Fig. 7 reports the invariant mass of the selected events. If no bound system was formed, this should peak, within the experimental resolution (4 MeV *FWHM* in this energy region), at about 2.37 GeV/c^2 , corresponding to the sum of the masses of $K^- + p + p$, decreased of ~ 30 MeV/c^2 to take into account the binding of the two protons inside the nucleus. Actually, a sharp peak is present at about 2.34 GeV/c^2 , but the bulk of the events distribute in a broad peak centered at a lower energy value, supporting the hypothesis of the formation of a K^-pp bound state. The selected events, corrected for the detector acceptance and fitted with a Lorentzian function folded with a gaussian to take into account the detector resolution (inset of fig. 7), give a binding energy $B_{K^-pp} = 115_{-6}^{+5} \text{stat } {}_{-4}^{+3} \text{sys}$ MeV and a width $\Gamma = 67_{-11}^{+14} \text{stat } {}_{-3}^{+2} \text{sys}$ MeV. Work is in progress to refine this result and to search also for K^-pn bound states.

3 Talks to international conferences by LNF authors in year 2004

- Meson 2004 Conference, Krakow, Poland, June 4-8, 2004.
- Dafne 2004. Physics at meson factories, LNF, Frascati, Italy, June 7-11, 2004.

4 Talks to international conferences by FINUDA authors in year 2004

- VIII International Conference on Hypernuclear & Strange Particle Physics. Jefferson Lab, Newport News, Virginia-USA, October 14-18 2004.
- XLII International Winter Meeting on Nuclear Physics, Bormio, Italy, January 25 - February 1, 2004.
- Meson 2004 Conference, Krakow, Poland, June 4-8, 2004.
- Dafne 2004. Physics at meson factories, LNF, Frascati, Italy, June 7-11, 2004.
- International Nuclear Physics Conference INPC 2004, Goteborg, Sweden, June 27-July 2, 2004.
- Strangeness Nuclear Physics 2004, July 29-31, 2004, Osaka, Japan.
- 19th European Conference on Few-Body Problems in Physics, August 23-27, 2004, Groningen, The Netherlands.
- Fifth Italy-Japan Symposium. Recent Achievements and Perspectives in Nuclear Physics, November 3-7, 2004, Naples, Italy.

GRAAL

O. Bartalini (Dott.), P. Levi Sandri (Resp.)

1 Introduction

The Graal experiment aims at a more detailed knowledge of the baryon spectrum via the precise measurement of polarisation observables in photo-induced reactions on the nucleon.

The use of the electromagnetic probe and of its polarisation, coupled to large acceptance detectors with cylindrical symmetry and high efficiency in the detection of all final state particles, is the technique chosen in many laboratories to perform the ambitious program of a full determination of the scattering amplitude of a given photonuclear reaction. Such determination requires the measurement of the cross section, of the three single polarisation observables and of four appropriately chosen double polarisation observables.

The Graal experiment is performed in collaboration between 6 INFN Sections (Roma2, LNF, Catania-LNS, Roma1, Genova and Torino), IPN-Orsay, ISN-Grenoble and INR-Moscow) The Frascati group is responsible of running and maintaining the $\Delta E/\Delta x$ scintillator barrel detector, the Montecarlo simulation program LAGGEN, the off-line reconstruction of events in the BGO calorimeter and the data analysis for coherent η photoproduction off the deuteron.

2 The Graal Beam and the Lagrange apparatus

The Graal facility provides a polarised and tagged photon beam by the backward Compton scattering of laser light on the high energy electrons circulating in the ESRF storage ring¹⁾. Using the UV line (350 nm) of an Ar-Ion laser we have produced a gamma-ray beam with an energy from 550 to 1470 MeV. Its polarisation is 0.98 at the maximum photon energy and the energy resolution has been measured to be 16 MeV (FWHM).

The Lagrange detector is formed by a central part surrounding the target and a forward part. Particles leaving the target at angles from 25° to 155° are detected by two cylindrical wire chambers with cathode readout, a barrel made of 32 strips of plastic scintillator parallel to the beam axis, used to determine the $\Delta E/\Delta x$ of charged particles, and the BGO rugby-ball made of 480 crystals of BGO scintillator.

The BGO ball is made of crystals of pyramidal shape with trapezoidal basis which are 21 radiation lengths long (24 cm). This calorimeter has an excellent energy resolution for photons²⁾, a good response to protons³⁾ and is very stable in time due to a continuous monitoring and calibration slow control system⁴⁾.

Particles moving at angles smaller than 25° encounter two plane wire chambers, (xy and uv) two walls of plastic scintillator bars 3 cm thin located at 3 m from the target point, that provide a measurement of the time-of-flight for charged particles (700 ps FWHM resolution) followed by a shower wall made by a sandwich of four layers of Lead and plastic scintillators 4 cm thick that provides a full coverage of the solid angle for photon detection (with 95 percent efficiency) and a 20 percent efficiency for neutron detection.

Finally, two disks of plastic scintillator separated by a disk of Lead complete the solid angle coverage in the backward direction.

The beam intensity is continuously monitored by a flux monitor, composed by three thin plastic scintillators and by a lead/scintillating fibre detector that measures energy and flux⁵⁾.

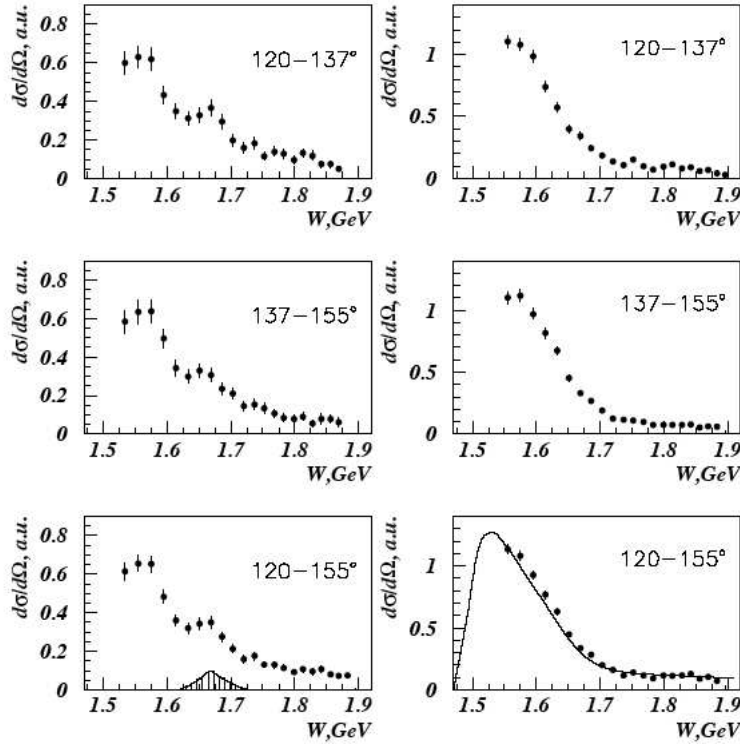


Figure 1: Preliminary ηn (left) and ηp (right) photoproduction cross sections. Dashed area simulates the contribution of a narrow state at $W=1.675$ GeV.

3 2004 activity

During the year 2004 the Graal experiment has suspended the data taking in order to install the polarised HD target. The activity was mainly focused in data analysis for various channels especially concentrating in the meson photoproduction on quasi-free neutron. Following the announced results coming from SPRING-8, a search for pentaquark states (θ^+ and non-strange antidecuplets members) was performed and some preliminary positive results were presented in international conferences. The $S=+1$ narrow resonance was searched in the reaction

$$\gamma + D \rightarrow \theta^+ + \Lambda, \quad (1)$$

while the possible signal of non strange members of the antidecuplet was searched for in the cross section. The preliminary results of the cross section for η photoproduction on the quasi-free neutron are shown in figure 1. A clear peak is evident in the cross section on the quasi-free neutron and absent in the cross section on the quasi-free proton: this peak could be ascribed to a narrow baryon resonance at $W=1.675$ GeV and could be an indication of a non strange antidecuplet pentaquark member. Further investigations (i.e. beam asymmetry) need to be performed to confirm this result, and more data are necessary to better fix the resonance properties.

4 A serendepic result

The excellent stability of the ESRF electron beam and, consequently, of the Graal photon beam and in particular of its Compton edge, has allowed to study, during many years of Graal data taking, the fluctuations in the speed of light with respect to the apex of the dipole of the Cosmic

Microwave Background radiation. The results have enabled to obtain a conservative constraint on the anisotropy in the light speed variations

$$\Delta c(\theta)/c < 3 \cdot 10^{-12} \quad (2)$$

improving the existing limit by two orders of magnitude.

5 Activity in 2005 and conclusions

The Graal experiment started data taking in 1997. It was run both with the green laser line giving rise to a photon beam of maximum energy of 1100 MeV and with UV multi-line with the corresponding gamma-ray beam of 1470 MeV maximum energy. The typical intensity was $2 \cdot 10^6 s^{-1}$ for the UV line and $5 \cdot 10^6 s^{-1}$ for the green line, reaching the design intensity. The detector was found very stable during the eight years of operation, with only minor maintenance problems.

Proton and deuteron targets of different lengths were used and asymmetry data and cross sections have been produced for η , π^0 , π^+ , $2\pi^0$ and ω photoproduction channels providing, for these reactions, the most extended and coherent data base available until now. The analysis of the Compton process on the proton, and of all the mentioned photoreactions on the quasi-free neutron of the deuteron target are underway.

During the year 2005 Graal will resume the data taking with deuteron (and other medium nuclei) in order to increase the available statistics for the θ^+ signal and to study the behavior of η photoproduction cross section as a function of the atomic number A.

6 Main recent publications

V. G. Gurzadyan et al., Mod. Phys. Lett. **A20**, (2005),19.

References

1. Graal Collaboration, Nucl. Phys. **A622**, (1997) 110c.
2. P. Levi Sandri *et al.* Nucl. Inst. and Meth. in Phys. Research **A370**, (1996), 396.
3. A. Zucchiatti *et al.*, Nucl. Inst. and Meth. in Phys. Research **A321**, (1992), 219.
4. F. Ghio *et al.*, Nucl. Inst. and Meth. in Phys. Research **A404**, (1998), 71.
5. V. Bellini *et al.*, Nucl. Inst. and Meth. in Phys. Research **A386**, (1997), 254.

HERMES

E. Avetisyan (Ass.), N. Bianchi (Resp. Naz.), A. Borysenko (Ass.),
G.P. Capitani (Resp. Loc.), E. De Sanctis, P. Di Nezza, A. Fantoni, A. Funel (Dott.),
C. Hadjidakis (Ass.), D. Hasch (Ass.), V. Muccifora, K.A. Oganessyan (Ass.),
A. Orlandi (Tecn.), W. Pesci (Tecn.), E. Polli, A.R. Reolon, A. Viticchié (Tecn.)

1 Introduction

HERMES (HERa MEasurement of Spin) is an experiment at DESY mainly dedicated to study the spin structure of the nucleon. Nucleons (protons and neutrons) are the basic ingredients of the matter of the known universe and their most important quantum number is the spin $1/2$. The nucleon is a composite object which can be described in terms of moving quarks of different flavors (up, down and strange) in different configurations (valence and sea) and gluons. Up to year 2000, HERMES collected data with a longitudinally polarized positron beam of 27.5 GeV on longitudinally polarized H, D and ^3He internal gas targets. From these runs HERMES provided the most accurate and complete data set for the polarized structure function g_1 and allowed a direct flavor decomposition of the nucleon spin (see Fig. 1). Runs on several unpolarized nuclear gas targets have been also collected.

In 2002-2004, data with a transversely polarized hydrogen target have been collected. The analysis on a reduced data sample has shown a small but clearly non-zero azimuthal asymmetry for both positive and negative pions (see Fig. 2). These data provide the first evidence of the so called Collins effect, which is related to the convolution of the chiral-odd transversity distribution $h_1(x)$ with a time-odd spin-dependent fragmentation function, and of the so called Sivers effect, which is related to chiral-even and time-odd distribution and spin independent fragmentation function. The transversity distribution $h_1(x)$ is the missing function in the leading twist description of the nucleon, together with the better known momentum $f_1(x)$ and helicity $g_1(x)$ distributions. Peculiarities of transversity are its relation with the relativistic motion of quarks and its pure non-singlet Q^2 -evolution due to the decoupling with gluons in the helicity flip. First moment of transversity distribution provides the tensor charge which has been calculated to be large from Lattice QCD. The Sivers distribution function is related to the still unknown orbital angular momentum of quarks. Much more data will be available in the current data taking and analysis.

2 The LNF HERMES group

HERMES is a Collaboration of about 180 physicists from 31 Institutions from 12 Countries. Italy participates with 4 groups and more than 30 physicists from Bari, Ferrara, Frascati and Rome. A Frascati physicist (P. Di Nezza) is the deputy spokesman and run-coordinator of the experiment. A Frascati physicist (D. Hasch) is the analysis coordinator of the experiment. The Frascati group is responsible for the electromagnetic calorimeter and has participated in the project and in the construction of two dual RICH detectors. It is currently involved in the project of a new recoil detector to be installed in summer of 2005. A Frascati physicist (C. Hadjidakis) has the responsibility of the analysis working groups of azimuthal asymmetries in semi-inclusive processes and of the pseudoscalar meson exclusive production. A Frascati physicist (P. Di Nezza) has the responsibility of the nuclear physics analysis working group. Frascati physicists are involved in the analysis of many other physics processes. In addition they are playing a major role in the physics paper draftings and in the editorial process being the leading authors of about one third of the HERMES Collaboration physics publications.

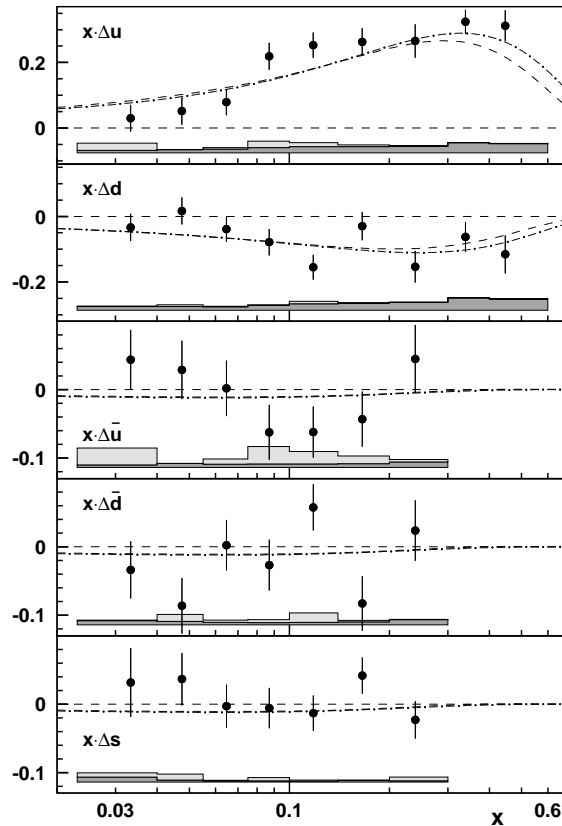


Figure 1: Quark helicity distributions at $\langle Q^2 \rangle = 2.5 \text{ GeV}^2$, as a function of Bjorken x , compared to two LO QCD fits to previously published inclusive data. The error bars are statistical and the bands at the bottom represent the systematic uncertainties, where the light area is the contribution due to the uncertainties of the fragmentation model, and the dark area is the contribution due to those of the asymmetries.

3 Experimental activity of the LNF group in 2004

3.1 Calorimeter and TOF

The HERMES calorimeter consists of a wall of 840 Lead-Glass blocks. The calorimeter is the basic detector for the main trigger and for the positron-hadron separation. It is used to reconstruct energy and angle of photons, π^0 and η . The responsibility of the calorimeter required the on-line monitoring and check of the status of detector for the whole period of data taking. During 2004 several reproductions of existing data with the re-calibration of all detectors, including the calorimeter were performed.

A precise energy and position reconstruction of the electromagnetic showers allowed a comparison with the lepton momentum reconstructed by the tracking system. In addition the single photon, from deeply virtual Compton scattering processes, and the double photon, from π^0 decays (see Fig 3-left), events were reconstructed by taking into account the photon early showering in the preshower detector in front of the Calorimeter.

HERMES has two sets of scintillator hodoscope paddles which were mainly designed for

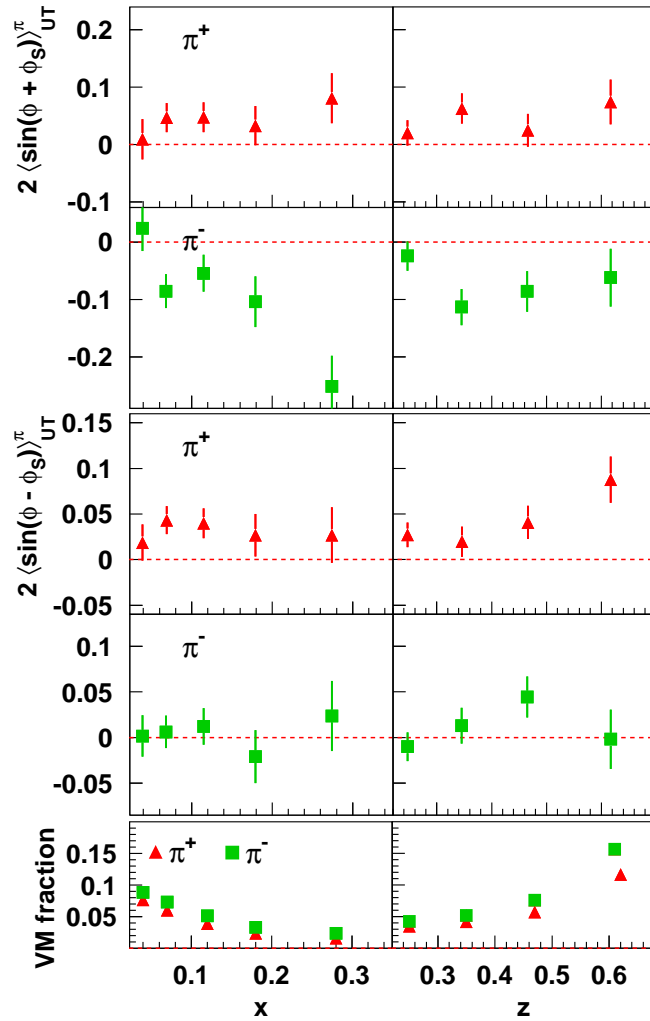


Figure 2: Virtual-photon Collins (Sivers) moments for charged pions as labeled in the upper (middle) panel, as a function of x and z , multiplied by two to have the possible range ± 1 . The error bars represent the statistical uncertainties. In addition, there is a common 8% scale uncertainty in the moments. The lower panel shows the relative contributions to the data from simulated exclusive vector meson production.

charge particle triggering and lepton/hadron separation. The second one is also working as a preshower detector. Nevertheless, it turned out that they can be used also as a time-of-flight system to distinguish different hadron types from each other by their mass extracted from speed and momentum. A method was therefore developed to allow a nice separation of pions from protons in the momentum range of 0.6-3 GeV/c with total efficiency of 98% and pion contamination in proton sample of less than 5% (see Fig. 3-right). This momentum range is complementary to the one provided by the HERMES dual RICH detector.

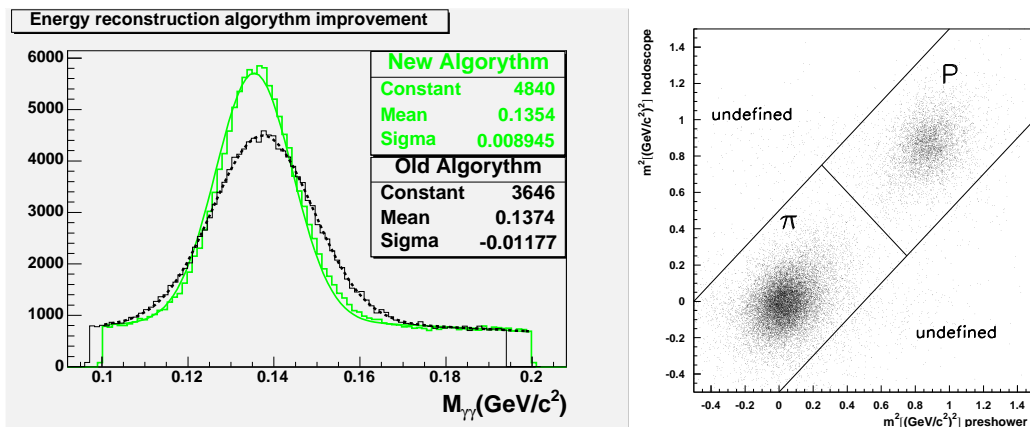


Figure 3: Left : Reconstruction of π^0 in the calorimeter with improved algorithm. Right : Identification of charged pions and protons of low momenta with Time of Flight.

3.2 Recoil detector

The recent proof of factorization for exclusive processes and their interpretation in terms of Generalized Parton Distributions to describe the nucleon structure, suggested the detailed investigation of these processes in which a fast meson or a photon is emitted in the forward direction while the slow nucleon is recoiling intact at large angle. Several exclusive processes have been already investigated by HERMES with the missing mass technique. To better identify these processes, a compact Recoil Detector (see Fig. 4 during the assembling) has been constructed to be installed around the target in summer 2005. Basically, it will consist of silicon detectors located under vacuum inside the beam pipe, a SciFi tracking system and a Lead-Scintillator barrel. The Frascati group has built the latter detector which will be used to detect photons from the π^0 decay. It consists of three layers of scintillating strips with a WLS fiber system readout. Multi-anode photomultipliers are used with specially designed fan-in/preamplifiers to ensure capable transmittance of the signal. In 2004 the photon detector has been fully assembled in Frascati. It was transported to DESY, installed inside the superconducting magnet and tested with cosmic rays with different trigger configurations. The reconstruction algorithm, the event display and the wire maps were developed, ensuring effective data acquisition, data processing and interpretation for standard HERMES software analysis tools. The Gain Monitoring System (GMS) of the detector was also successfully tested. The value of GMS signal was at the level of 4 MIPs. After the installation of the SciFi tracker and the silicon detector, the full Recoil Detector is now starting the complete and final test before the debugging on the beam line.

3.3 Technical software

LNF members were main responsible for Particle Identification (PID). In particular they worked on the maintenance and code development of the PID library function, on the PID calibration, on the data productions, on the flux corrections to PID for different physics analyzes.

During 2004 the LNF group acted also as HERMES Linux administrator and represented HERMES on DESY Linux user meeting, where user requirements and future strategy for Linux support were discussed. HERMES has a powerful Linux-based PC-farm with 2 work-groups servers, 4 file-servers and 30 batch nodes for various types of analysis. The maintenance of the computers is provided

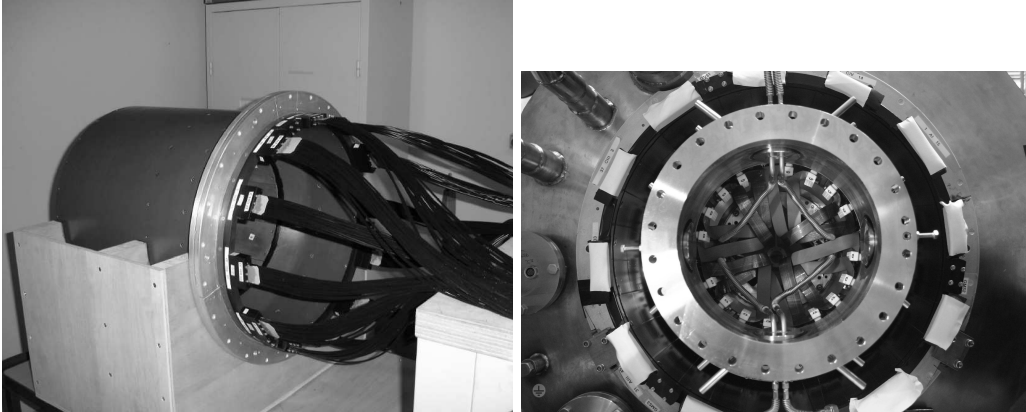


Figure 4: The Photon Detector and the full Recoil Detector during the assembling in DESY.

through SNMP protocol plugged through an SMS gateway, which allows immediate knowledge in case of failures. In addition, there are about 40 desktop PCs acting as terminals for users and about 20 notebook computers for working use.

4 Data analysis and physics results of the LNF group in 2004

4.1 Beam-spin asymmetry in SIDIS

Single-spin asymmetries in semi-inclusive deep-inelastic-scattering (SIDIS) are known as a powerful tool for probing the structure of the nucleon. They give access to transverse momentum dependent parton distributions and time-reversal-odd fragmentation functions with prominent examples like the transversity h_1 and Sivers f_{1T}^\perp distributions and Collins H_1^\perp fragmentation functions. These quantities have been studied so far with unpolarized beam and both transverse and longitudinally polarized targets. Recently, the analyzing power for a beam spin asymmetry with unpolarized beam has been also investigated (see Fig.5-left). This asymmetry can be related to the twist-3 p_T dependent unpolarized distribution $e(x)$ and requires a non-zero Collins fragmentation function.

4.2 Exclusive production of single pion

The interest in the hard exclusive electroproduction of mesons has grown since a QCD factorization theorem was proved in the case of longitudinal photon at large Q^2 . The amplitude for such reactions can be factorized into a hard lepton scattering part and two soft parts which parametrize the produced meson by a distribution amplitude and the target nucleon by four Generalized Parton Distributions. In the case of exclusive electroproduction of pion, the reaction provides essential information of the largely unknown space-like pion form factor and of the polarized GPDs (\tilde{H} and \tilde{E}). First preliminary results for the unpolarized $ep \rightarrow en\pi^+$ has been extracted in a wide Q^2 - and x -ranges (see Fig.5-right). For the total cross section determination an exclusive Monte Carlo based on GPDs has been developed to account for detector acceptance and efficiency. The data are compared with theoretical prediction for the longitudinal part of the cross section. However, since the transverse contribution is predicted to be suppressed by a power of $1/Q^2$, the data at larger Q^2 are expected to be dominated by the longitudinal part. The power corrections in the calculation include the effect of the intrinsic parton momentum and mainly of the soft overlap in the pion distribution amplitude.

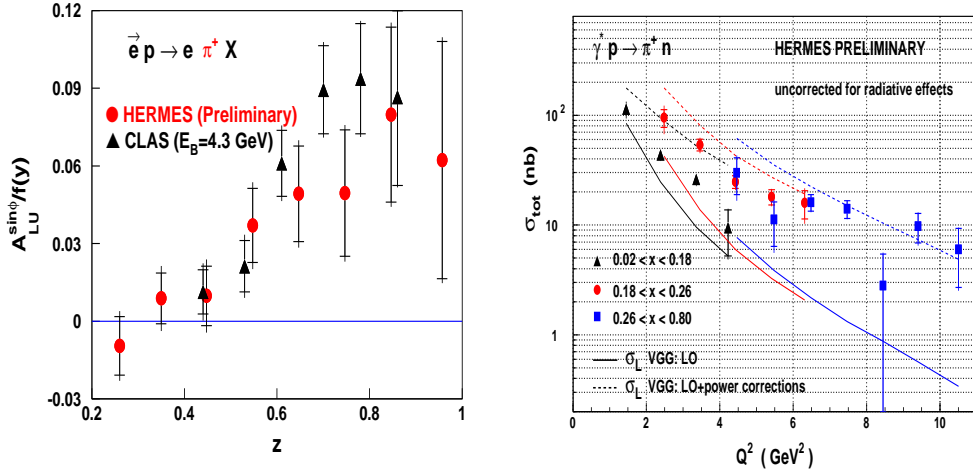


Figure 5: Left : Beam spin asymmetry for semi-inclusive π^+ production as function of the pion relative energy. The preliminary HERMES data are compared with CLAS results by taking into account a relative kinematic factor $f(y)$. Right : Total cross section for exclusive π^+ production as function of Q^2 and for different x -bins. The HERMES preliminary data are compared with calculations for the longitudinal part of the cross section based on Generalised Parton Distributions at leading order and with the inclusion of power corrections for the pion form factor.

Furthermore, SSA on a transverse polarized target are now in the stage of the analysis. This observable is expected to be less sensitive to corrections to QCD leading order and will be directly compared to GPD's predictions. Results on the single spin asymmetry (SSA) on a longitudinal polarized target have already been published.

4.3 Exclusive production of $\pi^+\pi^-$ pairs

Hard exclusive electroproduction of $\pi^+\pi^-$ pairs is sensitive to the interference between isospin $I = 1$ (P-wave) and $I = 0$ (S, D-wave) channels and provides new constraints on certain combinations of GPDs. By studying the angular distribution of the pair and by evaluating the relevant Legendre moments P_n , it is possible to single out at the amplitude level the weaker isoscalar channel which is generally suppressed in the cross section. In Fig. 6 are shown two of these Legendre moments as a function of the pair invariant mass. P_1 is sensitive to P-wave (mainly the ρ vector meson) interference with S and D-waves (mainly σ , f_0 and f_2 mesons), while P_3 is sensitive to only P-wave interference with a D-wave. As it is seen, large interference effects are present for P_1 in general agreement with GPDs calculation with the inclusion of the two-gluon exchange contribution. In the insert the study of the possible effect from f_0 interference is also shown together with a calculation which explicitly considers this effect. The data presented are related to large- x kinematics. Currently an analysis is under development in the low- x region to search for possible signatures of interference between Pomeron and Odderon exchanges.

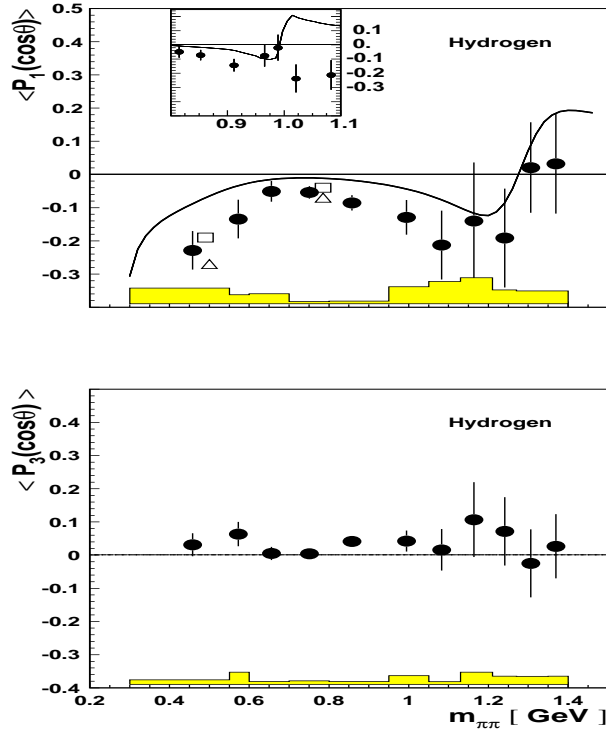


Figure 6: The $m_{\pi\pi}$ -dependence of the Legendre moments P_1 and P_3 . For P_1 leading twist predictions are shown as solid curves. Open points shows the range of the same prediction without the two-gluon exchange contribution. In the insert panel, the prediction for the effect of the f_0 decay is also presented. The systematic uncertainty is represented by the error band.

4.4 Nuclear effects in two hadron electroproduction

Medium modification of dihadron fragmentation function has been studied by considering the relative yield of two hadrons (leading and sub-leading) over the leading one in nuclei with respect to deuterium. Double hadron leptonproduction offers a way to disentangle hadronization occurring inside versus outside the nucleus. In Fig. 7-left the preliminary HERMES data show an effect which is substantially smaller in magnitude and reduced in the A -dependence compared to the previously measured single hadron multiplicity ratio. The solid curves are model theoretical prediction which use the quark concept for the prehadronic cross section and a hadron formation time $\tau_f = 0.5$ fm/c. The dashed curves are calculations with a purely absorptive treatment of the hadron final state interaction which is clearly ruled out by the preliminary HERMES data. New data on a Xenon target has been collected to explore a wider atomic mass range.

5 Phenomenology on HERMES physics of the LNF group in 2004

5.1 Quark-hadron duality

The quark-hadron duality was introduced in 1970 by Bloom and Gilman who noted a relationship between the resonance and deep inelastic scattering physics. A perturbative QCD NLO analysis

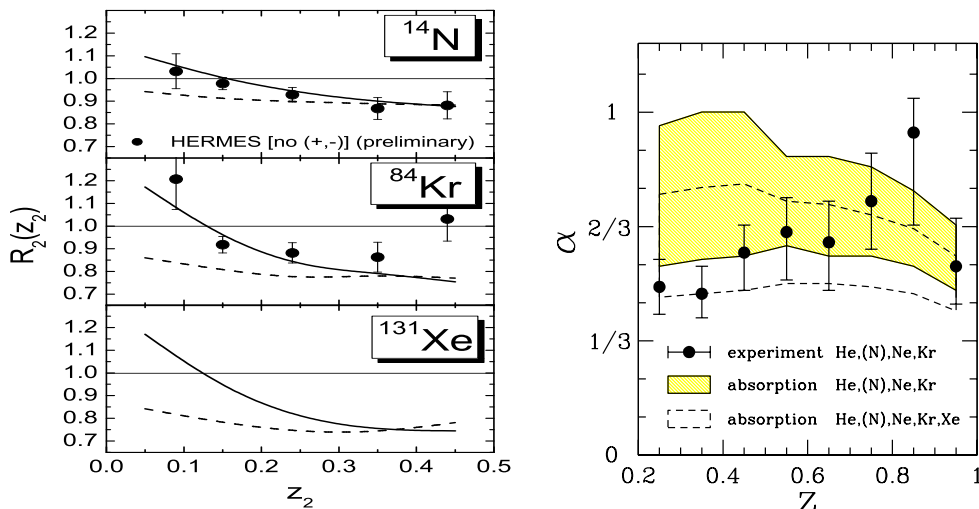


Figure 7: Left : Two hadron relative yield for different nuclei with respect to deuterium and as a function of the relative energy of the sub-leading hadron. Preliminary HERMES data are shown in comparison with different assumption for the hadronization process. Right : Values of α as function of the hadron relative energy derived from HERMES preliminary data (dots) and from pure absorption model computation. α is the power of the mass dependence A^α of the medium effect in the fragmentation function modification.

including target mass corrections and large x re-summation effects has been extended to the integrals of both unpolarized and polarized structure functions in the resonance region. Both effects have been quantified and disentangled for the first time. A different behavior for unpolarized and polarized structure functions has been found. The discrepancy of the ratio from unity has been interpreted in terms of higher twists (HTs). While the size of the HT contributions is comparable in both polarized and unpolarized scattering at larger x and Q^2 values, at low x and Q^2 large negative non-perturbative contributions have been found only in the polarized case (see Fig. 8). The HT coefficients of the present extraction in the resonance region have been compared with all existing results of HTs in the DIS region.

5.2 Nuclear medium effects in fragmentation

A theoretical model for the interpretation of the hadron production in lepton-nucleus DIS has been developed. In this model, the early stage of hadronization in the nuclear medium is dominated by prehadron formation and absorption, controlled by flavor-dependent formation lengths and absorption cross sections. The mass number dependence of hadron attenuation is shown to be sensitive to the underlying hadronization dynamics. Contrary to common expectations for absorption models, a leading term proportional to $A^{2/3}$ is found (see Fig. 7-right). Deviations from the leading behavior arise at large mass-numbers and large hadron fractional momenta.

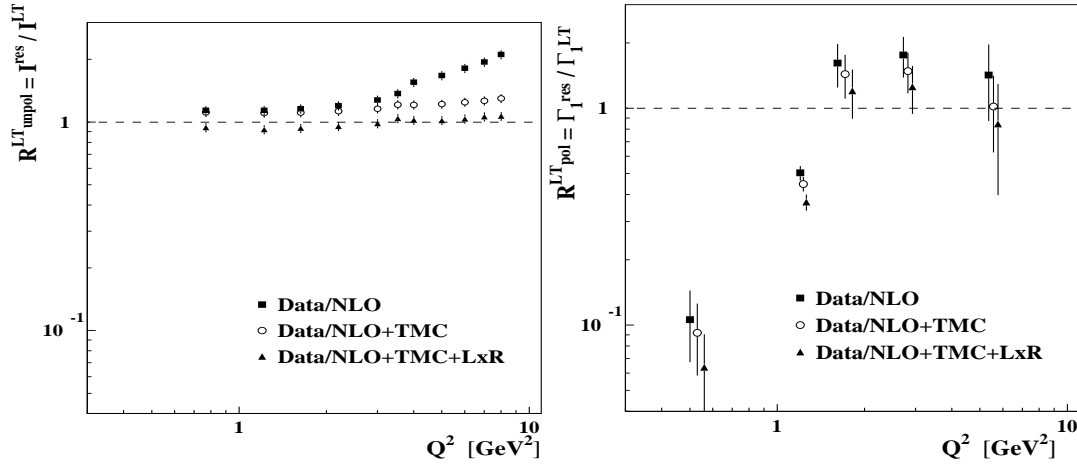


Figure 8: Ratio between the integrals of the measured structure functions and the calculated ones plotted as a function of Q^2 for the unpolarized case (left) and the polarized one (right). The calculation includes one by one the effects of NLO pQCD.

6 Outlook

The data taking with a transversely polarized hydrogen target will continue up to summer 2005. Then, the Recoil Detector will be installed on the beam line and debugged. The ongoing physics analysis and the phenomenological investigations will be completed.

7 Conferences by LNF Authors in Year 2004

7.1 Conference Talks

1. E. Avetisyan, Beam-spin asymmetries in π^+ electr., DIS 2004, Strbske Pleso (Slovakia).
2. E. Avetisyan, HERMES e.m. calorimeter, Nato workshop, Nor Amberd (Armenia).
3. E. Avetisyan, Beam-spin asymmetries in π^+ electroproduction, XC SIF, Brescia (Italy).
4. N. Bianchi, Fragmentation inside nuclei, Gordon Conference, New London (USA).
5. N. Bianchi, Status of polarized DIS experiments, Few Body XIX, Groningen (Holland).
6. N. Bianchi, Experimental review on transversity, Baryons 2004, Palaiseau (France).
7. N. Bianchi, Electroproduction of hadrons in nuclei, In-Medium workshop, Giessen (Germany).
8. P. Di Nezza, Hadron suppression in DIS, Quark Matter 2004, Oakland (USA).
9. P. Di Nezza, The spin of the nucleon, II PANDA physics workshop, Frascati (Italy).
10. P. Di Nezza, The spin of the nucleon, VIII Electron-Nucleus Scattering, Marciana M. (Italy).
11. P. Di Nezza, Spin structure of the nucleon, QCD 04, Montpellier (France).
12. P. Di Nezza, Results from HERMES, Wissenschaftlicher Ausschuss, Hamburg (Germany).
13. A. Fantoni, Quark-Hadron Duality, VIII Electron-Nucleus Scattering, Marciana M. (Italy).
14. A. Fantoni, Quark-Hadron Duality and Higher Twist High X 2004, Marseille (France).
15. A. Fantoni, Recenti risultati di HERMES, XC SIF, Brescia (Italy).
16. A. Funel, Effetti nucleari nella produzione di adroni ad HERMES, XC SIF, Brescia (Italy).

17. C. Hadjidakis, Exclusive production at HERMES, Rencontres de Moriond, La Thuile (Italy).
18. C. Hadjidakis, Exclusive π^+ production at HERMES, DIS 2004, Strbske Pleso (Slovakia).
19. C. Hadjidakis, Exclusive π^+ production at HERMES, Meson 2004, Krakow (Poland).
20. C. Hadjidakis, Exclusive production at HERMES, XC SIF, Brescia (Italy).
21. C. Hadjidakis, Exclusive π^+ production at HERMES, Baryon 2004, Palaiseau (France).
22. D. Hasch, Newest results from Hermes, DPG Spring meeting, Cologne (Germany).
23. D. Hasch, Future measurements, ECT* Workshop on Transversity, Trento (Italy).
24. D. Hasch, Spin physics with longitudinal targets, RHIC-Spin workshop, Torino (Italy).
25. D. Hasch, Spin physics at Hermes, Spin04 conference, Trieste (Italy).
26. V. Muccifora, Hadron Production in nuclear DIS, NuInt04, LNGS (Italy).
27. V. Muccifora, Nuclear effects in DIS at HERMES, QNP 2004, Bloomington (USA)
28. V. Muccifora, Space-time charact. of hadronization, Physics of Nuclei at 12 GeV, Jlab (USA).

7.2 Conference organization and advisory, Projects, Seminars, Lectures

1. N. Bianchi, (Advisor) Physics of Nuclei at 12 GeV, Jlab (USA).
2. E. De Sanctis, (Organizer) ECT* Workshop on Transversity, Trento (Italy).
3. E. De Sanctis, (Organizer) Spin04, Trieste (Italy).
4. E. De Sanctis, (Convener) N7-Transversity, I3HP Project.
5. E. De Sanctis, (Convener) Misura della Trasversalita' del Nucleone, Cofinanziamento MIUR.
6. E. De Sanctis, (Convener) HERMES-LNF TARI at DESY.
7. V. Muccifora, (Convener) Physics of Nuclei at 12 GeV, Jlab (USA).
8. D. Hasch, (Lectures) Spin structure of the nucleon, Graduate School Tuebingen (Germany).
9. D. Hasch, (Lectures) Physics with Hermes, Desy Summer Students Program (Germany).
10. D. Hasch, (Lectures) Spin structure of the nucleon, Munich University (Germany).

8 Publications of LNF Authors in Year 2004

1. A. Accardi, D.Grunewald, V.Muccifora and H.J.Pirner, "Atomic Mass Dependence of Hadron Production in Deep Inelastic Scattering on Nuclei", Submitted to Nucl. Phys. A.
2. A. Airapetian *et al.*, "Flavor Decomposition of the Sea Quark Helicity Distributions in the Nucleon from Semi-inclusive Deep-inelastic Scattering", Phys. Rev. Lett. **92** (2004) 012005.
3. A. Airapetian *et al.*, "Evidence for a Narrow $|S|=1$ Baryon State at a Mass of 1528 MeV in quasi-real Photoproduction", Phys. Lett. **B 585** (2004) 213.
4. A. Airapetian *et al.*, "Nuclear Polarization of Molecular Hydrogen Recombined on a non-metallic Surface", Eur. Phys. Jour. **D 29** (2004) 21.
5. A. Airapetian *et al.*, "Hard exclusive electroproduction of $\pi^+\pi^-$ pairs", Phys. Lett. **B 599** (2004) 212.
6. A. Airapetian *et al.*, "The time-of-flight technique for the HERMES experiment", Nucl. Instr. and Meth., in press.
7. N. Bianchi, A. Fantoni, and S. Liuti, "Parton-hadron duality in unpolarized and polarized structure functions", Phys. Rev. **D69** (2004) 014505.
8. L.P. Gamberg, D.S. Hwang, K.A. Oganessyan, "Chiral-Odd Fragmentation Functions in Single Pion Inclusive Electroproduction", Phys. Lett. **B 584** (2004) 276.
9. V. Muccifora, "Hadronization process in DIS at HERMES", Fizika **B13** (2004) 413.
10. V. Muccifora, "Hadronization in DIS at HERMES", J. Phys. **G30** (2004) S103.
11. P. Di Nezza, "Hadron suppression in DIS at HERMES", J. Phys. **G30** (2004) S783.

PANDA

P. Gianotti (Resp. Naz.), C. Guaraldo, O.N. Hartmann (Art. 23), M. Iliescu, V. Lucherini,
E. Pace, C. Petruscu, D. Sirghi (Bors. PD), F. Sirghi (Bors.)

1 Introduction

PANDA (\bar{p} Annihilation at Darmstadt) is one of the big future experiments at the Facility for Antiproton and Ion Research (FAIR), located at the Gesellschaft für Schwerionenforschung (GSI), Darmstadt, Germany.

At FAIR a storage ring for antiprotons, the High Energy Storage Ring (HESR), will provide an antiproton beam in the momentum range from ≈ 1 to 15 GeV/c, with a momentum spread of $\delta p/p=10^{-5}$ in the high resolution mode and a luminosity of $10^{32}\text{cm}^{-2}\text{s}^{-1}$ in the high luminosity mode. PANDA is an internal experiment at HESR, it will use proton and nuclear targets.

2 Physics Case

The physics program of PANDA covers various topics in hadron and nuclear physics which can be addressed by studying the interaction of antiprotons with nucleons and nuclei – the confinement of quarks within hadrons, the origin of the mass of hadrons, self-interaction among the exchange particles of the strong interaction, the gluons. With the antiproton beam available at HESR, all hadrons up to the $\Omega_c\bar{\Omega}_c$ production can be accessed, as Fig. 1 shows.

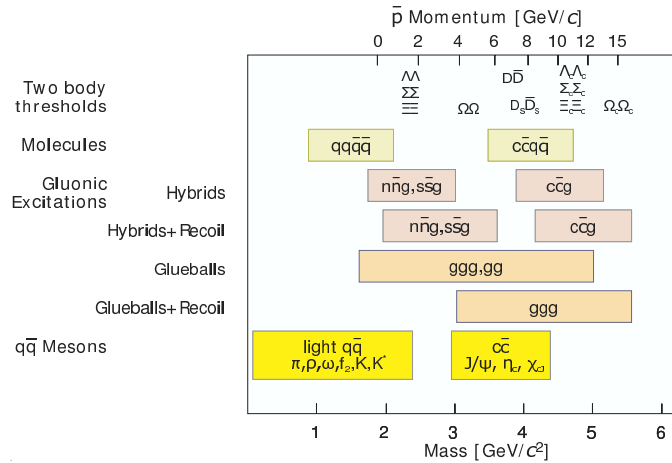


Figure 1: Accessible mass range of PANDA at HESR.

- Charmonium

The precision spectroscopy of all charmonium states with mass, width, decay branches, is a key experiment to be done at PANDA. From that, information on the quark confining potential can be extracted.

- **Gluonic Excitations: charmed hybrids, glueballs**
Another important topic is the search for objects like charmed hybrids and glueballs as they are predicted by QCD. $\overline{\text{P}}\text{ANDA}$ will extend the search for those objects into the charmonium mass range (3-5 GeV/c²), with high statistics and spin-parity analysis in fully exclusive measurements.
- **Charm in Nuclei**
Furthermore, the search for in-medium-modifications of hadrons (mesons) and their possible relation to a (partial) restoration of chiral symmetry in the nuclear medium will be pursued, especially for mesons containing open or hidden charm, which will shed light on the gluon contribution in this sector.
- **Hypernuclei**
At $\overline{\text{P}}\text{ANDA}$, double and single Λ hypernuclei can be produced abundantly. An experiment with precision γ ray spectroscopy of hypernuclei for extracting information on their structure, hyperon-nucleon and hyperon-hyperon interaction is planned. In addition, Ω atoms can be formed and studied.
- **Open Charm, GPD's, CP violation, Transversity, timelike EM form factors**
These are additional topics which can be studied at $\overline{\text{P}}\text{ANDA}$, some of them need the HESR running at highest luminosity and thus are planned for a later stage of the program.

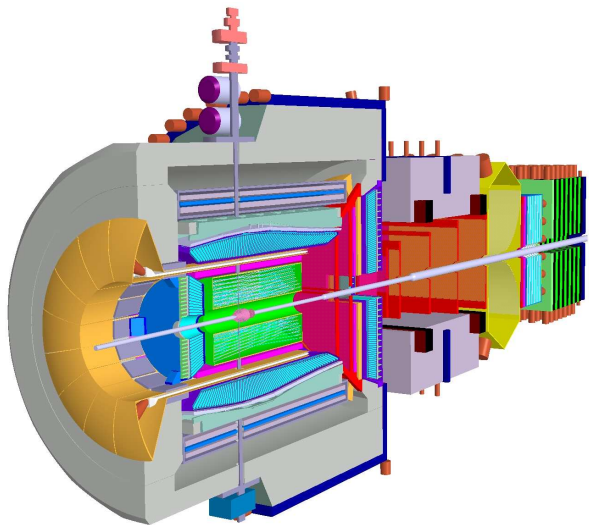


Figure 2: View of the $\overline{\text{P}}\text{ANDA}$ detector as proposed in 3).

3 The proposed Detector

The $\overline{\text{P}}\text{ANDA}$ collaboration has proposed a multipurpose detector to satisfy all the requirements given by the physics of interest. The concept is described in 1) 2) 3).

The fixed target geometry of $\overline{\text{P}}\text{ANDA}$ reflects in the design of the detector system which is built out of a target spectrometer and a forward spectrometer, using a superconducting solenoid with a

2 T field and a dipole with 2 Tm bending power, respectively. In Fig. 2, a schematic drawing of the whole detector is shown, the beam is coming from the lower left.

The target spectrometer houses the interaction point. The target techniques to be exploited are frozen pellets of hydrogen, cluster jets, as well as wire/fibre/foil targets for the heavier target nuclei. The interaction point is surrounded by a microvertex detector (silicon pixel), an outer tracking system (straw tubes or time projection chamber), a Čerenkov counter (DIRC type), a time of flight barrel and an electromagnetic calorimeter. Towards the forward angles, drift chambers of the MDC type, additional Čerenkov counters and calorimeter crystals are foreseen. The forward spectrometer comprises drift chambers, a Čerenkov counter, an electromagnetic and a hadron calorimeter. The outer borders of the magnet iron yokes and the forward calorimeter will be equipped with detectors for muon identification. Thus, the detector will be able to identify charged and neutral particles in a slightly energy range.

For the hypernuclei program, an additional target point with a silicon tracking detector will be installed, and Germanium detectors for the γ -ray spectroscopy will be placed, instead of the backward endcap of the calorimeter.

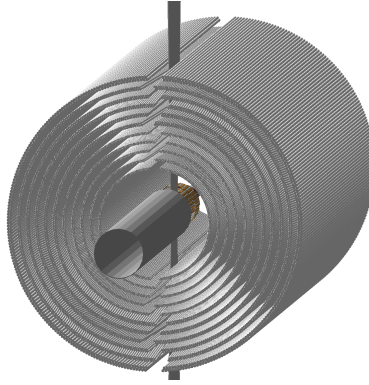


Figure 3: Eleven double layers of straw tubes around the interaction point (beam and target pipe are also visible).

4 LNF Activities

The Laboratori Nazionali di Frascati are in particular involved in the design, prototyping and construction of the central tracking detector, made from straw tubes. Here, Frascati is also coordinating the appropriate working group. In Fig. 3 an arrangement of eleven double layers of straw tubes around the target is shown. The straws should have a length of 150 cm, with diameters of 4, 6 and 8 mm. They will be arranged in double layers, parallel to the beam axis, applying a skew angle in the order of 2 to 3° to resolve ambiguities in the reconstruction of the z -coordinate.

For the hypernuclei physics program, a so-called primary target will be used in the antiproton beam. The task of this target is the production of hyperons which in a secondary target should form hypernuclei. The background from the \bar{p} annihilation on various target nuclei has been studied using a model based on UrQMD ⁴⁾ with an evaporation and multifragmentation part in addition ³⁾. Specially the neutron flux is critical since the use of germanium detectors is planned. Fig. 4 shows a differential polar angle distribution of the neutrons from the primary reaction $\bar{p}+A$. The numbers suggest that a target in lower mass range should be used.

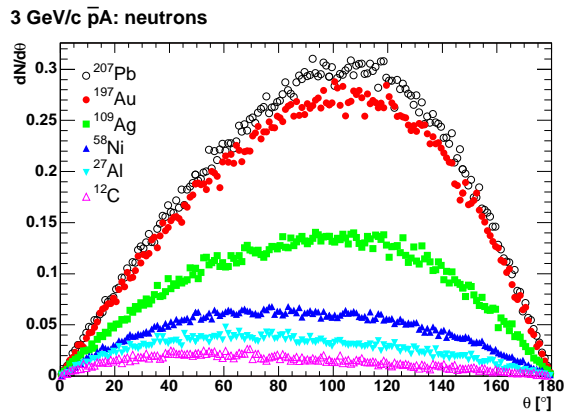


Figure 4: Polar angle distribution of neutrons from the reaction 3 GeV/c $\bar{p}+A$ for various target nuclei.

In March 2004, Frascati was organizing the 2nd \bar{P} ANDA physics workshop together with the 8th collaboration meeting at the LNF.

5 List of Conference Talks by LNF members in the year 2004

1. P. Gianotti, "From LEAR to HESR: past, present and future of meson spectroscopy with antiprotons", 19th European Conference on Few-Body Problems in Physics, Aug. 23-27, Groningen, Netherlands.
2. P. Gianotti, "The PANDA scientific program at the HESR of GSI", International Workshop on collaboration of physics programs between IMP and GSI, Sep. 16-18, Lanzhou, China.
3. P. Gianotti, "The PANDA experimental program", 10th Conference on Problems in Theoretical Physics, Oct. 4-9, Cortone, Italy.

References

1. An International Accelerator Facility for Beams of Ions and Antiprotons, Conceptual Design Report, GSI 11/2001.
2. Letter of Intent, PANDA Collaboration, 01/2004.
3. Technical Progress Report, PANDA Collaboration, 01/2005.
4. UrQMD coll., Prog. Part. Nucl. Phys. 41, (1998) 225, Journal of PhysicsG 25, (1999) 1859.

SIDDHARTA

M. Bragadireanu (Bors. UE), M. Catitti (Bors.), C. Curceanu Petrascu (Co-Resp. Naz.),
C. Guaraldo (Co-Resp. Naz.), M. Iliescu (Art. 23), V. Lucherini, F. Lucibello (Tecn.),
D. Sirghi (Bors. PD), F. Sirghi (Bors. PD)

1 The SIDDHARTA scientific program

The objective of the SIDDHARTA (Silicon Drift Detector for Hadronic Atom Research by Timing Application) experiment is to continue, to deepen and enlarge the successful scientific line, initiated by the DEAR experiment, in performing precision measurements of X-ray transitions in exotic (kaonic) atoms at DAΦNE.

The eV precise determination of the shift and width of the $1s$ level with respect to the purely electromagnetic calculated values, in kaonic hydrogen and kaonic deuterium, generated by the presence of the strong interaction, through the measurement of the X-ray transitions to this level, will allow the first precise experimental determination of the isospin dependent antikaon-nucleon scattering lengths.

The shift ϵ and the width Γ of the $1s$ state of kaonic hydrogen are related to the real and imaginary part of the complex s -wave scattering length, a_{K^-p} , through the Deser formula:

$$\epsilon + i\Gamma/2 = 2\alpha^3\mu^2 a_{K^-p} = (412 \text{ eV fm}^{-1}) \cdot a_{K^-p}, \quad (1)$$

where α is the fine structure constant and μ the reduced mass of the K^-p system. In the isospin limit, i.e. in the absence of the electromagnetic interaction and at $m_d = m_u$, a_{K^-p} can be expressed directly in terms of the scattering lengths for isospin $I=0$ and $I=1$:

$$a_{K^-p} = \frac{1}{2}(a_0 + a_1). \quad (2)$$

A similar relation applies to the case of kaonic deuterium and to the corresponding scattering length a_{K^-d} :

$$\epsilon + i\Gamma/2 = 2\alpha^3\mu^2 a_{K^-d} = (601 \text{ eV fm}^{-1}) \cdot a_{K^-d}. \quad (3)$$

An accurate determination of the K^-N isospin dependent scattering lengths will place strong constraints on the low-energy K^-N dynamics, which, in turn, constrains the SU(3) description of chiral symmetry breaking in systems containing the strange quark, contributing to the determination of the so-called kaon-nucleon sigma terms. These sigma terms are also important inputs for the determination of the strangeness content of the proton. This quantity depends on both kaon-nucleon and pion-nucleon sigma terms, being more sensitive to the first ones.

In 2002, DEAR (DAΦNE Exotic Atom Research) experiment has performed the most precise measurement of kaonic hydrogen X-ray transitions to the fundamental $1s$ level, to present:

$$\epsilon = -193 \pm 37(\text{stat.}) \pm 6(\text{syst.}) \text{ eV} \quad (4)$$

$$\Gamma = 249 \pm 111(\text{stat.}) \pm 39(\text{syst.}) \text{ eV}. \quad (5)$$

This measurement has triggered new interest and results from the theoretical groups working in the low-energy kaon-nucleon interaction field, as well related to non-perturbative QCD tests.

The new experiment SIDDHARTA, aims to improve the precision obtained by DEAR by an order of magnitude and to perform the first measurement ever of kaonic deuterium. Other measurements (kaonic helium, sigmonic atoms, precise determination of the charged kaon mass) are as well considered in the scientific program.

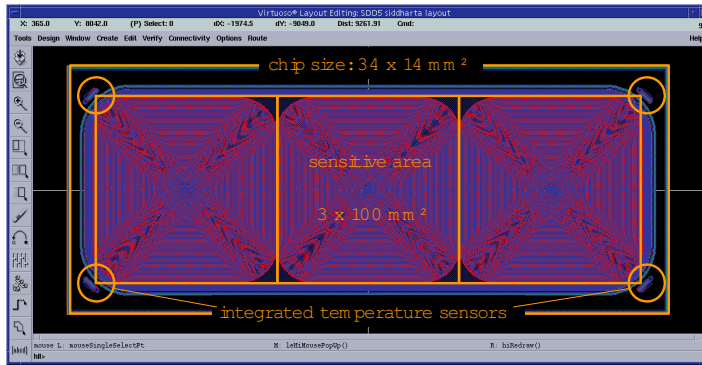


Figure 1: *SDD layout on the readout side.*

2 The SIDDHARTA experiment and preliminary tests

SIDDHARTA represents a new phase in the study of kaonic atoms at DAΦNE. The DEAR precision was limited by a signal/background ratio of about 1/70. In order to significantly improve this ratio a breakthrough is necessary. An accurate study of the background sources present at DAΦNE was re-done. The background includes two main sources:

- synchronous background: coming together with the K^- - related to K^- interaction in the setup materials and also to the ϕ -decay process; it can be defined hadronic background;
- asynchronous background: final products of electromagnetic showers in the machine pipe and in the setup materials originated by particles lost from primary circulating beams either due to the interaction of particles in the same bunch (Touschek effect) or due to the interaction with the residual gas.

Accurate studies performed by DEAR showed that the main background source in DAΦNE is of the second type, which shows the way to reduce it. A fast trigger correlated to the negative kaon entrance in the target would cut the main part of the asynchronous background.

While DEAR used for the X rays detection the CCD (Charge Coupled Device) detectors - excellent X-ray detectors, with very good energy resolution (about 140 eV FWHM at 6 keV), but having the drawback of being non-triggerable devices (since the read-out time per device is at the level of 10 s), a recently developed device, which preserves all good features of CCDs (energy resolution, stability and linearity) but additionally is triggerable - i.e. fast (at the level of $1\mu\text{s}$) was implemented. This new detector is represented by large area Silicon Drift Detector (SDD), specially designed for spectroscopic application. The development of the new 1 cm^2 SDD device is partially performed in the framework of an European Joint Research Activity (JRA10) within the FP6 program, the HadronPhysics I3.

A first successful test of a prototype array of 7 SDDs, 5 mm^2 each, was performed in July 2003 at the Beam Test Facility of Frascati (BTF), in realistic (i.e. DEAR-like) conditions. The results of this tests were very encouraging: a trigger rejection factor of $5 \cdot 10^{-5}$ was measured. Extrapolated to SIDDHARTA conditions, this number translates into a S/B ratio in the region of interest about 20/1. By triggering the SDDs, the asynchronous e.m. background (mainly due to Touschek effect) can therefore be eliminated.

The final large area SDD layout (see Fig. 1) was defined and the fabrication procedure started in 2004.

2.1 Summary of the 2004 activities

During the year 2004 the SIDDHARTA main activities at LNF were focussed on:

- i) long stability tests performed in the laboratory, as function of the incident rate and time, of the performance of the 7 SDD chips, 5 mm² each; these tests gave important information concerning the way in which the readout electronics should be built and the stabilization of the voltages on the SDD;
- ii) tests of a preliminary readout electronics, giving input for the design of the final electronics readout chip;
- iii) tests of a larger, 30 mm², prototype SDD chip in laboratory and at the BTF facility;
- iv) definition of the trigger system, based on back-to-back signature of the $\phi \rightarrow K^+ K^-$ process;
- v) Monte Carlo simulations of the setup and of its performance.

In the next paragraph we present the results of the 30 mm² SDD chip test at the BTF facility at Frascati.

2.2 30 mm² SDD chip tested at BTF

One of the main activities of SIDDHARTA at LNF in 2004 was the test of a 30 mm² SDD chip, Figure 2. The detector was firstly tested in the laboratory with very positive results: experimental resolution of about 140 eV at 6 keV, see Figure 3.

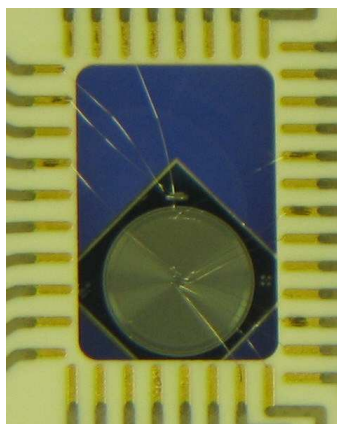


Figure 2: *The 30 mm² SDD chip used for testing in the laboratory.*

In the period 13-28 July 2004 a trigger test of the 30 mm² SDD chip was performed at the BTF facility.

Fig. 4 shows a scheme of the setup configuration. The beam coming from the BTF (510 MeV electrons, 50 Hz) hits a thin scintillator to provide a fast trigger signal, then is degraded in a 2 cm thick lead layer. The emerging secondaries from the e.m. cascade generated in lead, hit a set of selected materials (Cu, Zr) disposed at about 45 degrees with respect to the primary

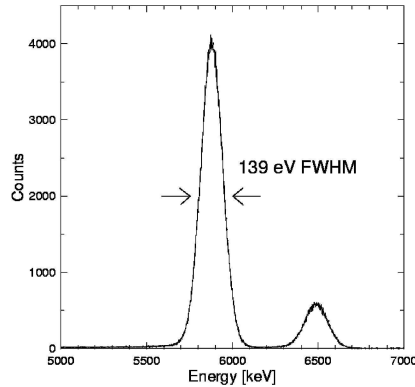


Figure 3: *The X-ray spectrum from an Iron source as measured in the laboratory with the 30 mm² SDD chip.*

beam line. Fluorescence X-ray transitions are then excited and reach the SDD. The detector can see the “signal” represented by the Cu and Zr fluorescence lines, superimposed to a continuous (synchronous) background represented by the secondaries (electrons, positrons, photons) generated in the e.m. cascade. To generate an “asynchronous” background, i.e. not time-correlated with the “signal”, two radioactive sources were employed (see Fig 3). One, a Sr source, due to its beta spectrum of maximum energy 2.24 MeV, produced a continuous background of soft electrons and photons. The other, a Fe source, produced a structured asynchronous background represented by the K_{α} and K_{β} Manganese lines.

A trigger test (1 μ s window), with an incident rate about 30 times higher than the one met in DEAR for the asynchronous background, confirmed on the larger 30 mm² SDD chip the $5 \cdot 10^{-5}$ rejection factor measured in 2003.

The remaining synchronous background was studied by Monte Carlo simulations and the result is a S/B ratio of the order 8/1.

3 Activity in 2005

The LNF activity of SIDDHARTA in 2005 is focussed in the following directions:

- test of the first production run of front-end electronics; participation in the design of the second production run and testing;
- design and testing of the DAQ system;
- test of a prototype for kaon trigger and start construction of the final trigger system;
- measurements in the lab and on BTF of 1 cm² SDD test setup;
- design of a multi-channel high voltage control system and biasing of the SDD detectors;
- finalize the setup design and start construction;
- Monte Carlo simulation of the system performance.

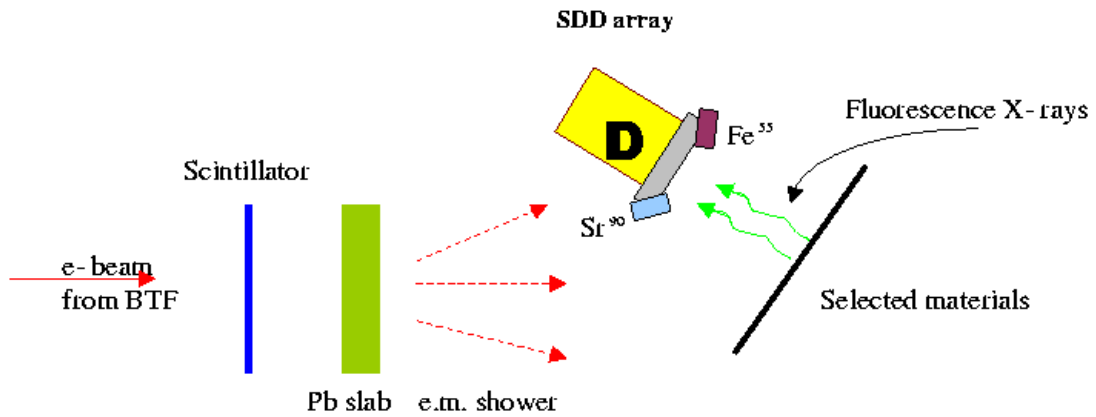


Figure 4: *The test experimental setup mounted in the BTF area*

4 Publications 2004

4.1 Conference Talks given by LNF Authors in Year 2004

1. C. Curceanu (Petrascu), **DEAR and SIDDHARTA: present and future precision measurements on kaonic hydrogen and kaonic deuterium**, "XLII International Winter Meeting on Nuclear Physics" Bormio, Italy, January 25-February 1, 2004.
2. D. Sirghi, **Kaonic atoms measured by DEAR at DAΦNE**, LNF Spring School in Nuclear, Subnuclear and Astroparticle Physics, Frascati (Italy), May 17th - 21st, 2004.
3. F. Sirghi, **Future precision measurement of kaonic atoms at DAΦNE**, LNF Spring School in Nuclear, Subnuclear and Astroparticle Physics, Frascati (Italy), May 17th - 21st, 2004.
4. M. Iliescu, **SIDDHARTA: The future of exotic atoms research at DAΦNE**, DAΦNE2004: Physics at meson factories, 7-11 June 2004, LNF Italy.
5. C. Curceanu (Petrascu), **Measurement of kaonic atoms at DAΦNE: what we can learn from their study**, International School of Physics "Enrico Fermi", Summer Courses 2004 Hadron Physics 22 June - 2 July 2004.
6. C. Curceanu (Petrascu), **Precision measurements on kaonic hydrogen and kaonic deuterium: present and future**, The 19th European Conference on Few-Body Problems in Physics, Groningen, The Netherlands, August 23-27, 2004.
7. C. Curceanu (Petrascu), **Misure di precisione di atomi kaonici a DAΦNE**, XC Congresso Nazionale Societa' Italiana di Fisica, Brescia, 20-25 Settembre 2004.

8. M. Iliescu, **Precision measurements on kaonic hydrogen and deuterium: DEAR and SIDDHARTA**, International Conference on the Structure of Baryons, Ecole Polytechnique, Palaiseau, France, October 25-29, 2004.
9. C. Guaraldo, **Measurement of kaonic hydrogen with DEAR at DAΦNE and future perspectives**, 5th Italy-Japan Symposium "Recent Achievements and Perspectives in Nuclear Physics", November 3-7, 2004, Naples, Italy.
10. C. Curceanu (Petrascu), **The kaonic helium case**, 5th Italy-Japan Symposium "Recent Achievements and Perspectives in Nuclear Physics", November 3-7, 2004, Naples, Italy.

4.2 Papers and Proceedings

1. C. Curceanu (Petrascu) *et al.*, **Last results from the DEAR experiment at DAΦNE**, American Institute of Physics (AIP), Editors E. Klempt, H. Koch, H. Orth, vol. 717 (2004) 175.
2. T. Ishiwatari *et al.*, **Kaonic nitrogen X ray transition yields in a gaseous target**, Phys. Lett. **B593** (1-4) (2004), 48.
3. C. Guaraldo *et al.*, **First results on kaonic hydrogen from DEAR at DAΦNE**, Eur. Phys. J. **A19** (2004) 185.
4. T. Ishiwatari *et al.*, **Performance of CCD X-ray detectors in exotic atom experiments**, Nucl. Instr. and Methods A, in press.
5. M. Cargnelli *et al.*, **Kaonic hydrogen measurement with DEAR at DAΦNE**, Proceedings of "MESON 2004, 8th International Workshop on Meson Production, Properties and Interaction", Krakow, Poland 4-8 June 2004.
6. J. Zmeskal, **First measurement of kaonic hydrogen and nitrogen X-rays at DAΦNE**, Proceedings of the DAΦNE2004 Conference: Physics at meson factories, 7-11 June 2004, LNF Italy.
7. M. Cargnelli *et al.*, **The SIDDHARTA project - experimental study of kaonic deuterium and helium**, Proceedings of the Hadron Structure 2004, Smolenice Castle, Slovakia, 30 August-3 September 2004.
8. J. Marton *et al.*, **DEAR: results on kaonic hydrogen**, Proceedings of the Hadron Structure 2004, Smolenice Castle, Slovakia, 30 August-3 September 2004.

4.3 Technical Notes

1. M. Bragadireanu *et al.* (SIDDHARTA Collaboration), **Tests of trigger on 30 mm² Silicon Drift Detector prototype performed at the Beam Test Facility (BTF) of LNF in the period 13 -28 July 2004**, SIDDHARTA Note-IR-5, November 2, 2004.
2. M. Bragadireanu *et al.* (SIDDHARTA Collaboration), **Rate dependence of the SDD response (signal, position and resolution) during the trigger tests on a 30 mm² chip performed at the Beam Test Facility (BTF) of LNF in the period 13 - 28 July 2004**, SIDDHARTA Note-IR-6, November 10, 2004.

VIP

S. Bartalucci, S. Bertolucci, M. Catitti (Bors.), C. Curceanu Petrascu (Resp. Naz.),
C. Guaraldo, M. Ilescu (Art. 23), F. Lucibello (Tecn.),
D. Sirghi (Bors. PD), F. Sirghi (Bors. PD), L. Sperandio (Osp.)

1 The VIP scientific case

The Pauli Exclusion Principle (PEP) represents one of the fundamental principles of the modern physics and our comprehension of the surrounding matter is based on it. Even if today there are no compelling reasons to doubt its validity, it still spurs a lively debate on its limits, as testified by the abundant contributions found in the literature and in many topical conferences and it is still possible to speculate that it is only an approximation of a more fundamental law, and that there may be tiny violations. The indistinguishability and the symmetrization (or antisymmetrization) of the wave-function should be then checked independently for each particle, and accurate tests were and are being done.

The VIP (Violation of the Pauli Exclusion Principle) experiment, an international Collaboration among 5 Institutions of 4 countries, has the goal to improve the current limit on the violation of the Pauli Exclusion Principle (PEP) for electrons, ($P < 1.7 \times 10^{-26}$ established by E. Ramberg e G. A. Snow: *Experimental limit on a small violation of the Pauli principle*, Phys. Lett. **B 238** (1990) 438) by four orders of magnitude ($P < 10^{-30}$), exploring a region where new theories allow for a possible PEP violation.

What actually VIP is doing is the search of “anomalous” X-ray transitions, i.e. electron transitions to states already occupied by the maximum allowed number of electrons compatible with the Pauli exclusion principle. The basic idea is to introduce “new” (fresh) electrons in a copper bar (new in the sense that the already existing ones in the copper bar had already all the time to perform the allowed and “prohibited” transitions) and measure the K-series ($2p \rightarrow 1s$) X-ray transitions for which the 1s level is already occupied by 2 electrons. Such transitions, obviously, would violate the PEP. The “anomalous” transitions in copper are identified by their energy shift, because instead of the normal 8.05 keV energy of the $2p \rightarrow 1s$ transition in Copper, one gets a value closer to the one corresponding to a (Z-1) atom (7.5 keV in this case), which can be readily measured by a high resolution X-ray detector as the one used in VIP - the Charge Coupled Device (CCD).

2 Experimental setup

The VIP setup is going to be built starting from the DEAR (DAΦNE Exotic Atom Research) one, which was successfully used to measure other exotic X-ray transitions (kaonic nitrogen and hydrogen) in the same energy region at the DAΦNE accelerator. DEAR ended its activity in 2003. The idea of performing a measurement of PEP for electrons was already present in the DEAR Collaboration, and a test measurement already done in 1998, applying the same method of Ramberg and Snow, for a period of three months, in the basement of the Neuchatel laboratory. The setup used 3 CCDs (Charge-Coupled Device) as X-ray detectors, with an energy resolution of 400-500 eV FWHM, already about 3 times better than the Ramberg and Snow setup. With the improved detector resolution and geometry, taking into account the integrated circulated current, the geometry and the material characteristics, an upper limit of $P < 0.95 \times 10^{-27}$ was obtained. After DEAR has finished its data taking being replaced by SIDDHARTA in the search of exotic atoms transitions at DAΦNE, the VIP experiment was prepared, presented and approved by INFN Nuclear Physics Commission in September 2004.



Figure 1: *The 2 CCD experimental test setup installed at LNGS - December 2004.*

The most important modification of the DEAR setup is the replacement of the plastic vessel, which contained the target gas, with a copper conductor that must be able to carry a large current close to the surface. At the moment, the design of this copper target is undergoing - few solutions being identified.

First tests at the LNGS laboratories were already performed in December 2004 with a 2 CCD setup, shown in Fig. 1, with encouraging results.

3 Activities in 2005

In first months of 2005 the background measurements at LNGS will continue, with the goal of optimizing the shielding to be used for the final setup. The copper-target is being actually built. The VIP setup will be installed before Summer and start taking data.

4 Publications 2004

- The VIP Collaboration, **The VIP Proposal**, presented at the LNGS Scientific Committee, October 2004.
- C. Petrascu *et al.*, **Interpretation of the background measurement results**, VIP Technical Note-IR-1, 20 November 2004.

FA51: FISICA ASTROPARTICELLARE

E. Nardi (Resp.)

1 Summary of the project

The main goal of the project during year 2004 has been that of carrying out a detailed study of the effects of neutrino masses on the neutrino signal from a future Galactic core-collapse supernova (SN). In a detector like SuperKamiokande (SK), a Galactic SN would yield several thousands of neutrino events within a time interval of a few tens of seconds, and for each event precise informations on the neutrinos arrival times and energies will be available. Since no laboratory experiment nor any other event in nature could yield such a large number of neutrinos in such a short time, it is worthwhile studying what informations on neutrino masses could be obtained at present detectors as well as at future large volume neutrino detectors.

2 Description of the 2004 activity

In ¹⁾ we presented the basic ideas underlying a new method to study a SN neutrino signal, together with some preliminary results. Differently from most of the methods proposed in the past, our method allows to study possible neutrino time-of-flight delays relying exclusively on the analysis of the detected signal, and therefore it is independent of particular astrophysical assumptions and does not require the occurrence of additional phenomena to measure the neutrinos time lags. The original statistical approach, that in ¹⁾ was justified mainly in terms of intuitive reasoning, has been put on a more rigorous basis by means of Bayesian inference reasoning in ²⁾. In this second paper the sensitivity of present and future water Čerenkov and scintillator neutrino detectors to neutrino mass effects was studied in detail. Since the method is based on the accurate reconstruction of the time evolution of the neutrino flux and spectrum, it can be successfully applied only to large statistics neutrino samples. In particular, it is not well suited to analyze the few hundreds of events expected in scintillator detectors like LVD or KamLAND. However, since KamLAND is located in the same site than SK, earth-matter effects on neutrinos will be the same for both detectors, and moreover the same clock could be used for timing both SK and KamLAND events. This allows to carry out a combined analysis of the SK and KamLAND data (see table 1).

To test the sensitivity of our method, we have analyzed a significant number of neutrino samples, grouped into different ensembles containing about 40 samples each. Each ensemble corresponds to a particular set of input conditions in the Monte Carlo (MC): we use two different SN models (model 1 and 2) and vary in turn the SN-earth distance (5, 10, and 15 Kpc) and the detection parameters (fiducial mass, threshold and energy resolution) specific for two operative detectors (SK and KamLAND) and for two proposed detectors (HyperKamiokande (HK) and LENA). Two kind of estimates are carried out: *i)* we estimate the upper limits at 95% c.l. that could be put on the neutrino mass from the analysis of the data, in case m_ν is too small to produce observable time-of-flight delays; *ii)* we estimate for which value of the mass, a massless neutrino can be rejected with good confidence. The results of our study are resumed in table 1. The conclusion is that from the observation of the neutrino signal from a future Galactic SN, detectors presently in operation could set limits on the neutrino masses of the order of 1 eV. This is better than current limits from tritium β -decay experiments, competitive with the most conservative results from neutrino-less double β -decay, less precise but remarkably less dependent from prior assumptions

Table 1: Results for the fits to the neutrino mass using two different SN models, at the SK (for three different SN-earth distances), SK plus KamLAND, HK (proposed) and LENA (proposed) detectors. The number of expected neutrino events are given in columns 2 and 5. The 95% c.l. upper limits that could be put on m_ν when the mass is vanishingly small are given in columns 3 and 6. The quoted ‘error’ is indicative of the statistical fluctuations of the analysis. The smaller values of m_ν for which in the majority of the runs a massless neutrino could be excluded at 95% c.l. are given in columns 4 and 7.

	Model 1			Model 2		
Detector	N. events ($\times 10^3$)	$\bar{m}_{\text{up}} \pm \Delta m_{\text{up}}$ eV	$\sqrt{m_{\text{min}}^2}$ eV	N. events ($\times 10^3$)	$\bar{m}_{\text{up}} \pm \Delta m_{\text{up}}$ eV	$\sqrt{m_{\text{min}}^2}$ eV
a) SK (10 kpc)	10.0	1.1 ± 0.2	1.1	5.9	1.2 ± 0.3	1.2
b) SK (5 kpc)	40.0	1.2 ± 0.2	1.2	23.7	1.2 ± 0.3	1.2
c) SK (15 kpc)	4.4	1.4 ± 0.3	1.5	2.6	1.7 ± 0.6	1.8
d) SK+KL (10 kpc)	10.4	1.1 ± 0.2	1.0	6.1	1.2 ± 0.3	1.2
e) HK (10 kpc)	170	0.5 ± 0.1	0.6	100	0.6 ± 0.1	0.6
f) LENA (10 kpc)	12.6	1.0 ± 0.2	1.0	7.5	1.0 ± 0.3	1.1

than cosmological bounds. Future megaton water Čerenkov detectors will allow for about a factor of two improvement. However, they will not be competitive with the next generation of laboratory experiments.

To carry out this study, a package of MC computer codes for generating realistic supernova neutrino signals under different initial conditions (fluxes, spectra, flavor mixing patterns, etc.) had to be written. This SUPernova Neutrino Generation (SUNG) package has now been equipped with a user-friendly interface, and made publicly accessible (in test mode) at <http://www.sungweb.tk/>. We think that it can provide a useful aid for further SN neutrino studies also for other groups.

References

1. E. Nardi and J. I. Zuluaga, “Exploring the sub-eV neutrino mass range with supernova neutrinos”, Phys.Rev.D **69**:103002, 2004.
2. E. Nardi and J. I. Zuluaga, “Constraints on neutrino masses from a Galactic supernova neutrino signal at present and future detectors”, E-Print Archive: hep-ph/0412104, (Submitted to Nucl. Phys. B).
3. E. Nardi, “Measuring neutrino masses with supernova neutrinos”, Proceedings of the 10th Marcel Grossmann Meeting on General Relativity, Gravitation and Relativistic Field Theories (MG X MMIII), Rio de Janeiro, Brazil, 20-26 Jul 2003. Edited by M. Novello, S. Perez-Bergliaffa and R. Ruffini, World Scientific, Singapore, 2005; e-Print Archive: astro-ph/0401624.
4. E. Nardi, “Supernova neutrinos and the absolute scale of neutrino masses: a Bayesian approach”, to appear in the proceedings of 5th Latin American Symposium on High Energy Physics (V-SILAFEA), Lima, Peru, 12-17 Jul 2004; e-Print Archive: hep-ph/0412024.

LF-11: SYNCHROTRON RADIATION SPECTROSCOPIES AND THE PHYSICS OF STRONGLY CORRELATED ELECTRON SYSTEMS

S. Bellucci, M. Benfatto, S. Di Matteo (Ass.), K. Hatada (Ass), K. Hayakawa (Ass), C.R. Natoli (Resp.), P. Onorato (Ass), N. Perkins (Visit.), A. Tenore, Wu Ziyu (Visit.)

1 The Project

The aim of this project is the theoretical analysis of strongly correlated electron systems, both in three and lower dimensions. In the first category systems showing orbital degeneracy (manganites, cuprates and transition metal oxides), geometrical frustration (spinel, pyrochlore lattices) or exotic magnetic structures ($\text{Li}_2\text{VOSiO}_4$), show very interesting physical phenomena, while on the low dimensional side nanotubes and nanostructures present novel quantum mechanical features that are particularly intriguing. Indeed both categories hold quite fundamental as well as technological interest. When appropriate methods borrowed from field theory and statistical mechanics are used to bear on the description of the essential physics of such systems. At the same time in-depth theoretical studies of significant synchrotron radiation spectroscopies (absorption, dichroism, elastic and inelastic resonant x-ray scattering, etc.) that can shed light on charge and magnetic correlations in such systems are carried out. Finally the theory underlying the multiple scattering programs used to analyse such spectroscopies is improved and applications are made to obtain structural and electronic information in condensed matter systems, with an eye to systems of biological relevance.

2 Physics of strongly correlated electron systems in 3D

The research in this field has developed along three main directions:

- Analysis of synchrotron radiation experiments (resonant x-ray scattering, absorption and dichroism) in V_2O_3 , $\text{Li}_2\text{VOSiO}_4$ and pyrochlore materials (MgTi_2O_4 , ZnV_2O_4).
- Examples of the polar (magnetic) and axial (non-magnetic) toroidal multipoles in chiral systems and their detection by means of x-ray resonant scattering.
- Investigation of the physics of the complex magnetic oxides like LiV_2O_4 , MgTi_2O_4 , ZnV_2O_4 , $\text{Li}_2\text{VOSiO}_4$, V_2O_3 , Sr_2FeWO_6 , $\text{Nd}_{1-x}\text{Sr}_x\text{Mn}_{1-x}\text{Ru}_x\text{O}_3$ and perovskites.

2.1 Analysis of synchrotron radiation experiments

We have extended the tensor analysis derived for circular and linear dichroism in photoemission and photoabsorption to Bragg-forbidden reflections in anomalous diffraction.

In one case we have studied the bidimensional frustrated magnetic material $\text{Li}_2\text{VOSiO}_4$, which is described by a J-J' square Heisenberg Hamiltonian. Here, contrary to previous reports based on neutron diffraction, it has been demonstrated that the ordered model in the low-temperature phase is very close to the value expected for the square lattice Heisenberg model (about 0.6 Bohr magnetons). The possibility to perform numerical simulations of the magnetic low-temperature signal in this case proved to be essential for the correct interpretation of the experimental data of resonant magnetic scattering¹).

In order to treat magnetic effects, we have developed a relativistic extension of the Schrödinger Equation, obtained by eliminating the small component of the wave-function in the Dirac Equation, thereby working with the usual non relativistic set of quantum numbers (l, m, σ) for the angular and

spin momenta. Spin polarized atomic potentials were obtained following the prescription by von Barth and Hedin starting from non self-consistent but realistic spin dependent charge densities. Electric dipole-dipole (E1-E1), dipole-quadrupole (E1-E2) and quadrupole-quadrupole (E2-E2) transition were considered altogether.

We have in this way interpreted recent x-ray resonant scattering experiments carried out in the monoclinic phase of V_2O_3 at the vanadium K-edge by Paolasini (L. Paolasini et al, Phys. Rev. Lett. 82, 4719 (1999)) We have obtained satisfactory agreement with experiments, both in energy and azimuthal scans. As a result we are able to show that all the main features of the Bragg-forbidden reflections with $h + k + l = \text{odd}$ and h odd or even can be interpreted in terms of the antiferromagnetic ordering only, i.e. they are of magnetic origin. No reduction of symmetry from the magnetic space group suggested by neutron scattering experiments, either due to orbital ordering or some other still unknown effect, is necessary to explain the observed patterns. In particular the energy scan of the (1,1,1) monoclinic reflection excludes the possibility of any kind of orbital ordering, contrary to what previously suggested by other authors ²⁾.

Another question again involving V_2O_3 concerns the nature of the magnetic space group in its monoclinic phase. All experiments performed before 2000 had shown that the system admitted a different magnetic space group than suggested by a recent dichroic experiment at vanadium K edge (Goulon *et al.* Phys. Rev. Lett. 85, 4385 (2000)). The authors of this latter work found that the systems allows non-reciprocal effects, implying that time-reversal and inversion symmetries are broken and only their product conserved, contrary to previous findings. This situation led to a further experiment to resolve this inconsistency (S. Di Matteo, A.G.M. Jansen, Phys. Rev. B 66, R100402 (2002)): however no magnetic-electric effect was detected in the system, and this finding is not compatible with the presence of a non-reciprocal gyrotropic linear dichroism. This result solved a problem but raised another question: the correct interpretation of the dichroic experiment at the vanadium K edge. For this reason we have analysed this experiment in more detail, in order to give a consistent interpretation of all the recent x-ray resonant scattering and dichroic experiments in V_2O_3 ³⁾. Moreover, we have performed numerical simulations based on the multiple scattering theory for both dichroic and resonant scattering spectra, analysing the experimental implications related to the different magnetic space symmetries. We have shown in this way the paradoxical consequences of the interpretation proposed by Goulon *et al* quoted above on the physics of this system and suggested how to perform unambiguously the dichroic experiment in order to dissipate any doubt on the properties of the system. Following this suggestion a new linear dichroism experiment has been performed, which confirms our previous interpretation: the results are analyzed in Ref. ⁴⁾.

The last argument involving V_2O_3 has concerned the study of the monoclinic "nucleation" in the corundum phase of the Cr-doped samples when cooled from the paramagnetic insulating to the antiferromagnetic insulating phase. Contrary to what observed in the pure system and to theoretical expectations, a breakdown of the trigonal symmetry, already slightly below room temperature, is observed. Such a study has been published in ⁵⁾.

In section 2.3 below we show how the analysis of resonant x-ray scattering can shed light on the ground state properties in frustrated spinels, like $MgTi_2O_4$ and ZnV_2O_4 .

Finally the interpretation of iron K edge absorption spectra in naturally layered silicates has led to the description of their magnetic transition as an order/disorder one ⁶⁾, definitively ruling out the possibility, advanced in the literature, of a high-spin to low-spin transition.

2.2 Analysis of the magnetic and non-magnetic anomalous scattering

The second direction of research is concerned with the analysis of the polar (magnetic) and axial (non-magnetic) toroidal multipoles of a system by means of x-ray dichroism and resonant scattering.

In this field a lot has been done, especially in russian literature, but very little has been said in connection with the detection of toroidal moments by means of resonant scattering. For this reasons, a general discussion of (magnetic and non-magnetic) toroidal multipolar expansion in condensed matter systems has been given, with the aim of applying it to the theory of anomalous x-ray resonant scattering. The idea turned out to be fruitful, and the main results of such a work regard the possibility to detect the toroidal moment and its multipoles in centrosymmetric magnetic systems by means of RXS and to separate in a similar way all the parity and time-reversal odd multipolar components. We have found that, e.g., the system $\text{Li}_2\text{VOSiO}_4$ is well suited for such an analysis, ¹⁾ and have performed a detailed simulation by means of a relativistic extension of the FDMNES program, that illustrates under which conditions the magnetic toroidal moment can be detected ⁷⁾. A more general work regarding parity and time-reversal even/odd multipole detection through resonant spectroscopies has recently been completed ⁸⁾.

2.3 Investigation of the physics of the complex magnetic oxides

The third direction of research concerns the investigation of the physics of complex magnetic oxides such as LiV_2O_4 , MgTi_2O_4 , ZnV_2O_4 , Sr_2FeWO_6 , $\text{Nd}_{1-x}\text{Sr}_x\text{Mn}_{1-x}\text{Ru}_x\text{O}_3$ and the manganites which exhibit a whole variety of interrelated phenomena such as metal-insulator transitions, orbital and magnetic ordering, double exchange, geometrical frustration, heavy fermion behaviour and colossal magnetoresistance.

The interest in frustrated systems lies in the fact that their ground state is highly degenerate and can evolve in a variety of ways: they can freeze on cooling forming ice, remain liquid down to the lowest temperature due to quantum effects or, finally, lift their geometrical degeneracy through a phase transition that lowers the local symmetry. One of them is the intriguing paramagnetic transition-metal oxide LiV_2O_4 . This compound has a spinel structure and its lattice consists of corner-shared tetrahedrons of $\text{V}^{+3.5}$ ions (pyrochlore lattice) located in slightly distorted oxygen octahedron. It is the first metal showing heavy fermion behavior without f orbitals, moreover LiV_2O_4 has some peculiar magnetic properties. The magnetic susceptibility and inelastic neutron scattering measurements indicate a spin liquid behavior over a large range of intermediate temperatures (for example, S.-H. Lee *et al.*, Phys. Rev. Lett. **86**, 5554 (2001)). On the other hand, analysis of recent neutron scattering experiments (A.P. Murani *et al.*, J. Phys.:*Condens. Matter* (2004)) revealed that in addition to antiferromagnetic correlations, ferromagnetic-like correlations on V sites appeared over some temperature range. The minimal model, that we have considered by means of an exact diagonalization study, includes both purely Heisenberg-like contribution from the super-exchange interaction among localized spins and an effective ferromagnetic double-exchange contribution driven by the itinerant electronic excitations. We have calculated the total spin correlation functions and, consistently with experimental observations, their temperature dependence shows a crossover from antiferromagnetic to ferromagnetic behavior when the temperature is increased. The increasing population of the magnetic states with temperature results in the formation of a non-zero residual magnetic moment which is also observed in the experiments. ¹³⁾

MgTi_2O_4 is another spinel, which recently has attracted much attention because of its tendency to dimerize. It undergoes a metal-insulator transition on cooling below $T = 260\text{K}$, which is accompanied by strong lattice distortion leading to the formation of helical chains of short and long bonds running along the tetragonal c axis, a unique example of chiral ordering of the spinel structure. In order to study the low temperature phase of MgTi_2O_4 , we have derived an effective spin-1/2, pseudospin-1 Hamiltonian and demonstrated that the orbital degrees of freedom can remove the infinite spin-degeneracy of the "pyrochlore" structures and induce a spin dimerization. Moreover, we have shown that the residual orbital degeneracy can be lifted by the spin-lattice

interaction forcing a tetragonal distortion to the chiral structure actually observed. We propose to investigate such a low-symmetry phase by means of x-ray natural circular dichroism. The work has been published in Phys. Rev. Lett.⁹⁾ We have then extended the previous idea of spin-lattice interaction to a quantitative model taking into account all the normal modes of the tetragonal low-temperature lattice: this has led us to a better description of the experimental data, and is presently considered for publication in Phys. Rev. B.¹¹⁾

Moreover, we have found out that the introduction of a spin-orbit interaction, that does not modify the situation with Ti^{3+} ion, strongly affects the physics of V^{3+} ion, as in ZnV_2O_4 . Here the interplay of superexchange, spin-orbit, and spin-lattice interactions is so deep that the ground state of the system with V^{3+} ion is completely different from that of the Ti^{3+} ion, the former being a one dimensional antiferromagnet, while the latter was a dimerized singlet state. Thus, spin-orbit coupling can exert a strong influence on these systems, even though its magnitude is much smaller than the typical superexchange energies (20 meV vs. 80 meV). Remarkably, we have found that it is possible to single out all orbital and magnetic orderings that appear in the phase diagram of this system by means of resonant x-ray scattering, with different polarization conditions and/or exchanged wave vectors. This work has been submitted for publication to Phys. Rev. Lett.¹²⁾

Another field of growing interest is that of the so-called double perovskites, that are becoming more and more important after the discovery of their colossal magnetoresistance. We focused on the insulating double perovskite Sr_2FeWO_6 , and derived its phase diagram on the basis of an effective spin-orbital Hamiltonian. The technique adopted for such a derivation and for the construction of the effective hamiltonian was borrowed from our previous experience on V_2O_3 . In this case, however, we had to deal with the much more complicated case of 4 electrons in 5 Fe-orbitals and include the empty W-orbitals. Our results predicted two transition temperatures, the higher to an antiferromagnetic state and the lower to an orbitally ordered state. We have suggested a possible experiment to detect both kinds of ordering.¹⁰⁾

In collaboration with the neutron diffraction group in Dubna, we also studied the compound $\text{Nd}_{1-x}\text{Sr}_x\text{Mn}_{1-x}\text{Ru}_x\text{O}_3$. In this case, the correlated doping of A- and B-sites with Sr and Ru ions in $\text{Nd}_{1-x}\text{Sr}_x\text{Mn}_{1-x}\text{Ru}_x\text{O}_3$ leads to long-range ferrimagnetic ordering but leaves the system insulating. Such an experimental fact has been observed for the first time and, in order to explain it, the role of Ru-doping has been analyzed under several aspects. The mean-field phase diagram of this compound has been studied as a function of the doping x .¹⁴⁾

Finally some structural properties have been investigated at the metal K-edge of 3d transition-metal compounds.¹⁵⁾

3 Improving the analysis of synchrotron radiation spectroscopies

3.1 Multichannel multiple scattering theory

The collaboration between the Frascati group and P. Kruger, from the University of Bourgogne (Dijon), on the Multichannel Multiple Scattering Theory (MMST) has produced a methodological paper.¹⁶⁾ Here a formalism for the calculation of x-ray absorption in condensed matter that combines eigenchannel R-matrix and multiple scattering theory and allows to take account for local correlation effects in a configuration interaction scheme, has been presented.

At present, the type of correlations that can be handled at this level are limited to those between one electron in a delocalized state and a finite number of electrons/holes in sufficiently localized orbitals, in which the wave function is negligibly small beyond the atomic radius. This applies exactly to inner-core shells and well to the 4f-shell in rare earths. Extensions of the method to include correlation effects between several delocalized electrons are under way. This last case includes the 3d-electrons of transition metal ions of the first series, some of which are of

great biological significance. After this extension the computer code will be made available to the interested SR scientific community through the SRRTNet program.

In a second paper an application of the method with an eye to biological problem has been made. 17)

3.2 Fitting of the XANES spectra by a full multiple scattering procedure

Applications of the method, already described in the previous reports, to problems of biological interest or to significant test cases have continued, as exemplified by refs.. 18, 23) For these applications the computer code has been adapted to parallel processing in a portable way, which means distributing different parts of the calculation across multiple processors (in a PC CLuster) based on the MPI Protocol. This entails a gain in computing speed by an order of magnitude or more. After publication, this computer code will be made available to the scientific community through the SRRTNet program

3.3 Beyond the muffin-tin approximation in Multiple Scattering Theory

An efficient new method for solving the 3-dimensional Schrodinger Equation with an arbitrary local potential and generating local solutions to fit in a Multiple Scattering Scheme has been devised and tested on known solutions. A Non-Muffin-Tin (NMT) MS code has been set up and is being tested for convergence in the various angular momentum expansions appearing in the theory (A. Gonis and W.H. Butler, Multiple Scattering in Solids, GTCP series, Springer-Verlag, N.Y. 2000). Due to the difficulty in controlling several expansion parameters in a user friendly mode, we are trying to formulate the theory (and accordingly the computer code) in such a way as to have only one expansion parameter. This latter governs the expansion of the global solution in local basis functions inside any particular of the set in which the whole physical space has been partitioned. The conditions for the validity of such an approach are being studied.

4 Nanotubes and Nanostructures

4.1 Quantum dots

In this respect, we investigated the effects of a strong transverse magnetic field in 2DEG Quantum Wires and Quantum Dots in the presence of Rashba Spin Orbit coupling. As we know magnetic field enhances the spin selection in the current and also give very singular spin textures in the nanostructures. We proposed these systems as possible devices for the spin filtering at low and intermediate temperature regime.

4.2 Carbon nanotubes

Another class of systems we have investigated is that of carbon nanotubes. We have examined several distinct issues.

A scaling approach allows us to encompass the different values of the critical exponent (α) measured for the tunneling density of states in carbon nanotubes. Our results can be compared with those from recent experiments, where measurements of the tunnelling conductance have been carried out in doped Multi Walled Carbon Nanotubes (MWNT), with a number of subbands at the Fermi level $N_s=10$ (in the outer layer). Our results show an overall agreement with the exponents measured in MWNT. We predict that further reduction of α should be observed in multi-walled nanotubes with a sizeable amount of doping.

Recent experiments about the low temperature behaviour of a Single Wall Carbon Nanotube (SWNT) showed typical Coulomb Blockade peaks in the zero bias conductance. We gave a theoretical explanation of this behaviour starting from a microscopic model of the many electron system, comparing results for SWCNT with those obtained for an ideal vertical Quantum Dot. Defects and doping can break some symmetries of the system, as revealed by the experimental data, so we introduce an appropriate model in order to approach this problem.

Starting from the recent experiment by Kanda *et al.* ²⁴⁾, in which an intermediate regime has been explored, measuring the zero-bias conductance at temperatures where the thermal energy becomes comparable to the level spacing in the discrete spectrum of a MWNT, we developed a theoretical approach to the low-energy properties of 1D electron systems aimed at encompassing the mixed features of Luttinger liquid and Coulomb blockade behavior observed in the crossover between the two regimes. For this purpose, we extend the Luttinger liquid description by incorporating the effects of a discrete single-particle spectrum. The intermediate regime is characterized by a power-law behavior of the conductance, but with an exponent that oscillates as a function of the gate voltage, in agreement with recent experimental observations. Our construction also accounts naturally for the existence of a crossover in the zero-bias conductance, mediating between two temperature ranges in which the power-law behavior is preserved but with a different exponent.

We also developed some theoretical approaches to the properties of 1D electron systems under the action of a strong transverse magnetic field B in order to evaluate the critical exponent α measured for the tunneling density of states: Renormalization group methods were used for studying the low-energy behavior of the unscreened Coulomb interaction in MWNT. Our results imply a variation with B in the value of the exponent for the tunneling density of states, which is in fair agreement with that observed in transport experiments. We apply the Luttinger model, in order to analyze the effects of the short range term of the interaction and the magnetic field on the electron liquids in Quantum Wires and especially on their power-law behaviour in all correlation functions. The focal point is the rescaling of all the repulsive terms of the interaction between electrons with opposite momenta, due to the edge localization of the electrons and to the reduction of the magnetic length. Because of the same two reasons we found some interesting effects of the magnetic field concerning the backward scattering due to the presence of one impurity and the corresponding conductance. We extended the dimensional regularization approach, in order to deal with the low-energy effects of the long-range Coulomb interaction when a strong transverse magnetic field acts on a quasi 1D electron system. Thanks to this method we can avoid the infrared singularities arising from the long-range Coulomb interaction at $D = 1$. Also this approach allows us to fit the variation with B in the value of the exponent for the tunneling density of states, which is in fair agreement with that observed in transport experiments for MWNT.

Channeling of a particle beam in straight and bent single-wall nanotubes, with a strong potential impact onto the accelerator world, has been studied in computer simulations (Monte Carlo). The first results identify the range of carbon nanotube parameters (diameter, length, curvature) suitable for channeling of GeV particles. This may be used to create a very elegant technique of beam handling at accelerators. ²⁵⁾

We reported on a scanning tunneling microscopy (STM) of AlN nanotubes synthesized by gas phase condensation using the solid-vapour equilibrium. We showed that the AlN nanotubes have different morphologies from usual straight ones and that they appear in twisted and helicoidal arrangements showing a period of 2.0 -2.5 nm. We found two kinds of helicoidal structures: one is correlated to the different atomic arrangements of AlN molecules leading to the thermodynamic equilibrium and the other to slip dislocations induced by stress. The former ones are compared with the theoretical predictions reported by other workers on AlN. ²⁶⁾

References

1. A. Bombardi, J. Rodriguez-Carvajal, S. Di Matteo *et al.*, “Direct determination of the magnetic ground state in the square lattice $S=1/2$ antiferromagnet $\text{Li}_2\text{VOSiO}_4$ ”, *Phys. Rev. Lett.* **93**, 027202 (2004).
2. Y. Joly, S. Di Matteo, and C.R. Natoli, “Ab-initio simulations of resonant x-ray scattering on the insulating phase of V_2O_3 compared with recent experiments”, *Phys. Rev. B* **69**, 224401 (2004).
3. S. Di Matteo, “On the nature of the magnetic space group in the monoclinic phase of V_2O_3 ”, accepted for publication in *Physica Scripta* (September 2004).
4. C. Meneghini, S. Di Matteo, C. Monesi *et al.*, “Structural dichroism in the antiferromagnetic insulating phase of V_2O_3 ”, *submitt. to Phys. Rev. B*.
5. A. Bombardi, F. de Bergevin, S. Di Matteo *et al.*, “Precursor symmetry breaking in Cr-doped V_2O_3 ”, *Physica B* **345**, 40-44 (2004).
6. A. Marcelli, G. Cibir, S. Di Matteo *et al.*, “Octahedral low spin symmetric configurations vs. high spin octahedral distorted configurations: The case of Fe in natural layered silicates”, *Jour. Phys. Chem. Solid* **65**, 1491 (2004).
7. S. Di Matteo, “Resonant x-ray scattering as a probe of toroidal moments in centrosymmetrical systems: The case of $\text{Li}_2\text{VOSiO}_4$ ”, *Phys. Rev. B* **70**, 165115 (2004).
8. S. Di Matteo, Y. Joly, and C.R. Natoli, “Detection of electromagnetic multipoles by resonant x-ray spectroscopies”, *submitt. to Phys. Rev. B*.
9. S. Di Matteo, G. Jackeli, C. Lacroix, and N.B. Perkins, “Valence bond crystal in a pyrochlore antiferromagnet with orbital degeneracy”, *Phys. Rev. Lett.* **93**, 077208 (2004).
10. N.B. Perkins, S. Di Matteo, and G. Jackeli, “An effective spin-orbital Hamiltonian for Sr_2FeWO_6 ”, *Int. Jour. Mag. & Mag. Mat.* **272-276**, 132 (2004).
11. S. Di Matteo, G. Jackeli, and N.B. Perkins, “Valence-Bond Crystal, and Lattice Distortions in a Pyrochlore Antiferromagnet with Orbital Degeneracy”, *submitted to Phys. Rev. B*.
12. S. Di Matteo, G. Jackeli, and N.B. Perkins, “Orbital and magnetic ordering in vanadium spinels”, *submitt. to Phys. Rev. Lett.*
13. S. Burdin, N.B. Perkins and C. Lacroix, “Electronic states and magnetic excitations in LiV_2O_4 ”, *Journal of Physics: Condensed Matter* **16**, S621 (2004).
14. A.M. Balagurov, S.N. Bushmeleva, V.Yu. Pomjakushin, D.V. Sheptyakov, V.A. Amelichev, O.Yu. Gorbenko, A.R. Kaul, E.A. Gan’shina and N.B. Perkins, “Magnetic structure of NdMnO_3 consistently doped with Sr and Ru”, *Phys. Rev. B* **70**, 014427 (2004).
15. Wu ZY, Xian DC, Hu TD, Xie YN, Tao Y, Natoli CR, Paris E, Marcelli A, “Quadrupolar transitions and medium-range-order effects in metal K-edge x-ray absorption spectra of 3d transition-metal compounds”, *Phys. Rev. B* **70**, 014427 (2004).
16. P. Kruger and C. R. Natoli, “X-ray absorption spectra at the Ca- $L_{2,3}$ -edge calculated within multichannel multiple scattering theory”, *Phys. Rev. B* **70**, 245120 (2004).

17. P. Kruger and C. R. Natoli, "Theory of Ca-L_{2,3} edges using a novel multichannel multiple scattering method", *J. Synchrotr. Rad.* **12**, 80-84 (2005).
18. Benfatto M, Della Longa S, Qin Y, *et al.*, "The role of Zn in the interplay among Langmuir-Blodgett multilayer and myelin basic protein: a quantitative analysis of XANES spectra", *Biophys Chem* **110**, 191-201 (2004).
19. Sepulcre F, Proietti MG, Benfatto M, *et al.*, "A quantitative XANES analysis of the calcium high-affinity binding site of the purple membrane", *Biophys J* **87**, 513-520 (2004).
20. D'Angelo P, Lucarelli D, della Longa S, *et al.*, "Unusual heme iron-lipid acyl chain coordination in *Escherichia coli* flavohemoglobin", *Biophys J* **86**, 3882-3892 (2004).
21. D'Angelo P, Benfatto M, "Effect of multielectronic configurations on the XAFS analysis at the FeK edge", *J Phys Chem A* **108**, 4505-4514 (2004).
22. Bubacco L, van Gastel M, Benfatto M, *et al.*, "What are the structural features of the active site that define binuclear copper proteins function?", *Micron* **35**, 143-145 (2004).
23. Hayakawa K, Hatada K, D'Angelo P, Della Longa S, Natoli CR and Benfatto M., "Full Quantitative Multiple-Scattering Analysis of X-ray Absorption Spectra: Application to Potassium Ferro- and Ferricyanide Complexes", *J. Am. Chem. Soc.* **126**, 15618-15623(2004).
24. S. Bellucci, J. Gonzalez, P. Onorato, "Doping- and size-dependent suppression of tunneling in carbon nanotubes", *Phys. Rev. B* **69**, 085404 (2004).
25. S. Bellucci, Biryukov VM, Britvich GI, *et al.*, "Crystal undulator as a new compact source of radiation", *Phys. Rev. ST Accel. Beams* **7**, 023501 (2004).
26. Balasubramanian C, Bellucci S, Castrucci P *et al.*, "Scanning tunneling microscopy observation of coiled aluminum nitride nanotubes", *Chem. Phys. Lett.* **383**, (2004) 188.
27. S. Bellucci, V. Biryukov, CERN Cour. 44N6 (2004) 19.
28. S. Bellucci, V.M. Biryukov, A.G. Afonin, *et al.*, "Accelerator Tests of Crystal Undulators", Invited talk at the NATO ARW "Advanced Photon Sources and Their Application" (Nor Hamberd, Armenia August 29 - September 02, 2004), physics/0412159.
29. S. Bellucci, "Testing the X-rays production from crystal undulators at positron facilities", Proc. of the 9th Topical Seminar on Innovative Particle and Radiation Detectors on 23-26 May, 2004 in Siena, Italy, *Nucl. Phys. B Proc. Suppl.* (in press).

LF21: PHENOMENOLOGY OF ELEMENTARY PARTICLE INTERACTIONS AT COLLIDERS

G. Isidori, F. Mescia (Ass. Ric.), G. Pancheri (Resp.),
O. Shekhovstova (Bors. PD), C. Smith (Bors. PD), S. Trine (Bors. PD)

1 Summary of the project

The research topics investigated by this project can be divided into two main areas:

- Flavour physics.
- Total hadronic cross-sections.

The first area, discussed in Section 2, concerns the possibility to perform new low-energy precision tests about the mechanism of quark-flavor mixing, by means of K and B meson decays. The second area, discussed in Section 3, is in itself divided into two sections, one related to precision determination of the total hadronic cross-section in electron-positron colliders at low energy, while the other is related to the QCD description of hadronic and photonic total cross-section at high energies.

2 Flavour Physics

Despite the Standard Model (SM) provides a successful description of particle interactions, it is natural to consider it only as the low-energy limit of a more general theory, or as the renormalizable part of an effective field theory valid up to some still undetermined cut-off scale Λ . Since the SM is renormalizable, we have no direct indications about the value of Λ . However, theoretical arguments based on a natural solution of the hierarchy problem suggest that Λ should not exceed a few TeV.

One of the strategies to obtain additional clues about the value of Λ is to constrain (or find evidences) of the effective non-renormalizable interactions, suppressed by inverse powers of Λ , which encode the presence of new degrees of freedom at high energies. These operators should naturally induce large effects in processes which are not mediated by tree-level SM amplitudes, such as $\Delta F = 1$ and $\Delta F = 2$ flavour-changing neutral current (FCNC) transitions. Up to now there is no evidence of these effects and this implies severe bounds on the effective scale of dimension-six FCNC operators. For instance the good agreement between SM expectations and experimental determinations of $K^0-\bar{K}^0$ mixing leads to bounds above 10^3 TeV for the effective scale of $\Delta S = 2$ operators, i.e. well above the few TeV range suggested by the Higgs sector.

The apparent contradiction between these two determinations of Λ is a manifestation of what in many specific frameworks (supersymmetry, technicolour, etc.) goes under the name of *flavour problem*: if we insist with the theoretical prejudice that new physics has to emerge in the TeV region, we have to conclude that the new theory possesses a highly non-generic flavour structure. Interestingly enough, this structure has not been clearly identified yet, mainly because the SM, *i.e.* the low-energy limit of the new theory, doesn't possess an exact flavour symmetry. The attempt to clarify this structure, both at the phenomenological level (with the help of precision data on rare decays) and at a more fundamental level (with the help of new symmetry principles), is one

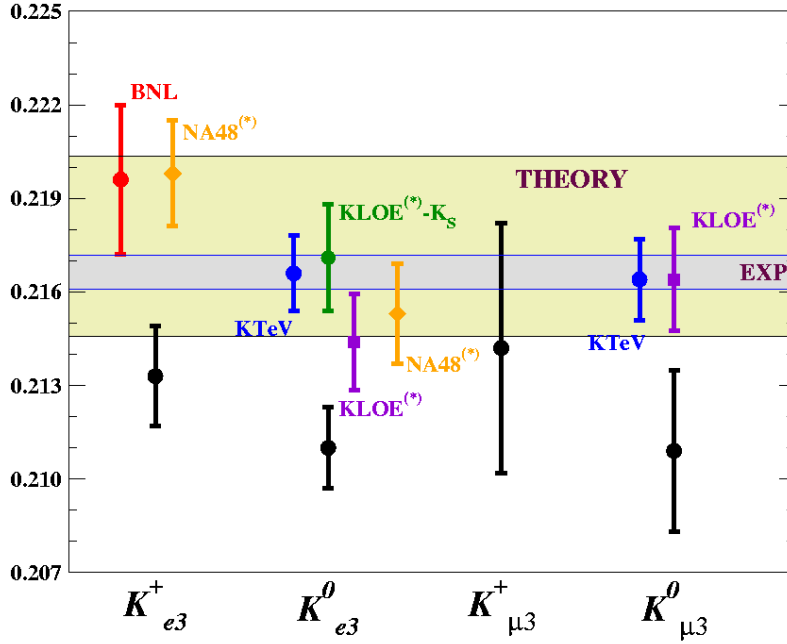


Figure 1: *Experimental results on $|V_{us}| \cdot f_+(0)$. ⁴⁾ The internal narrow band indicates the average of the new experimental results ($|V_{us}| \cdot f_+(0) = 0.2166 \pm 0.0005$), as reported at the ICHEP 2004 conference (the '*' marks results which are still preliminary); the lower (black) points without labels are the old PDG values. The larger band represents the unitarity prediction combined with our recent lattice ³⁾ determination of the vector form factor $[(1 - |V_{ud}|^2 - |V_{ub}|^2)^{1/2} \cdot f_+(0) = 0.2175 \pm 0.0029]$.*

of the main activity of our group. ¹⁾ A closely related subject –which is also one of the primary research objectives of our group– is a better understanding of the SM itself, fixing his fundamental couplings (quark masses, CKM angles, non-perturbative condensates, ...) by means of precise low-energy observations. Within this general framework, last year we have performed a series of works aimed at:

- i. The extraction $\pi\pi$ scattering lengths (and the determination of the quark condensate) from $K \rightarrow 3\pi$ decays. ²⁾
- ii. The precise determination of the the Cabibbo angle from $K_{\ell 3}$ decays ^{3, 4, 5)} (see figure 1).
- iii. The estimate of the hadronic parameter B_K which control the $K-\bar{K}$ mixing amplitude. ⁶⁾
- iv. Understanding the role of QCD anomalies in weak decays. ⁷⁾
- v. Predicting with high accuracy the rate of the rare decays $K_L \rightarrow \pi^0 \mu^+ \mu^-$, an observable particularly sensitive to new physics. ^{8, 9)}

3 Hadronic cross-sections

This project is divided into two separate areas, precision physics at the ϕ -factory DAΦNE and the rise of all total cross-sections with energy.

3.1 Final-state radiation in electron-positron annihilation into a pion pair

The process of e^+e^- annihilation into a pion pair and a photon is relevant to the estimate of the hadronic cross-section at low energies. The amplitude of this reaction consists of the model independent initial-state radiation (ISR) and model-dependent final-state radiation (FSR). The general structure of the FSR tensor was constructed from Lorentz covariance, gauge invariance and discrete symmetries in terms of the three invariant functions. To calculate these functions we have applied Chiral Perturbation Theory (ChPT) with vector and axial-vector mesons. The contribution of e^+e^- into charged pion pair process to the muon anomalous magnetic moment has been evaluated, and the results compared with the dominant contribution in the framework of a hybrid model, consisting of VMD and point-like scalar electrodynamics¹⁰⁾. The developed approach allows also to calculate the $\pi^+\pi^-$ charge asymmetry. Work is in progress to compare this approach with various Monte Carlo simulations and experimental data from KLOE and Novosibirsk.

3.2 Quantum chromodynamics (QCD) and the energy behaviour of total hadronic cross-sections

The energy behaviour of total proton and photon cross-sections is the focus of this line of research and its description through QCD is the ultimate goal of this project. QCD indeed provides various mechanisms to explain the energy dependence, although quantitatively rigorous studies are yet to come. The goal would be to obtain a QCD description of the initial decrease and the final increase of total cross-sections through soft gluon summation and QCD calculable jet x-sections, also known as mini-jets in this context. The resulting physical picture includes multiple parton collisions, whose number increases with energy, and soft gluon emission dressing each collision, with a reducing effect.

3.2.1 *The Eikonal Minijet Model for protons and photons*

In the Eikonal Minijet Model (EMM) the rise can be obtained using the QCD calculable contribution from the parton-parton cross-section, whose total yield increases with energy. For a unitary description, the jet cross-sections are embedded into the eikonal formalism, where the eikonal function contains both the energy and the impact parameter distribution in b-space. The simplest formulation, with minijets to drive the rise and hadronic form factors for the impact parameter distribution, can be applied to all the available x-sections. One finds¹¹⁾ that proton-antiproton and proton-proton high energy data can be reproduced by this model, using currently used parton densities, like the ones from GRV parametrization, and a reasonable minimum transverse momentum cut-off of $\approx 2 \text{ GeV}$. However, one also finds that, with a single set of parameters, it is not possible to describe both the early rise, which in proton-antiproton scattering takes place around $10 \div 50 \text{ GeV}$, and the Tevatron data.

Photo-production data can be described through the same simple eikonal minijet model, with the relevant parton densities for the jet cross-sections, scaling the non perturbative part with VMD

and quark counting factors. However, just like in proton-proton, the case for extrapolation of the EMM to higher energies is not convincing. Because of too fast a rise of the minijet cross-section, the set of parameters which allow to describe the high energy data points will reproduce the low energy ones with quite some uncertainty and viceversa ¹²⁾.

Going to purely photonic processes like $\gamma\gamma$, the theoretical uncertainties from pp and γp conjure to obtain predictions which differ by factors 2 and 3 at very high energies. A compilation of $\gamma\gamma$ data, including present LEP data, done for future Linear ¹³⁾ and Photon Colliders ¹⁴⁾ indicated many problems with all the models for photon-photon total hadronic cross-section at high energy ¹⁵⁾. In particular one can see that while the EMM describes quite well the rise at present energies, the extrapolation to even higher energies appears unrealistic and may need to be modified, as found in the proton case.

A possible way to decrease the uncertainty in the predictions is to refine the QCD analysis, through resummation of soft gluon emission from the initial state partons, a feature absent from most simple EMM.

3.2.2 *Soft Gluon Summation and the impact parameter distribution of partons*

A model for the impact parameter space distribution of parton in the hadrons has been developed and applied to the proton and photon cross-sections in order to obtain a better description of total cross-section. The physical picture underlying this model is that the fast rise due to mini-jets and the increasing number of gluon-gluon collisions as the energy increases, can be reduced if one takes into account that soft gluons, emitted mostly by the initial state valence quarks, determine an acollinearity between the partons which reduces the overall parton-parton luminosity. This model can describe very well all available data for proton collisions as we show in fig.(2) from ¹¹⁾ and appears flexible enough to be applied to photon processes ¹⁶⁾.

4 Work Program for the year 2005

Most of the activity previously described will be continued into the year 2005. The work on QCD and total cross-sections, a long term project, will focus mainly on discussing the complementarity between the coming measurements at LHC and the prospects of measuring total cross-sections at the Linear Colliders.

References

1. G. Isidori, "Kaon decays and the flavour problem", *Annales Henri Poincare* **4** (2003) S97.
2. N. Cabibbo and G. Isidori, "Pion pion scattering and the $K \rightarrow 3\pi$ decay amplitudes", hep-ph/0502130, submitted to JHEP.
3. D. Bećirević, G. Isidori, V. Lubicz, G. Martinelli, F. Mescia, S. Simula, C. Tarantino, G. Villadoro, "The $K \rightarrow \pi$ vector form factor at zero momentum transfer on the lattice", *Nucl. Phys. B* **705** (2005) 339.
4. F. Mescia, " V_{us} from K_{l3} decays", hep-ph/0411097, talk presented at ICHEP 2004.

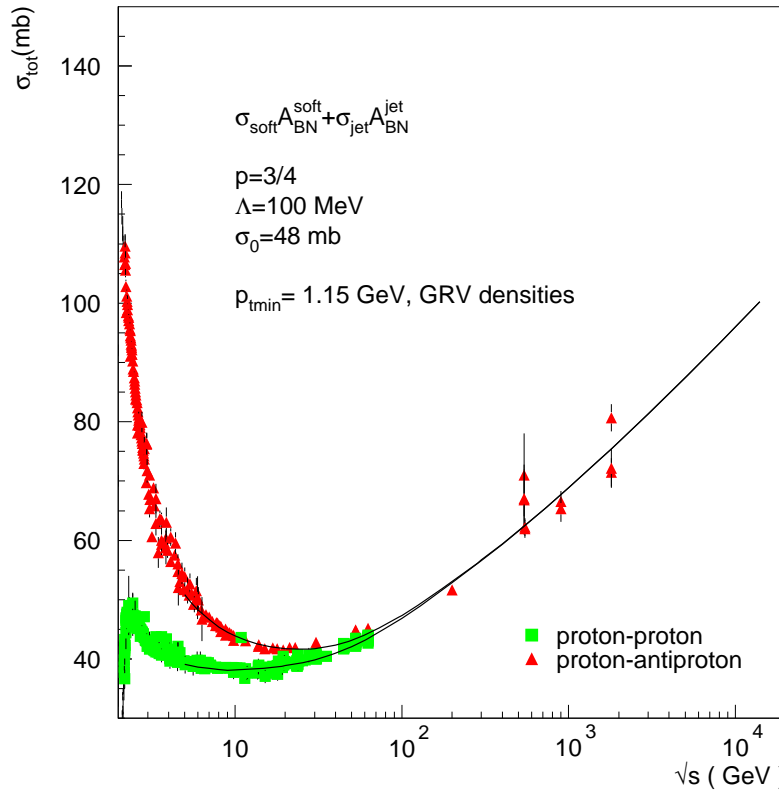


Figure 2: Total pp and $\bar{p}p$ cross-sections, in an eikonal formulation with soft gluon resummation (BN) and GRV densities in the mini-jet cross-section, for an indicative set of parameters, and in comparison with present data.

5. D. Becirevic *et al.*, “SU(3)-breaking effects in kaon and hyperon semileptonic decays from lattice QCD”, hep-lat/0411016, talk presented at Lattice 2004.
6. J. M. Flynn, F. Mescia and A. S. B. Tariq [UKQCD Collaboration], “Sea quark effects in B_K from $N_f = 2$ clover-improved Wilson fermions”, JHEP **0411**, (2004) 049.
7. J. M. Gerard and S. Trine, “QCD anomalies in hadronic weak decays”, Phys. Rev. D **69**, (2004) 113005.
8. G. Isidori, C. Smith and R. Unterdorfer, “The rare decay $K_L \rightarrow \pi^0 \mu^+ \mu^-$ within the SM”, Eur. Phys. J. C **36**, (2004) 57.
9. C. Smith, “Recent progress on the rare decay $K_L \rightarrow \pi^0 \mu^+ \mu^-$ ”, hep-ph/0407361, talk presented at DAPHNE 2004.
10. S. Dubinsky, A. Korchin, N. Merenkov, G. Pancheri, O. Shekhovtsova, “Final-state radiation in electron-positron annihilation into a pion pair”, e-Print Archive: hep-ph/0411113. Published electronically in EPJC as <http://www.springerlink.com/index/10.1140/epjc/s2004-02109-7>.
11. R.M. Godbole, A. Grau, G. Pancheri, Y.N. Srivastava, “Soft Gluon Radiation and energy dependence of total hadronic cross-sections”, submitted to Phys. Rev. D; e-Print Archive: hep-ph/0408355.

12. G. Pancheri, A. De Roeck, R.M. Godbole, A. Grau, Y.N. Srivastava, “Total cross-sections:cross-talk between HERA, LHC and LC”, talk given at International Conference on Linear Colliders (LCWS 04), Paris, France, 19-24 Apr 2004, e-Print Archive: hep-ph/0412189.
13. CLIC Physics Working Group *et al.*, “Physics at the CLIC Multi-TeV Linear Collider”, CERN-2004-005, e-Print Archive: hep-ph/0412251.
14. B.Badelek *et al.*, “The Photon Collider at TESLA”, Intern. Journ. Mod. Phys A **19**, (2004) 5097-5186.
15. R.M. Godbole, A. De Roeck, A. Grau, G. Pancheri, “Hadronic Cross-sections in two photon processes at a future Linear Collider”, JHEP 0306:061,2003 e-Print Archive: hep-ph/0305071.
16. G. Pancheri, R. Godbole, A. Grau and Y. Srivastava “Total cross-sections and Bloch-Nordsieck gluon summation”, Acta Physica Polonica B **36**, (2005) 735.

Iniziativa specifica MI11

M. P. Lombardo, F. Palumbo (Resp.)

In the standard regularization of gauge theories on a lattice the fermion fields are time-split in their coupling to the chemical potential. Then, as a consequence of gauge invariance, this coupling also involves temporal gauge links, a feature which has been considered of physical significance. I have shown ¹⁾ instead that this time splitting, as well as the temporal links, can be avoided getting a coupling of the chemical potential closer to the continuum definition.

The above result has been obtained by defining the chemical potential in the operator form of the partition function and then deriving its functional form. I have also reviewed other applications of such a procedure to identify physical degrees of freedom in the path integral formalism ²⁾.

I constructed a new method of bosonization valid for many-body systems and relativistic field theories of fermions ³⁾. It is based on the functional evaluation of the partition function restricted to the bosonic composites of interest. In this way the action of the effective bosons is determined in closed form, respecting all the fermion symmetries. This also allows numerical simulations avoiding the sign problem. As an illustration I investigated the foundations of the Interacting Boson Model of Nuclear Physics and determined the rule of the fermion-boson mapping of operators.

The main results obtained by MPL concern QCD at nonzero temperature and baryon density ^{4, 5, 6, 7, 8, 9, 10}).

References

1. F.Palumbo, "Different couplings of the chemical potential with identical partition function in QCD on a lattice", Phys.Rev. D **69**, 074508 (2004).
2. F.Palumbo, "Path integrals and degrees of freedom in many-body systems and relativistic field theories", hep-th/0412073; vol. in honor of prof. Yu. S. Simonov, Phys. Atom. Nucl., **5**, (2005).
3. F.Palumbo, "Bosonization in many-body systems and relativistic field theories", nucl-th/0405045.
4. Massimo D'Elia and Maria Paola Lombardo, Phys.Rev.D**70**:074509, (2004).
5. Maria Paola Lombardo, Prog.Theor.Phys.Suppl.**153**:26-39, (2004).
6. N. Brambilla et al.. "Heavy Quarkonium Physics", e-Print Archive: hep-ph/0412158, to appear as CERN Yellow Report.
7. G. Akemann, E. Bittner, M. P. Lombardo, H. Markum, R. Pullirsch , "Density profiles of Small Diarc Operator Eigenvalues", to appear in the proceedings of 22nd International Symposium on Lattice Field Theory 21-26 Jun 2004; e-Print Archive: hep-lat/0409045.
8. Massimo D'Elia, Maria Paola Lombardo "Lattice Results Confront Models", to appear in the Proceedings of the 6th Conference on Strong and Electroweak Matter, Helsinki, Finland, 16-19 June 2004; e-Print Archive: hep-lat/0409010.
9. M. D'Elia, M. P. Lombardo, Nucl.Phys.Proc.Suppl.**129**:536-538, (2004).
10. M.P. Lombardo, M.L. Paciello, S. Petrarca, B. Taglienti, Nucl.Phys.Proc.Suppl.**129**:635-637, (2004).

MI12

S. Bellucci (Resp.), P.-Y. Casteill, M. Cini (Ass.), S. Ferrara (Ass.), E. Latini (Dott.),
A. Marrani (Dott.), F. Morales, E. Orazi (Dott.), E. Perfetto, C. Sochichiu

1 Research Activity

The project under consideration is devoted to study the vast problems of high energy theoretical physics which arise from modern development of superstring theory. At present, the superstring theory is more and more treated as a basic theory providing the unification of all fundamental interactions in Nature including the unification of particles and forces, bosons and fermions, quantum mechanics and general relativity. The superstring theory operates with extended physical objects like strings and branes and demands to formulate physics in higher dimensions. Central trend of development of modern theoretical physics is mainly associated now with study of the various low-energy aspects of superstring theory which allows to provide the understanding the physics beyond standard model. In low energy limit, the superstring theory leads to new field theory models possessing the remarkable properties like supersymmetry and non-commutativity. Besides, the superstring theory describes the higher spin bosonic and fermionic particles, hence the superstring theory can be naturally related with higher spin field theory. Thus, a development of superstring theory seted up the new complicated problems in classical and quantum field theory, study of which demands the new methods and approaches. Series of such problems was formulated and solved for the first time in framework of the project. In process of project realization the a large number of pioneer results in superstring theory, extended supersymmetric field theory, supergravity and quantum filed theory has been obtained.

2 Non-commutative field theory

Such theories can arise in low-energy limit of superstring theory and can be formulated in deformed spaces with non-(anti)commuting bosonic (fermionic) coordinates. A series of supersymmetric field models in nilpotently deformed harmonic superspace induced by nonanticommutating fermionic coordinates has been constructed for the first time. The renormalization of composite operators and energy momentum tensor in noncommutative scalar field theory has been realized for the first time. These results impact on development of noncommutative field theory, on understanding the profound relation between superstring theory and field theory.

3 Construction of new superstring and superparticle models and their quantization

Superstring theory possesses a very rich structure of vacuum states which can be studied considering the string models coupled to background fields. Another way to study the various aspects of superstring theory is to construct one-dimensional superparticle models having properties analogous to superstrings. The exact solution of quantum superstring theory in maximally supersymmetric plane wave background has been found. This result was one of the most bright achievements in superstrig theory for the last years and impacted on modern development of superstring theory on the whole. A number of particle models possessing the extended supersymmetry have been constructed. Quantization of superparticle propagating in $N=1$, $D=4$ superspace with tensorial cooordinates has been carried out. These results point to the many interesting links between supersymmetric field theory and one dimensional quantum mechanics and allow one to clarify the aspects of superstring theory with help of simplified models.

4 Correlation functions of in N=4 supersymmetric Yang-Mills theory

Extended supersymmetry imposes strong restriction on a quantum structure of N=4 SYM theory, so that the correlation functions of gauge invariant operators can be practically exactly found on the ground of only symmetry properties. These correlation functions have close relations to AdS/CFT correspondence in superstring theory and their study clarifies many complicated aspects both in superstring theory and superconformal invariant quantum field theories. The exact structure of four-point correlation functions in N=4 super-Yang-Mills theory has been studied in details. General solution of the Ward identities for the correlations functions of gauge invariant operators has been found and applied to correlation functions of stress tensor multiplets. Four-point correlator of half-BPS operators of weight 4 in N=4 SYM theory, which are dual to massive Kaluza-Klein modes in AdS(5) supergravity has been exactly calculated on the base of general field theoretical and symmetric analysis. The results have the pioneer significance and determine a modern state of research on finding the exact results in superconformal quantum field theory. They impact on developing the new profound relations between superstring theory and N=4 super-Yang-Mills theory.

5 List of Conference Talks by LNF Authors in Year 2003

1. S. Bellucci, "Nuovi modelli di meccanica superconforme con N=8", Congresso di Fisica Teorica "Cortona 2004", Cortona, Italy, 27 May 2004.
2. S. Bellucci, "Quantum Hall effect on complex projective spaces, Low Dimensional Field Theory at Work in Condensed Matter and String Theory", Anacapri (SA), Italy, 21 Sept. 2004.
3. S. Ferrara, "Orientifolds, Brane Coordinates and Special Geometry", "DeserFest", Ann Arbor, Michigan, 3-6 April 2004.
4. S. Ferrara, "No-scale supergravity from higher dimensions", Annual International Conference on Strings, Theory and Applications (Strings 2004), Paris, France, 28 Jun - Jul 2, 2004.
5. S. Ferrara, "Generalized dimensional reduction of supergravity with eight supercharges", 10th International Symposium on Particles, Strings and Cosmology (PASCOS 04 and Pran Nath Fest), Boston, Massachusetts, 16-22 Aug 2004.

References

1. S. Bellucci, A. Yeranian, "Noncommutative Quantum Scattering in a Central Field", hep-th/0412305, Phys. Lett. **B** (to appear).
2. S. Bellucci, P.-Y. Casteill, A. Marrani, C. Sochichiu, "Spin bits at two loops", hep-th/0411261, Phys. Lett. **B** (to appear).
3. S. Bellucci, A. Galajinsky, E. Latini, "New insight into WDVV equation", hep-th/0411232, Phys. Rev. **D** (to appear).
4. S. Bellucci, S. Krivonos, A. Sutulin, "N=8 Supersymmetric Quaternionic Mechanics", hep-th/0410276, Phys. Lett. **B** (to appear).
5. S. Bellucci, S. Krivonos, A. Nersessian, A. Shcherbakov, "2k-dimensional N=8 supersymmetric quantum mechanics", hep-th/0410073, presented at the XI International Conference "Symmetry Methods in Physics", 2004, June 21-24, Prague, Czech Republic.
6. S. Bellucci, S. Krivonos, A. Nersessian, "N=8 supersymmetric mechanics on special Kaehler manifolds", hep-th/0410029, Phys. Lett. **B** (to appear).
7. S. Bellucci, C. Sochichiu, "On matrix models for anomalous dimensions of Super Yang-Mills theory", hep-th/0410010, submitted to Nucl. Phys. **B**.

8. S. Bellucci, P.-Y. Casteill, F. Morales, C. Sochichiu, SL(2) spin chain and spinning strings on AdS(5)xS(5), hep-th/0409086, Nucl. Phys. B (to appear).
9. S. Bellucci, P.-Y. Casteill, F. Morales, C. Sochichiu, "Chaining spins from (super)Yang-Mills", hep-th/0408102, Contribution to the XI International Conference on Symmetry Methods in Physics (SYMPHYS-11).
10. S. Bellucci, S. Krivonos, E. Orazi, Phys.Lett. **B597** (2004) 208.
11. S. Bellucci, A. Nersessian, A. Yeranian, Phys. Rev. **D70** (2004) 085013.
12. S. Bellucci, E. Ivanov, S. Krivonos, O. Lechtenfeld, Nucl.Phys. **B699** (2004) 226.
13. S. Bellucci, C. Sochichiu, "On the dynamics of BMN operators of finite size and the model of string bits", hep-th/0404143, Contribution to BW2003 Workshop, 29 August - 02 September, 2003 Vrnjacka Banja, Serbia.
14. S. Bellucci, P.-Y. Casteill, F. Morales, C. Sochichiu, Nucl. Phys. **B699** (2004) 151.
15. S. Bellucci, A. Galajinsky, E. Latini, Phys. Rev. **D70** (2004) 024013.
16. S. Bellucci, I.L. Buchbinder, V.A. Krykhtin, Nucl. Phys. **B693** (2004) 51.
17. S. Bellucci, A. Nersessian, "Supersymmetric Kaehler oscillator in a constant magnetic field", hep-th/0401232, Contribution to the proceedings of the international workshop "Supersymmetry and Quantum Symmetries" SQS03 Dubna, 24-29 July 2003.
18. S. Bellucci, A. Nersessian, A. Yeranian, Phys. Rev. **D70** (2004) 045006.
19. S. Bellucci, E. Ivanov, S. Krivonos, O. Lechtenfeld, Nucl. Phys. **B684** (2004) 321; S. Ferrara, E. Sokatchev, Phys. Lett. **B579** (2004) 226.
20. C. Angelantonj, S. Ferrara, M. Trigiante, Phys.Lett. **B582** (2004) 263.
21. N. Beisert, M. Bianchi, J.F. Morales, H. Samtleben, JHEP 0402 (2004) 001.
22. C. Angelantonj, R. D'Auria, S. Ferrara, M. Trigiante, Phys. Lett. **B583** (2004) 331.
23. R. D'Auria, S. Ferrara, M. Trigiante, Phys. Lett. **B587** (2004) 138.
24. L. Andrianopoli, S. Ferrara, M.A. Lledo', JHEP 0404 (2004) 005.
25. R. D'Auria, S. Ferrara, M. Trigiante, Nucl. Phys. **B693** (2004) 261.
26. S. Ferrara, E. Ivanov, O. Lechtenfeld, E. Sokatchev, B. Zupnik, Nucl. Phys. **B704** (2005) 154.
27. L. Andrianopoli, S. Ferrara, M.A. Lledo', Class. Quant. Grav. 21 (2004) 4677.
28. L. Andrianopoli, S. Ferrara, M.A. Lledo', JHEP 0406 (2004) 018.
29. L. Andrianopoli, S. Ferrara, M.A. Lledo', "Generalized dimensional reduction of supergravity with eight supercharges", hep-th/0410005, Contribution to the proceedings of "NathFest" at PASCOS conference, Northeastern University, Boston, Ma, August 2004.
30. R. D'Auria, S. Ferrara, M. Trigiante, "No-scale supergravity from higher dimensions", hep-th/0409184, To appear in the proceedings of Annual International Conference on Strings, Theory and Applications (Strings 2004), Paris, France, 28 Jun - Jul 2, 2004.
31. R. D'Auria, S. Ferrara, M. Trigiante, "Orientifolds, Brane Coordinates and Special Geometry", hep-th/0407138, contribution to the proceedings of "DeserFest", Ann Arbor, Michigan, 3-6 April 2004.
32. F. Fucito, F. Morales, R. Poghossian, JHEP 0410 (2004) 037.
33. F. Fucito, F. Morales, R. Poghossian, Nucl. Phys. **B703** (2004) 518.
34. N. Beisert, M. Bianchi, J.F. Morales, H. Samtleben, JHEP 0407 (2004) 058
35. R. Flume, F. Fucito, J.F. Morales, R. Poghossian, JHEP 0404 (2004) 008.
36. E. Perfetto and M. Cini, Phys. Rev. **B 69** (2004) 092508.

Iniziativa specifica PI31

F. Palumbo (Resp.)

As a first step to derive the IBM (Interacting Boson Model) from a microscopic nuclear Hamiltonian, we ¹⁾ bosonized the pairing Hamiltonian in the framework of the path integral formalism respecting both the particle number conservation and the Pauli principle. Special attention was paid to the role of the Goldstone bosons. We constructed the saddle point expansion which reproduces the sector of the spectrum associated to the addition or removal of nucleon pairs.

The method of bosonization described in the report of the activity in the framework of MI11 has been reported, as far as nuclear physics is concerned, in the Paestum conference.

An application of the scissors mode has been done in condensed matter ²⁾. We suggested that in an anisotropic crystal there should be a new mechanism of dichroism related to a scissors mode, a kind of excitation observed in several other many-body systems. Such an effect should be found in crystals, amorphous systems and also metallo-proteins. Its signature is a strong magnetic dipole transition amplitude, which is a function of the angle between the momentum of the photon and the anisotropy axis of the cell. The identification of such mode can be relevant to the study of the structures of the above systems and their modifications.

1 List of Conference Talks in Year 2004

1. F. Palumbo, "Bosonization and IBM", invited talk at the 8th International Spring Seminar on Nuclear Physics: Key Topics in Nuclear Structure, Paestum, Italy, 23-27 May 2004; nucl-th/0412042.

References

1. M.B. Barbaro, A. Molinari, F. Palumbo and M.R. Quaglia, "Path integral bosonization of the pairing Hamiltonian", Phys. Rev. C **70**, 034309 (2004).
2. K. Hatada, K. Hayakawa and F. Palumbo, "Scissors Mode and dichroism in an anisotropic crystal", cond-mat/0402193, Phys. Rev. B, (in press).

ARCHIMEDE

G. Cinque (Resp.), G. Cibin (Bors.), E. Burattini(Ass.), A. Marcelli, A. Raco (Tecn.),
A. Soldatov (Osp.) and M. Mazuritskiy (Osp.)

1 Summary

The experiment ARCHitects of Mirror Extreme ultraviolet DEvices (ARCHIMEDE), concerns the design and study of high reflectivity optical systems - at quasi normal incidence - for the X-rays in the so-called water window, i.e. wavelenghts from 44 to 24 Å). This collaboration between INFN laboratories exploits the expertises of the Laboratori Nazionali di Legnaro (LNL), for tayloring and growing speciphic multilayers devices, and of the Laboratori Nazionali di Frascati (LNF), for characterizing the diffracting optics in reflectivity by X-ray Synchrotron Radiation (SR) at DAΦNE-L Laboratory.

2 Activity

The project ARCHIMEDE is devoted to grow and study multilayer mirrors with high reflectivity for X-rays in the energy window between O and C absorption edges (circa 280 - 540 eV). This spectral region is strategically important for multidisciplinary applications ranging from astrophysics to nano-lithography, as well as focusing optics for new X-ray sources like laser plasma or Free Electron Lasers (FEL). As for SR research, the scientific importance is straightforward: for soft X-ray microscopy on organic structures, e.g. cells and their organelles in aqueous environment, and more generally for X-ray microprobe spectroscopy. Since all these fields of research require an efficient collection of most of the X-rays emitted from a source, multilayer mirrors are studied to preferentially work at normal incidence. Because of the limited size of the multilayers, the project intend to test the feasibility design of multistep devices consisting of several multilayer elements, to cover X-ray energy ranges not accessible by crystals, working at quasi-normal incidence to the beam, allowing full exploitation of angular aperture, in a focusing geometry.

The maximum reflectivity of multilayer devices requires sharp and flat interfaces of the alternate high/low refractive index layers (with minimal overall absorption). Design and deposition of these devices has been progressed at LNL after an optimization phase of deposition conditions

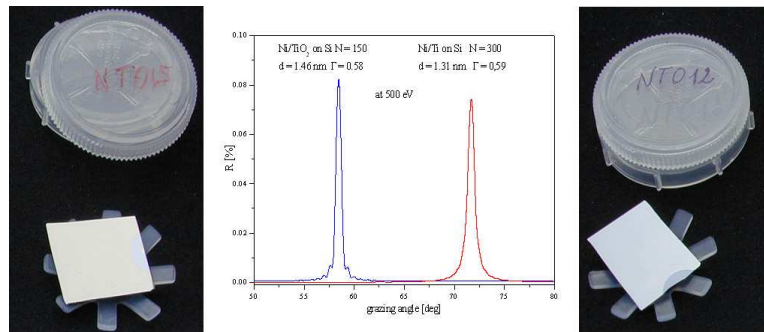


Figure 1: Ni/Ti (left) and Ni/TiO_2 multilayer samples for the X-ray water window with their estimated reflectivity at 500 eV as a function of the sample diffraction angle (ω scan).

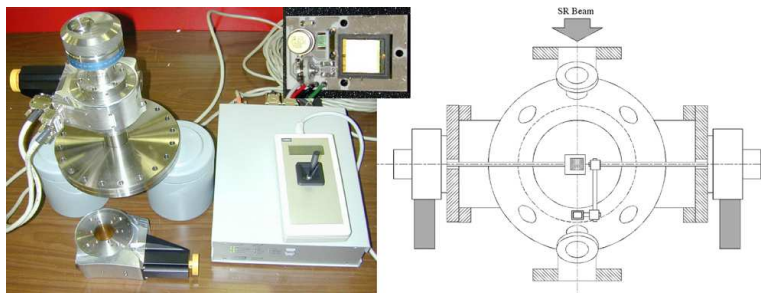


Figure 2: The X-ray reflectometer under construction on the soft X-ray beamline. Right: detailed drawing of the $\theta - 2\theta$ system. Left: precision goniometer, rotary feedthrough and control unit. Top inset: absolute photodiode and UHV preamplifier.

(mainly growth rate and surface roughness) in the new sputtering chamber. Among the best material candidates for these soft X-ray optics, the first Ni/Ti and Ni/TiO₂ multilayers have been grown (Fig. 1). To our knowledge, these are the first results concerning the growth of pure metal layers (Ni) on different metal oxide (TiO₂). At present, technological limitations constrain the maximum number of deposited layers, respectively $N = 150$ and 300 . Bulk diffusion and interface mixing on samples have been preliminarily checked by Rutherford Backscattering Spectroscopy.

In 2004, several improvements of the soft X ray beamline have been completed with new equipment, in particular (Fig.2): i) tests of diffraction crystal with large lattice spacing, KAP(100), for low energy monochromatization; ii) implementation of UHV/HV ultrathin windows for high soft X-ray transmission; iii) installation of an absolute X-ray photodiode (including UHV compatible preamplifier) for the direct detection of diffracted X ray beams; iv) installation of two-goniometer system, and remote control unit, with guaranteed angular precisions and accuracy movements better than $1/1000^\circ$ both in open and closed loop; iii) final project and acquisition of two UHV all-magnetic rotary feedthroughs ready-to-use for $\theta - 2\theta$ measure in the vacuum chamber iv) software control of the angular movements, readout of absolute angular encoders and one signal acquisition channel (photodiode). These changes in the soft X-ray energy side extend the working region down to the oxygen K-edge, and the main instrumentation of the $\theta - 2\theta$ UHV compatible reflectometer is completed. We will proceed first with the direct measure of the multilayer reflectivity under vacuum in the water window by (white/monochromatic) SR beam. The experimental techniques to be used for the optical characterization are:

- 1) energy resolved assessment of reflectivity with fixed detector and sample;
- 2) ω scan for determination of the multilayer rocking curve;
- 3) θ - 2θ diffraction measurement by fixed energy monochromatic beam.

The double-crystal *boomerang* monochromator in operation at the soft X-ray beamline allows routinely performing X-ray Absorption Spectroscopy (XAS) in transmission of light elements (K-edges) and transition metal (L-edges) on thin samples (see DAΦNE-L report pag. 231). The analysis of the optical device interfaces will benefit of XAS technique for the characterization of their inter- and intra-atomic layer structures. The experimental research at DAΦNE-L will be completed within 2005 with diffraction measurements by means of X-rays of the first optical-grade multilayers in terms of energy bandwidth (rocking curve) and absolute reflectivity. Tests of the multistep planar and/or spherical supports will proceed with studying the multilayers fixing by optical contact to minimize stress on the diffracting surfaces. The study of a multiple assembly onto large substrates, to increase the optical aperture, eventually shaped according to spherical geometries, for final refocusing, takes advantage of the experience acquired by the LNF group in collaboration with A. Soldatov and M. Mazuritskiy from Rostov University–Russia (previous experiment MUST of Gr V).

CAPIRE

A. Calcaterra, L. Daniello (Tecn.), R. de Sangro, G. Mannocchi (Ass.)
P. Patteri, M. Piccolo (Resp.), L. Satta (Ass.)

1 Abstract

CAPIRE is a program to develop large area parallel plate detectors, carried out in collaboration with INFN Milano and INFN Torino. In 2004 the Collaboration has completely refurbished both long term test facilities in Milano Bicocca and in Frascati. The gas distribution was redone either with copper or stainless steel tubing; water contamination for the detectors under test is now below the 30 ppm level. Long term tests are being carried out at the two cosmic ray facilities. New techniques for silk printing of the external electrodes have been tested with the use of U.V. drying inks. In the two weeks of running at the Frascati BTF we continued studying (several) small prototypes performances both for what local rate capability and spatial efficiency and resolution are concerned.

2 Measurements and Results

During 2004 a new silk printing technique has been tested: the most relevant change with respect to the original one, has been the use of a new U.V. drying ink that, if found viable, might reduce considerably electrodes production times and improve reliability and uniformity. Six relatively large detectors ($50 \times 50 \text{ cm}^2$) have been produced with this new technique and they are now under test in the Frascati cosmic ray test facility.

The same technique has been used for the smaller prototypes ($20 \times 20 \text{ cm}^2$) exposed to the BTF beams. The BTF runs have been carried out in April and October and were used to test the operational behaviour of detectors with gas mixtures producing relatively small streamer pulses. The rationale for this bears with the fact that smaller pulses grant a better local rate capability, which in turns translates in better linearity for (digital) calorimetric applications.

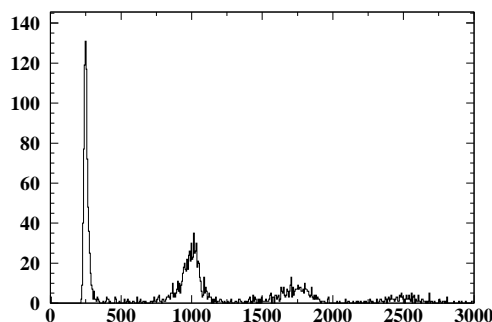


Figure 1: *The raw pulse height from the total absorption calorimeter, used a particle counting device. The peaks at 0,1,2 and 3 particles can be easily seen.*

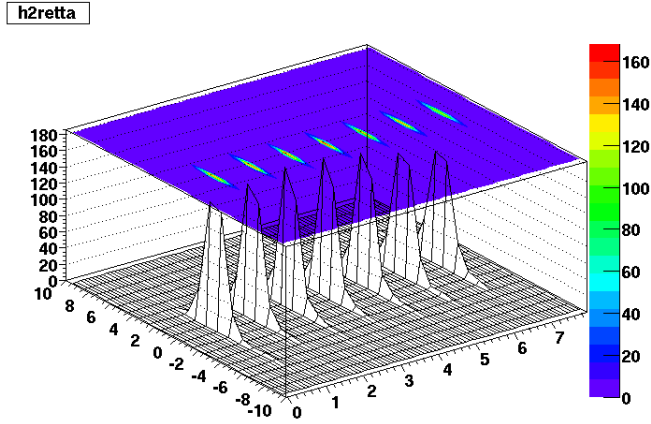


Figure 2: *The radial occupancy distribution for the seven prototype chambers under test: the beam was unfocused. The evolution of the beam spot shape is quite evident.*

The prototype chambers were equipped with strips on both sides so that vertical and horizontal coordinates were measured; in addition the horizontal strips were connected to an analog adder and fed to a commercial ADC: on a trigger, provided by the beam R.F., the digital response of the two electrode planes and the ADC value were recorded for each chamber, together with the pulse height of a small beam defining scintillation counter and of a particle counting crystal calorimeter.

In order to quantify the local rate capability of these detectors, the knowledge of the beam spot shape is of paramount importance: the overall imaging capability of the setup is shown in fig. 2, here the radial beam distributions are shown for the seven chambers under test: effects like beam divergence and multiple scattering can be easily disentangled, given the redundancy of the spatial measurements of the setup.

One of the instrumentation problems we had to face was the relatively low sensitivity of the digital electronics we had available. The possibility of using pulse height measurements did help in this respect: the equivalent threshold of the ADC, set by environmental noise, was about one third to one half pCoul.

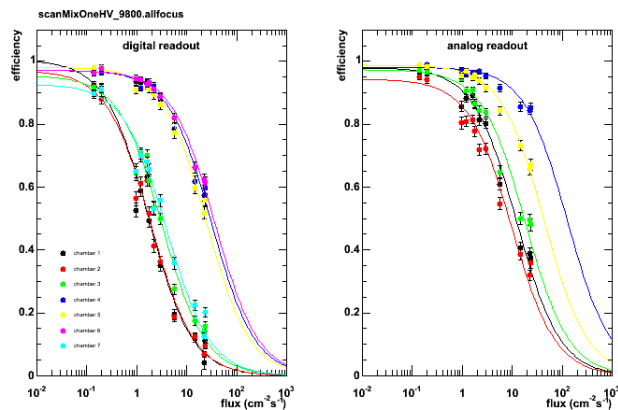


Figure 3: *Local rate capability for the prototype chambers: left plot, digital readout right plot analog (ADC) readout. Clear differences can be seen: rate capability for 2 mm thick chambers seems to be definitely better than the one for the 3 mm thick chambers. It has to be noted, however, that the glass resistivity in the first case (2 mm) is roughly four times smaller than in the other one (3 mm).*

As already mentioned, the main measurements obtainable at the BTF concern the local rate capability, Preliminary results on such a quantity are shown in Fig. 3. Noticeable differences can be seen for different chambers, and this could be in principle explained by the different glass characteristics (e.g. resistivity value). However the analysis is quite tricky and as of now we are still working trying to understand subtle local effects that could be relevant in the interpretation of the data.

3 2005 plan

In the coming year, the Collaboration will keep on the long term test on a substantial amount of detectors ($\approx 15 \text{ m}^2$) at Milano and Frascati. Furthermore, we plan to produce detectors drawing the pick up electrodes directly within the silk printing process. We also envisage running at the BTF to test local rate capabilities in different operational conditions (avalanche regime).

4 Conference presentations and Publications

- T. Tabarelli de Fatis, “Contribution to LCWG 2004”, Paris, April 2004, in press.
- G. Trincherò, “Contribution to IEEE NSS”, Rome, October 2004, in press.
- M. Piccolo, “Contribution to the Muon and special detector session for ALCPG”, Victoria Island (Canada), July 2004.
- A. Calcaterra *et al.*, N.I.A.M **A533**, 2004 pg. 154-158.

CORA

D. Alesini (Art. 23), R. Boni, M. Ferrario, A. Gallo (Resp.), F. Marcellini, M. Vescovi

1 Activity

The object of the CORA experiment is the study and fabrication of RF accelerating structure prototypes aimed to the particle bunch length reduction by means of the “RF compression” technique. The experimental test of the RF linear compression concept will be part of the scientific program of the so called “SPARC phase II”.

The velocity buncher concept is based on the longitudinal focussing properties of the slow waves, and allows compressing the bunch length up to a factor 20. It consists in a modified accelerating structure allowing the inside propagation of a wave whose phase velocity v_{ph} is close to but slightly less than the light velocity c (slow wave, $v_{ph}/c = 0.999 \div 1$). The required gradients are similar to that of the standard S-band structures, that means in the 20-25 MV/m range.

The accelerating slow wave can be obtained by linearly scaling the dimensions of a standard, synchronous RF accelerating structure ($v_{ph} = c$). In this case the relative phase velocity variation is proportional to the scaling factor $\Delta f/f$ through a constant equal to the ratio between the phase and the group velocity of the structure:

$$\Delta v_{ph}/v_{ph} = \Delta f/f (1 - v_{ph}/v_g) \approx -\Delta f/f \cdot v_{ph}/v_g. \quad (1)$$

In a standard SLAC type section the value of the ratio is $v_{ph}/v_g \approx 100$, which means that deformations of the order of 10^{-5} are sufficient to produce phase velocity variation of the order of 10^{-3} . Since the Copper linear thermal expansion coefficient is $\approx 1.6 \cdot 10^{-5}/^\circ\text{C}$, a variation of 1°C of the operating temperature of the structure produces a variation of the structure phase velocity larger than desired. This means that a special accelerating section equipped with a thermal regulation system capable to stabilize the section temperature at a small fraction of 1°C can be used as a slow wave velocity buncher. The phase velocity in the buncher can be tuned by changing the temperature set point of the thermal regulation system, assuming that the real section temperature can be maintained equal to the set value within a very narrow range (of the order of 0.1°C). The CORA experimental activity is mainly orientated to the demonstration of the feasibility and reliability of such a temperature regulation system to precisely control the phase velocity in the RF compressor.

In order to relax the stability specifications of the temperature control system, the basic cell of the RF accelerating structure has been re-designed to obtain a larger group velocity with respect to a SLAC structure. In this case the phase velocity variation associated to a given temperature fluctuation is smaller since the magnification factor v_{ph}/v_g of (1) is reduced. The use of a standard SLAC accelerating sections as velocity buncher has another potential drawback since this structure is of “constant gradient” type. This means that the iris diameter decreases along the section to compensate the wave attenuation keeping the accelerating E-field constant. As a consequence, the group velocity has a significant variation along the structure and, in the thermal deformation regime, the phase velocity will not be perfectly uniform. A “constant impedance” structure, with constant iris diameter and no modulation of the group velocity, will still show a uniform phase velocity even in presence of thermal deformation. In order to relax the temperature stability specifications of the regulation system and to maintain the uniformity of the phase velocity along the structure, a special high group velocity, constant impedance accelerating section named “Alma 5” has been designed. In table I the “Alma 5” parameters are compared to the standard

Table 1: *Characteristics of different cell design.*

	Mark IV (SLAC)	Alma5
Cavity radius [cm]	4.124	4.248
Iris radius [cm]	1.130	1.54
Septum thickness [cm]	0.584	0.59
Cell length [cm]	3.5	3.5
Mode	$2\pi/3$	$2\pi/3$
Frequency [MHz]	2856	2856
Q	13200	13205
Shunt imp. [$M\Omega/m$]	53	41
Vg/c	0.012	0.034
ΔT [$^{\circ}C$]	0.6	2.0

SLAC “Mark IV” section ones. The group velocity has been increased of a factor of 3 to fulfill the requirement on thermal sensitivity. The shunt impedance reduction is acceptable since the nominal gradient of 20 MV/m is obtained with 66 MW of input RF power, a power rate available from the SPARC RF system. The last row in the table shows the power required to the Klystron that feeds the structure. Using the parameters reported in the table, a set of simulations have been carried out using codes as Homdyn and Astra to verify the behavior of a full scale model composed of a slow wave structure followed by two standard SLAC cavities. The results show that the compression factor obtainable is of the order of 7, and that it varies of about 20 % for 0.1 $^{\circ}C$ variation of the compressor temperature. The thermal control of the structure has been studied using finite elements analysis. The best solution to guarantee temperature uniformity and stability has been found embedding the channels for water flow within the cells body to take advantage of the whole copper mass available. The cooling water will be provided to the structure by a compact cooling unit (Neslab HX300). This refrigeration unit has been selected as the basic element of the cooling plant since it is specified for a maximum power load of 10kW with a stability of the operating point of 0.1 $^{\circ}C$. The cooling plant has been tested on a 3 meter long standard SLAC cavity. The cavity has been thermal insulated from the outside to reproduce as close as possible the characteristics of the ALMA 5 cooling circuits and the RF power load has been simulated by a controlled resistive load. The results show that the cooling system is capable of keeping the structure temperature within 0.1 $^{\circ}C$ and the measured resonant frequency variations of the SLAC structure agree with the measured temperature stability. Finally, 9-cell of the ALMA 5 structure has been fabricated and are going to be brazed at CERN to produce a full-scale 9-cell model. A bench test of the phase velocity tuning through a fine temperature regulation will be performed on the model. We expect the test will confirm that the ALMA 5 structure is about 3 times less sensitive to temperature variations respect to a standard SLAC one, so that its phase velocity can be precisely tuned by means of the selected cooling plant. The expected validation of our approach to the SPARC RF compressor design would represent the achievement of the main goal of the whole CORA experiment.

2 Publications

D. Alesini *et al.*, “The design of a prototype RF compressor for high brightness electron beams”, Proceedings of the 2004 European Particle Accelerator Conference, Lucerne (Switzerland), July 5-9, p. 698.

DEUTER

C. Catena (Ass.), F. Celani, (Ass.), A. Di Michele (Ass.), A. Marcelli,
G. Onori (Ass. Resp.), A. Paciaroni (Ass.), E. Righi (Resp. Naz.), G. Trenta (Ass.)

The DEUTER research, typically imprinted by a serendipity character, started up as a microbiological research appended to a cold fusion experiment to inquire the reasons of the following two outcome:

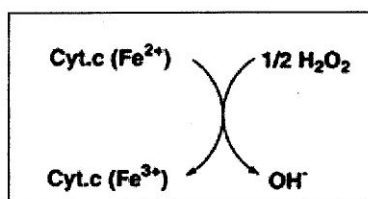
- the strong pH variability of D₂O used to overloading deuterium in palladium,
- the disappearance of the mercury used to patch the micro-slits of the palladium wire.

This microbiological research ended with a discovery of two new bacterial species resulted responsible of the two reminded experimental outcome. Namely the bacteria, named by the discovering researchers: “*Ralstonia detusculanense e Stenotrophomonas detusculanense*”, cause the pH instability with their organic catabolites; similarly their presence explained the reason of the mercury disappearance, being they highly voracious of heavy metals. Therefore to improve the reproducibility of the cold fusion experiment, we attacked the undesirable microbiologic guests treating the D₂O with high gamma ray dose (17 kGy from Calliope facility of ENEA-Casaccia). A literature review disclosed a lot of data undoubtedly interesting from the biochemical, biological and biomedical point of view. In this connexion the judgement many researcher advanced on the subject saying the biological effects of D₂O be extensively studied but rarely deepened seems to be completely shared . It also clearly came out a complete lack of bibliographic references on the biological effects inducible by heavy water irradiated to high dose, whereas there is a large lot of data on the radiolysis induced in H₂O. This remark, undoubtedly interesting from the scientific point of view, gave to INTRABIO and FREEDOM research groups (now gathered in the FREETHAI/DEUTER Group) a sound justification to carry out a comparative study on the biological effects due to non irradiated D₂O in comparison with D₂O irradiated to high dose.

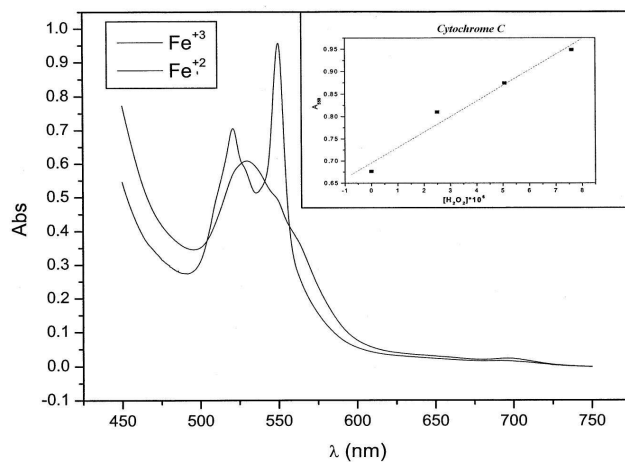
A first “in vitro” experimental research was carried out on the stabilized cell lineage U937 taken rise from an histiocytic pleural Lymphoma. It confirmed the expected result of the cytotoxic effect of non irradiated D₂O. More specifically the experiment showed that D₂O concentrations up to 10% in the culture medium are compatible with the cell growth, whereas concentrations greater than 30% are certainly cytotoxic. This first study phase did not allow to perceive the extent of the greater cytotoxic efficacy of the irradiated D₂O with the respect to the non irradiated D₂O. The subsequent research was carried on evaluating the cytotoxic effect on other cancer cell lineage with not irradiated and with irradiated (17kGy) D₂O: the intent was to evaluate better the biological different behaviour of the two variants. During this phase the stronger increase of the biological effect of the irradiated versus the non irradiated D₂O was clearly demonstrated. Together with the cell survival, it was also evaluated another biological parameter: the apoptosis; this was to obtain more deeper knowledge on the cytotoxic effect due to the two D₂O variants.

To probe into this cytotoxicity kind, certainly due to the radiolysis consequences on the living matter, some other experiments were carried out using both H₂O and D₂O more recently irradiated with 17kGy. Concentrations lesser than 5% of irradiated D₂O caused on the CEM cell lineage a strong lethal effect with a CL50 vs. a concentration of 0,7%. The DAUDI cell lineage, because of a reduced number of experimental data, seems to show a reduced effect, but the lethal effectiveness trend is coherent with the expected consequences. To explain the strengthening of the lethal effect induced by the high dose irradiated D₂O it was necessary a comparison with the data obtained by H₂O irradiated with a similar dose. The results of the experiment showed the two variants (irradiated D₂O and H₂O) cause a similar cytotoxic efficacy, but with a decay time shorter for the H₂O than for the D₂O. Those experimental observations gave rise to the question on the possible mechanisms that induce a lethal cell damage to low concentration of D₂O irradiated to high dose.

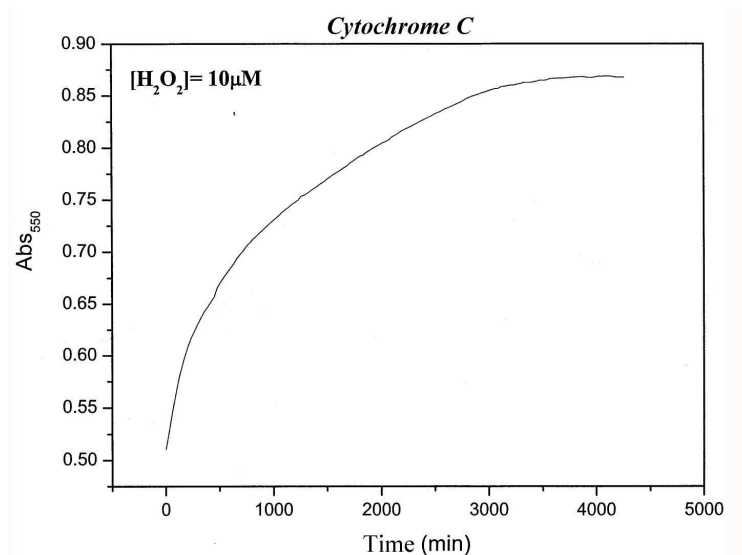
Therefore in the latest phase of this research the main concern was addressed to the qualitative and to quantitative study of the deuterium free radicals, to understand their different biological behaviour and to interpret the long time persistence of the high cytotoxic efficacy of irradiated D₂O. As the aftermath of a meeting in July 2004 on the DEUTER experimental results with the Perugia University research group led by the Prof. Giuseppe Onori, a collaboration was signed on. The aims of it was a study on a comparative analysis between the free radicals of irradiated D₂O and H₂O and on the investigation of the basic reasons why the irradiated D₂O has the peculiar exhibited biological behaviour. The investigation would be carried out using both physical tools and chemical techniques (like: EPR, infrared spectroscopy, interactions of ROS with the scavengers enzymes, ...). For the time being this synergy was useful also to reinstate the researcher number of the DEUTER group; namely this group during the 2004 year fell into a big trouble because of a drastic reduction in number (particularly because of the breaking off of the radiobiologist work contract). The first objective at this point was to set-up a spectrophotometric system able to detect the expected concentration of oxidative compounds at about 10⁻²⁰ μM level as it could be found in a gamma irradiated sample. Namely our observations of hydrogen peroxide at 30% in natural water in the near and medium infrared allowed to appreciate a H₂O₂ concentration of about 100mM; it was too high for our requirements. So we thought to use a probe that reacting with micromoles of oxidizing agents would be able to show measurable infrared absorption variations. We selected the cytochrome-c that, reacting with the hydrogen peroxide, is able to oxidize the iron atom of its heme-group from oxidation number +2 to +3 in accordance with the following scheme:



The absorption band between 500 and 600 nm of the cytochrome-c changes with the iron oxidation; therefore adding H₂O₂ up the 530 nm peak disappears and two new peaks at 520 and 550 nm appear. With an excess of cytochrome, the absorption at 550 nm increases and after a time needed to reach the equilibrium, the absorption efficacy grows linearly with the H₂O₂ concentration (see the insert in the following figure).



The time absorption increase of a cytochrome-c solution in the presence of H_2O_2 raises slowly, depending from the protein and from the hydrogen peroxide concentration. The following figure shows the result for a cytochrome-c $60 \mu\text{M}$ solution with $10 \mu\text{M}$ of H_2O_2 . In those conditions the reaction is completed after about three days.



The previous results show clearly that the depicted system is suitable for our purposes. Therefore we can use in our future research the spectrophotometric system we set up to evaluate low quantity of oxidizing agents in a watery solution. Namely the system, a new one compared with the traditional ones utilized at this purpose, on the one hand allows to estimate oxidizing agents concentration in water up to an extent of $\pm 10^{-6}$ M/l and to the other to show a biological effect on a biomolecule.

The foregoing system will therefore be used:

- a) to make a comparative analysis of the radioinduced free radicals in H_2O and in D_2O ,
- b) to analyse the correlation between the biological effects of irradiated H_2O and D_2O and the kinds and concentration of oxidizing agents.

To this purpose optical spectroscopy techniques in the infrared, visible and ultraviolet bands will be employed using the instruments belonging to the Biophysics department of the Perugia University as well as the DAΦNE infrared radiation of the INFN Frascati National Laboratories. We hope that the quantitative evaluation of the oxidizing agents in irradiated H_2O and D_2O , joined with the correlation of the observed biological effects, will be able to allow the better understanding of the responsible mechanism causing the cytotoxic effects of the irradiated water and to clear the differences between the effects due to H_2O and to D_2O .

1 Publications and Conferences

1. C. Catena, D. Pomponi, G. Trenta, F. Celani, P. Marini, G. De Rossi, E. Righi, "Acqua pesante (D_2O) irradiata: dal reattore nucleare alla cellula". LNF-04/09(P), 6 Maggio 2004.
2. G. Trenta, "La contaminazione dell' ambiente: vie di ritorno all' uomo e valutazioni modellistiche predittive" – Convegno AIRM-AIRP, CNR–Roma, Aprile 2004.

3. G. Trenta, "Radiocontaminazione esterna e interna: Basi fisiche e biologiche, valutazioni, criteri e mezzi di decontaminazione", Master in emergenze NRBC - Università di Roma La Sapienza II Facoltà di Medicina e Chirurgia, Osp. S. Andrea - Roma, Giugno 2004.
4. G. Trenta, "Utilizzo della PC negli USA ed in Italia" – "Scienza medica e diritto", Convegno AIRM, INAIL, ISPESL, Riva del Garda, Giugno 2004.
5. G. Trenta, – Fisica e metrologia delle radiazioni – Corso di Radioprotezione – Università degli studi di Napoli Federico II Facoltà di Medicina e Chirurgia - Napoli, Giugno 2004
6. G. Trenta – Medical surveillance - Scuola Europea di Studi Avanzati in Tecnologie Nucleari e delle Radiazioni Ionizzanti – Anno accademico 2003-2004 – Istituto Universitario di Studi Superiori, Pavia (Luglio 2004).
7. G. Trenta – Diagnostica nelle radiocontaminazioni: metodi diretti e metodi indiretti. - 18° corso avanzato di radioprotezione medica – Radiazioni: lesività e protezioni – Università degli studi di Padova, INFN, AIRM – Settembre 2004.
8. E. Righi – L' esame ematologico: "gold standard" in Radioprotezione medica? – 18° corso avanzato di radioprotezione medica – Radiazioni: lesività e protezioni – Università degli studi di Padova, INFN, AIRM – Settembre 2004.
9. G. Trenta - Probability of causation: aggiornamenti metodologici – 18° corso avanzato di radioprotezione medica – Radiazioni: lesività e protezioni Università degli studi di Padova, INFN, AIRM – Settembre 2004.
10. G. Trenta – Il terrorismo nucleare e radiologico - Antidotes in Depth 2004 and NBCR Emergencies, Clinical and Public Health Issues. International Continuing Educational Course in Clinical Toxicology – Società Italiana di Tossicologia – Pavia, Settembre 2004.
11. G. Trenta – Aspetti medici della protezione del paziente – Corso di formazione in Radioprotezione per Radiologi e Medici nucleari – ASL n.1 Sassari, Ottobre 2004.
12. E. Righi – Significato e limiti dell' ipotesi NTL. – Congresso nazionale della Società Italiana di Radiobiologia (AIRB) - CNR, Roma 9-10 Dicembre 2004.
13. G. Trenta, "Le dosi diagnostiche. Giustificazione e ottimizzazione", Congresso nazionale della Società Italiana di Radiobiologia (AIRB) - CNR, Roma 9-10 Dicembre 2004.
14. G. Trenta, E. Righi, E. Strambi, "Il Polmone" – in: Aggiornamenti di Radioprotezione – n. 26, Anno XII, 1 (7-16), Marzo 2004.
15. G. Trenta, "Il radon" – in: Aggiornamenti di Radioprotezione – n. 26, Anno XII, 1 (17-25), Marzo 2004.
16. G. Trenta, "Informazione, correttezza scientifica e deontologia medica" – in: Aggiornamenti di Radioprotezione, n. 27, Anno XII, 2 (17-25), Marzo 2004; (www.galileo2001.it).
17. E. Righi, "Interventi nella irradiazione esterna", relazione al Master sulle Emergenze, 2ª Facoltà di Medicina dell' Università La Sapienza - Roma.

E-CLOUD

A. Balerna, M. Biagini, M. Boscolo, R. Cimino (Resp.), A. Drago,
S. Guiducci, M. Migliorati, L. Palumbo, C. Vaccarezza, M. Zobov

In the second year of activity of the project E-CLOUD (study of the vacuum chamber surface electronic properties influencing electron cloud phenomena), we continued studying the surface electronic properties of the vacuum chamber material of accelerators. Some of this surface properties may enhance the formation, inside the accelerator vacuum chamber, of what is called an “electron cloud”. The low energy electrons forming such an “e-cloud” inside the vacuum chamber may interact with the high energy circulating beam (specially if formed by positively charged particles) inducing, in certain cases, beam instabilities which may deteriorate accelerator ultimate performance. One aspect of this work, hence, is to analyse in details the surface properties of relevance in this context by means of surface science techniques, studying in details also the time dependence of such phenomena. In fact it is now clear that the surface properties change during accelerator functioning, so that the surface conditions must be followed and studied also as a function of commissioning time. The other essential aspect of this project is to try to understand the impact of a measured parameter on the machine performances. This can be done using the measured parameters as input to “ad hoc” refined Beam Induced Electron Multipacting (BIEM) codes which can simulate the beam stability, in the presence of an electron cloud, for the different machines under study. This has been successfully done in the case of the Large Hadron Collider (LHC) ^{1, 2, 3, 4} and has been started on DAΦNE ⁵.

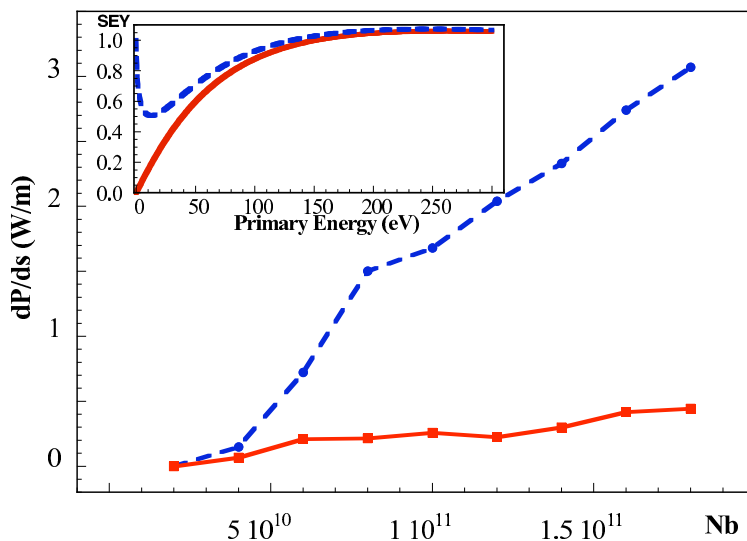


Figure 1: Simulated average heat load in an LHC dipole magnet as a function of proton bunch population at 0.45 TeV, calculated by extrapolating the best fit to the experimental data (shown in the insert) for a SEY with $\delta_{\max}^* = 1.7$ and $E_{\max} = 240$ eV, considering the elastic reflection (dashed line) or ignoring it (full line) ³.

For LHC a number of surface related properties, such as photon reflectivity ², electron ^{1, 3, 4} and photon induced electron emission, and their modification during machine commissioning and operation has been studied and the measured parameters implemented into the codes. In this

contest the most striking result obtained was the observation that total electron yield (SEY) from the industrially prepared Cu co-laminated material, the adopted LHC beam screen material, approaches unity at very low energy electron beam. This suggests that, at low energy, most of the impinging electrons are reflected by the Cu surface ¹⁾. Fig 1 shows the impact on heat load estimates for LHC dipoles if this experimentally derived Cu surface property is feed into the codes (dashed line) as compared to the situation when zero elastic reflection was considered (full line) ³⁾. The impact on the estimate of heat loads is indeed significant, both for LHC, and for all “cold dipole” based machine which may potentially suffer from e-cloud.

Within this project, we also started the analysis of detrimental effects of an eventually present electron cloud at DAΦNE. One of the reason to do that was that, at the design stage of the DAΦNE e+e- collider, preliminary simulations predicted significant e-cloud induced beam instabilities in the positron ring for the design machine parameters. Such calculations were not refined to simulate e-cloud instabilities using more realistic parameters (i.e. chamber geometry, measured secondary emission yield (SEY), photon reflectivity and actual beam conditions). DAΦNE has been routinely operated with more than 1A of circulating positron current, without clear evidence of the predicted e-cloud limitations. Present measurements ⁵⁾ of the tune shift of both positron and electron beam as a function of the total current do show a clear difference of the horizontal tune behaviour for the two beams. For the electrons the slope of the current induced tune shift is equal (opposite sign) for the two planes, while for the positrons the growth of the horizontal tune is clearly steeper than the vertical one. The electron beam behaviour can be related to resistive wall effects due to a rectangular vacuum chamber cross section but it is also conceivable that an electron cloud may have contributed to the observed horizontal instability and tune shift of the positron beam. We set the necessary collaborations and computing tools to be able to run the simulation study of the electron cloud build-up using the E-cloud codes at LNF ⁵⁾.

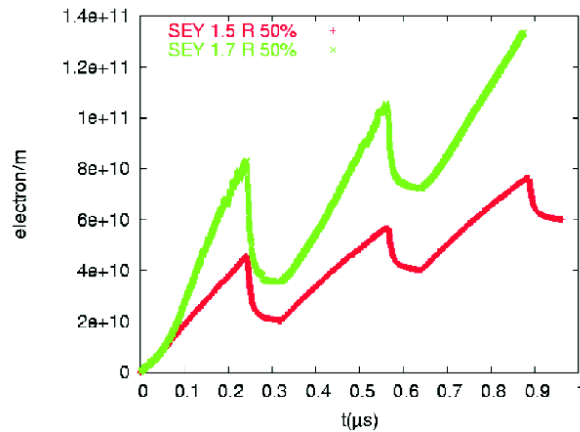


Figure 2: Photoelectron linear density build-up for the drift zone at the arc exit. Three complete turns are plotted.

The result shown in fig.2 consider the drift zone at the arc exit which receives about 9 degrees of the synchrotron radiation emitted by the upstream dipole, not intercepted by the slot. Only the results with an estimated value of 50 % reflectivity are here reported. Simulation done taking for the reflectivity value 15% gives photoelectron densities is about one half. This justify the ongoing experimental activity to measure, with Synchrotron radiation, the actual Al 5083 photon reflectivity

to obtain more reliable simulations. In fig.2 two different values of the maximum secondary emission yield (SEY) were considered as indicated confirming the importance of measuring the actual SEY value of the Al used. In any case, the simulated electron cloud build-up turns out to be severe. More realistic calculations including experimentally measured surface properties as well as considering the presence of fringe fields due to the nearby magnetic elements is foreseen, in order to arrive at a more accurate scenario.

1 List of Conference Talks by LNF Authors in Year 2004

1. R. Cimino, "Surface-Related properties as an essential ingredient to electron-cloud simulations", invited talk at the 31st ICFA Advanced Beam Dynamics Workshop on Electron-Cloud Effects ELOUD'04; Napa (California), April 19-23, 2004.
2. C. Vaccarezza *et al.*, "Experimental observations and e-cloud simulations at DAΦNE", 31st ICFA Advanced Beam Dynamics Workshop on Electron-Cloud Effects ELOUD'04. Napa (California), April 19-23, 2004.

References

1. R. Cimino, and I. R. Collins, "Vacuum chamber surface electronic properties influencing electron cloud phenomena", Applied Surface Science 235, 231-235, (2004).
2. N.Mahne *et al.*, "Photon reflectivity distributions from the LHC beam screen and their implications on the arc beam vacuum system", Applied Surface Science 235, 221-226, (2004).
3. R. Cimino, I. R. Collins, M.A. Furman, F. Ruggiero, G. Rumolo and F. Zimmermann, "Can Low Energy Electrons Affect High-Energy Physics Accelerators?", Physical Review Letters 93, 14801 (2004).
4. R. Cimino, "Surface-Related properties as an essential ingredient to electron-cloud simulations", Proceedings of the 31st ICFA Advanced Beam Dynamics Workshop on Electron-Cloud Effects ELOUD'04. Napa (California), <http://icfa-ecloud04.web.cern.ch/icfa-ecloud04>.
5. C. Vaccarezza *et al.*, "Experimental observations and e-cloud simulations at DAΦNE", Proceedings of The 31st ICFA Advanced Beam Dynamics Workshop on Electron-Cloud Effects ELOUD'04. Napa (California), <http://icfa-ecloud04.web.cern.ch/icfa-ecloud04>, to appear in: PRST-AB Special Editions, Conference Editions, and Special Collection.

FLUKA

M. Carboni, M. Pelliccioni (Resp.), S. Villari (Ass.)

1 Report year 2004

The angular distribution of the secondary radiation produced by the galactic component of cosmic rays has been determined simulating the penetration in the Earth's atmosphere of the primary spectra with the FLUKA code. The calculated results at a typical cruise altitude for a civil aircraft have been fitted with simple mathematical equations.

The irradiation of a mathematical model of aircraft, developed with the combinatorial geometry package of FLUKA, has been simulated using the calculated angular distributions. A significant shielding effect from the aircraft structures has been observed in the middle of the passenger cabin.

Work has been done on the software technological aspects concerning the management and improvement of the FLUKA web server. In particular, a web form has been prepared to provide a FLUKA user questionnaire and a system of monitoring of the server itself has been implemented. Work started in order to build a web interface to run FLUKA with the final aim of developing a FLUKA web demonstrative calculator.

2 Conference Talks in 2004

1. M. Pelliccioni (co-authors A. Ferrari and R. Villari), An aircraft mathematical model for the evaluation of structure shielding on the aircrew exposure, paper presented at the Conference ICRS10-RPS2004, Madeira, Portugal, 10-14/5/2004.
2. M. Pelliccioni (co-authors G. Battistoni, A. Ferrari and R. Villari), Evaluation of the doses to aircrew members by considering the aircraft structures, COSPAR2004, Paris, France, 19-25/7/2004 [solicited paper].

3 List of Publications 2004

1. A. Ferrari, M. Pelliccioni and R. Villari, Evaluation of the influence of aircraft shielding on the aircrew exposure through an aircraft mathematical model, *Radiat. Prot. Dosim.* 109, 91-105, 2004.
2. M. Pelliccioni, The impact of Publication 92 on the conversion coefficients for cosmic ray dosimetry, *Rad. Prot. Dosim.* 109, 303-309, 2004 [invited paper].
3. G. Battistoni, A. Ferrari, M. Pelliccioni and R. Villari, Monte Carlo calculation of the angular distribution of cosmic rays at flight altitudes, *Rad. Prot. Dosim.*, 112, 331-343, 2004.
4. A. Ferrari, M. Pelliccioni and T. Rancati, Calculations for Cosmic Ray Dosimetry at Aircraft Altitudes using FLUKA, in *Radiation Protection 140, Cosmic Radiation Exposure of Aircraft Crew, Compilation of Measured and Calculated Data*, European Commission, Final Report of EURADOS WG 5, 2004.

FREETHAI

V. Andreassi, F. Celani (Resp. Naz.), G. D' Agostaro (Osp.),
P. Quercia (Osp.), E. Righi (Ass.), A. Spallone (Ass.), G. Trenta (Ass.)

Collaboration with Companies/University: EURESYS (Rome); Pirelli Labs (Milan);
Centro Sviluppo Materiali (Castel Romano); CESI (Milan); ORIM (Macerata);
STMicroelectronics (Cornaredo, Milan); Mitsubishi Heavy Industries (Yokohama-Japan);
Hokkaido University (Sapporo-Japan); University and INFN Lecce.

1 Foreword

Starting from 2004, the experiment FREETHAI included also the activity of previous INTRABIO experiment (see the Activity Report (AR) of year 2003): biological use of Heavy Water. It was renamed DEUTER in 2004. In such group are involved also researcher of Perugia INFN section, that have a close collaboration with LNF because some of their scientific activity is performed at LNF using the Infrared Synchrotron Light coming out from DAΦNE e^+e^- collider.

* The common aspect of both experiments is the use of Deuterated compounds.

* Here we will report on the nuclear results, key activity of FREETHAI.

* The aim of DEUTER is to explore the possible use of Heavy Water, irradiated by gamma radiation (energies of 1173 keV and 1332 keV) coming out from a high intensity ^{60}Co source (“Calliope” facilities at ENEA-Casaccia), as a possible anti-cancer agent. Details are given in the DEUTER activity report.

2 Introduction

The experimental task of FREETHAI (Fusion Research by Electrolytic Experiments: Tritium and Heat Anomalous Increase), 2nd year of activity, is to develop innovative and reproducible techniques to maximize the values of Hydrogen (H) and Deuterium (D) concentrations in Palladium (Pd), i.e. the so-called overloading, ($\text{H,D/Pd} \gg 0.95$) through light (H) or heavy (D) electrolytic solutions (water and/or hydro-alcoholic). The aim is to get short waiting times for the overloading (50 hours) and long time stability (> 4 hours). It is a further developing of the FREEDOM experiment ended in December 2002: see the AR of such experiment for further details.

Our experimental pathway consists in the development of very innovative methods for overloading Pd (surface and/or bulk) using light H and, later on, in the transfer and adaptation of the successful methods to the use of heavy (water, alcohol) solutions. Such two steps procedure was demonstrated to be overall quite efficient because the experiments using light H did not need particularly sophisticated cares (for example the solutions are insensible to ambient humidity). The employment of heavy H solutions (i.e. the Deuterium, D) is, on the contrary, very time consuming and experimentally complex. All the deuterated compounds are strongly hydro-scopic: the H contamination of D solutions (with H arising from ambient humidity), was an uncontrollable parameter in our D-based experiments: it could work as a poison with respect to the D electrolyte. The resulting main drawback of such a procedure is that it is necessary to build at least a twin experimental set-up, electronic data acquisition system together with full-time dedicated people.

In the case of the D based experiments, we were looking for “the anomalous production” of excess heat, tritium and “transmutations” also, i.e. the quite “strange” and unusual thermal and/or nuclear ashes related to the so-called, and still now controversial, “Cold Fusion” (CF) phenomenology. Anyway, recently, the “transmutations” phenomena received a significant acceptance in the scientific community mainly because of the **reproducible** experiments carried out at Mitsubishi Heavy Industries Laboratories (Yokohama, Japan). We note that some of the Mitsubishi

Group (headed by Yasuhiro Iwamura) results were independently confirmed also by our experimental group in Italy at INFN Frascati National Laboratories, using a complementary methodology (wet electrolytic environment instead of dry gaseous one).

During the overloading experiments we changed from water based electrolyte to hydro-alcoholic solution. The scientific explanations for the use of such an unconventional electrolyte are stated in details in our previous AR. In short, we used a main solution made of heavy ethyl alcohol (C_2H_5OD) and heavy water (D_2O) with a ratio 90-95% to 10-5%. The main dissolved cations were Strontium (as $SrCl_2$) and Mercury (as $HgCl_2$) ions, at a typical concentration as low as 10 micromolar and 1 micromolar respectively. The pH, "mild", was kept at about 4 (acidic). For the sake of comparison, most of the electrolytic "Cold Fusion" experiments (several thousands) performed in the world use pure D_2O adding $LiOD$ at a concentration of $0.1 \div 1$ molar, i.e. obtained strong basic solutions (pH about $13 \div 14$). Solutions of the latter type follow the "teachings" of Martin Fleischmann and Stanley Pons (Utah University-USA) who in 1989 at first claimed, worldwide, the possible "nuclear" origin of some anomalous heat in their, D_2O - $LiOD$ (0.1M), electrolytic cell operated (for several months) at a cathode current density between 60 and 600 mA/cm². We emphasize that, thank to the mild pH (4) and very low current density (only $5 \div 20$ mA/cm² at the cathode surface and five times less at anode) it is possible to reduce, at a great deal, the corrosion of components inside the electrolytic cell: such effect is typical of "conventional" electrolytic experiments. As a consequence, it is possible to make elemental composition analysis of both cell residual powders and Pd wire (by: Inductively Coupled Plasma-Mass Spectroscopy ICP-MS; Inductively Coupled Plasma-Optical Emission Spectroscopy ICP-OES; Scanning Electron Microscopy SEM with micro analysis) after electrolysis, in a quite reliable way. We suggest to read our AR of 2002 and 2003 about a general discussion on ICP-MS results.

We use as cathode Pd electrodes consisting of wires 50 to 100cm long with diameter as thin as 50 microns instead of the most diffused rods (according to Fleischmann and Pons) or plates (according to Akito Takahashi, Osaka University-Japan, 1992). We experienced that some suggestions from Giuliano Preparata and Emilio Del Giudice (University and INFN Milan, 1994) about the peculiarity of long-thin wires are substantially correct, although some interpretations of their results have to be, according to our recent experiments, updated. Before the use, the wire Pd cathodes are: carefully cleaned (by organic solvent-water-nitric acid-water sequence), bulk lattice strain released and surface oxidized (both by a specific protocol of Joule heating-room temperature cooling). We introduced (1996), and continuously improved, such protocol.

As reported in detail in the papers quoted in our previous AR, we performed a series of experiments with hydro-alcoholic solutions containing small amounts of Sr salts and Hg ions during which we found excess heat (see ref. 22 in Pub.1 at AR 2003) and tritium (see ref. 24 in Pub.1 at AR 2003) well above background. We found that in the hydro-alcoholic environment, during the anodic phases (that is for some hours every 1-3 days) of our loading cycles, the Pd electrode is eroded. Significant amounts of very fine Pd particles are found at the bottom of the cell at the end of the experiments. ICP-MS analysis after electrolysis showed the presence of Pd together with some unexpected elements, in such black powder (see ref. 26 in Pub. 1 at AR 2003). Moreover, after several electrolytic loading-unloading cycles, the Pd wire eroded surface could absorb the D dissolved in the solution (whose maximum overpressure is only 50mbar in our experimental apparatus), quickly and without applied electrolytic current. The effect is remarkable: a mean D/Pd ratio up to 0.75 was reached in some very recent experiments (December 2004). The improved performance about spontaneous D self-loading, up to a value equivalent to a gas pressure of over 10 bar, was due a new, specific procedure of electrolysis. Such procedure (together with electronic circuitry design), was developed fully in our group and is under consideration for a **patent**. Recently we got evidence, by SEM analysis, that in the Pd surface were build a kind of nano-structures and fractal geometry of Pd (see Ref. 27 in Pub.1 of AR 2003 for further comments about the

importance of nano-structure in Cold Fusion experiments, as pointed out by Yoshiaki Arata at Osaka Univ.-Japan). *We are almost convinced that the growing up of nano-structure and/or fractal geometry at Pd surface (spontaneous, as a side-effect of Deuterium absorption/desorption cycles; controlled, by proper procedures) play a key role in the production of all the anomalous effects detected in Cold Fusion experiments.*

We recall that Y. Iwamura, at Mitsubishi Heavy Industries of Yokohama-Japan (see ref. 25 in Pub. 1 of AR 2003), first showed that Sr is apparently transmuted into Molybdenum (Mo), or Cesium (Cs) into the rare earth Praseodymium (Pr) when a proper multilayer of Pd/Pd-CaO/Sr or Pr is forced to be grown at enough high rate (>3 SCCM), by D_2 gas for enough long time (several hundred of hours). We tried to check whether such a “transmutation” could occur also after the repeated D-Pd loading/deloading/loading cycles in our experimental set-up. In July 2002 we were ready to perform an independent variant of the Iwamura experiment.

Before starting we analyzed, by ICP-MS, all the components present in the cell (C_2H_5OD , D_2O , $SrCl_2$, DCl , $HgCl_2$, Pd), and pieces of 2 Pt wires (anode and reference electrodes). At the end of the repeated D-Pd loading/deloading experiment, the electrolytic solution was vacuum dried, the residue was collected and again analyzed by ICP-MS together with the Pd cathode (all dissolved in hot-concentrated aqua regia). Mo was found in excess of any conceivable contamination, its isotopic composition of the Mo was different from the natural one (see ref. 26 in Pub.1 of AR 2003). It appears that the phenomenon, first discovered by Y. Iwamura in a flowing deuterium gas system, also occurs in our electrolytic cell when it is operated according to our loading-deloading-loading procedure for a time length of the order of 500–1000 hours.

3 Main Experimental results in 2004

About the reasons to use Thorium salts as main electrolyte, together with our specific procedures to clean the cell and purify reagents, see our previous AR2002 and 2003.

In short, we got both excess heat (best result was an energy gain of about 10 for several days) and several strong indications of the “production” of new elements, some of these with an isotopic composition different from the natural one.

About the new elements “produced”, some (Cu, Zn) are the same as those obtained by using Sr as the main electrolyte, others are peculiar respectively of Strontium (i.e. Mo) or of the Thorium addition (i.e. Pb). Further details can be found in the papers published (see Pub.1, 4 in AR2003). Significantly, it were found large differences between H and D based experiments.

1) Surprisingly, we found that the electrolyte consumption was much larger than could be expected according to the Faraday’s law. We suspect that this loss is caused by the heat being generated in a few hot spots at wire surface, where the temperature might raise to rather high values. This local over-heating could evaporate the solution so that gaseous D_2O and C_2H_5OD are lost in addition to D_2 and O_2 . Because this effect, we build, in July 2004 a new cell made out of PTFE, quartz, and used an IR thermo-camera (NEC-Nikon, model TH7100) in order to detect the IR radiation that might issue from the deuterated Pd wire surface. Some results, although preliminary, were quite intriguing: some hot area were detected along the Pd wire, at D (mean) overloading situation. The hot area were not stable over time.

2) A series of test were made aimed to cross check, in a systematic way and operating conditions more severe than in our typical experiments, if the new element detected can arise from an uncontrolled source of contamination in the cell itself. The cell was exactly the same of usual (i.e. chemical borosilicate glass 3.3) and the reagents were the same Th and Hg salts (usually used in “heavy water” experiments) dissolved in few cc of D_2O . Only the main electrolytes, about 750cc of C_2H_5OH and H_2O , were changed from Deuterium based to Hydrogen based. In other words, the total amount of D_2O (due to Th and Hg solutions) in H_2O was about 10% The electrolytic current was about 3 times the usual, in order to “stress” the system. The total “new” elements

detected were from 10 to 100 times less than in Deuterium based experiments (Pub. 7). Results were presented at International Conference on Cold Fusion 11 (ICCF11) as Invited Paper by F. Celani.

3) We developed an innovative procedure to measure, in situ, the resistive thermal coefficient of Pd wire versus loading. Such a measurement is needed to avoid ambiguous interpretation of results when there is an increase of Pd wire resistance. The origin of such increase can be two, one “bad” (Pd wire deloading), one “good” (resistance increase because some excess heat generated by the Pd wire). The measurements were made both for H and D based electrolytes. Some of the experimental results, by D electrolyte and wire in overloaded conditions, showed a behavior completely different from H one. Up to now, the analysis of data is made only off-line. The data about Deuterium were anticipated at 5th Asti Workshop on Cold Fusion (Invited Paper), Pub. 1, and later “enriched” with Hydrogen data at ICCF11 (Invited Paper, both presented by F. Celani, Pub. 7). Moreover, the results presented at ICCF11 were previously presented and discussed, deeply, during the Italian Physical Society Annual Meeting. Two contributed papers (Pub. 5, Pub. 6) were presented by F. Celani. We would like to note that, as usual during presentation of Cold Fusion results, the people attending the talk was quite large and the discussions continued quite longer than the time allotted (extra 2 hours, this time). *We are proud to inform that such procedure, although not fully automated up to now, was the first one developed in the world and received an enthusiastic acceptance from the scientific groups involved in “Cold Fusion” experiments: it solved one of the open problems about ambiguity in excess heat measurements.*

4) It was continued the systematic study on different electrolytes and loading procedures, using Hydrogen based solutions (Contributed Papers, presented by Antonio Spallone, at 5th Asti Workshop Pub. 2 and later, with further details, at ICCF11, Pub. 8).

5) We made some collaborations, with a group leaded by Tadahiko Mizuno of Okkaido University (Japan), aimed to cross-check the fully unexpected emission of neutrons from pressurized Deuterium gas kept at low temperature (77K) and under strong magnetic field (8kG). The results, still in progress, were presented by Tadahiko Mizuno, before at 5th Asti Meeting (Pub. 3) and later, with further test, at ICCF11, Invited Paper (Pub. 9).

6) We made some collaboration, obviously, with Lecce Group of FREETHAI which aim is to stimulate production of new elements using laser excitation in Pd-H and Pd-D gaseous system. The paper (Pub.4) was presented by Antonella Lorusso of Lecce INFN section.

7) We made a close collaboration with Yasuhiro Iwamura (and co-workers) at Mitsubishi Heavy Industries (Yokohama, Japan), aimed to study possible transmutations of Thorium and Mercury, i.e. the key elements of LNF-INFN electrolytic experiments, using only gaseous systems and the specific multilayer of Pd compound developed by Iwamura. The experiments were performed, in Japan, using the apparatus developed by Iwamura group. Because law constrains about use of radioactive materials, it was not possible to use pure Th (like at INFN-LNF) but just a W-Th alloy. The results, about Mercury, were qualitatively in agreement with what found in INFN-LNF experiments: presented jointly by Y. Iwamura and F. Celani at ICCF11, Invited Paper (Pub. 10).

4 Conclusions

After a large number of experiments performed during 15 years of research work aimed to find out anomalous effects in systems forced to a high concentration of deuterium, we are confident that most of the observed effects occur at the interface between the solution and the Pd bulk. A properly thin-formed layer of a third element is necessary. Non-equilibrium situations are also necessary to trigger the effects. Recently, we found that deuterated hydro-alcoholic, slightly acidic solutions, works very well at producing the so called anomalous effects. Additions of Th and Hg salts within the micromolar concentration range improve the effects even at very low electrolytic current density ($<10\text{mA}/\text{cm}^2$). We think that the model developed by Akito Takahashi about

multi-body resonance fusion of deuterons (see ref. 31 in Pub.1, AR2003) can explain most of the thermal and isotopic anomalies, including foreign elements that we have recently observed. Further work is necessary to fully characterize the system and increase the magnitude of the effects.

5 Publications

1. F. Celani, A. Spallone, E. Righi, G. Trenta, C. Catena, G. D'Agostaro, P. Quercia, V. Andreassi, P. Marini, V. Di Stefano, M. Nakamura, A. Mancini, P.G. Sona, F. Fontana, L. Gamberale, D. Garbelli, F. Falcioni, M. Marchesini, E. Novaro, U. Mastromatteo, "Problematics related to Th-Hg salts in Cold Fusion Experiments", invited paper at the "5th Asti Workshop on Anomalies in Hydrogen/Deuterium loaded Metals", Asti, March 19-21, 2004; <http://www.iscmns.org/meetings/Asti/papers/celani.doc>.
2. A. Spallone, "A method to achieve H/Pd=1; a review of 10 years of studies", contributed paper at the "5th Asti Workshop on Anomalies in Hydrogen/Deuterium loaded Metals", Asti, March 19-21, 2004; <http://www.iscmns.org/meetings/Asti/papers/spallone.ppt>.
3. T. Mizuno, H. Kenichi, A. Takahashi, F. Celani, "Neutron emission from low temperature D₂ gas in a magnetic field", invited paper at the "5th Asti Workshop on Anomalies in Hydrogen/Deuterium loaded Metals", Asti, March 19-21, 2004; <http://www.iscmns.org/meetings/Asti/papers/mizuno.ppt>.
4. A. Lorusso, V. Nassisi, E. Filippi, M. Di Giulio, D. Manno, G. Buccolieri, F. Celani, "Modification of Pd-H₂ thin films processed by UV lasers", invited paper at the "5th Asti Workshop on Anomalies in Hydrogen/Deuterium loaded Metals", Asti, March 19-21, 2004; <http://www.iscmns.org/meetings/Asti/papers/lorusso.doc>.
5. F. Celani *et al.* (same authors as Pub.1), "Metodo innovativo per la misura, in situ, del coefficiente termico resistivo nel Palladio iperdeuterato tramite elettrolisi", contributed paper at the "XC Congresso Nazionale Società Italiana di Fisica", Brescia-Italy, September 20-25, 2004; <http://www.sif.it>.
6. F. Celani *et al.* (same authors as Pub.1), "Evidenza sperimentale, tramite analisi ICP-MS, di elementi con composizione isotopica anomala in celle elettrolitiche con catodo di Palladio iperdeuterato", contributed paper at the "XC Congresso Nazionale Società Italiana di Fisica", Brescia-Italy, September 20-25, 2004; <http://www.sif.it>.
7. F. Celani *et al.* (same authors as Pub.1), "Innovative procedure to measure, in situ, resistive thermal coefficient of H(D)/Pd during electrolysis and cross-comparison of new elements detected in Th-Hg-Pd(H) electrolytic cells", invited paper at the "International Conference on Cold Fusion 11", Marseille (France), October 31-November 5, 2004; to be published in the conference proceedings.
8. A. Spallone, F. Celani, P. Marini, V. di Stefano, "An overview of experimental studies of H/Pd over-loading with thin Pd wires and several different electrolytic solutions", contributed paper at the "International Conference on Cold Fusion 11", Marseille (France), October 31-November 5, 2004; to be published in the conference proceedings.
9. T. Mizuno, T. Akimoto, A. Takahashi, F. Celani, "Neutron emission from D₂ gas in magnetic field under low temperature", invited paper at the "International Conference on Cold Fusion 11", Marseille (France), October 31-November 5, 2004; to be published in the conference proceedings.
10. Y. Iwamura, F. Celani *et al.*, "Th-W and Hg transmutations experiments by D₂ gas permeation through Pd/CaO/Pd complexes", invited paper at "International Conference on Cold Fusion 11", Marseille (France), October 31-November 5, 2004; to be published in the conference proceedings.

LAZIO-SiRad

G. Bisogni (Tecn.), S. Dell’Agnello (Resp.), A. De Paolis (Tecn.),
M. A. Franceschi, E. Iacussa (Tecn.)

The R&D experiment called LAZIO-SiRad (Low Altitude Zone Ionization Observatory ¹⁾) is part of the Italian Soyuz Mission 2 (ISM2) to the International Space Station (ISS). LAZIO-SiRad was launched with a PROGRESS spacecraft (unmanned Soyuz) from the Baikonur cosmodrome on February 28, 2005. The experiment is being built by a collaboration of several Universities and Laboratories, led by INFN within the GR. V activities. The LNF group has built four structural mechanical parts.

- 1) The LAZIO-SiRad Main Electronics Box (MEB), which is the main mechanical enclosure (**both** the *qualification* model, QM, and the *flight* model, FM).
- 2) The EGLE MB box (**both** QM and FM versions), external to the MEB. LAZIO is equipped with the high precision low frequency magnetometer EGLE (Esperia’s Geomagnetometer for a Low frequency wave Experiment ²⁾). Magnetic field signals detected by the EGLE magnetic head probe are amplified, filtered and acquired by the EGLE acquisition and data handling board located into the EGLE MB box.

Although LAZIO-SiRad is not a large project (the MEB is about $464 \times 314 \times 260$ mm³, and the whole payload is 28 Kg and the number of detector channels is not high), it is a very integrated space mission, since it involves several space agencies and has to be launched with a tight time schedule (in practice less than 6 months).

The goal of LAZIO-SiRad (see Fig. 1) will be to monitor the real-time variations of the radiation environment on the ISS and to measure the activity of the Van Allen belts in LEO (Low Earth Orbits). Three scintillators are used to trigger on the passage of charged particles and eight silicon detectors will measure their charge up to $Z=25$ (iron nuclei) in the range ~ 10 to ~ 100 MeV, with a large geometric aperture ($GF \sim 40$ cm²sr). Together, they will record particle arrival times, their line of arrival (pitch angle), their direction of arrival. This will provide measurements of the pitch angle distribution within short time intervals (from few seconds to few minutes depending on the position on the orbit). EGLE will measure the magnetic environment inside the ISS concurrently to the measurement of charged particle fluxes and will examine potential pre- and post-seismic effects. LAZIO-SiRad is also equipped with 16 scintillator tiles with WLS fibers readout by some of the very first prototypes of Silicon Photomultipliers operated in space ³⁾.

LAZIO-SiRad integration was done in Rome Tor Vergata, where a first acceptance test carried out by ESA was performed successfully on December 15, 2004. Afterwards, SQ tests were done at the SERMS SQ facility ⁴⁾ of INFN-Perugia. An acceptance test for off-gassing occurred at the ESTEC SQ site (Holland) on January 10, 2005. The experiment passed the final acceptance test in Moscow at the end of January 2005 and the payload was shipped successfully to the ISS with the PROGRESS launch of February 28, 2005. There it awaits the ISM2 crew, that will be launched around mid April 2005. The Italian ESA astronaut Roberto Vittori, part of this crew, will operate the experiment and bring back the data to Earth at the end of the mission.

A review of LAZIO-SiRad and of the goals of ISM2 was given at the meeting “INFN-SPAZIO/2” held at LNF, on February 16, 2005 and can be found in its web site ⁵⁾.

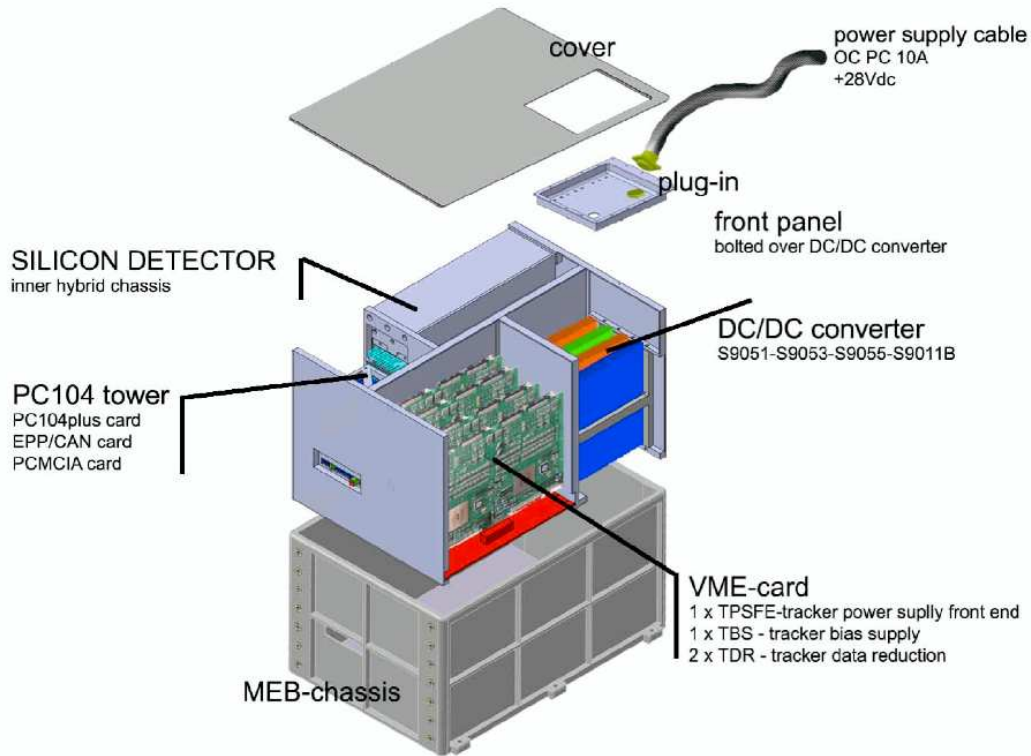


Figure 1: Exploded view of the LAZIO-SiRad experiment on the International Space Station.

References

1. See the presentation of R. Battiston at http://www.pg.infn.it/home/battiston/PUBLIC/LAZIO-SIRAD/Presentazione_PIs_13Settembre2004.ppt (GR. V meeting).
2. [HTTP://www.fis.uniroma3.it/it.php?page=ricerca&argo=gruppi&cat=FisicaTerrestre-Ambiente&gruppo=40](http://www.fis.uniroma3.it/it.php?page=ricerca&argo=gruppi&cat=FisicaTerrestre-Ambiente&gruppo=40). See also V. Sgrigna http://www.agu.org/meetings/fm04/fm04-sessions/fm04_T53C.html.
3. Silicon PhotoMultipliers: NIMA 504 (2003) 48.
4. SERMS is located in Terni, Italy; see <http://serms.unipg.it/>.
5. "INFN-SPAZIO/2: meeting on the prospects for astro-particle physics in space within INFN", LNF, February 16, 2005. <http://www.lnf.infn.it/conference/2005/spazio/>.

Ma - Bo

D. Di Gioacchino, U. Gambardella (Resp.), G. Celentano,
A. Mancini, P. Tripodi, S. Pace

1 Purposes of the project

The *Ma-Bo* experiment is devoted to analyze the use of the magnesium diboride MgB_2 compound. As it becomes superconducting at temperatures below 39 K, its potentiality either in wire applications (magnets) or in thin films applications (RF applications or electronics) have been investigated. Six INFN sections are involved: Genova (group leader), Milano, Torino, LNF, LNL, and Napoli, in collaboration with INFN Genova, CNR Genova, and ENEA Frascati.

2 The Frascati group activity

The Frascati group, made of LNF and ENEA, takes care of studying the process of thin film depositions, their structural and morphological properties, as well as to analyze the MgB_2 superconducting properties by means of current transport and *ac* susceptibility measurements in high magnetic fields.

2.1 Thin film synthesis

The activity carried out was focused to improve the process to realize MgB_2 superconducting thin films. During 2004 from the sputtering processes with alternate layer depositions MgB_2/Mg , followed by different heat treatments in Ar gas at temperatures lower than 600 C¹⁾, we switched to a single deposition of MgB_2 process followed by a high temperature treatment in a Mg vapour. According to the literature this process is the more reliable to attain high quality films useful for applications. This process is performed without vacuum break, as in the deposition chamber it has been realized a Nb box where samples can be sealed in with bulk Mg pieces and heated up to 900 C. The system (mechanics, heater, Nb box) has been assembled late 2004 and we expect to test it early 2005.

2.2 AC susceptibility measurements

The superconducting dynamic response²⁾ in zero field cooling (ZFC) of MgB_2 bulk samples using the 3rd harmonic *ac* susceptibility measurements has been studied. The responses are characterized from the critical states that decay in glass states via creep processes. In this analysis different frequency values at fixed H_{dc} investigate different current density levels, J , through the relation

$$J(\text{time}) \approx \left[\ln\left(\frac{t}{t_0}\right) \right]^{-\frac{1}{\mu}} . \quad (1)$$

In this way, different pinning regimes in the Collective-Glass (CG) pinning framework, as single vortex (*sv*), small bundle (*sb*), large bundle (*lb*) have been studied. In fact the curvature K of the $E-J$ relationship is strictly connected with the 3rd harmonic modulus of the *ac* magnetic susceptibility. The theoretical $K(J)$, in various pinning CG regimes, has been calculated for YBCO as all the parameters are well known. In fact the mathematical $K(J)$ slopes for different CG pinning regimes have general validity for a superconductor described with the CG pinning theory. Then the computed slopes will be used to explain the experimental *ac* magnetic 3rd harmonic modulus

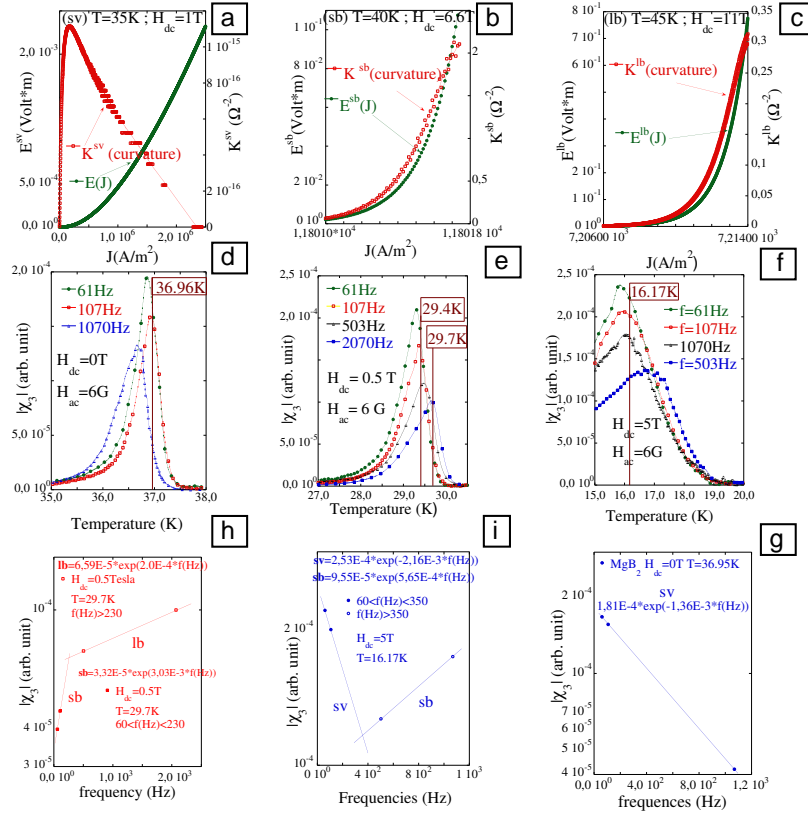


Figure 1: *a,b,c*) curvature $K(J)$ for '*sv*' '*sb*' '*lb*' pinning regimes in collective pinning approach; *d,e,f*) the 3^{rd} harmonic measurements for bulk MgB_2 sample; *g,h,i*) flux pinning dynamic behaviour of MgB_2 .

susceptibility for a MgB_2 sample. The theoretical curvature $K(J)$ in the *sv* behavior, assumes lower values compared to other pinning regimes. The curvature $K(J)$ versus J shows an abrupt increase followed by an exponential decrease. Analyzing $K(J)$ for *sb* and *lb*, the curvature shows significantly higher values with a monotonic exponential increase. In case of *sb*, the parameter K/J is one order of magnitude higher than in the *lb* case. This led us to separate the pinning regime (fig.1a,b,c). In fig.1d,e,f are shown the 3^{rd} harmonic behaviour versus temperature for $H_{dc}=0, 0.5, 5$ Tesla. For example the 3^{rd} harmonic modulus vs. frequency, at $T=36.96K$ and $H_{dc}=0T$, shows a decrease with the frequency. Only *sv* pinning regime has this kind of behavior (fig.1g). In fig. 1h and fig.1i the 3^{rd} harmonic modulus versus frequency at $H_{dc}=0.5T$ and $T=29.7K$ and at $H_{dc}=5T$ and $T=29.4K$ and are shown. In fig.1h a *sv* regime is evident for frequency in the range $[60 \leq f \leq 260 Hz]$, the modulus exponentially increases for $f > 260 Hz$ and shows a *sb* flux dynamics regime, in this figure a flux transition regime is present. Thus that a change of the frequency is able to give rise to a flux dynamic transition.

References

1. G. Grassano, U. Besi Vetrella, V. Boffa, G. Celentano, U. Gambardella, A. Mancini, T. Petrisor, A. Rufoloni, M. Vadrucchi, "In-situ growth of MgB_2 thin films with different techniques assisted by Mg thermal evaporation", IOP Conference Series 181 (2004), 1367.
2. D. Di Gioacchino, P. Tripodi, J. D. Vinko "Glass-Collective Pinning and Flux Creep Dynamic regimes in MgB_2 bulk", IEEE Trans. on Appl. Supec. (2005), in press.

MINCE

C. Balasubramanian, S. Bellucci (Resp.), S. Bini,, G. Giannini, A. Marcelli,
A. Raco (Tecn.), F. Tombolini (Dott.).

1 External collaborating Institutions:

Univ. Roma La Sapienza (School of aerospace engineering), Univ. Modena, Univ. Roma Tor Vergata-Policlinico Tor Vergata, IHEP-Protvino (Russia), VARIAN (Torino), CSM (Pomezia), HITESYS (Aprilia), Univ. Pune (India), Burnham Institute (La Jolla, CA, USA), Lviv Univ (Ukraine), ILL (Grenoble, France), Univ. Cosenza.

2 Relevant results achieved:

Good quality samples of: a) roughly aligned ropes of SWNT, with the tube diameter in the range 1-2 nm and a bundle diameter of 20-40 nm, as well as MWNT with diameter of 20-60 nm; b) high yield in terms of C nanotube density in the sample (above 50%).

Good field emission properties of the samples, with activation fields as low as 0.4 V/micron and a typical current emission of about 10 mA/cm² (for a voltage of 1 V/micron: I-V measurements). These results are competitive with the best results reported by Saito, Carbon 38 (2000) 169. We continued the study of the stability of the emitted current, which is a very important constraint for the proposed applications. We also repeated the measurements of the emitted current for samples obtained using different synthesis conditions. We started sample purification procedures using nitric acid.

Fourier Transform Infra Red (FTIR) characterization of the nano-AlN samples produced in collaboration with the Univ. of Pune were performed for both mid-IR (600 - 4000 cm⁻¹) as well as far-IR (200 - 600 cm⁻¹). MIR gives an insight into the molecular structure through the specific vibrational frequencies; whereas the FIR domain probes the phonon modes and consequently the long range periodicity of the 1-D crystalline structure. Extensive FTIR studies were carried out at the SINBAD facility (the synchrotron radiation IR beamline at DAΦNE) for three different samples. The samples studied were: Samples containing a high concentration of nanotubes/nanocoils; Samples containing a high concentration of nanoparticles; Commercially obtained bulk (micron sized) AlN powder (for comparison between nano and bulk characteristics). The transmission spectra were recorded for the samples for both room temperature as well as low temperature (LN₂). The analysis of the results is in progress.

A large part of the interest involved with carbon nanotubes, is due to the fact that they can be used as a main constituent of composite materials characterized by exceptional mechanical and electrical properties, very suitable for aerospace applications, due to their light weight, mechanical strength and flexibility. Recent results we obtained in collaboration with the Aerospace Engineering School at the Univ. Rome La Sapienza and the industrial Center for the development of materials (CSM), concerning our measurements of the electrical and mechanical properties (resilience and Young Modulus, conductivity) of a polymer matrix, reinforced with carbon nanotubes synthesized by arc discharge. Stress and numerical analysis of aerospace structures using carbon nanotubes reinforced composite materials were obtained by us. The evaluation of the reduction weight of a typical aerospace structure has also been carried out.

Nanomaterials are being developed for medical and biotechnological applications including gene delivery, drug delivery, enzyme immobilization, and biosensing. The most commonly used materials are gold, silica and semiconductors. Silica nanoparticles have been widely used for

biosensing and catalytic applications due to their large surface area to volume ratio, straightforward manufacture, and the compatibility of silica chemistry with covalent coupling of biomolecules. A key challenge in nanotechnology is the more precise control of nanoparticle assembly for the engineering of particles with the desired physical and chemical properties. Much research is currently focused on new CNT composite materials, such as CNTs with a thin surface cover or CNTs bound to nanoparticles, in order to tailor their properties for specific applications. We obtained, in collaboration with the Univ. of Roma Tor Vergata, the Policlinico of Tor Vergata and the Burnham Institute, a novel tunable approach for the synthesis of carbon nanotube-silica nanobead composite structures; control of nanotube morphology and bead size, and the versatility of silica chemistry, make these structures an excellent platform for the development of biosensors, optical, magnetic or catalytic applications.

3 Level of leadership in the international context, competing experiments:

In SWNT synthesis and field emission studies, we confirmed that our experimental parameters are in line with the best achievements in the international community active on this topic. Our group organizes since 2000 a series of international meetings in the area of nanotechnology www.lnf.infn.it/conference/nn2004. Part of the yearly event consists in a school dedicated to training of Ph.D. students and young postdocs in the basics of nanoscience. Also, our group in Frascati has been selected as the host of the 2004 international conference on relativistic channeling and coherent phenomena in strong fields www.lnf.infn.it/conference/rc2004.

4 Potential relevance for other INFN experiments:

The enhancement in the efficiency and stability of directional electron emission in cold cathodes, for the production of interesting electron sources, at low cost and with a long lifetime. Potential applications of field emitters producing a stable current of low energy electrons can have a big impact on the monitoring of purity of the liquid Ar inside neutrino detectors (such as for the ICARUS or the OPERA experiments). As it is well known, there are methods developed for measuring the electronegative contamination of liquid Ar, based on the transport of electrons emitted from a metallic photocathode (see G. Carugno, et al., Nucl. Instr. Meth. A 292, 580 (1990)). In principle, one could replace the emitters with low-cost C nanotube based ones, measuring the purity through the observed ratio of collected to emitted charges, as in the standard case. We started in 2004 to develop this application in collaboration with ICARUS research group at the Univ. of L'Aquila. Also, our results based on field emission effects from C nanotubes can be useful for benchmarking with other techniques developed at INFN, based on high temperature diamond emission (ad es. DIAMANTE3). C nanotube based table-top low-energy X-ray sources can be of interest for groups with an interest in national security, artistic and archeological patrimony protection, biomedical and environmental applications. A study of the toxicity of nanotubes is in progress in collaboration with the Univ. of Roma Tor Vergata, the Policlinico of Tor Vergata and the Burnham Institute. This research is carried out in collaboration with the INFN Servizio Medicina del Lavoro.

5 Potential relevance for other scientific disciplines:

Production of micro and nanostructured films, as promising candidates for producing X-ray sources and gas discharge tubes, for potential applications in radiotherapy, biomedical applications and structural applications for aerospace research.

6 Impact for applied research and industrial applications:

Our activity attracts interest from collaborating enterprises, including large companies (VARIAN, CSM) which are world leaders in their fields (vacuum technology, sensors), as well as SME (HITESYS) with an eminent position in the market of electro-medical devices.

7 List of Conference Talks by LNF Authors in Year 2004

1. S. Bellucci, "Channeling in Micro- and Nano-structures for Micro- and Nano-beams and New Radiation Sources", International Workshop on Interactions between Nanostructure and Particle Beams, Shanghai, 11 March 2004.
2. S. Bellucci, "Testing the X-rays production from crystal undulators at positron facilities", 9th Topical Seminar on Innovative Particle and Radiation Detectors, Siena, 26 May 2004.
3. S. Bellucci, "Nanotubes of Aluminium Nitride: Synthesis and study of properties", Institute Laue-Langevin, Grenoble, 14 June 2004.
4. S. Bellucci, "Electrical properties of carbon nanostructures", First Symposium on Developments in Nanotechnology: Defense Applications, Rome, 30 June 2004.
5. S. Bellucci, "Carbon Nanotube based Field Emitters for Vacuum Gauges", IUVSTA meeting, Venice, 1 July 2004.
6. S. Bellucci, "Carbon Nanotubes: Physics and Applications", International Conference on Defects in Insulating Materials, Institute of Solid State Physics, Univ. Riga, 16 July 2004.
7. S. Bellucci, "Carbon Nanotubes and Semiconducting Nanostructures: current views and future perspectives", CANEUS Conference, Monterey, 1 November 2004.
8. S. Bellucci, "Composite materials based on carbon nanotubes for aerospace applications", International Conference on Experimental Mechanics, Singapore, 29 November 2004.
9. S. Bellucci, "New Radiation Sources from Channeling in Micro- and Nano-structures", International Conference on Experimental Mechanics, Singapore, 30 November 2004.

References

1. C. Balasubramanian, et al., Chem. Phys. Lett. 383, 188 (2004).
2. S. Bellucci, J. Gonzalez, P. Onorato, Phys. Rev. **B** 69, 085404 (2004).
3. S. Bellucci, V. Biryukov, A. Cordelli, "Channeling of high-energy particles in a multi-wall nanotube", con Phys. Lett. **B** (in press).
4. S. Bellucci, V. Biryukov, "From bent crystals to nanostructures", Cern Courier 44 N6, 19 (2004).
5. S. Bellucci, S. Bini, G. Giannini, V.M. Biryukov, G. I. Britvich, et al., "Crystal Undulator As A Novel Compact Source Of Radiation" Phys. Rev. ST Accel. Beams 7, 023501 (2004).
6. S. Bellucci, V.M. Biryukov, A.G. Afonin, et al., "Accelerator Tests of Crystal Undulators", presented at the NATO ARW "Advanced Photon Sources and Their Application" (Nor Hamberd, Armenia August 29 - September 02, 2004), physics/0412159.
7. S. Bellucci, "Nanotubes for Particle Channeling, Radiation and Electron Sources", Nucl. Instr. Meth. **B** (in press).
8. S. Bellucci, "Testing the X-rays production from crystal undulators at positron facilities", 9th Topical Seminar on Innovative Particle and Radiation Detectors (Siena, 23-26 May 2004), Nucl. Phys. **B** (Proc. Suppl., in press).

9. S. Bellucci, "Carbon Nanotubes: Physics and Applications", *Physica Status Solidi* (c, in press).
10. S. Bellucci, "New Radiation Sources from Channeling in Micro- and Nano-structures", Proc. of the International Conference on Experimental Mechanics, (Singapore, 29 November - 1 December 2004).
11. S. Bellucci, "Channeling in Micro- and Nano-structures for Micro- and Nano-beams and New Radiation Sources", Proc of the International Workshop on Interactions between Nanostructure and Particle Beams, Shanghai, 11-13 March 2004.
12. S. Bellucci, "Carbon Nanotube based Field Emitters for Vacuum Gauges", Proc. of the IU-VSTA meeting (Venice, 28 June - 2 July 2004).
13. S. Bellucci, C. Balasubramanian, F. Mancia, M. Marchetti, M. Regi, F. Tombolini, "Composite materials based on carbon nanotubes for aerospace applications", Proc. of the International Conference on Experimental Mechanics, (Singapore, 29 November - 1 December 2004).
14. S. Bellucci, "Carbon Nanotubes and Semiconducting Nanostructures: current views and future perspectives", Proc. of the CANEUS Conference, (Monterey, 1-5 November 2004).
15. S. Bellucci, "Positron Facilities Tests of the X-Rays Produced by Crystalline Undulators", *Mod. Phys. Lett. B* (in press).
16. M. Bottini, L. Tautz, H. Huynh, E. Monosov, N. Bottini, M. I. Dawson, S. Bellucci and T. Mustelin, "Covalent decoration of multi-walled carbon nanotubes with silica nanoparticles", *Chemical Communications* (in press).

MIVEDE2

M. Pallotta (Resp.), M. Caponero (Ass.)

1 Aim of the experiment

The aim of MIVEDE2 is to apply optical fiber sensing techniques for permanent and real-time structural and geometrical monitoring of large civil engineering structures, with particular reference to highway and railway bridges. MIVEDE2 proposes to use FBG type optical fiber sensors because of their long term signal stability and chemical endurance, that make them suitable for embedding within concrete castings, resin matrixes and gluing layers. Experience in the use of FBG sensors for permanent and real-time monitoring was gained within the research activity carried out for the previous experiment MIVEDE, devoted to high resolution metrological survey of HEP vertex detectors. MIVEDE2 will allow the development of structural and geometrical monitoring techniques based on a large number of FBG sensors distributed on large volume structures, that are of potential great interest for large scale HEP devices, with particular reference to linear and ring accelerators.

2 2003 Activity

In 2003 the activity of MIVEDE2 has been devoted to the project planning and to the testing of a distributed FBG sensor system composed of 24 sensors, installed on the 1.6Km long bridge on the Po river of the A21 Torino Brescia Italian Highway. The FBG sensor system is intended for overall health monitoring of critical bridge structures with early damage detection capabilities. The bridge is a concrete structure, and sensors are applied on various rebar components. The sensors were installed directly on the rebars, adopting a special technique specifically developed for permanent concrete embedding. MIVEDE2 developed the specific algorithms applied to carry out the remote continuous monitoring of the structures, with real time acquisition of the dynamic and quasi-static deformations inferred by both the road traffic and the daily and seasonal thermal variations.

3 2004 Activity

In 2004 the activity of MIVEDE2 has been devoted to enhancing the algorithms developed for monitoring the structural integrity of the bridge structures. The enhanced technique is based on the analysis of the FBG signals in the frequency domain, to detect resonance frequency shifts in the long-term acquired data¹⁾. Moreover, the analysis of the FBG signals in the time domain, based on peak amplitude thresholds control, provides real-time information about overstressing or structural collapse. Finally, the enhanced analysis technique also allows the evaluation of the speed of the transiting vehicle, based on time gradient analysis of amplitude analysis of FBG data. In order to characterize time endurance of both FBG sensor and the techniques adopted for their bonding to the monitored structures, MIVEDE2 has performed extensive aging test by use of specimens subject to hydro-thermal cycling in chemically aggressive atmosphere. Results confirm that reliable monitoring can be assumed for tens of years even in the most severe expected environment.

References

1. M.A. Caponero, D. Colonna, M. Gruppi, M. Pallotta, R. Salvatori, "Use of FBG Sensors for Bridge Structural Monitoring and Traffic Control", in Second European Workshop on Optical Fibre Sensors; J. M. Lopez-Higuera, B. Culshaw Eds.; Proc. SPIE Vol. 5502, p. 480-483, (2004).

POLYX

G. Cappuccio (Res. Ass.), G. Cibin (Ass.), S. B. Dabagov (Art. 23), A. Esposito,
D. Hampai (Osp.), A. Marcelli, V. Sessa (Osp.), C. Veroli (Osp.),
M. A. Kumakhov, R. V. Fedorchuk.

Participant Institutions:

Italy: INFN - LNF, INFN - Milano Bicocca
CNR - ISMN, Istituto per lo Studio dei Materiali Nanostrutturati, Roma
CNR - IPCF, Istituto Per i Processi Chimico Fisici, Pisa
Dip. Scienze e Tecnologie Chimiche, Univ. 'Tor Vergata', Roma
Russia: P. N. Lebedev Physical Institute, Moscow
IRO - Institute for Roentgen Optics, Moscow
Switzerland: Unisantis S.A., Geneva

1 Introduction

The POLYX project for the research and development of polycapillary optics in X-ray applications, previously supported by INFN Gr. V, is in progress due to a collaboration between the Institute for the Study of Nano-structured Materials of the National Research Council (ISMN-CNR) and LNF, in the framework of the MIUR project: "Impianti innovativi multiscopo per la produzione di radiazione X ed ultravioletta" - Legge 449/97.

2 Activities in 2004

Accordingly with the above, during the 2004 the basis for an X-ray optical laboratory was set up. To fulfill the safety regulations imposed by the LNF Radiation Protection Group, a special large cabinet with lead windows, supported by a solid table (Fig. 1), was designed by our team and manufactured by the OET¹ firm. A heavy "research grade" optical table is placed inside the cabinet on four pneumatic supports in order to damp vibrations. A range of instruments can be logged on rack unit holders under the table. On the optical table, inside the cabinet, a low power X-ray source, i.e. a 50 W Cu tube with air-cooling systems, is fixed on an optical rail. A scintillation detector with a FET preamplifier, a H.V. power supply, counting electronic equipment, and various optical holders complete the system. The optical bench inside the cabinet will be used to characterize and test X-ray optics with special attention paid to polycapillary lenses. For the optics alignment along the source-detector axis, the polycapillary lenses will be fixed at the center of a gimbal mount supported by a xyz platform. All the cinematic movements are remotely controlled through linear actuators, using an "ad hoc" software program.

To evaluate the lens parameters (focal points, gain, etc.) an original program, named "PolyCAD", was developed and is continuously upgraded (Fig. 2). This program, written in FORTRAN, allows us to compare the image shape experimentally collected at the focal plane with the theoretical one. A review of the results was presented during the second "International Conference on X-Ray and Neutron Capillary Optics", held in September 2004 at Zvenigorod, Russia.

In November 2004, our group also organized the International Workshop "Channeling 2004", at Frascati. Sixty-six people from the USA, Russia, China, Central and East Europe attended the meeting. The workshop was a success and greatly appreciated by all the participants, many of whom were leading experts in the research field. The workshop contribution will be published as a special issue of SPIE Proceeding Series.

¹Officina Elettrotecnica di Tenno , Via Duina 5, 38077 Bleggio Inferiore (Tn) - Italy.



Figure 1: Cabinet with a “research grade” optical table to be used for characterization of different kind of X-ray optics.

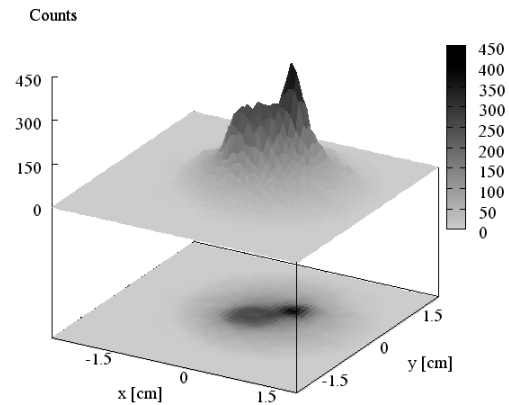


Figure 2: X-ray intensity distribution beyond cylindrical polycapillary. The image is a 2D and 3D reconstruction of an X-ray beam impinging on two spheres located at different distance from the optics entrance.

3 Activity in 2005

The year 2005 will see the start a systematic complete characterization of many of the polycapillary optics supplied by the Institute for Roentgen Optics through the “Unisantis” company. After a test period, a special lens designed for micro-diffraction experiments will be mounted on the X-ray diffraction station, which is operative at the “Laboratory Dafne Light”. In the framework of the CNR-MIUR Project, in collaboration with the Institute for the Chemical Physics Processes (IPCF) at Pisa, polycapillary half-lenses will be used to convert the divergent X-ray beam, coming from an X-ray plasma source, into a parallel beam. If this optical match is successful, the source-lens configuration will be utilized in 2006 for X-ray microscopy experiments in collaboration with the Physics Department of the University “Milano Bicocca”.

References

1. D. Hampai, S. B. Dabagov, G. Cappuccio, Preprint INFN - LNF **04/3 (IR)**, 1-11 (2004).
2. G. Cappuccio, S. B. Dabagov, D. Hampai, V. Sessa, C. Veroli, *Quaderni di Ottica e Fotonica* **11**, 133-139 (2004).
3. D. Hampai, S. B. Dabagov, G. Cappuccio, *Quaderni di Ottica e Fotonica* **11**, 188-193 (2004).
4. P. Cacchio, R. Contento, C. Ercole, G. Cappuccio, M. P. Martinez, A. Lepidi. *Geomicrobiology Journal* **210**, 497-509 (2004).
5. D. Hampai, S. B. Dabagov, G. Cappuccio and G. Cibirin, *Proceedings of Spie, International Conference on X-Ray and Neutron Capillary Optics (Zvenigorod, Russia, September 22-26 2004)*, (in press).
6. D. Hampai, S. B. Dabagov, G. Cappuccio and G. Cibirin, *Proceedings of Spie, Channeling 2004 (Frascati, Italy, November 2-6 2004)*, (in press).

SAFTA2

D. Alesini (Art. 2222), V. Fusco (Dott.), M. Migliorati (Ass.),
A. Mostacci (Ass.), L. Palumbo (Ass.), B. Spataro (Resp.),
M. Zobov (Art. 2222)

1 Aim of the experiment

The aim of SAFTA2 group is mainly related to the study of the electromagnetic interaction between a particle beam and the accelerator beam pipe, the generation of the parasitic fields, the related energy loss and the instability effects. The main investigation subjects are: the coupling impedance of the LHC and SPS machines and the realization of a standing wave accelerating structure. The first activity, done in collaboration with AB/ABP group at CERN, consists of estimating the longitudinal and transverse coupling impedance budget of the LHC and SPS rings in order to evaluate the instability thresholds. Results obtained from simulations have been cross-checked with analytical estimations, and, whenever possible with experimental results. The second activity has been the design, realization and measurements of a prototype compact standing wave accelerating structure operating at 11 GHz to be used for linearizing the longitudinal phase space in the Frascati Linac Coherent Light Source (SPARC).

2 2004 Main results

The energy losses, the parasitic resonances, the longitudinal and transverse impedances of several beam components, and the standing wave accelerating structure have been studied with the MAFFIA3D, HFSS, ABCI, OSCAR2D and SUPERFISH codes.

The Cold to Warm transition of the SPS machine (COLDEX section) with different geometries, shapes and holes has been studied. The analysis of the results suggested an optimization of the design in order to obtain acceptable values of the coupling impedance and energy loss. The first measurements performed with LHC type protons showed large heat load dissipated onto cold bore and beam screen.

The numerical calculations have been carried out by using the MAFFIA3D code in time domain and by performing the Fourier transform of the wake potentials for the impedance estimations.

The numerical estimations of the coupling impedance have been compared to a theoretical model showing a good agreement. From the impedance study it resulted that the power losses into COLDEX due to the impedance seen by the beam is negligible as compared to the measured value. The measured heat load is therefore attributed to the presence of an electron cloud activity which appears above a given bunch current threshold inside the COLDEX beam screen.

In order to strongly reduce the heating of cold/warm section, the change of the shape, sizes and holes of the previous installed vacuum chamber inside SPS machine was required. Numerical studies and experimental activity gave no specific problem for the SPS machine operation. Moreover, additional studies to evaluate the longitudinal broad-band impedance and parasitic resonances on the symmetric and asymmetric collimators with no tank and tapers have also been performed. In this last subject an optimization has been proposed about the tapered vacuum chamber of the IP4 region of LHC where the synchrotron radiation monitor will be installed.

The SAFTA2 group has been invited to participate at the first Care HHH-APD-Workshop organized by CERN and held at Geneve, 8-11 November 2004. In particular, the SAFTA2 group presented a poster regarding the coupling impedance of the SPS machine components, A. Mostacci presented an invited talk on the impedance measurements and simulations, L. Palumbo was the

coordinator of the panel discussion on the instabilities and M. Zobov was member of the panel discussion on the impedance and instabilities.

Concerning the linear accelerating structure operating on π mode at a frequency $f = 11.424$ GHz a prototype in copper was realized. The section constituted by 9 cells was designed to obtain a 5 MeV accelerating voltage. To feed the structure there are two lateral antennas, each one at the end cavity, and a waveguide coupling (coaxial-transition) or coupler in the central cell. Then, in each cell a tuner is inserted in order to properly tune the frequency of the operating mode.

Calculations for the 2D profile design have been carried out using the e.m. codes SUPERFISH, OSCAR2D while the coupler has been designed using HFSS code.

The antennas allow to excite and characterize all the electromagnetic configuration (structure modes) and mostly those of the dispersion diagram of our concern. The coupler allows to feed the section in high power and to get a better isolation of the π mode respect to the closest one.

At room temperature, bead-pull measurements with the perturbation method of the relevant RF parameters are in good agreement with the numerical results.

As an example, in Fig. 1 we report the measurement setup. The measured frequency spectrum by feeding the section with the lateral antennas is illustrated in Fig. 2 and the corresponding one by exciting the section with the coupler is shown in Fig. 3.



Figure 1: *RF measurement set-up.*

It is worth noticing that when we excite the structure with the coupler, we observe only 5 over 9 possible modes of the diagram dispersion because of a non-zero field in the coupling cell. On the contrary, by feeding the structure from the antennas, we excite all 9 modes of the dispersion curve. Additional measurements as the electric field flatness, the loaded quality factor Q_l , the structure form factor R/Q where R is the longitudinal shunt impedance are in progress.

3 Activity 2005

The continuation of the successful collaboration with the AB/ABP group of CERN is foreseen in order to study other components of the LHC chamber under definition. In particular, the colli-

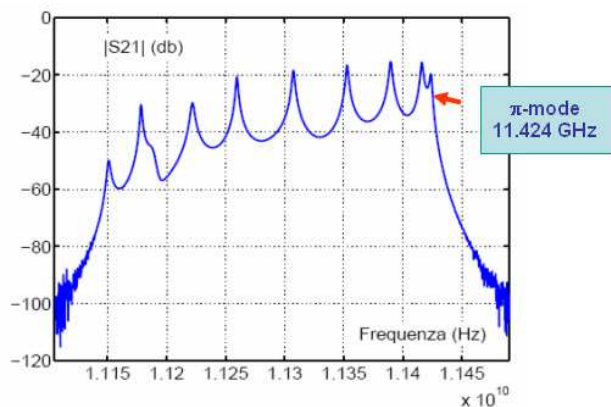


Figure 2: *Detection of the structure modes with an antenna.*

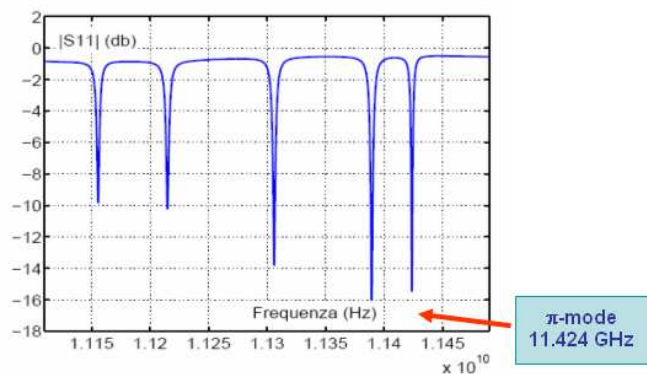


Figure 3: *Detection of the structure modes with the input coupler.*

mators behavior and the whole vacuum chamber where the SRM (synchrotron radiation monitor) will be installed, will be investigated in detail.

References

1. B. Spataro, M. Migliorati, A. Mostacci, L. Palumbo, F. Ruggiero, “Coupling impedances of the LHCb recombination chamber (IR8)”, LHC Project Note 348, 17 June 2004.
2. A. Mostacci, L. Palumbo, B. Spataro and F. Caspers, “RF coupling impedance measurements versus simulations”, CARE-HHH-APD- WORKSHOP, Geneve 8-11 November 2004.
3. B. Spataro, D. Alesini, M. Migliorati, A. Mostacci, L. Palumbo, F. Ruggiero, “Cold to warm transition impedances in the SPS machine”, CARE-HHH-APD-WORKSHOP, Geneve 8-11 November 2004.
4. K. L. Bane, K. Oide, M. Zobov, “Impedance calculation and verification in Storage Rings”, CARE-HHH-APD-WORKSHOP, Geneve 8-11 November 2004.

5. M. Ferrario, V. Fusco, S. Guiducci, B. Spataro, M. Migliorati and L. Palumbo, "Wake fields in the Sparc Linac", WORKSHOP on Charged and Neutral Particles Channeling Phenomena, Frascati (Rome) Italy, November 2-6, 2004.
6. A. Bacci, M. Migliorati, L. Palumbo, B. Spataro, "An X-band structure for a longitudinal emittance correction at Sparc", LNF-03/008(R), 6 Maggio 2003.
7. R. Bartolini, C. Bruni, M. E. Couprie, G. Dattoli, L. Giannessi, D. Garzella, L. Mezi, M. Migliorati, G. Orlandi, A. Renieri, "Saturation and electron-beam lifetime in a storage ring free-electron laser", **Physical Review**, E 69, 036501 (2004).
8. D. Alesini, *et al.*, (The SPARX Study Group), "Status of the SPARC project", **Nuclear Instruments and Methods in Physics Research**, A 528 (2004), pp. 586-590.
9. G. Dattoli, M. Migliorati, H. M. Srivastava, "Some families of generating functions for the Bessel and related functions", **Georgian Mathematical Journal**, Vol 11, N. 2 (2004), pp. 219-228.
10. D. Alesini, R. Boni, A. Gallo, F. Marcellini, M. Migliorati, L. Palumbo, M. Zobov, "Third harmonic cavity design and RF measurements for the Frascati DAΦNE collider", **Physical Review Special Topics - Accelerators and Beams**, 7, 092001 (2004).
11. G. Dattoli, M. Migliorati, H. M. Srivastava, "A class of Bessel summation formulas and associated operational methods", **Fractional Calculus & Applied Analysis**, Vol 7, N. 2 (2004), pp. 169-176.
12. G. Dattoli, L. Mezi, M. Migliorati, "An operational solution for the motion equation of bodies in non-inertial frames", **Il Nuovo Cimento**, Vol. 119 B, N. 6 (2004), pp. 565-569, anche ENEA (ISSN/0393-3016), RT/2004/23/FIS.
13. M. Biagini, M. Boscolo, M. Ferrario, V. Fusco, L. Giannessi, S. Guiducci, L. Mezi, M. Migliorati, M. Quattromini, C. Ronsivalle, J. B. Rosenzweig, C. Sanelli, L. Serafini, F. Tazzioli, C. Vaccarezza, "SPARC photoinjector working point optimization, tolerances and sensitivity to errors", European Particle Accelerator Conference 2004, pp. 396-398, Lucerne, Switzerland, July 2004, anche SPARC-GE-04/001, Frascati, 13 Luglio 2004.
14. D. Alesini, *et al.*, (The SPARX Study Group), "Status of the SPARC project", European Particle Accelerator Conference 2004, pp. 399-401, Lucerne, Switzerland, July 2004, anche SPARC-GE-04/001, Frascati, 13 Luglio 2004.
15. M. Ferrario, V. Fusco, M. Migliorati, L. Palumbo, B. Spataro, "Wake fields effects in the SPARC photoinjector", European Particle Accelerator Conference 2004, pp. 405-407, Lucerne, Switzerland, July 2004, anche SPARC-GE-04/001, Frascati, 13 Luglio 2004.

SI-RAD

L.Bongiorno (Ass. Ric.), G.Mazzenga (Tecn.), M.Ricci (Resp.), B.Spataro

Participant Institutions:

ITALY: INFN LNF, Firenze, Roma2, Trieste

RUSSIA: MePhi, IBMP, RKK"Energiya" (Moscow)

SWEDEN: KTH (Stockholm)

1 Introduction

The SI-RAD experiment is a continuation of the activity that the Collaboration has carried out for the experiments SIEYE1 and SIEYE2 on board the Russian Space Station MIR and SIEYE3/ALTEINO on board ISS in the years 1995-2002 ^{1, 2, 3, 4, 5, 6, 7, 8, 9}. SI-RAD will be installed on board the International Space Station (ISS) to study and monitor the radioactive environment internally and externally of ISS. At the same time, the investigation, with a more sophisticated instrument, of the "Light Flashes" phenomenon ¹⁰, will be conducted to improve and refine the results obtained with the previous SIEYE experiments. The instrument will consist of a 16-plane tower of double-sided silicon detectors (8x8 cm² area) equipped with trigger and anticoincidence counters. The total weight is 13 kg and the total power consumption should not exceed 30 W. The experimental program will be completed through three steps by the construction of a laboratory prototype model, an engineering model and the final flight, space qualified model. The activity in 2004 has been focused on the parallel development of the following systems of the engineering model:

- Trigger system.
- Study on Silicon Photomultiplier (SI-PM) technology for space applications.
- Design and realization of a highly integrated silicon board (16 cm x 16 cm).
- Realization and test of a low-power, low-mass Digital Processing Unit (DPU).

In 2005, the planned activity includes the completion of the flight unit equipped with autotrigger capabilities for heavy nuclei and a trigger for crossing protons and nuclei. The interface with the ISS Space Station will be realized with an intermediate CPU to manage the telecommands from ground and the download of the data.

2 Activity of the LNF group

The LNF group has taken the responsibility of the design, construction and test of the mechanical structures and interfaces of the three models of the detector contributing also to the integration of the mechanical support for the DAQ. This activity is carried out with the support of the LNF Service of Development and Construction of Detectors (SSCR). The activity in 2004 has been mainly devoted to the mechanical support of the engineering model and to the interfaces of the front-end and DAQ with the detector. The LNF group also participates in the beam test activities at GSI/Darmstadt and TSL/Uppsala having the responsibility of the beam trigger counters.

3 Publications in 2004

- 1) “The ALTEA/ALTEINO projects: studying functional effects of microgravity and cosmic radiation; L.Narici *et al.*, Adv. Space Res. **33** (2004) 1352.

References

1. G.Furano *et al.*: “Measurement of Nuclear Mass Distribution of Primary and Recoil Heavy Ions inside MIR Space Station with SilEye Silicon Detector”, Proc. XXVI ICRC, Salt Lake City **Vol.5** (1999) p. 128.
2. S.Avdeev *et al.*: “The SilEye nuclei cosmic ray and eye light flash experiment onboard the Mir Space Station”, Proc. XXVII ICRC, Hamburg (2001) p. 1745.
3. M.Casolino *et al.*: “Cosmic ray measurements on board space station MIR with SILEYE-2 experiment”, Proc. XXVII ICRC, Hamburg (2001) p. 4011.
4. V.Bidoli *et al.*: “In-flight performances of SilEye-2 Experiment and cosmic ray abundances inside space station MIR”; Journal of Physics G: Nuclear and Particle Physics **27**(2001) 2051.
5. S.Avdeev *et al.*: “Eye light flashes on the Mir Space Station”; Acta Astronautica, **50** (2002) 511.
6. L.Narici *et al.*: “The ALTEA facility on the International Space Station”; Physica Medica Suppl. 1 **17** (2001) 255.
7. M.Casolino *et al.*: “The Sileye/3-Alteino experiment on board the International Space Station”; Nucl.Phys. **113B** (2002) 88.
8. V.Bidoli *et al.*: “Dual origin of light flashes in space”; Nature **422** (2003) 680.
9. P.Maponi *et al.*: “A syncitium model for the interpretation of the phenomenon of anomalous light flashes occurring in the human eye during space missions”; Nuovo Cim., **116B** (2001) 1173.
10. G. Horneck: “Radiobiological experiments in space: a review”, Nucl. Tracks Radiat. Meas., **20** (1992) 185 .

SUE

E. Burattini (Resp.), A. Grilli (Tecn.), F. Belloni (Bors.), D. Bettega (Ass.), P. Calzolari (Ass.),
F. Malvezzi Campeggi (Ass.), F. Monti (Ass.), L. Tallone (Ass.), S. Crema, L. Doneda.

1 Aim of the experiment

The variation of the ozone layer observed in the last decades can lead to an increase in the UVB component of the solar spectrum transmitted onto the earth surface. Since the biological effectiveness of UV radiation is strongly wavelength dependent, even a low increase in the UVB irradiance can lead to a significant increase of its biological effects, especially at shorter wavelengths. It is then important to evaluate their dependence as a function of the dose at each wavelength. To this aim, in the framework of the SUE (Solar Ultraviolet Effects) experiment, we are carrying out a systematic study of early and delayed biological effects induced in *in vitro* human cell cultures by monochromatic radiation in the UVB band (280÷320 nm) at the UV beamline of the DAΦNE-Light Synchrotron Radiation Facility.

The experimental hutch is equipped with a Jobin-Yvon monochromator where a holographic diffraction grating blazed at 250 nm allows to select photons in the range 200÷600 nm within a 0.1÷0.3% spectral band. The beam travels in air after a 38 mm diameter, 2 mm thick sapphire window and is focussed on the entrance slits of the monochromator by two remotely controlled Al-coated mirrors. Photons of wavelength shorter than 180 nm are not transmitted through the sapphire window, ensuring the absence of higher order contamination in the monochromatic beam at the exit of the monochromator.

The cell cultures are grown on the quartz base (13 mm diameter) of small teflon cylinders. After the exit slits of the monochromator, a suitable sample holder allows to fix the teflon cylinder at the right distance for uniform (within 10%) spatial exposure. The photon distribution at the sample position is determined by microdensitometry on UV sensitive photographic plates.

Dosimetry is accomplished using a calibrated Hamamatsu Silicon photodiode sensitive in the range 200÷1200 nm whose active area is 1 cm². Before irradiation, at each wavelength, the power and the irradiance on the sample per unit of the current circulating in the DAΦNE electron ring are determined. During irradiation, the circulating current $I(t)$ is continuously monitored and the dose is calculated as the irradiance per unit of the circulating current multiplied by the $\int I(t)dt$. The linearity of the photodiode response versus the circulating current has been verified in the range 0.1÷1A.

In the five irradiation sessions performed, cultures of human hybrid cells CGL1 (HeLa x human skin fibroblast) were exposed to monochromatic beams of four different wavelengths (285, 292, 295 and 300 nm) in the dose range between 5 and 100 J/m². The power on the sample area per unit of the circulating current in a 2.5÷3 nm bandwidth went from around 4 mW/A during the first three sessions up to around 8 mW/A in the last sessions, hence allowing to do measurements at 300 nm and at higher doses; the average irradiance during an exposure was 20 mW/m² and 40 mW/m², respectively. Treatment of the cell cultures after irradiation is performed at the Radiobiology Laboratory of the Department of Physics of the University of Milan. Three

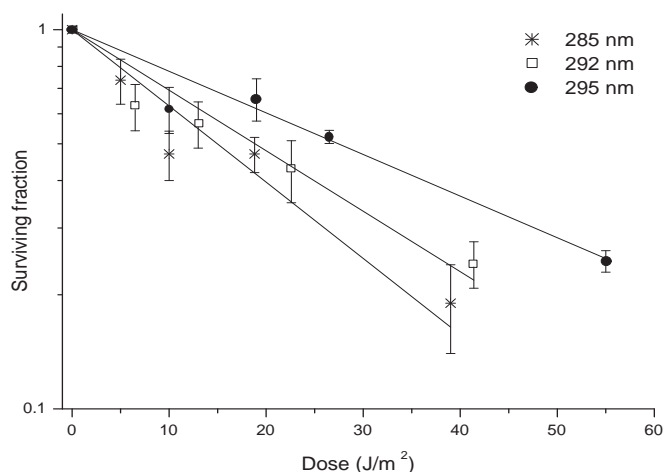


Figure 1: *Survival of the irradiated cells vs the dose.*

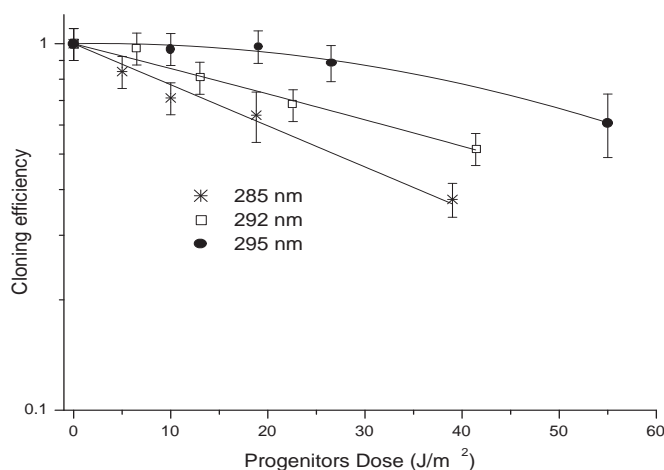


Figure 2: *Cloning efficiency of the survived cells vs the dose.*

different biological effects have been studied as a function of the dose at each wavelength: survival of the irradiated cells, delayed reproductive death (i.e. cloning efficiency of the survived cells) and neoplastic transformation. Data analysis after the last irradiation sessions has still to be completed but it substantially confirms previous results up to 300 nm, i.e.: the radiation effectiveness depends on the wavelength and increases at decreasing wavelength at all wavelengths (Fig.1, Fig.2, Fig.3); the rate at which the radiation effectiveness increases at decreasing wavelength is higher for the two delayed effects (delayed reproductive death and neoplastic transformation) than for the early effect (cell survival) (Fig.4). These results suggest that the action spectrum of UVB radiation may be different for delayed and early biological effects.

2 List of Conference Talks in 2003

1. P. Calzolari, F. Monti, "Studio di Effetti Biologici a Lungo Termine Indotti in cellule umane della linea CGL1 con fasci UVB monocromatici presso la linea UV di Luce di Sincrotrone dei LNF", I Convegno Nazionale della Federazione Italiana per le ricerche sulle Radiazioni-

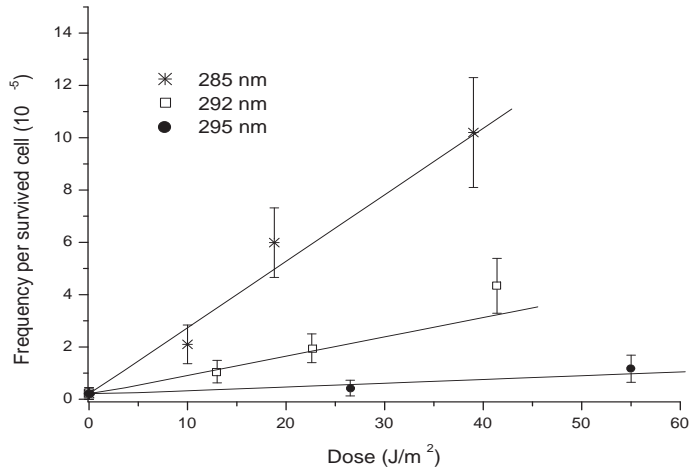


Figure 3: Neoplastic transformation per survived cell vs the dose.

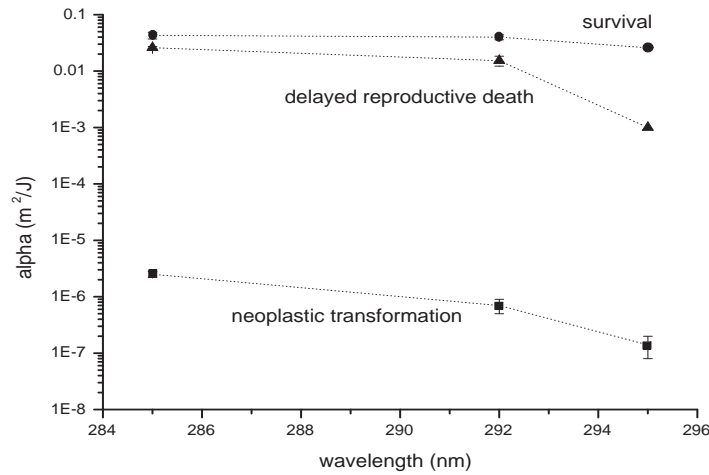


Figure 4: Slope (alpha) of the curves for each biological effect vs wavelength.

Radiazioni in medicina e biologia: stato delle ricerche e applicazioni cliniche.
Legnaro (Padova), 20-22 November 2003.

References

1. Stanbridge *et al.*, *Science* **215**, 252 (1982).
2. J.L. Redpath *et al.*, *Rad. Res.* **110**, 468 (1987).
3. Mendonca *et al.*, *Rad. Res.* **131**, 345 (1992).
4. D. Bettega *et al.*, *Int. J. of Rad. Biol.* **72**, 523 (1997).
5. J. Little *et al.*, *Int. J. of Rad. Biol.* **74**, 663 (1998).
6. D. Bettega *et al.*, *Int. J. of Rad. Biol.* **77**, 963 (2003).

DAΦNE

The DAΦNE Team: D. Alesini, G. Benedetti, M.E. Biagini, C. Biscari, R. Boni, M. Boscolo, A. Clozza, G. Delle Monache, G. Di Pirro, A. Drago, A. Gallo, A. Ghigo, S. Guiducci, M. Incurvati, C. Ligi, F. Marcellini, G. Mazzitelli, C. Milardi, L. Pellegrino, M. Preger, P. Raimondi (Resp.), R. Ricci, C. Sanelli, M. Serio, F. Sgamma, B. Spataro, A. Stecchi, A. Stella, C. Vaccarezza, M. Vescovi, M. Zobov

The DAΦNE Technical Staff: G. Baccarelli, G. Baldini, P. Baldini, A. Battisti, A. Beatrici, M. Belli, B. Bolli, L. Cacciotti, G. Ceccarelli, R. Ceccarelli, A. Cecchinelli, S. Ceravolo, R. Clementi, O. Coiro, S. De Biase, M. Giabbai, M. De Giorgi, N. De Sanctis, R. Di Raddo, M. Di Virgilio, G. Ermini, G. Fontana, U. Frasacco, C. Fusco, F. Galletti, O. Giacinti, E. Grossi, F. Iungo, R. Lanzi, V. Lollo, V. Luppino, C. Marchetti, M. Marchetti, C. Marini, M. Martinelli, M. Masciarelli, A. Mazzenga, M. Monteduro, A. Palleschi, M. Paris, E. Passarelli, V. Pavan, S. Pella, D. Pellegrini, R. Pieri, G. Piermarini, G. Possanza, S. Quaglia, F. Ronci, M. Rondinelli, U. Rotundo, F. Rubeo, M. Sardone, M. Scampati, G. Sensolini, R. Sorchetti, A. Sorgi, M. Sperati, A. Spreccacenero, P. Tiseo, R. Tonus, T. Tranquilli, M. Troiani, V. Valtriani, R. Zarlenga, A. Zolla

1 Introduction

DAΦNE is an “electron-positron factory” operating at Frascati since 1997. Factories are storage rings for electrons and positrons delivering a high rate of mesons to high resolution experiments which require an extremely large number of events. To reach such high rates, the factories are designed to work at the energies of the meson resonances, where the production cross section peaks. To obtain the required production rate it is also necessary that the collider luminosity (the number of events per unit time of the reaction under investigation divided by its cross section weighted by the acceptance of the detector) is very high, between one and two orders of magnitude larger than that obtained in the conventional colliders with a single ring, where electrons and positrons run on the same orbit in opposite directions. When sharing the same ring the two N-bunch trains cross in 2N points and the maximum obtained luminosity is limited by the electromagnetic beam-beam interaction. The unwanted effects of this interaction can be reduced with a very strong focussing (called “low- β ”) at each crossing point, obtained by means of quadrupole doublets or triplets. At the same time these magnetic structures take up much room and excite chromatic aberrations which must be corrected elsewhere in the ring. A large number of bunches can be stored only with twice the number of low- β points and due to the compactness of the DAΦNE machine only two of these regions can be realized, therefore only a single electron bunch and a single positron one could be stored in a single ring.

This limitation does not hold for the double ring option, consisting in two separate rings crossing at two low- β points. The number of bunches that can be stored in such a collider is limited only by the geometry of the IR’s.

DAΦNE is a system consisting of a double-ring collider, a linear accelerator (LINAC) an intermediate damping ring to make injection easier and faster and 180 m long transfer lines connecting these machines. The beam accelerated by the Linac can also be switched into a laboratory called “Beam Test Facility (BTF)”, for dedicated experiments and calibration of detectors. The accelerator complex has been designed to fit into the existing ADONE buildings (ADONE was the 3 GeV center of mass electron-positron collider in operation at LNF from 1969 to 1993); the complex is shown schematically in Fig. 1.

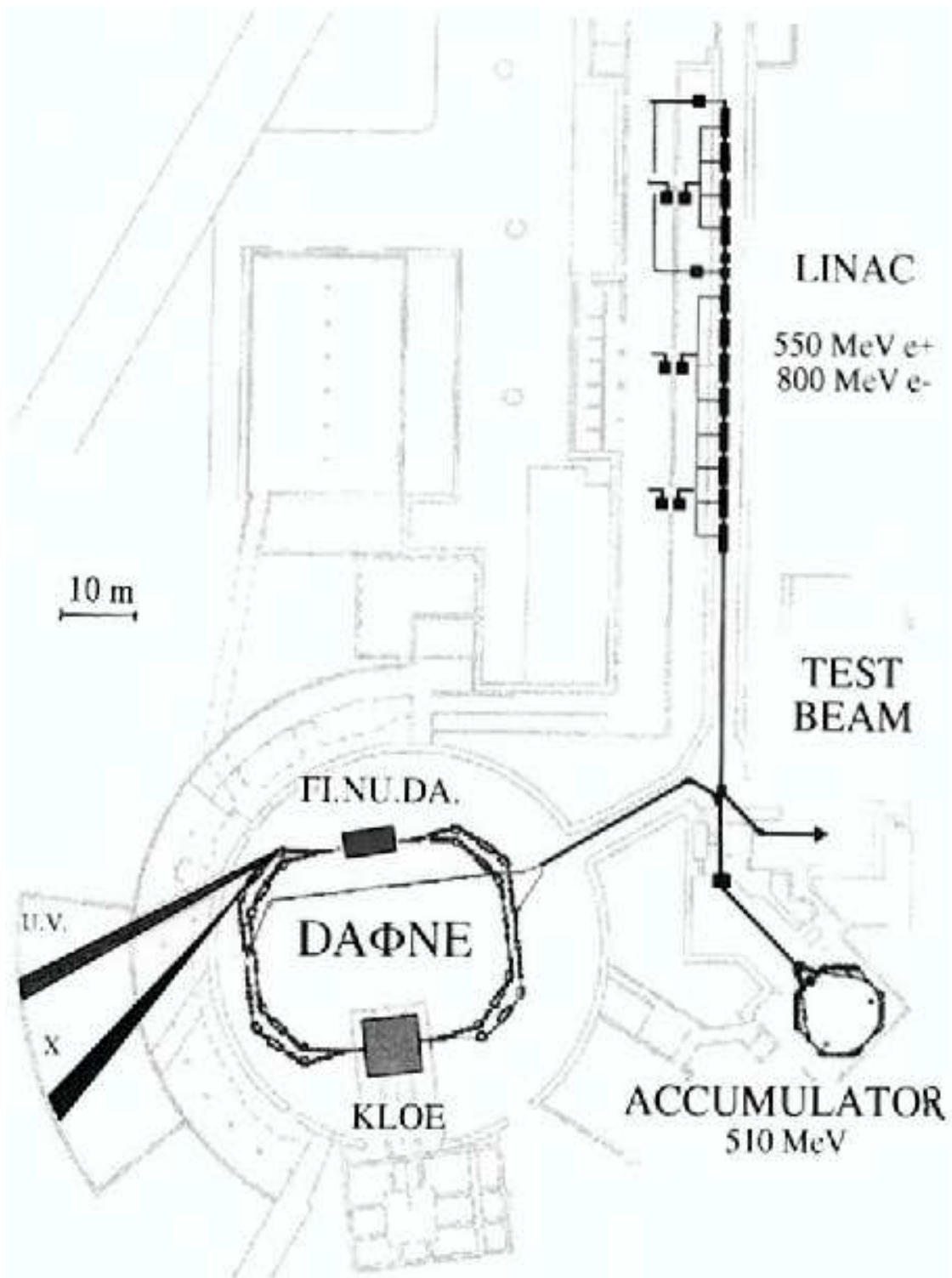


Figure 1: The layout of the DAΦNE accelerator complex inside its buildings.

In the DAΦNE collider the two beam trajectories cross at the interaction point (IP) at an angle of ≈ 1.5 degrees in the horizontal plane. A positron bunch leaving the IP after crossing an electron one will reach the following electron bunch at a distance of half the longitudinal separation between bunches from the IP. Due to the horizontal angle between the trajectories of the two beams, the distance in the horizontal direction between the two bunches is equal to the horizontal angle times half the longitudinal distance between the bunches in the beam. The beam-beam interaction can be harmful to the beam stability even if the distance in the horizontal direction between bunches of opposite charge is of the order of few bunch widths at points where the β function is high and this sets a lower limit on the bunch longitudinal separation and therefore on the number of bunches which can be stored in the collider. For DAΦNE the minimum separation is 80 cm, and the maximum number of bunches to be stored in each ring is 120. This number determines the frequency of the radiofrequency cavity which replaces at each turn the energy lost in synchrotron radiation, which must be 120 times the revolution frequency. The luminosity of the collider can therefore be up to 120 times larger than that obtainable in a single ring with the same size and optical functions.

Crossing at an angle could in principle be a limitation to the maximum single bunch luminosity. In order to make the beam-beam interaction less sensitive to this parameter and similar to the case of single ring colliders where the bunches cross head-on, the shape of the bunches at the IP is made very flat (typical r.m.s. sizes are 30 mm in the longitudinal direction, 2 mm in the horizontal and 0.01 mm in the vertical one).

The double ring scheme with many bunches has also some relevant drawbacks: the total current in the ring reaches extremely high values (5 A in the DAΦNE design) and the high power emitted as synchrotron radiation (≈ 50 KW) needs to be absorbed by a complicated structure of vacuum chambers and pumping systems in order to reach the very low residual gas pressure levels necessary to avoid beam loss. In addition, the number of possible oscillation modes of the beam increases with the number of bunches, calling for sophisticated bunch-to-bunch feedback systems.

The double annular structure of the DAΦNE collider is shown schematically in Fig. 2.

Both rings lay in the same horizontal plane and each one consists of a long external arc and a short internal one. Starting from the IP the two beams travel together inside a common vacuum chamber and their distance increases until it becomes ≈ 12 cm at the level of the magnetic separators called “splitters” (SPL). These are special magnets with two regions of opposite field which deflect the two beams in opposite directions, allowing them to reach the separate vacuum chambers of the long and short arcs. Each arc consists of two “almost achromatic” bends (deflecting the beam by 81 degrees in the short arc and 99 degrees in the long one) similar to those frequently used in synchrotron radiation sources, with a long straight section in between. Each bend consists of two dipoles, three quadrupoles, two sextupoles and a wiggler. This structure is used for the first time in an electron-positron collider and it has been designed for the particular requirements of DAΦNE: the amount of synchrotron radiation power emitted in the wigglers is the same as in the bending magnets and the wigglers can be used to change the transverse size of the beams. The increase of emitted power doubles the damping rates for betatron and synchrotron oscillations, thus making the beam dynamics more stable, while the possibility of changing the beam sizes makes the beam-beam interaction parameters more flexible.

The straight section in the long arc houses the pulsed magnets used to store into the rings the bunches coming from the injection system, while in the short straight arc there are the radiofrequency cavity and the equipment for the feedback systems which are used to damp longitudinal and transverse instabilities.

The most delicate part of the whole structure are the IR's. The collider can host two experiments, even if only one at a time can get useful luminosity. Three detectors have been realized, KLOE, DEAR and FINUDA. KLOE is permanently installed in the first IP, while DEAR and

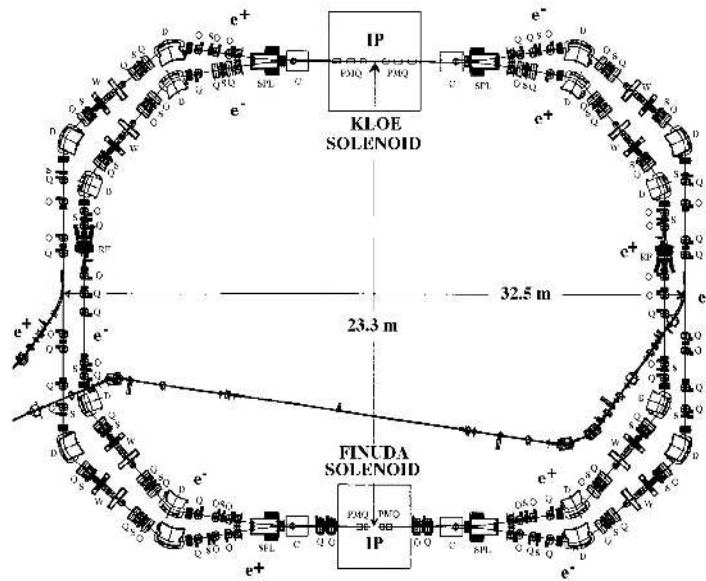


Figure 2: *The DAΦNE Main Rings.*

FINUDA are alternatively running on the second one. The detectors of KLOE and FINUDA are surrounded by large superconducting solenoid magnets for the momentum analysis of the decay particles and their magnetic fields represent a strong perturbation on the beam dynamics. This perturbation tends to induce an effect called “beam coupling”, consisting in the transfer of the betatron oscillations from the horizontal plane to the vertical one. If the coupling is not properly corrected, it increases significantly the vertical beam size leading to luminosity reduction. For this reason a superconducting solenoid magnet with half the field integral of the detector one and of opposite direction is placed near each splitter in such a way that the overall field integral in the IR’s vanishes. However, this is not sufficient to obtain full compensation of the beam coupling induced by the main solenoids. In the case of KLOE the low- β at the IP was originally designed with two quadrupole triplets. Due to the flat shape of the beam at the IP, the low- β is realized only in the vertical plane. The quadrupoles cannot be of the conventional electromagnetic type for two reasons: the first is that the iron of the yoke would degrade the flatness of the magnetic field in the detector and the second is that the overall transverse size of a conventional quadrupole is at least twice its useful aperture. Therefore quadrupoles realized with permanent magnets have been built, which exhibit an excellent field quality, very small transverse size and are fully transparent to external fields. The region of space around the IP occupied by machine elements, which is unavailable for the detection of decay particles by the experiment consists in two cones with the vertex at the IP and a half aperture of only 9 degrees. In order to obtain a good compensation of the above mentioned coupling effects induced by the solenoids, these quadrupoles are rotated around their longitudinal axis by angles between 10 and 20 degrees and are provided with actuators to finely adjust their rotation.

The structure of the FINUDA IR is quite similar. Since its superconducting solenoid magnet has half the length (but twice the field) of the KLOE one, the low- β focusing at the IP is obtained by means of two permanent magnet quadrupole doublets inside the detector and completed with two other conventional doublets outside. Both IR’s have been further modified during the 2003

shutdown.

The DEAR experiment, which was installed on the IR opposite to KLOE, took data during the years 2002-2003. It does not need magnetic field and therefore only conventional quadrupoles were used for the low- β . FINUDA rolled-in at DEAR's place in the second half of 2003 and took data until spring 2004. It was then removed from IP2 in order to run the KLOE experiment with only one low- β section at IP1.

Two synchrotron radiation lines, one from a bending dipole and the other from the wiggler are routinely operated by the DAΦNE-LIGHT group in a parasitic mode, providing to the users radiation from the infrared to soft x-rays.

The vacuum chambers of the arcs have been designed to stand the high level of radiation power emitted by the beams (up to 50 KW per ring): they consist of 10 m long aluminum structures built in a single piece: its cross section exhibits a central region around the beam and two external ones, called the antechambers, connected to the central one by means of a narrow slot. In this way the synchrotron radiation hits the vacuum chamber walls far from the beam and the desorbed gas particles can be easily pumped away. The chambers contain water cooled copper absorbers placed where the radiation flux is maximum: each absorber has a sputter ion pump below and a titanium sublimation pump above.

The single cell copper radiofrequency cavities, one in each ring, are capable of running at 368 MHz and 250 KV and are designed with particular care to avoid high order modes which could induce longitudinal instabilities in the multibunch structure of the beams. This is obtained by means of external waveguides terminated on 50Ω loads. A sophisticated longitudinal feedback has, however, been built to maintain a reasonable safety margin on the threshold of multibunch instabilities. The system is based on the digital signal processing technique and acts on each single bunch individually. Additional feedback systems on the betatron motion have been also realized following the observation of coherent instabilities during collider operation.

The correct superposition of the beams at the IP is of course critical for the luminosity of the ring. For this reason, 46 beam position monitors are available in each ring and 31 small dipoles can be used to steer the beam and correct orbit distortions caused by alignment errors or wrong currents in the magnetic elements by means of sophisticated software procedures implemented in the Control System of the collider. Additional beam diagnostics are two synchrotron radiation outputs, from which the transverse and longitudinal size of the beam can be measured, total beam current monitors and strip-line pickups delivering the charge of each bunch.

In a low energy electron-positron collider, such as DAΦNE, the lifetime of the stored current is mainly limited by the Touschek effect, namely the particle loss due to the scattering of the particles inside the bunches. In the present operating conditions it is of the order of half an hour. It is therefore necessary to have a powerful injection system, capable of refilling the beam without dumping the already stored one. In addition, flexibility of operation requires that any bunch pattern can be stored among the 120 available buckets. The injection system of DAΦNE is therefore designed to deliver a large rate of particles in a single bunch at the working energy of the collider.

It starts from a linear accelerator (LINAC, see Fig. 1) with a total accelerating voltage of 800 MV. Electrons are accelerated to ≈ 250 MeV before hitting a tungsten target (called positron converter) where positrons are generated by bremsstrahlung and pair production with an efficiency of $\approx 1\%$. The positrons exit from the target with an energy of few MeV and are then accelerated by the second section of the LINAC to their final energy of ≈ 0.51 GeV. The positrons are then driven along a transfer line and injected into a small storage ring, called Accumulator, at a frequency of 25 Hz. Up to 19 positron pulses are stacked into a single bucket of the Accumulator, then injection stops and the bunch damps down to its equilibrium beam size and energy spread, which are much smaller than the LINAC ones. Damping takes ≈ 0.1 seconds and then the beam is extracted

from the Accumulator and injected into the positron main ring at an overall repetition rate of 2 Hz. A powerful and flexible timing system allows the storage of any desired bunch pattern in the collider. In the electron mode, the converter is extracted from the LINAC and electrons are directly accelerated to 0.51 GeV and injected into the Accumulator in the opposite direction with respect to positron operation. They are then extracted like in the positron case and injected into the electron main ring through the second transfer line.

The Accumulator has been introduced for the following reasons: the first is that the LINAC can deliver 10 ns pulses with a charge of ≈ 1 nC. Since the design charge of the main ring at the maximum luminosity is $1.5 \mu\text{C}$ and the longitudinal acceptance of the main rings is only 2 ns, the number of pulses necessary to fill the ring is of the order of 10^4 . In order to avoid saturation it is therefore necessary that at each injection pulse a fraction smaller than 10^{-4} of the already stored beam is lost, and this is not easy to achieve. The Accumulator instead can work with a lower frequency RF cavity and therefore with a larger longitudinal acceptance. In this way the full charge coming from the LINAC can be stored. The number of pulses into the Accumulator is only 19, and after damping the whole charge stacked into an Accumulator bunch can be stored into the main ring. In this way a single main ring bucket can be filled with only one pulse from the Accumulator, reducing to 120 the number of injection pulses into each main ring. As an additional benefit, the transverse beam size and energy spread of the beam coming from the Accumulator are at least one order of magnitude smaller than those of the LINAC beam, and this strongly reduces the aperture requirements of the main ring and, as a consequence, the overall cost of the collider.

2 DAΦNE main changes during 2003

During the six months shutdown occurred in 2003 the main machine modifications can be summarized as follows:

- KLOE IR extraction and reassembling according to a modified optics design and vacuum chamber upgrade: the IR lattice was changed from a triplet to a doublet structure in order to have the same low- β^* characteristics while lowering the chromaticity with an overall improvement of the beam lifetime and beam-beam performance. At the same time the increased tunability of the low- β^* lattice allows to double the number of colliding bunches (from 50 to 100) avoiding the parasitic crossings drawback on the luminosity.
- FINUDA detector installation, together with the insertion of a new Be vacuum chamber and four Permanent Magnet (PM) quadrupoles; as for the KLOE IR, the mechanics has been modified in order to allow for full rotation of the PM quadrupoles.
- wiggler magnets modification to increase the width of the good field region and get rid of the high order terms of the magnetic field. The main effect on the beam dynamics is a strong octupole term contribution affecting the dynamic aperture of the ring. A reduction of the octupole term by a factor ≈ 2.5 turned out from the measurements.

Further details of the overall machine modifications performed in 2003 can be found in the previous LNF Activity Report. In the following section the activities carried on during the year 2004 are described in detail.

3 Year 2004 activity

The DAΦNE activity in 2004 has mainly been dedicated to both the FINUDA and KLOE experiments; in summary, the following items have been addressed:

- FINUDA operation up to March 2004 (started on October 2003, $\approx 250pb^{-1}$ delivered);
- removal of the FINUDA detector and IR2 in April 2004;
- KLOE operation start in May 2004 (until the end of 2005, final target $2fb^{-1}$);

3.1 FINUDA Operation

The FINUDA detector was completely installed by the end of July 2003. At the end of the same year the total integrated luminosity delivered to the experiment was $\approx 80pb^{-1}$. By the end of March 2004 $\approx 250pb^{-1}$ were delivered with a peak luminosity of $6 \times 10^{31}s^{-1}cm^{-2}$, and a daily integrated value close to $4pb^{-1}$.

The new lattice for FINUDA operation was designed by taking into account all hardware modifications. Special care has been devoted to the new wiggler model included in the machine optics simulation code. The whole magnet has been described as a sequence of 2 m long hard edge dipoles and straight sections representing the linear part of the beam motion. The non-linear terms have been introduced by adding at both pole sides higher order multipole terms. All the model parameters have been derived from the measurement of the vertical component of the magnetic field in the horizontal midplane, measured on a spare wiggler.

The new KLOE IR gives a smaller contribution to the chromaticity, which is almost corrected in the horizontal plane by an additional sextupole introduced in each wiggler by means of a special reshaping of one terminal pole. The machine model has been validated by comparing its predictions with the beam measurements. Simulations and experimental data are in satisfactory agreement both for the linear part (betatron functions, betatron tunes and dispersion) and for the non-linear one (second order dispersion and second order chromaticity), as can be seen from Fig. 3.

To perform collisions at FINUDA IP, the KLOE solenoidal field ($Bd1 = 2.4 Tm$) is off.

For this operation mode the horizontal beam emittance is smaller by 44% with respect to the previous one ($\epsilon_x = .34 \mu m$), allowing for a separation of $\approx 13\sigma_x$ at the first parasitic crossing, 0.4 m from the IP. The dynamic aperture has been improved by optimizing the relative phase advance between sextupoles. The betatron functions at the IP have been set to $\beta_x^* = 2.33$ m, a reasonable trade off between the need to keep β_x low at the IP and at the first parasitic crossing, and $\beta_y^* = .024$ m, compatible with the limit imposed by the hourglass effect. The horizontal crossing angle at the IP has been set to $\theta_x = .021$ rad which was found to minimize background on the detector.

A local betatron coupling correction has been performed by minimizing the coupling terms extracted from the measured Response Matrix (C matrix) for the two rings. Using the matrix M, as computed from the machine model, that links the IR quadrupole rotation angles to the resulting coupling terms, a linear equation system can be written and solved with the singular value decomposition. After few iterations the rms value of the coupling terms has been reduced by 40% yielding a residual coupling value of $\approx 0.3\%$.

The upgraded wigglers yield a significant reduction of the unwanted high order terms in the field responsible for the quadratic behaviour of the horizontal betatron tune versus beam displacement in the wiggler. Tests with the beams confirmed the reduction of the non-linear terms, as well as an improvement by a factor ≈ 2 in the energy acceptance (see Fig. 4).

At the end of FINUDA operation the machine performance was:

- number of bunches per beam: 100 + 100;
- total current per beam e-/e+: 1.1/0.8 A;
- peak luminosity $\approx 0.6 \times 10^{32}cm^{-2}s^{-1}$;
- average luminosity during runs $\approx 0.3 \times 10^{32}cm^{-2}s^{-1}$;

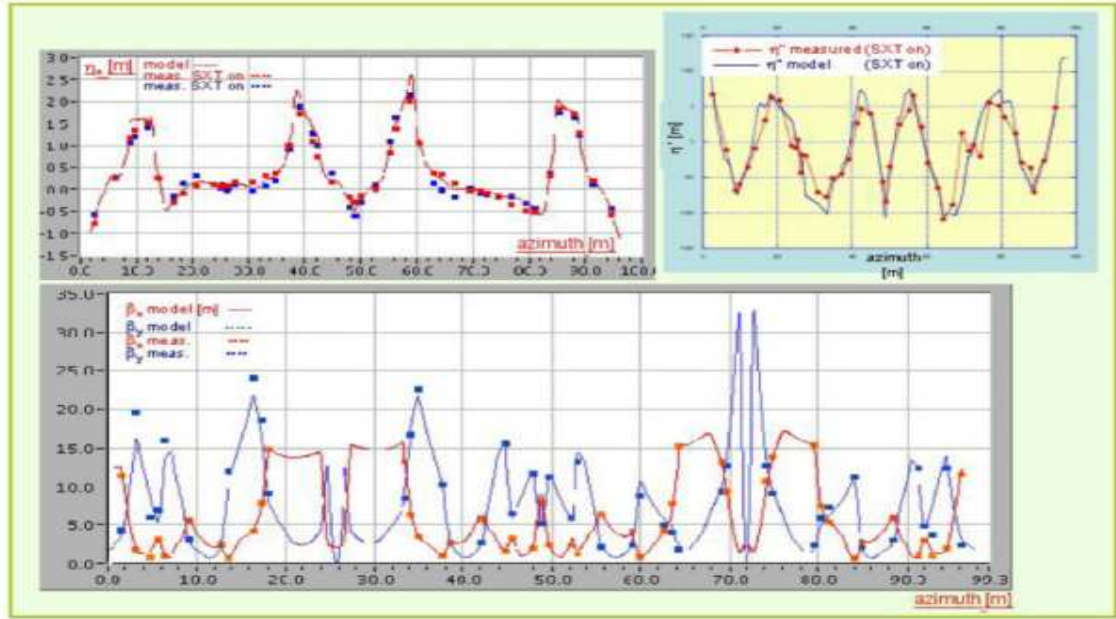


Figure 3: DAΦNE optic functions comparison between simulation results (line) and experimental data (dots)- up: first and second order dispersion; down: horizontal and vertical betatron functions (FINUDA configuration).

- maximum integrated luminosity per day $\approx 4 pb^{-1}$;
- luminosity lifetime: 0.6 h;
- number of fillings per hour: 2;
- injection frequency e-/e+: 2/1 Hz;
- data acquisition during injection: OFF.

Fig. 5 shows the daily and integrated luminosity from mid-October 2003 to March 2004. The FINUDA experiment has completed the first stage of its scientific program and data analysis is under way.

3.2 KLOE operation

After the FINUDA detector removal, KLOE operation was resumed starting from May 2004 with a luminosity delivery goal of $2 fb^{-1}$ before the end of 2005. At the end of July the value of the delivered luminosity was $5.2 pb^{-1}/day$, with electron and positron peak currents $I_{peak}^- = 1.25 A$ and $I_{peak}^+ = 1.0 A$ respectively. After the August shutdown the transverse and longitudinal feedbacks were improved by reducing the unwanted noise and increasing the system gain for the positron horizontal feedback. This led us to reach higher currents for the two beams namely $I_{peak}^- = 1.7 A$ and $I_{peak}^+ = 1.25 A$ respectively. At the same time the time-duration of the injection kickers pulse was halved in order to increase the injection efficiency while reducing the excitation of horizontal

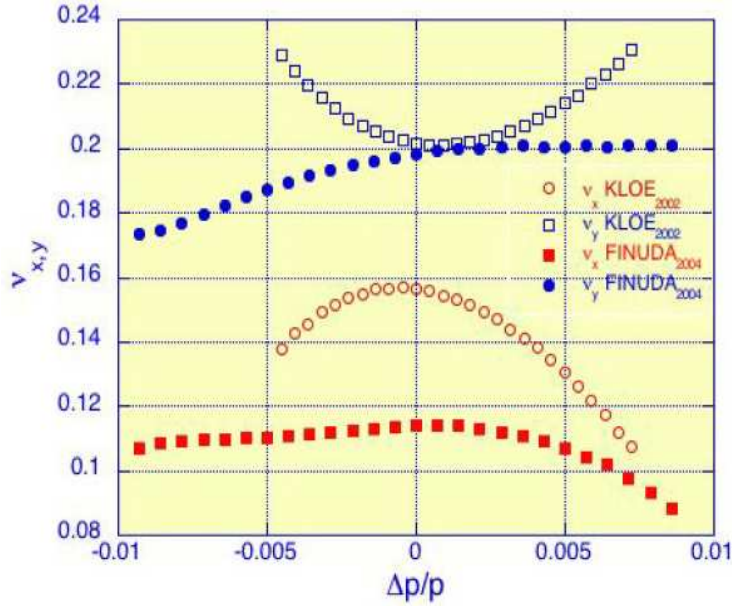


Figure 4: *Tune shift dependence on energy measured in the positron ring before and after the wiggler upgrade.*

instabilities during beam injection. An optimization on sextupole and octupole magnet settings was performed to increase the dynamic aperture and the beam lifetimes. By the end of 2004 the the following performance was reached:

- number of bunches per beam: 105 + 105;
- total current per beam e-/e+: 1.7/1.25 A;
- peak luminosity $\approx 1.23 \times 10^{32} \text{cm}^{-2} \text{s}^{-1}$;
- number of fillings per hour: 3;
- data acquisition during injection: ON.
- maximum integrated luminosity per day $\approx 7.4 \text{pb}^{-1}$;
- maximum integrated luminosity per month $\approx 150 \text{pb}^{-1}$;
- integrated luminosity in 2004 $> .8 \text{fb}^{-1}$;

The peak and integrated luminosity delivered to KLOE since May 2004 are shown in Fig. 6.

3.2.1 KLOE optics

In this configuration the fine tuning of the betatron functions at the IR is close to its optimum. A 20% smaller value was tried for the β_x^* resulting in a 5% reduction of the luminosity, while an higher value turned out to be not compatible with 105 bunch operation. A 3% reduction on

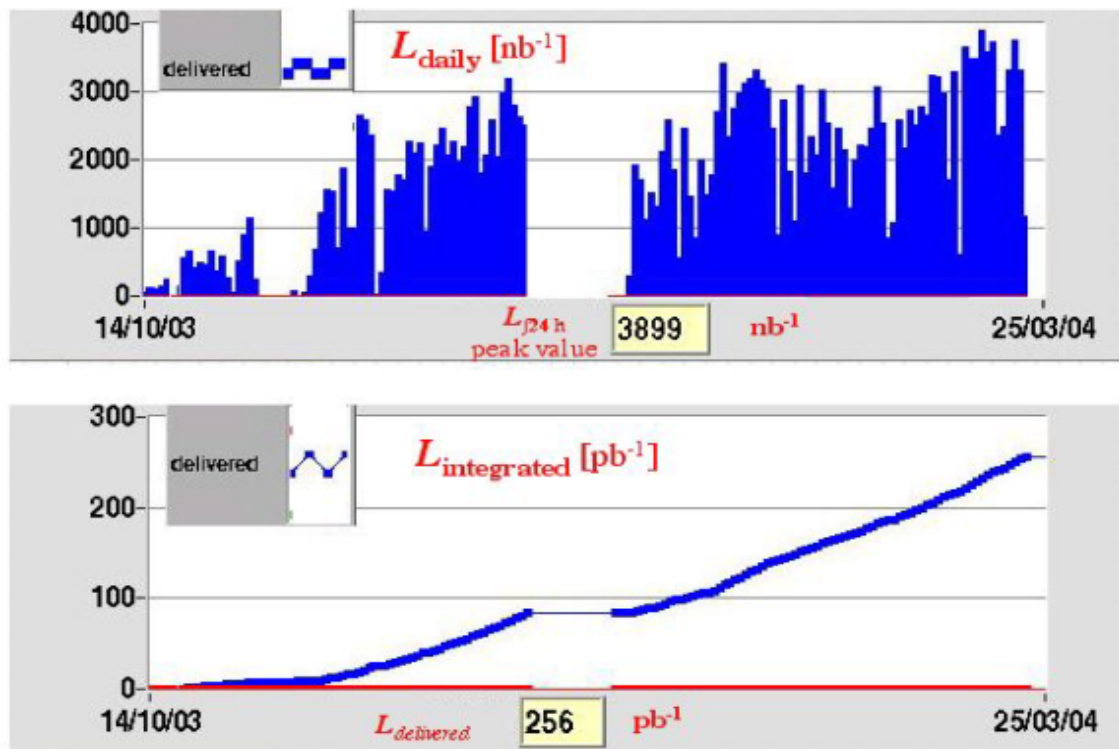


Figure 5: *Daily and Total Integrated luminosity per day delivered to FINUDA.*

β_y^* could be realized at the cost of increased chromaticity and beam instability. Both tunes are now very close to the integer (around $Q_x=0.10$, $Q_y=0.17$, lower values not tried yet in collision), and seem to be the best compromise between minimum beam-beam blow-up and several other parameters such as lifetime, ion trapping, maximum storable positron current, injection efficiency etc. As in FINUDA configuration a satisfactory agreement persists between the calculated values of the optical functions and the measurements, see Fig. 7.

4 Future Plans

The present physics program of DAΦNE should be completed by 2007. In the next decade physics with kaons at 1 GeV c.m. will be appealing only if the luminosity can be enhanced by at least one order of magnitude with respect to the present one. Studies on light quarks near the nucleon threshold at 2 GeV c.m. have also been proposed with less challenging requirements on luminosity. Two possibilities have been envisaged for the DAΦNE upgrade:

- to transform the collider into a light quark source by increasing the maximum center of mass energy from 1.4 GeV to ≈ 2.2 GeV;
- to upgrade it to a super factory with a luminosity larger by one to two orders of magnitude with respect to the present best performances, namely in the $10^{33} \div 10^{34} \text{cm}^{-2}\text{s}^{-1}$ range.

A dedicated Physics and Accelerator Workshop was held in Alghero (Sardinia, Italy) in September 2003 to study both the machine feasibility and the physics cases in the 1-2 GeV range.

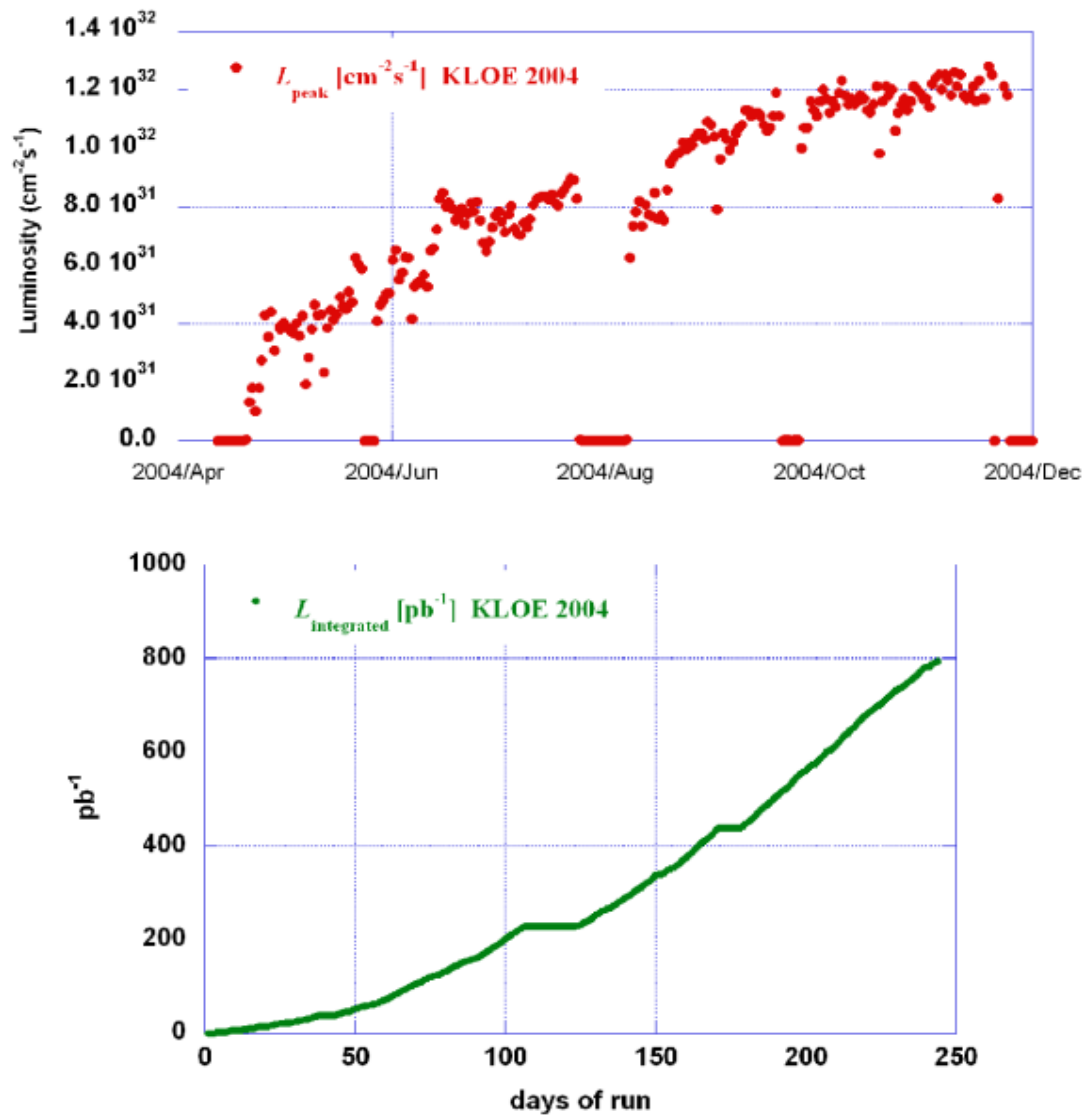


Figure 6: Peak and Integrated luminosity delivered to KLOE.

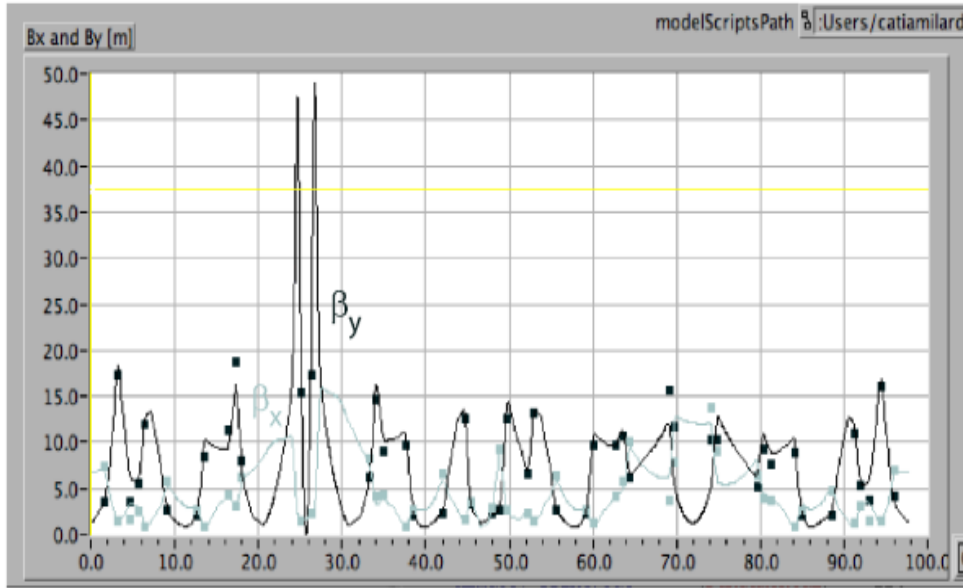


Figure 7: *DAΦNE* betatron functions comparison between simulation (line) and measurements (dots) - black: horizontal, grey: vertical (*KLOE* configuration).

Participation was shared between Experimental, Theoretical Physics and Accelerator Physics on the case for the c.m. energy between 1 and 2 GeV and the luminosity issues at these energies, leading essentially to discuss two options.

The first one, the increase in energy by at least a factor 2, needs changes of some of the present systems: dipoles, Interaction Region and injection. All other systems, RF, feedback, vacuum, quadrupoles, sextupoles, corrector magnets, diagnostics, are already compatible with the higher energy. The required luminosity is similar to the one already achieved in *DAΦNE* at the lowest energy, $10^{32}\text{cm}^{-2}\text{s}^{-1}$. The project for this upgrade is called *DAΦNE2*, where the “F” stays for Frascati and the “2” for the c.m. energy. The dipole preliminary designs, fitting the present vacuum chambers, are based on the use of two materials, steel and permendur. The last one, having a higher saturation field, will be used on the poles in order to increase the magnetic field on the beam axis, up to the necessary 2.2 T. The luminosity requirements can be achieved with a total current of 0.5 A in 30 bunches. The corresponding beam-beam tune shifts are $\xi_x/\xi_y = 0.014/0.024$, below the limit already achieved in *DAΦNE*. The IR design, based on the same principles of the present ones, could use superconducting quadrupoles very similar to those used at *CESR*. Two possibilities are being considered for injection: a Linac upgrade to 1 GeV for on-energy injection, or energy ramping; the first one is better for the average luminosity, while the second one is cheaper.

The second option, named *DAΦNE-II*, on which a preliminary conceptual design has been presented at Alghero, is based on the “strong RF focusing” principle, very high radiation emission and negative momentum compaction ring configuration. The strong RF focusing is a modulation of the bunch length along the ring, obtained by a very large longitudinal phase advance, corresponding to synchrotron tune near half integer. The minimum bunch length occurs at the IP, the maximum at the RF cavity position. Such a scheme needs a large absolute value of the momentum compaction and a high RF voltage, and the ring acts as a magnetic compressor. The strong radiation emission can be obtained with a new lattice based on cells with positive and negative dipoles, yielding a

damping time of the order of few msec, about a factor 5 less than in DAΦNE. In this lattice the dispersion oscillates around zero and in each dipole has the sign opposite to the bending angle and a large value, so that its contribution to the momentum compaction is always negative and high, almost an order of magnitude with respect to the present DAΦNE one. The advantages of the negative momentum compaction regime, like shorter bunches, and more regular bunch shape are therefore included in the design. An RF system at 500 MHz, with voltage of the order of 10 MV, for a 100m long ring, and momentum compaction near -0.2, will give bunch lengths at the IP near 2 mm. The IR fitting the existing KLOE detector is based on superconducting low- β quadrupoles very close to the IP, to focus β_y^* to few millimeters.

The preliminary collider layout fits the existing DAΦNE hall (see Fig. 8) and could utilize all existing infrastructures and sub-systems. The collider should have only one IR, while the opposite section could be used for injection and RF system. The elements yielding the major contribution to the ring impedance should be placed in the sections where the bunch length is longer, so that the perturbation to the bunch distribution is minimized.

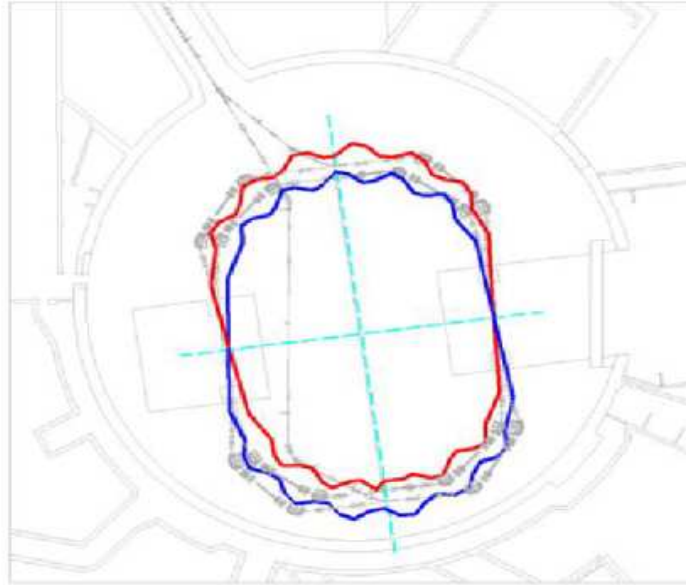


Figure 8: *Layout of DAΦNE-II in the DAΦNE Hall.*

Both options seem to be appealing to the Physics community. DAΦNE is the only e^+e^- collider in Europe, and the only one in the world, at present, operating at such a low energy. Its upgrade, both towards higher luminosity or energy, would allow continuing the tradition of the Frascati Laboratory in designing, building and operating e^+e^- storage rings.

Besides these future machine upgrades, in July 2005 a proposal was presented for DAΦNE as powerful source of ultrastable Coherent Synchrotron Radiation (CSR) in the terahertz frequency region. This kind of radiation occurs when the particle bunch becomes shorter than the emitted wavelength. In DAΦNE such a regime can be reached in the far infrared by realizing a machine lattice with an almost vanishing momentum compaction (α_c) at very low bunch currents. An

important issue for the high current operation of DAΦNE and for the proposed strong RF focusing experiment is the evaluation and understanding of the effect of the machine impedance on the bunch length and energy spread. One effect which has not yet been considered is the microbunching instability (MBI) driven by the radiation impedance. This can be of high relevance for such mode of operation. In fact when the current per bunch is above the MBI threshold, the longitudinal dynamics starts to be perturbed by the instability. For most storage rings and just above the MBI threshold, the perturbation is weak and shows measurable effects only as bursts of CSR in the far infrared (FIR). For currents much higher than the MBI threshold the effects could be relevant, inducing average bunch lengthening and strong transient modulation of the longitudinal distribution. If the current per bunch is kept below the MBI threshold, DAΦNE could become an interesting source of stable CSR in the terahertz frequency range. In fact several beneficial features are simultaneously present in the Frascati collider: the relatively low energy contributes to obtaining short bunches; the small bending radius and the large dipole gaps reduce the shielding of the vacuum chamber that tends to suppress the CSR emission; the aluminum vacuum chamber minimizes the contribution of the resistive wall impedance that induces bunch lengthening; several families of sextupole and octupole magnets allow for a precise control of the linear and nonlinear terms of the momentum compaction, which is a fundamental requirement when tuning the machine to vanishing α_c for short bunches. Last but not least, DAΦNE is equipped with SINBAD, a beamline optimized for the far-infrared (FIR) in the electron ring.

A limitation is the existing RF system which allows for relatively low voltage in the cavities. However, with the proposed strong focusing RF scheme using a 1.3 GHz superconducting cavity operated at several megavolts, DAΦNE could become an outstanding source of CSR.

A preliminary evaluation of the MBI effects on DAΦNE was carried on: the CSR issues associated with DAΦNE have been analyzed and the threshold for the MBI calculated. The results showed that MBI is not a concern in the present high current collision operation while it could appear at larger currents per bunch. MBI could be important in the proposed strong RF focusing scheme, where shorter bunches are foreseen. Experimental characterization of MBI in DAΦNE, well above the single bunch threshold, will help to better understand the problem. Two cases, one with the present RF system, the other with the superconducting 1.3 GHz one foreseen in the strong RF focusing scheme, were investigated. The results are very interesting and show the high potentiality of DAΦNE as a CSR source.

5 Publications

1. B. Spataro *et al.*, “On Trapped Modes in the LHC Recombination Chambers: Numerical and Experimental Results”, Nuclear Instruments and Methods in Physics Research A 517 (2004) 19-27.
2. A. Gallo *et al.*, “Design Considerations For Future DAFNE Upgrades”, DAFNE 2004: Physics at meson factories, Invited Review Talk in Plenary Session, Frascati, 7-11 June, 2004. Frascati Physics Series Vol. XXXVI(2004).
3. P. Raimondi: “Towards Higher Luminosities in B and Phi Factories”, Proceedings of EPAC2004, 5-7 July, 2004 Lucerne, Switzerland; LNF-04/18(P), 30/07/04.
4. C. Milardi *et al.*, “DAFNE Operation with the FINUDA Experiment”, Proceedings of EPAC2004, 5-7 July, 2004 Lucerne, Switzerland; LNF-04/18(P), 30/07/04.
5. C. Biscari *et al.*, “Feasibility Study for a Very High Luminosity F-Factory”, Proceedings of EPAC2004, 5-7 July, 2004 Lucerne, Switzerland; LNF-04/18(P), 30/07/04.

6. C. Vaccarezza *et al.*, Experimental Observations and E-Cloud Simulation at DAFNE, Proceedings of the 31st ICFA Advanced Beam Dynamics Workshop (E-CLOUD '04), CERN-2005-001 (12 January 2005).
7. A. Gallo *et al.*, "Proposal of a Strong RF Focusing Experiment at DAFNE", Proceedings of EPAC2004, 5-7 July, 2004 Lucerne, Switzerland; LNF-04/18(P), 30/07/04.
8. S. Guiducci *et al.*, "The Modified DAFNE Wigglers", Proceedings of EPAC2004, 5-7 July, 2004 Lucerne, Switzerland; LNF-04/18(P), 30/07/04.
9. L. Pellegrino, "Experience with Long Term Operation with Demineralized Water Systems at DAFNE", Proceedings of EPAC2004, 5-7 July, 2004 Lucerne, Switzerland; LNF-04/18(P), 30/07/04.
10. Alessandro Drago, "Horizontal Instability and Feedback Performance an DAFNE e+ Ring", Proceedings of EPAC2004, 5-7 July, 2004 Lucerne, Switzerland; LNF-04/18(P), 30/07/04.
11. D. Alesini *et al.*, "Third Harmonic Cavity Design and RF Measurements for the Frascati DAFNE Collider", Physical Review Special Topics - Accelerators and Beams, Volume 7, 092001 (2004).
12. C. Biscari *et al.*, "Terahertz Coherent Synchrotron Radiation at DAFNE", ICFA Beam Dynamics Newsletter No. 35, December 2004.
13. S. Guiducci, "Report on the ILC Workshop KEK (Japan) November 2004", ICFA Beam Dynamics Newsletter No. 35, December 2004.

DAΦNE BTF

B. Buonomo (Bors.), G. Mazzitelli (Resp.), P. Valente (Art.23)

The DAΦNE Operation Staff: G. Baldini, P. Baldini, M. Belli, B. Bolli, G. Ceccarelli, R. Ceccarelli, A. Cecchinelli, S. Ceravolo, R. Clementi, O. Coiro, S. De Biase, M. De Giorgi, N. De Sanctis, M. Di Virgilio, G. Ermini, O. Giacinti, E. Grossi, F. Iungo, R. Lanzi, C. Marini, M. Martinelli, M. Masciarelli, E. Passarelli, V. Pavan, D. Pellegrini, R. Pieri, G. Piermarini, S. Quaglia, M. Sardone, M. Scampati, G. Sensolini, A. Sorigi, M. Sperati, A. Spreccacenero, R. Tonus, T. Tranquilli, M. Troiani, R. Zarlenga

1 Description of the DAΦNE BTF 2004 Activities

During the 2004 the DAΦNE Beam Test Facility (BTF) ¹⁾ continued the electron/positron beams delivering for many user groups, while in March an upgrade ²⁾ of the beam line has been performed in order to increase the duty cycle limited by topping up operations of KLOE experiment data taking. The schedule has been divided in three periods.

- From January to March the BTF delivered beams in a parasitic way during the data taking of the FINUDA experiment. Typically 20-30 minutes were available between two DAΦNE main rings injections, leaving 15-20 minutes runs for the BTF experiments.
- During the FINUDA roll out in the last three weeks of March, the common beam line of DAΦNE and the BTF was completely dismantled and reassembled in a different configuration, in order to have a complete separation of the beam test channel.
- In May the BTF resumed operation with the new line till the end of the year.

The Beam Test facility staff also continued the optimization of the beam characteristics, the improvement of the diagnostic tools ³⁾, as well as of the DAQ system, user devices, controls and management software. The beam parameters achieved in single particle operation mode during year 2004 ⁴⁾ are summarized in Tab. 1.

Parameter	Value
Energy range	25÷750 MeV (e ⁻ /e ⁺)
$n_{average}$	1÷10 ⁷
Pulse Duration	1-10 ns
Repetition Rate	0÷50 Hz
Energy Resolution	≈ 1%
Spot Size	≈ 2 × 2 mm

Table 1: The year 2004 operated parameters of the DAΦNE BTF.

2 2004 Users Experience

During year 2004 many different test-beams and experiments have used the DAΦNE BTF, requiring very different beam characteristics and operating conditions, as briefly reported below:

High multiplicity in a wide range of energies.

AIRFLY ⁵⁾: the experiment is dedicated to the measurement of AIR Fluorescence Yield and lifetime; it requires the modulation of the beam multiplicity between 1 to 10^7 electrons per pulse, 1 ns pulse length, in a variable energy range, with as low as possible contamination from the low energy particles background. The experiments continued the measurements started in 2003 improving the sensitivity of the detector and the background discrimination. The introduction of the tiny beryllium exit window of the BTF line during the upgrade has permitted to lower the minimal energy of the beam down to 25 MeV. The experiment had 4 shifts assigned for about 50 days of operation partially shared with other experiments. The work was partially funded by Transnational Access to major Research Infrastructures, TARI.

RAP ⁶⁾: “Rivelazione Acustica di Particelle”, is aimed to the measurement of particle energy conversion efficiency in acoustic vibration of the fundamental modes of a cryogenic detector, as a function of its thermodynamic temperature. The experiment needs a large integrated number of particles, in order to release more than 100 TeV energy in the detector. Also this experiment continued the data taking started in 2003 with the first successfully run at 4 K. During the March upgrade a low noise beam monitor detector has been mounted at the end of the BTF transfer line in order to improve the precision in monitoring the beam intensity in the range of a few pC beam charge. One shift of three weeks has been assigned.

APACHE ⁷⁾: (Aerogel Photographic Analysis of Cerenkov Emission), test of the light diffusion within the aerogel that is usually limiting the performance of this material as Cerenkov radiator for the LHCb-RICH detector. The experiment had 3 shifts assigned for a total of 25 days of test. In those first periods the APACHE group studied the feasibility of the measurements of aerogel homogeneity with photographic emulsions that will be replaced in the next future by electronics read out system, close to the final setup that will be installed in LHCb CERN experiment.

FLAG ⁸⁾: test of very high sensitivity beam fluorescence detector. Different fluorescence targets were tested in nC-pC charge conditions. The experiment, started in 2003, has been installed in the second (straight) beam line of the BTF. A shift of a week has been assigned.

Low multiplicity or single electron mode at different energies.

MCAL-AGILE ⁹⁾: The detector of MCAL, MINI-CALORIMETER of AGILE satellite detector, has been characterized with high energy particles hitting the detectors in various positions. The effects of phosphorescence induced in CsI(Tl) scintillators for large amount of energy deposit has been studied as well as the electronics performance. The test had 4 shifts assigned for about 20 days of data taking.

LHCb-LNF ¹⁰⁾: test of efficiency for the MWPC and GEM detectors for the LHCb detector. The experiment already performed a run in 2003; one shift of 10 days has been assigned.

CaPiRe ¹¹⁾: (Camere a Piatti Resistivi): the test consisted in mapping the efficiency of glass RPC chamber as a function of the beam impinging position, gas mixture and repetition rate. The test continued the operation started in 2003 with two shifts for 14 days of beam.

SIDDHARTA ¹²⁾: test of triggerable Silicon Drift Detector, designed in order to replace the standard CCD detector in DEAR experiment to avoid the asynchronous background reducing

the sensitivity to kaonic atoms signal in previous DEAR measurements. A few tens of electrons impinging on a target of different materials were used to produce synchronous background. Fe and Sr sources were instead used to produce the asynchronous background. The group continued the measurement started at the end of 2003 with a dedicated shift of 14 days. The work was partially funded by Transnational Access to major Research Infrastructures, TARI.

CRYSTAL ¹³⁾: A shift of 14 days has been assigned to the study of the particle channeling effect via crystal structures. Well collimated positrons were sent to a crystal sample optimally aligned by a goniometric system. The profile of channeled positrons was monitored 5 meters far from the sample, by means of the BTF scintillating fiber profile monitor. Work partially funded by Transnational Access to major Research Infrastructures, TARI.

MEG ¹⁴⁾: The test is part of the experiment devoted to the search for the (flavour violating) decay $\mu^+ \rightarrow e^+ \gamma$ with a sensitivity of 10^{-13} . The aim of the measurements performed at the BTF is to study the time resolution of different scintillator samples, as a function of the positrons impact position and angle. Three shifts for 28 days has been assigned partially shared with other users.

LAZIO ¹⁵⁾: (Low Altitude Zone Ionizing Observatory): test of silicon and scintillators detectors (Wizard collaboration). This experiment requires a multiplicity of 1-10 electrons/s, 1-10 ns variable pulse length and an energy around 500 MeV. Four shifts for 28 days, partially shared with other experiments, were assigned.

BTeV ¹⁶⁾: The test was performed by the BTeV collaboration, and was aimed to measure the space resolution and efficiency of the MOX straw-tube detector for the main BTeV tracker. A single electron distribution has been provided at 500 MeV. One shift of 14 days has been assigned.

BTF LAB: part of the beam time, about 20 days, has been dedicated in parasitic way to experiments and test operation with an educational purpose. Students from Roma II and Roma I universities, as well as students and teachers from high schools, took part to simple experiments or in the operation of the facility.

3 BTF Upgrade

During the DAΦNE operation the availability of the facility is limited by the main DAΦNE experiments, KLOE, DEAR, and FINUDA. In particular the KLOE detector can take data also during the injection of the beams, practically leaving no time for BTF operation due to the very short luminosity lifetime, while during FINUDA operation the available duty cycle for the BTF was about of the 50%. In order to overcome these limitations, a complete separation between the DAFNE transfer line to the main rings and the BTF channel allows a large improvement in the duty-cycle ²⁾.

An independent transfer line for the BTF can now be operated with a dead-time coming only from the LINAC switching time and the time spent for filling the main rings. The chosen solution consisted in realizing a triple output from the LINAC transfer line Fig. 1:

1. a straight line towards the accumulator (and from there to main ring);
2. the spectrometer line at 6° , dedicated to the LINAC beam energy measurement;
3. an exit at 3° for the BTF channel.

A new small fast cycling DC magnet (DHSTB101) with a bending angle of 3° has been installed upstream the pulsed magnet used for the beam energy measurement (DHSTP001). The DC power supply of the DHSTB101 magnet will be soon replaced by a pulsed power supply in order to have a quasi-continuous injection in the BTF transfer line.

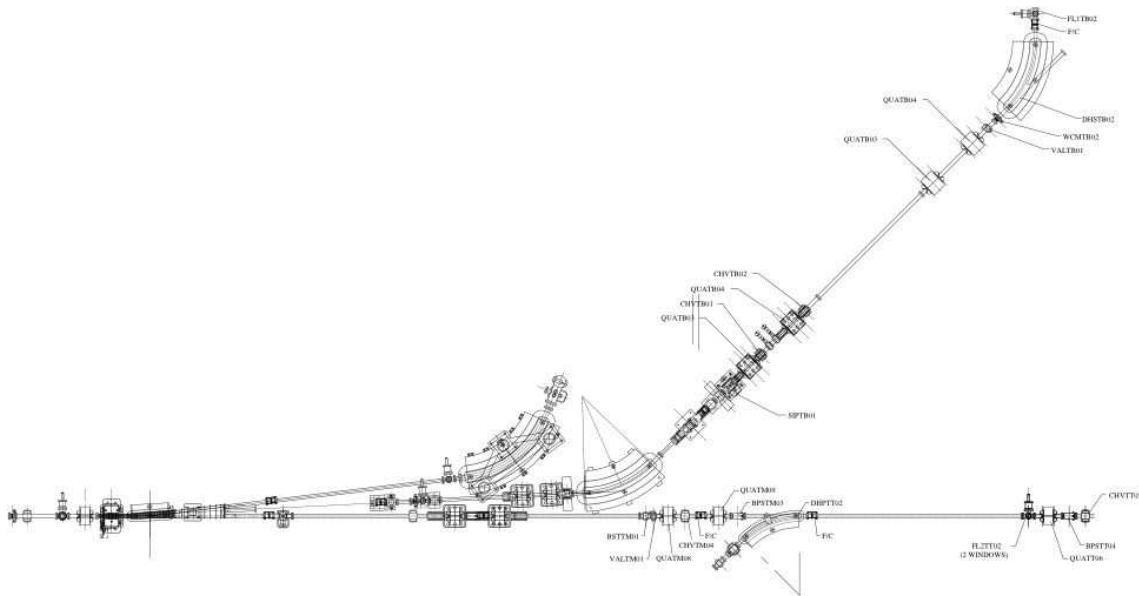


Figure 1: *Layout of the new configuration with the triple exit for the transfer line to the accumulator, the hodoscope line for LINAC energy measurement, and the BTF channel.*

This configuration leaves a completely independent line equipped with all the BTF elements (variable thickness target, quadrupoles, dipoles slits) at a nominal 3° angle with respect to the main channel. All magnets and devices needed for the BTF operation are now always switched on and set to the operation values, not only increasing the duty cycle, but also improving the reliability of the beam characteristics.

During the beam injection in the collider DHSTB101 magnet is off, and the beam follows the standard timing sequence and injection scheme: one LINAC bunch per second (out the available 50) is bent by 6° by the pulsed magnet DHSTP001, and sent to the hodoscope for energy measurement, while the remaining bunches follow the standard path to the accumulator and main rings. On the contrary, during the BTF operation DHSTP001 magnet is on, so that the beam is driven into the new transfer line at 3° . The pulsed magnet DHSTP001 then kicks one LINAC bunch per second by the additional 3° necessary to reach the hodoscope system. The required switching time between BTF and main rings injection configurations comes now only from ramping the two magnets DHSTB101 and DHSTP001, and is reduced to less than 10 seconds.

This upgrade allowed to run the facility during the KLOE operation with a duty cycle better than 40%. This value was limited in 2004 by the steady growing up of the injection time, during the operation for the KLOE experiment, in order to improve the delivered integrated luminosity. This limitation will be overcome in year 2005 thanks to the introduction of the pulsed power supply for the DHSTB101.

4 Diagnostics and Facility Improvements

Two new vertical slits have been installed, in addition to the horizontal collimators already present in the BTF line. The first one, upstream the attenuation target, is very effective in modulating the beam intensity at the end of the LINAC. This overcomes the problem of running the BTF with a special (lower intensity) LINAC setting, different from the normal DAΦNE main ring injection

setting, thus contributing to the improvement of the duty cycle. The second one has been installed downstream the DHSTB001 bending magnet, in order to adjust the vertical beam spot size.

A thin beryllium window has been installed, in place of the previously used 1.5 mm thick aluminum window, thus giving a decrease of the beam divergence at very low energy.

A low noise Beam Charge Monitor (Bergoz) has been positioned just before the last bending magnet, in order to improve the beam diagnostics in the pC range. The analog signal from the device is acquired by 12 bit, 25 fC/count QDC.

Tools and infrastructure were also improved:

- The BTF permanent DAQ system has been enlarged with many new devices; details are available in the technical BTF web page, <http://www.lnf.infn.it/acceleratori/btf/>.
- New high voltage supplies, positive 3-4KV and 15 KV maximum voltages, are now available in addition to the the already present negative boards.
- A database for user handling, beam request, and recording of the information connected to runs and shifts allocation has been developed, and a simple web interface has been created.
- A console system dedicated to beam control, structured LAN and WAN network, PCs for user implementation running Linux and Windows operating system, have been installed in the BTF control room and made available for user operation.

5 Future Plans and Conclusions

In the following table the beam time allocated during the available period of operation of the DAΦNE BTF are reported, showing the high interest for the facility. During the first two years of operation tens of papers and presentations at international conferences have been produced by the groups working with the DAΦNE BTF beam.

2004 shift	available (days)	assigned (days)
07/1 - 22/3	75	92
23/3 - 24/5	0 (61)	upgrade shutdown
25/5 - 31/7	78 (92-14)	72
01/7 - 19/9	0 (50-14)	summer shutdown
20/9 - 23/12	87 (94-7)	117

Table 2: The year 2004 operation of the DAΦNE BTF.

The upgrade performed during the 2004 was very successful and permitted to operate also during the KLOE data taking. In addition, the beam reliability improved thanks to the complete separation of the BTF channel. In general the facility performed very well and provided beam to a great number of user groups. In the next future the introduction of the pulsed power supply will allow a quasi-continuous operation. The plans for the year 2005 are, in addition to running the facility for all the available time, to continue the improvements of the diagnostics tools and of the infrastructure.

Publication and Conference Talks by LNF Authors in Year 2004:

1. B. Buonomo, G. Mazzitelli and P. Valente, *Diagnostic and Upgrade of the DAFNE BTF*, under publication in Nucl. Phys. B (Proceeding of 9th Topical Seminar on Innovative Particle and Radiation Detectors).
2. B. Buonomo, G. Mazzitelli and P. Valente, *Performance and Upgrade of the DAFNE BTF*, submitted to Trans. Nucl. Science (Proceeding of IEEE2004).
3. M. Anelli, B. Buonomo, G. Mazzitelli and P. Valente *A Scintillating-Fiber beam profile monitor for the DAFNE BTF*, LNF-04/24(IR).
4. B. Buonomo, G. Mazzitelli and P. Valente, *Status Report on the DAΦNE BTF* Commissione Nazionale II, Ott. 30, 2004, Roma, Italy.

Additional References to Experiments:

5. F. Arciprete *et al.*, “Air Fluorescence Induced by Electrons in a Wide Energy Range”, in proceeding of 28th ICRC (2003).
6. S. Bertolucci *et al.*, “RAP: Acoustic detection of particles at the DAΦNE BTF”, Frontier Detector for Frontier Physics (2003), Elba, Italy; Nucl. Instrum. Meth. A **518** (2004) 261-263.
7. C. Matteuzzi *et al.*, in proceedings of RICH2004 Mexico 2004.
8. D. Filippetto, “Studio sperimentale della radiazione emessa da schermi fluorescenti attraversati da fasci di elettroni relativistici”, Tesi di Laurea in Ingegneria Elettronica (2003), Università degli Studi di Roma “La Sapienza”.
9. M. Prest *et al.*, “The AGILE silicon tracker: an innovative γ -ray instrument for space”, Nucl. Instrum. Meth. A **501** (2003) 280-287.
10. M. Alfonsi *et al.*, “Triple GEM detector operation for high rate particle triggering”, Frontier Detector for Frontier Physics (2003), Elba, Italy. Nucl. Instrum. Meth. A **518** (2004) 106-112.
11. S. Calcaterra *et al.*, “Test of large area glass RPCs at the DAΦNE Test Beam Facility (BTF)”, Nucl. Instru. Method. A **533** (2004) 154-158.
12. C. Curceano *et al.*, “Future precision measurements on kaonic hydrogen and kaonic deuterium with SIDDHARTA”, in proceeding of Workshop on Hadronic Atoms, Trento, Italy (2003).
13. S. Bellucci *et al.* “Crystal undulator as a new compact source of radiation”, Phys. Rev. ST Accel. Beams **7** (2004) 023501.
14. T. Mori, “Search for Lepton Flavor Violation with Muons”, talk given at SUSY 2004, Tsukuba, Japan, June 17-23, 2004.
15. D. Babusci *et al.*, “elect Experimental Trends in Astro-Particle Physics in Space”, LNF - 04 / 26(IR).
16. E. Basile *et al.*, “A Novel Configuration for a Strawtube-Microstrip detector”, LNF-04-25(P), submitted to Trans. Nucl. Science (Proceeding of IEEE2004).

DAΦNE-L Lab

E. Burattini (Resp.), P. Calvani (Ass.), G. Cappuccio (Ass.),
 G. Cibin (Bors.), G. Cinque (Art. 23), S. Dabagov (Art. 23), G. Della Ventura (Ass.),
 M. Cestelli Guidi (Art. 23), A. Grilli (Tecn.), A. Mottana, (Ass.), A. Marcelli,
 F. Monti (Ass.), A. Nucara (Ass.), E. Pace, P. Postorino (Ass.), M. Piccinini (Ass. Ric.),
 M. Pietropaoli (Art. 15), A. Raco (Tecn.), G. Viviani (Art. 15)

1 Summary

During the 2004, DAΦNE-L continued the experimental activity and planned improvements on all Synchrotron Radiation (SR) installations. In particular, at the Synchrotron INfrared Beamline at DAΦNE (SINBAD) the commissioning of the IR microscope was completed. On the soft X-Ray beamline, technical improvements extended the range of samples measurable by X-ray Absorption Spectroscopy (XAS), and a new CDD instrumentation for X-ray imaging was tested. At the UltraViolet (UV) branch line, dedicated experimental runs continued for the Solar Ultraviolet Effect (SUE) in photobiology. The status of the commissioning of the IR beamline can be well evaluated looking at Fig. 1, where the SR gain over a conventional source is shown in the far- and mid-IR range. Being fully operative in the whole IR range, a report of SINBAD and its activity since 2001 has been submitted to an International Committee of referees.

SR experiments have been performed in full parasitic mode during both Finuda (till spring) and KLOE runs on DAΦNE collider. Within August, all previously approved projects within the EU FP5 framework Transnational Access to Research Infrastructure (TARI) at LNF have been successfully completed on SINBAD and in autumn several European users started the experimental activity at DAΦNE-L within the new TARI program, now included in the Integrated Infrastructure Initiative (I3 program). Since November the X-ray beamline operates also during the topping up e^+ injection.

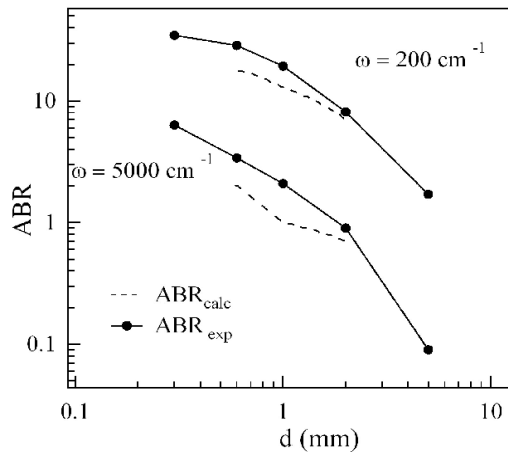


Figure 1: The Actual Brilliance Ratio (ABR_{exp}) (dots) is reported vs. the aperture diameter d and compared in the mid and the far infrared with the ABR_{calc} (dashed lines) obtained by ray tracing simulation of the optical system. Solid lines are just guides to the eye.

2 Activity

2.1 SINBAD

The SINBAD optical layout is the results of many technical considerations. Along ~ 25 m there are six gold-coated mirrors. All mirror adjustments are remotely controlled and seven cameras monitor the visible light along the SINBAD path. The final spot is affected by coma aberrations mainly in the horizontal plane produced by two spherical mirrors which determine a visible spot at the entrance of the interferometer with an area of about 2 mm^2 , and a divergence that well matches the f-number (4) of the interferometer. This latter is a BRUKER Equinox 55, suitably modified to work under vacuum, which covers a spectral range from 10 through 15000 cm^{-1} with a maximum spectral resolution 0.5 cm^{-1} . A port of the interferometer hosts a BRUKER IRscope 1 microscope, operating in the near- and mid-IR range.

The scientific activity at SINBAD was mainly associated to experiments performed within the EU framework of the previous TARI and also the new TARI access program supported by I3. Actually, in 2004 13 EU funded experiments run at SINBAD supporting more than 30 users for a total of 150 experimental days. In addition a few Italian teams had the chance to start tests on future experimental programs. During the year the SINBAD instrumentations has been used also by two students of Laurea Thesis of the La Sapienza University and by one Master of the INFN course who performed an investigation on Cultural Heritage applications aiming at characterizing samples of “lapis lacaedemonium” (*Verde di Grecia*) containing chalcedony and quartz inclusions. Although working in parasitic regime relevant results were achieved in these months.

Taking full advantage of high brilliance of the IR beam of the SINBAD beamline, room temperature far-IR absorption measurements have been carried out on different samples of manganites as a function of pressure by means of a diamond anvil cell. Very thin sample slabs ($4\text{-}5 \mu\text{m}$) have been obtained by pressing finely powdered manganite between diamonds. At present few papers on high-pressure far-IR measurements can be found in the literature and none devoted on manganites and similar compounds. The present results which have been submitted for publication represent a quite important technological achievement in itself, give a first insight to the delocalization processes induced by pressure in manganites, and provide a new opportunity for studying the role of the electron-phonon coupling in Jahn-Teller systems.

After the commissioning of the IRscope 1 several spectromicroscopy tests and experiments were performed. Among them we may underline the results obtained by the team of Wojciech M. Kwiatek of the Institute of Nuclear Physics Polish Academy of Sciences who performed tissues analysis on non-cancerous, hyperplasmic and cancerous prostate. The FTIR measurements delivered information on the specific bonds intensities which could help in understanding of protein structures. Although not optimized and in fully parasitic conditions FTIR data on hyperplasmic sample were collected with an aperture up to $5 \mu\text{m}$. Moreover, the measurement of the spatial distribution of CH_2 and CH_3 bonds with two-dimensional maps with spatial resolution of $20 \mu\text{m}$ were also performed.

Another relevant investigation which has been submitted for publication regards in situ synchrotron FTIR experiments performed during in-situ evaporation-induced self-assembly (EISA) of mesoporous films and the role of silica polycondensation in obtaining highly organized mesostructures. The organization through EISA of mesostructured silica materials is given by a delicate balance of different processes in competition between each other. The kinetics of silica polycondensation has been followed observing the IR transmission in the $1000\text{-}1250 \text{ cm}^{-1}$ range and comparison between the different kinetics of ethanol and water evaporation during EISA have been obtained from FTIR spectra using a 2D correlation analysis. As an example Fig. 3 shows the asynchronous spectra obtained correlating in 2D the IR absorption spectra. Evaporation of water is observed to take place in three different phases, with a first rapid evaporation followed by an

increase in H₂O content and a second evaporation stage (in press, J. Am. Chem. Soc., 2005).

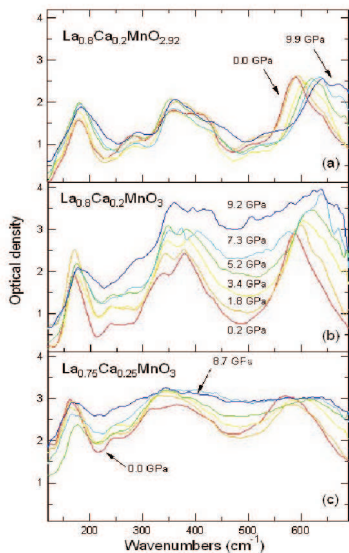


Figure 2: Pressure dependence of the optical density of $La_{0.75}Ca_{0.25}MnO_3$ (bottom panel); $La_{0.80}Ca_{0.20}MnO_3$ (central panel); $La_{0.80}Ca_{0.20}MnO_{2.92}$ (upper panel). Curves from ambient pressure up to about 10 GPa have been overimposed to show the behavior vs. pressure.

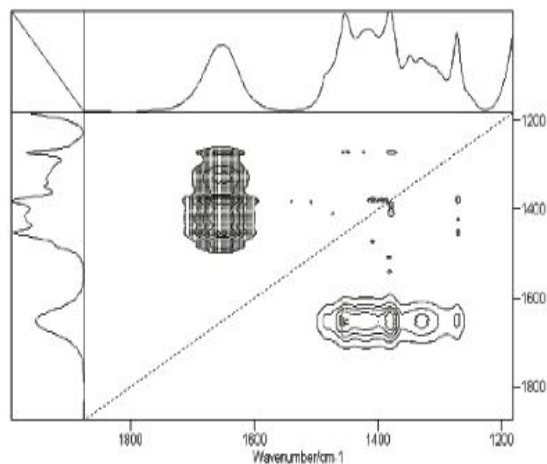


Figure 3: 2D asynchronous correlation of FTIR spectra of silice polycondensate a solution of MTES (methyltriethoxysilane), TEOS (tetraethylorthosilicate) and Pluronic F127.

By using the SINBAD beamline FTIR experiments in cooperation with the Roma Tre University were also performed on mineral samples and particularly on inclusions the lateral dimensions of which are smaller than 50 microns. As a matter of fact, using the microscope and the high brilliance of the IR synchrotron source, it was possible to measure small inclusions in the investigated systems with a spectral and spatial resolution unattainable by conventional sources. Since synchrotron radiation is characterized by a high degree of linear polarization, some experiments have also been carried out on natural mica crystals in order to study the anisotropy of this lamellar systems and in addition the structural configuration of water contained in them. Always in this research area, by using a cryostat which can operate down to about 20 K, very low temperature FTIR spectra were collected on a sample of the synthetic amphibole. The acquired data allowed verifying the structural model of the phase transitions of this compound, as it had turned out from X-ray diffraction techniques (in press on Am. Miner., 2005).

2.2 Soft X-Ray Beamline

The SR source of X-rays is one of the 6-pole equivalent planar insertion devices installed on the electron ring for radiation damping. This wiggler forces the electrons to emit a wide electromagnetic radiation fan that, in the X-ray region (above 1 keV), is fully polarized in the orbital plane. By over 1 A of circulating current an intense flux of soft X-rays is present, and used, well beyond one decade from the critical energy (~ 300 eV).

The front-end of the X-ray beamline is placed at about 4 m downward the wiggler magnet,

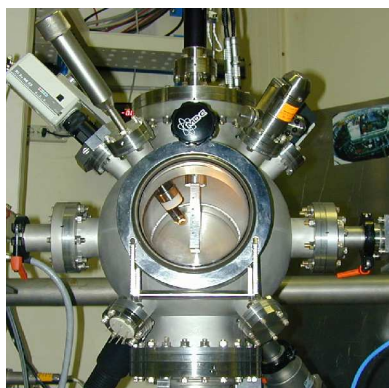


Figure 4: *New experimental chamber and instrumentations for soft X-ray experiments.*

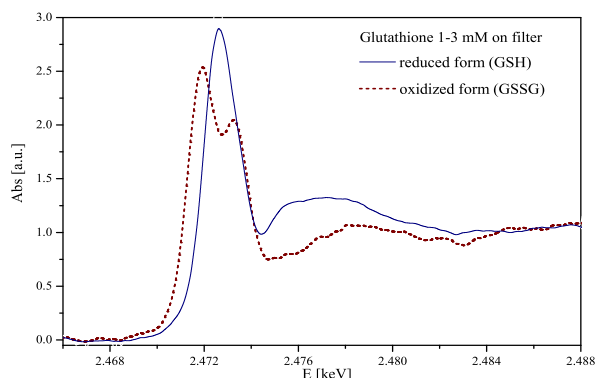


Figure 5: *XANES spectra of sulphur K absorption edge in a protein deposited in solution on paper filter. Data acquired in transmission mode by ion chambers at the energy resolution of 0.25 eV using Si(111) crystals.*

with the optical axis geometrically aligned to the insertion device itself. The exit flange is designed to accept all the vertical SR divergence, and more than 12 mrad of the photon fan in the orbit plane as seen from the wiggler midpoint. A vertical Au-coated silicon mirror is used for deflecting, in the horizontal plane and at a grazing angle of 2.2° , half of the SR fan into the UV branch line. Thin interchangeable windows of either Be ($8 \mu\text{m}$ thick) or polyamide (well below $1 \mu\text{m}$ of thickness) allow a high transparency to soft X-rays.

The wiggler beamline is equipped with a Toyama double-crystal monochromator in *boomerang* geometry to ensure a fixed beam exit within the Bragg's angle range $15^\circ - 75^\circ$. By a set of crystals including Si(111), Ge(111), α -Quartz (10-10) and KTP(011), the energy spectrum from 1.2 keV upward may be now covered. The newly installed multipurpose experimental UHV chamber (Fig. 4) can allocate several samples to be measured both in transmission and by secondary particles/radiation emission. The implemented detector equipment includes ion chambers, x-ray photodiodes and energy resolved PIN Si detector, plus electron channeltrons. In the experimental area, a $\theta - 2\theta$ goniometer is available for powder diffraction studies on using also the Cu K_α emission line from a 1000 W conventional source (see MicroPOLYX activity report pag. 181).

During 2004, the soft X-ray line has successfully delivered beamtime to external EU users, in the framework of the TARI program. In the following, selected examples are given of the experiments carried on in this year. X-ray Absorption Near Edge Spectroscopy (XANES) technique has been routinely applied on thin samples within the energy range 1,5 - 3,6 keV. All XANES spectra are acquired parasitically in transmission mode during runs from about 20 min (FINUDA runs) down to 10 minutes (KLOE runs), constraining the actual measuring time to 1-4 seconds per energy point. In spite of the very short acquisition time, soft X-ray absorption spectra are obtained with a sensible S/N ratio. On the higher energy side of the available X-ray spectrum, the XAS signal of the K edge of potassium atoms has been measured for the first time in samples of mineralogical interest (collaboration with Roma Tre University). These preliminary data are particularly appealing because of both the advantage of measuring the total cross section and because the intrinsic photon beam polarization can probe the atomic layers orientations in the sample. XANES spectrum of transition metal, namely the L edges elements like molybdenum palladium, antimony and silver have been also measured in the form of powders. In particular, Mo was extensively studied in compounds of different stoichiometry and magnetic properties, from non

magnetic upto giant magnetoresistance behaviour (TARI project of J. Chaboy, Zaragoza University). On the lower energy side, sulphur signal was measured for material science (TARI project by A. Kisiel⁸), Jagiellonian University) and in biomedicine. Fig. 5 refers to the XANES spectrum of S-bound or double-S-bound in Gluthathione protein. This reducing agent is a testbench organic compound endowed with well distinguishable redox states. Deposited onto a thin filter, both forms have been measured in concentration of few mM, i.e. almost like in vivo (collaboration with G. Bellisola of Verona University).

The lowest energy side was reached by quartz crystals: XANES spectra of aluminium K edge have been measured in powders of aluminum nitride nanotubes and nanoparticles. Nanomaterial are nowadays extensively studied since their peculiar mechanical and electronic properties, mostly dominated by the surface state due to their overwhelming surface to bulk ratio (TARI project of E. Kotomin, Riga University).

X-ray imaging tests have been studied onto leaves accumulating toxic metals as effective agents

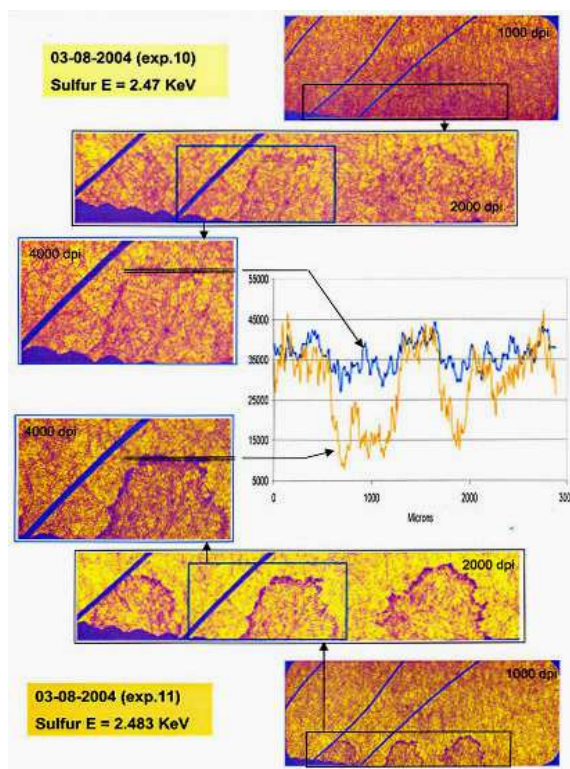


Figure 6: *Dual energy X-ray microradiography test (about 20 μ g/mm² of S per NiSO₄ on 8 μ m paper filter plus Cu reference wires). Imaging below (top) and above (bottom) the sulphur K edge (data by A. Faenov and T. Pikuz, MISDC – Russia).*

for the so-called phytoremediations of polluted environment. The idea is to apply dual energy X-ray microscopy on thin plant leaves supplied with Cd or Pb. An example of the technique, Fig. 6 shows a microradiography of diluted NiSO₄ solution on paper. Recorded by direct contact radiography on a 7 μ m-grain X-ray film at monochromatic energy, namely below (top) and at (bottom) the sulphur K edge energy, these results are rather promising for proceeding with a practical application of the dual energy X-ray imaging in light matrix samples such as biological systems

and biomedical tissues.

A new approach of spectrally tunable backlighting X-ray microscope based on spherically bent crystals of mica is under development. The investigated object is placed downstream the X-ray bent crystal which works as both energy monochromator and focusing system.

On regulating the Bragg's angle the X ray beam energy is selected, and a magnified image is recorded at increasing distances (collaboration with L'Aquila University).

Once widen the spectral range to the lighter element side, in order to include Si, Mg, Na K edges, including also the L absorption lines of transition metals as well as most of the M edges of rare earths, further improvements on the monochromator system and controls are expected to open the energy upper limit.

The use of polycapillary lenses is foreseen in order to increase the photon flux density on the samples for both X-ray spectroscopy and microscopy purposes. With an expected beamspot demagnification down to the micron scale, the main advantage of this optics for soft X-rays includes the intrinsic hollow structure and reduced chromatic aberration.

2.3 UV branch line

The deflected line on the wiggler beam has been devoted to the SUE experiment also in the 2004 (see SUE activity report pag. 189). During the year, refined investigations on the effects induced by irradiations of biological specimens with the UVB-band light have been collected during few dedicated runs. In addition, in cooperation with E. Pace (Department of Astronomy and Space Science) of the Florence University using the existing set up, preliminary tests of simple detectors based on crystalline diamonds have been performed between 200 and 500 nm¹¹).

3 List of Conference Talks by LNF Authors in Year 2004

1. P. Calvani, "Spectroscopy and Microscopy at SINBAD, the Synchrotron Infrared Beamline at DAΦNE", Joint 29th Int. Conf. on Infrared and Millimeter Waves and 12th Int. Conf. on Terahertz Electronics - Karlsruhe, Germany.
2. G. Cibin, "Interlayer Cation Characterization in Phyllosilicates: a XANES Investigation", 6th European Conf. on Mineralogy and Spectroscopy - Wien, Austria.
3. M. Piccinini, "Far-infrared synchrotron radiation spectroscopy of solids in normal and extreme conditions", 15th Int. Conf. on Defects in Insulating Materials (ICDIM 2004), Riga, Latvia.
4. B. Robouch, "Statistical strained-tetrahedron model of local ternary zincblende crystal structures", XV Ural Int. Winter School on the Physics of Semiconductors - Yekaterinburg, Russia.
5. B. Robouch, "Statistical analysis of inter-ionic distances and occupation preferences in ternary zincblende and wurzite structured crystals", Phonons 2004 - St. Petersburg, Russia.
6. B. Robouch, "Statistical strained-tetrahedron model of local ternary zincblende crystal structures", 7th Int. School of Physics - Otradnoe-Moscow, Russia.
7. S. Dabagov, "X-Ray Nanochannelling", E. Conf. X-Ray Spectrometry - (6 -11 June 2004 Alghero, Italy).
8. S. Dabagov, "X-Ray and Neutron Micro- and Nanochannelling, 2nd Int. Conf. X-Ray & Neutron Capillary Optics - Zvenigorod, September 22-26, 2004.

References

1. N.L. Saini *et al.*, Phys. Rev. B **70**, 094509 (2004).
2. Z.Y. Wu *et al.*, Phys. Rev. B **70**, 033104 (2004).
3. J.J. Polit *et al.*, J. Alloys and Compounds **317**, 172 (2004).
4. A. Marcelli *et al.*, J. Phys. Chem. Sol. **65**, 1491 (2004).
5. Z.Y. Wu *et al.*, Phys. Rev. B **69**, 104106 (2004).
6. F. Bonfigli *et al.*, Optics Comm. **233**, 43 (2004).
7. A. Marcelli and G. Cibin, in: Cryoalp - Una ricerca integrata sul ghiaccio alpino. Quaderni della Montagna, **3**, 33 (Bononia University Press, Bologna, 2004).
8. P. Zaidel *et al.*, J. Alloys and Compounds, (2004).
9. G. Cinque *et al.*. The soft X-ray beamline at Frascati, in: Proc. Channeling 2004 (Eds, S. Dabagov and G. Cappuccio, Frascati, November 2004) SPIE Proc. Series (2004).
10. J.J. Polit *et al.*, European Phys. J. - App. Physics, **27**, 321 (2004).
11. E. Burattini *et al.*, LNF Report 04/030(IR) (2004).
12. C. Biscari *et al.*, DAΦNE Tech. Note, INFN-LNF, G-61 (2004).
13. Z.Y. Wu *et al.*, Phys. Scripta (2004).
14. Z.J. Li *et al.*, Phys. Scripta (2004).
15. M.I. Abbas *et al.*, Phys. Scripta (2004).
16. M. Piccinini *et al.*, Phys. Stat. Sol. (C) **1**, 236 (2004).
17. N. Mironova-Ulmane *et al.*, Phys. Stat. Sol. (C) **1**, 704 (2004).
18. L.K. Vodopianov *et al.*, Phys. Stat. Sol. (c) **1**, 2836 (2004).
19. A. Mottana, G. Cibin and A. Marcelli, in: Spectroscopy Methods in Mineralogy (Eds. A. Beran and E. Libowitzky, Vienna, 2004) 526 (Eotvos University Press, Budapest, 2004).
20. E. Burattini, G. Cinque *et al.*, in: Proc. eight Int. Conf. on Synchrotron Radiation Instrumentation, (San Francisco, August 2003) AIP Conf. Proc. **7051**, 81 (2004).
21. A. Marcelli *et al.*, LNF Report 04/006(IR) (2004).
22. M. Cestelli Guidi *et al.*, LNF Report 04/004(IR) (2004).
23. M. Cestelli Guidi *et al.*, Infrared Phys. and Tech. **45**, 365 (2004)
24. M. Cestelli Guidi *et al.*, in: Proc. Joint 29th Int. Conf. on IR and Millimeter Waves and 12th Int. Conf. on Terahertz Electronics, 787 (2004).
25. A. Mottana, EMU Notes in Mineralogy **6**, 465 (2004).
26. M.F. Brigatti *et al.*, N. Jb. Miner. Mh. **3**, 117 (2004).
27. M. Montecchi *et al.*, Optical and Quantum El. **36**, 43 (2004).

GILDA

A. Balerna, S. Mobilio (Resp.), V. Sciarra (Tecn.), V. Tullio (Tecn.)

1 Introduction

GILDA (General Purpose Italian BeamLine for Diffraction and Absorption), is the Italian CRG beamline, built to provide the Italian scientific community with an easy access to the European Synchrotron Radiation Facility to perform experiments with a high energy and brilliance X-ray photon beam. GILDA is funded by the three Italian public research Institutes: Consiglio Nazionale delle Ricerche (CNR), Istituto Nazionale per la Fisica della Materia (INFN) and Istituto Nazionale di Fisica Nucleare (INFN). Experimental stations for X-ray Absorption Spectroscopy, Anomalous X-ray Scattering and X-ray Diffraction (XRD) are present at the GILDA beamline.

2 Activity on the GILDA beamline during 2004

1) The support for the second mirror was realized and will be used to install the new second mirror of the beamline. 2) Off-line tests of the new second mirror to control the surface roughness and the density of the coating were performed. 3) A new software to perform Quick XANES spectra has been developed and tests were performed. It is now possible to record near edge region XANES spectra in few seconds. 4) The new sample holder for X-ray diffraction experiments in grazing incidence was successfully tested. 5) For structural studies on catalysts, a new cell has been built and tested. It allows to monitor the structural evolution of the sample in a reaction environment, to heat the sample and to flow different gasses and control the output products. 6) The realization of a magnetron sputtering system to grow nanoclusters has been continued. The experimental chamber including the mounting of nanocluster substrate and its cooling system has been realized and installed.

3 Beamtime use during 2004 and scientific outcomes

At the end of 2004 the activity of the GILDA beamline was controlled by an International Review Panel. The scientific output of the experiments performed on GILDA has been considered of high quality and it was stressed that with the projected technical developments, the beamline can maintain its high status for the foreseeable future (next 5 years and beyond). During 2004 ESRF delivered beam for about 5000 hours; 3150 hours were used for users experiments, about 700 hours for in-house research, 600 hours for beamline improvement, maintenance and alignment; about 500 hours were delivered in single bunch mode and therefore used for tests. Totally 36 experiments were performed, 27 of Italian users and 9 of European users. Studies and results to be mentioned are the following:

1. Structural characterization of the NiO/Ag(001) interface. In recent years, the physical properties of two dimensional metal-oxide epilayers on metal substrates have become a topic of great interest. Films a few monolayers (ML) can be deposited epitaxially on metal substrates by ultrahigh vacuum techniques, yielding reproducible and well-characterized systems. It has been shown that the energy gap of the oxide, in the oxide/metal system, can be modulated by the film thickness T . It has also been argued that the presence of the metal substrate can

alter significantly the electronic structure of the oxide and influence its chemical properties. To provide an accurate estimate of the geometry of the NiO/Ag(001) interface a polarization dependent XAFS investigation was performed at GILDA and compared with ab-initio simulations. The data showed the absence of significant interdiffusion; the 3 ML epilayer of NiO/Ag(001) is pseudomorphically distorted with the in-plane lattice parameter equal to that of the substrate; an interface Ni-Ag signal was detected which is compatible with the growth of the epilayer with O on top of Ag and an interface distance which is expanded compared to both the Ag and NiO lattice parameters.

2. Origin of the colors in Renaissance lustre pottery. Metal-glass nanocomposites, formed by nanometer-sized crystalline metal clusters embedded in a glass matrix, are characterized by specific optical and magnetic properties. It has been recently found that lustre decorations, typical of the Medieval and Renaissance pottery of the Mediterranean basin, substantially is composed of a heterogeneous distribution of silver and copper nanoparticles of sizes ranging from 5 to 100 nm. These decorations show peculiar optical properties. In spite of the large historical documentation, only little scientific information on lustre is available. To investigate the presence of nanoparticles and of copper ions in the lustre glaze and to determine copper ion states and their local order, a study has been performed on the original samples of Umbrian Renaissance lustre pottery exclusively by nondestructive techniques. Elemental analyses indicate that silver and copper are present in gold decorations, while copper only is present in red decorations. Specifically, silver nanoparticles determine the gold colour, while the red colour is determined by nanoparticles of copper. EXAFS measurements, carried out at the Cu and Ag K edge, indicate that in both gold and red lustre copper is mostly in the oxidized form (Cu⁺ and Cu²⁺) with a large prevalence of Cu⁺. States and local environment of copper ions are similar to those found in copper-alkali ion-exchanged silicate glass samples. This strongly supports the view that lustre formation is mediated by a copper- and silver-alkali ion exchange as a first step, followed by nucleation and growth of metal nanoparticles. Ag K-edge EXAFS data recorded on gold lustre suggest the presence of both metallic and oxidized silver in this case.

4 2005 - GILDA Forseen Activity

During the 2005, the activity foresees: 1) installation of the new second mirror composed by a single piece of silicon, curved by a single actuator; 2) migration of the operating system of the beamline from Microware OS 9 to LINUX; 3) improvement of the present performances of x-ray fluorescence detection with tests on new SDD detectors; 4) test of a new Transition Edge Superconducting (TES) detector, specifically realized for synchrotron radiation applications by the MANU 2 experiment; 5) extension of the Quick XANES software to longer energy ranges to collect Quick EXAFS spectra; 6) first tests and study on the nanocluster samples produced by the nanocluster source under construction at Frascati.

References

1. A. Martorana, G. Deganello, A. Longo, A. Prestianni, L. Liotta, A. Macaluso, G. Pantaleo, A. Balerna, S. Mobilio *J. of Solid State Chem.* **177**, 1268 (2004).
2. F. d'Acapito, S. Mobilio, S. Scalese, A. Terrasi, G. Franz, and F. Priolo *Phys. Rev.* **B 69**, 153310 (2004).
3. C. Maurizio, D. Pergolesi, F. Gatti, F. D'Acapito, M. Razeti, A. Balerna, S. Mobilio, *Nucl. Instrum. Meth.* **A 520**, 610 (2004).

NTA.CLIC
CLIC TEST FACILITY 3

D. Alesini, G. Benedetti, C. Biscari, R. Boni, A. Clozza, A. Drago, D. Filippetto,
A. Gallo, A. Ghigo (Resp.), F. Marcellini, C. Milardi, L. Pellegrino, B. Preger,
M.A. Preger, R. Ricci, C. Sanelli, M. Serio, F. Sgamma,
A. Stecchi, A. Stella, M. Zobov

1 Introduction

The Compact Linear Collider (CLIC) project is a multi-TeV electron-positron collider for particle physics based on the two-beam acceleration concept; a high-intensity drive beam powers the main beam of a high-frequency (30 GHz) linear accelerator with a gradient of 150 MV/m, by means of transfer structure sections.

The aim of the CLIC Test Facility (CTF3) is to make exhaustive tests of the main CLIC parameters. An international collaboration participates to the construction of the machine and the LNF contributes to the realization of a large part of the recombination system, consisting in two rings which will multiply the bunch frequency and peak current by a factor of ten. CTF3 is under construction in the LEP preinjector complex existing building at CERN. It uses where possible the existing magnets, power supplies, equipments and ancillary system.

2 LNF group contribution in year 2004

The INFN Frascati laboratories have been provided the design and realization of the first of the two rings of the bunch train compression system, said Delay Loop, and of the Transfer line that connect the Linac to the Delay Loop including the magnetic Chicane that is used to vary the bunch length in a wide range. In summer 2004 the chicane and the transfer line have been installed and aligned in the tunnel; the vacuum chamber connected and tested together with the diagnostics devices. In autumn 2004 the commissioning of this part of the machine started and full set of measurements on electron beam have been performed. Electron beam trajectory and beam current transport efficiency along the line has been measured by means of beam position system and current monitors. The horizontal and vertical emittances of the linac beam have been measured with the quadrupole scan method monitoring the beam sizes on a carbon OTR screen. The bunch length versus the optical function configurations in the magnetic chicane has been measured using a 3GHz radio-frequency deflector. The electrons of the bunches, passing through the deflector cavities at field zero crossing point, are deflected depending on the longitudinal position; the longitudinal distribution is converted in the vertical distribution on an OTR screen intercepting the beam and measured via an optical system and CCD camera. The layout of the Delay Loop has been completed and the missing magnetic elements are in construction. The vacuum chamber components have been realized, tested and almost ready for installation. The mechanical drawings of the 1.5 GHz RF deflector, needed to inject into the Delay Loop, are ready and the deflector has been in construction. The 1.5 GHz wave-guide components have been selected and ordered.

3 Foreseen activity of the LNF group during year 2005

The foreseen activities for the year 2005 include: the installation of the Delay Loop ring that should be ready before September 2005; the test of all the installed magnetic and vacuum components; the test of beam diagnostics and RF deflector; the ring commissioning with the beam; the test of the recombination of the electron bunch trains.

4 References

1. D. Alesini and F. Marcellini, “Beam Loading in the RF Deflector of the CTF3 Delay Loop”, Proceedings of EPAC2004, 5-7 July, 2004 Lucerne, Switzerland; LNF-04/18(P), 30/07/04.
2. A. Ghigo *et al.*, “Status of CTF3 Stretcher-Compressor and Transfer Line”, Proceedings of EPAC2004, 5-7 July, 2004 Lucerne, Switzerland; LNF-04/18(P), 30/07/04.
3. F. Marcellini and D. Alesini, “Design Options for the RF Deflector of the CTF3 Delay Loop”, Proceedings of EPAC2004, 5-7 July, 2004 Lucerne, Switzerland; LNF-04/18(P), 30/07/04.
4. D. Alesini, C. Biscari, A. Ghigo, F. Marcellini, INFN/LNF; R. Corsini, CERN: “Longitudinal Phase Space Characterization of the CTF3 BEAM with the RF Deflector”, Proceedings of EPAC2004, 5-7 July, 2004 Lucerne, Switzerland; LNF-04/18(P), 30/07/04.
5. M. Preger, “Particle tracking through the measured field of the CTF3 Delay Loop dipole”, CTFF3-009, Apr. 21, 2004.

NTA TTF

L. Cacciotti (Tecn), M. Castellano (Resp), A. Clozza, G. Di Pirro, M. Ferrario,
O. Giacinti (Tecn), S. Guiducci, C. Milardi, R. Sorchetti (Tecn), F. Tazzioli, M. Zobov

1 Introduction

The TESLA Test Facility (TTF) is an international effort, based at Desy (Hamburg), aiming at the development of the technologies required for a Superconducting e^+e^- Linear Collider. High gradient superconducting RF cavities, with their high power coupling and tuning device, and low cost cryostats were the main goal of the project, but also the production of a high power, long pulse electron beam from a RF gun was required. This involved the development of new photocathode, an adequate laser source and new beam diagnostics. In addition to prove the possibility of producing and accelerating the kind of beam required for the future superconducting Linear Collider, TTF has also demonstrated that this beam was of enough good quality to be successfully used for the production of UV coherent radiation with the Self Amplified Spontaneous Emission (SASE) Free Electron Laser process. TTF is now transforming in the TTF VUV/FEL User Facility, becoming a test bench not only for the Linear Collider, but also for the European X-ray FEL Facility. INFN contribution comes from LNF, LNL, Sezione di Milano and Sezione di Roma2.

2 Activities in the year 2004

In 2004 the installation of TTF VUV/FEL (TTF2) was completed, with the last optical diagnostics installed in February, while in spring the first beam was transported from the gun through the first accelerating module and the first bunch compressor. The OTR screen system in the injector, produced and installed by our group, was heavily used to optimize the transport and to measure the beam emittance. In summer the whole diagnostic system based on OTR was commissioned, and used to transport the beam through the entire linac and the undulator. The transport through the second bunch compressor, with its small gap pipe, was accomplished without difficulties. This compressor was normally non operative, with the bunch going on crest in accelerating modules ACC2 and ACC3. The last two modules were kept at very low gradient, to limit the beam energy to 350 MeV for lasing in the 30 nm region. A Martin Puppert interferometer, a jointly effort of Desy, INFN and Sincrotrone Trieste, was installed after the second bunch compressor in order to measure the bunch length in a non intercepting way using the Coherent Diffraction Radiation emitted by a metallic screen with a variable aperture cut through which the beam can pass untouched. First tests, with the bunch compressed only by the first bunch compressor, have been performed to verify the correct alignment of the interferometer.

References

1. A. Cianchi *et al.*, - Commissioning of the OTR Beam Profile Monitor System at the TTF/VUV-FEL Injector, Proceedings of EPAC 2004, Lucerne, Switzerland 2619 (2004).



Figure 1: *The injector FODO structure with the 4 OTR screens for the emittance measurement.*

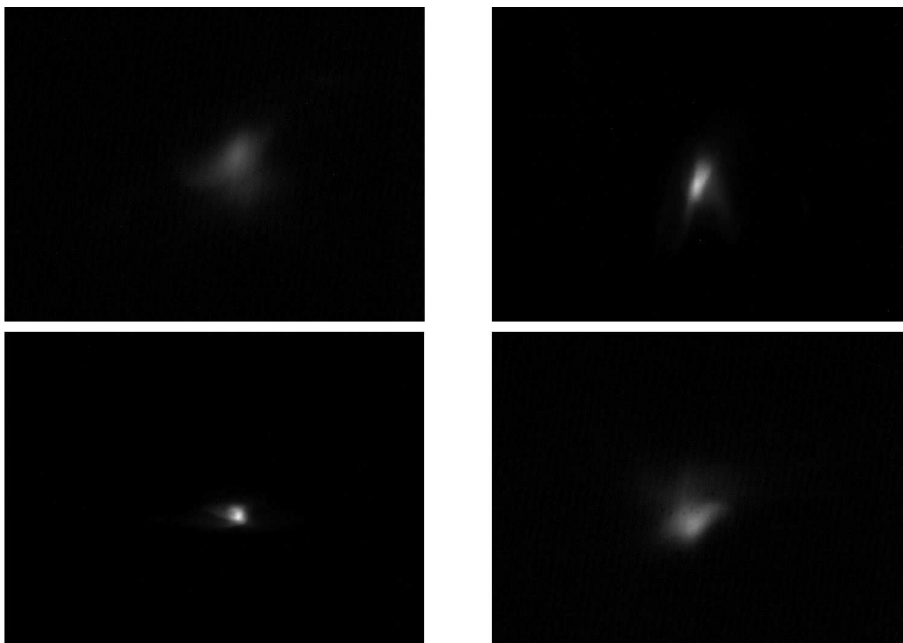


Figure 2: *Beam images for emittance measurement.*

SPARC

D. Alesini, M. Bellaveglia, S. Bertolucci, M.E. Biagini, R. Boni, M. Boscolo, M. Castellano, A. Clozza, G. Di Pirro, A. Drago, A. Esposito, M. Ferrario, D. Filippetto, V. Fusco, A. Gallo, A. Ghigo, S. Guiducci, M. Incurvati, C. Ligi, F. Marcellini, M. Migliorati, A. Mostacci, L. Palumbo (Resp.), L. Pellegrino, M. Preger, P. Raimondi, R. Ricci, C. Sanelli, M. Serio, F. Sgamma, B. Spataro, A. Stecchi, A. Stella, F. Tazzioli, C. Vaccarezza, M. Vescovi, C. Vicario, M. Zobov

F. Alessandria, A. Bacci, I. Boscolo, F. Broggi, S. Cialdi, C. DeMartinis, D. Giove, C. Maroli, V. Petrillo, M. Romè, L. Serafini (**INFN /Milano**)

D. Levi, M. Mattioli, P. Musumeci, G. Medici (**INFN /Roma1**)

L. Catani, E. Chiadroni, A. Cianchi, C. Schaerf, S. Tazzari (**INFN /Roma2**)

1 Aim of the experiment

The aim of the SPARC project (Phase 1) is to promote an R&D activity oriented to the development of a high brightness photoinjector to drive SASE-FEL experiments. It has been proposed by a collaboration among ENEA-INFN-CNR-Università di Roma Tor Vergata-INFN-ST and funded by the Italian Government and INFN with a 3 year time schedule (Phase 1). The main goals of the SPARC project are: 1) the generation of a high brightness electron beam able to drive a self-amplified spontaneous free-electron laser (SASE FEL) experiment in the green visible light and higher harmonics generation, 2) the development of an ultra-brilliant beam photo-injector needed for the future SASE FEL-based X-ray sources. The machine will be installed at LNF, inside an existing underground bunker, see Fig. 1. We foresee conducting investigations on the emittance correction and on the rf compression techniques up to kA level. The SPARC photoinjector can be used also to investigate beam physics issues like surface-roughness-induced wake fields, bunch-length measurements in the sub-ps range, emittance degradation in magnetic compressors due to CSR (SPARC Phase 2). Beams with the features anticipated in the SPARC project are also of strong interest for experiments into other cutting edge fields. The SPARC injector may allow investigations into the physics of ultra-short beams, plasma wave-based acceleration, and production of X-ray Compton back-scattering (PLASMON/MAMBO activities).

We present in this report the status of the design activities of the injector that is under the responsibility of the INFN. In the past year the design of the experiment and the main technological choices have been set up as follows. The proposed system to be built consists of: a 1.6 cell RF gun operated at S-band (2.856 GHz, of the BNL/UCLA/SLAC type) and high peak field on the cathode (120 MV/m) with incorporated metallic photo-cathode (Copper or Mg), generating a 5.6 MeV beam which is properly focused and matched into 3 accelerating sections of the SLAC type (S-band, travelling wave) which accelerate the bunch up to 150-200 MeV.

The choice of the S-band Linac with respect to a L-band is due to compactness of the system, the lower cost, and the existence at LNF of a 800 MeV Linac based on the same technology, with obvious advantages on the side of the expertise and spares components. Moreover, the higher RF frequency leads to a higher peak brightness attainable by an optimized photo-injector. In our case we expect a projected emittance < 2 mm-mrad, a slice emittance ~ 1 mm-mrad with a slice peak current of 100 A.

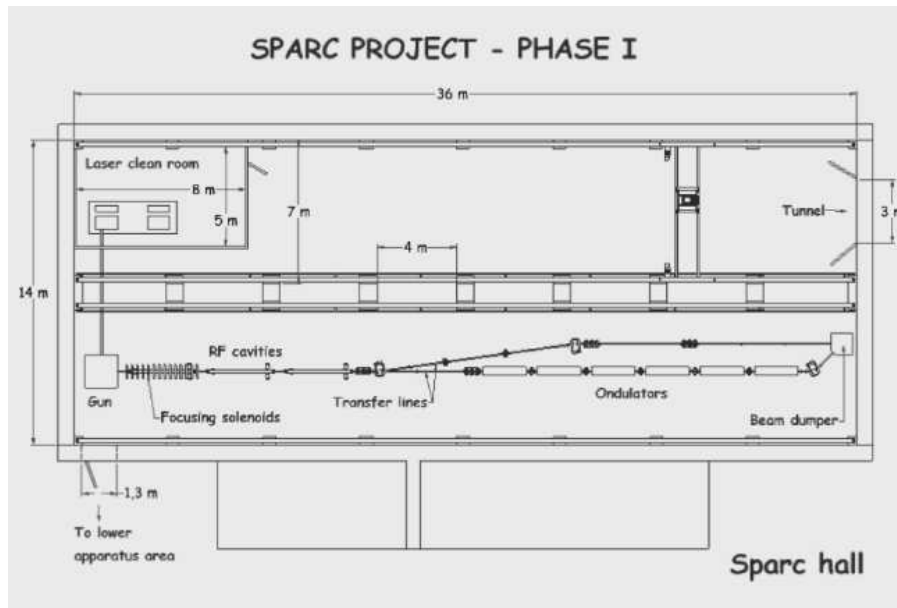


Figure 1: Schematic of layout of the SPARC photo-injector complex inside the SPARC experimental hall, including undulator, and by-pass line (Phase 1).

The production of highest brightness electron beams in the photo-injector requires that a temporally-flat, picosecond laser source be used to drive the photo-cathode. The laser system driving the photocathode will therefore employ high bandwidth Ti:Sa technologies with the oscillator pulse train locked to the RF. The Ti:Sa mode locked oscillator and amplifiers able to produce the requested energy per pulse ($500 \mu\text{J}$ at 266 nm) are commercially available. To obtain the desired time pulse shape we will test the manipulation of frequency lines in the large bandwidth of Ti:Sa, in order to produce the 10 ps long flat-top shape. We plan to use a liquid crystal mask in the Fourier plane of the non-dispersive optic arrangement or a collinear acousto-optic modulator (Dazzler crystal) for linear frequency manipulation.

2 Group activity in 2004

The completion of the Technical Design Report and the procurement of the machine components has been one of the major achievement of the group in the year 2004. This work includes the optimization of the machine layout, start to end simulations and optimization of the beam working point, simulations of beam measurements (virtual experiments program), the design of the main components of the injector such as laser, radiofrequency, magnetic, control and vacuum systems. In addition tender processes of the main components of the machine have been completed.

The experimental activity has also began with the laser pulse shaping measurements and the rf deflector cavity tests.

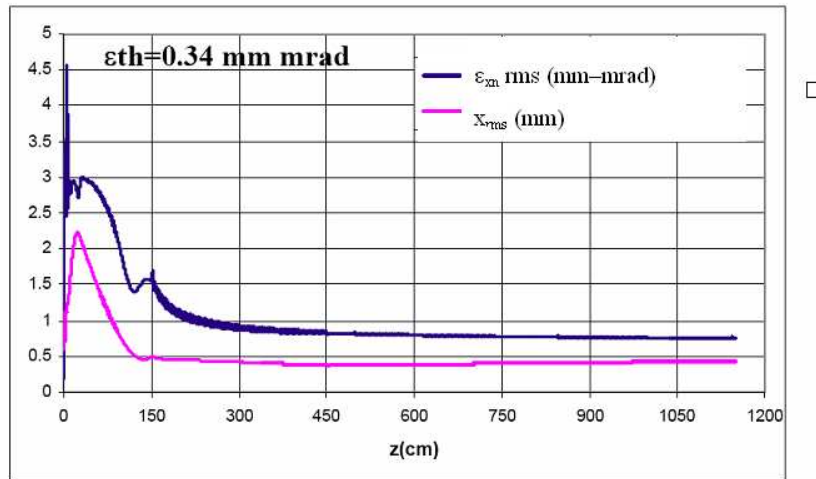
We discuss in the next sub-sections a restricted number of achievements, a more complete documentation about the SPARC activities, including the Preliminary Technical Design Report and the SPAC technical notes, can be found at the following dedicated web page: <http://www.lnf.infn.it/acceleratori/SPARC>

2.1 The Photo-Injector system

The main goals of this activity are the construction, commissioning and characterization of an advanced photo-injector system and the experimental investigation of the new ideas recently conceived: flat-top laser drive pulse manipulation, optimum working point for high brightness RF photo-injector, RF bunch compression technique.

Our simulations using the PARMELA code to track the electron beam from the photocathode to the end of the accelerating sections indicate that we can generate a beam as required by the FEL experiment at 150 MeV. The obtained rms correlated energy spread is 0.2% with rms-normalized emittance lower than $2 \mu\text{m}$ (at 1.1 nC bunch charge, 100 A peak current). The optimized emittance behavior along the channel is reported in Fig. 2. All over the bunch the slice energy spread and the slice normalized emittance at the undulator entrance, calculated over a $300 \mu\text{m}$ slice length, are below 0.05% and $1 \mu\text{m}$ respectively. The whole parameter range of the system has been deeply studied, in particular tolerances and sensitivities are being considered in the beam dynamics simulations.

Q=1.1 nC, pulse length (FWHM) = 10 psec, rise time=1 psec



$\phi_{\text{gun}}=33^\circ$, $r_{\text{cathode}}=1.13 \text{ mm}$, $B_{\text{gun}}=2.73 \text{ Kgauss}$, $B(\text{TW1})=750 \text{ gauss}$

Figure 2: PARMELA simulations of the rms normalized transverse emittance and bunch envelope evolution along the Photo-injector section (RF gun + linac sections, up to 11.5 m).

2.2 Laser pulse shaping experiment

The laser system for SPARC is required to deliver a $500 \mu\text{J}$ pulse of 266 nm wavelength photons to the photo-cathode at a repetition rate of 10 Hz. According to theory and simulation, the emittance compensation scheme requires a laser pulse with transverse and longitudinal profiles that are as uniform as possible. In fact, temporal and spatial flat top laser energy distribution on cathode has been demonstrated to reduce the emittance in recent experiments as well. Additional demands are placed on longitudinal (time) laser profile by the demand for the capability of changing the

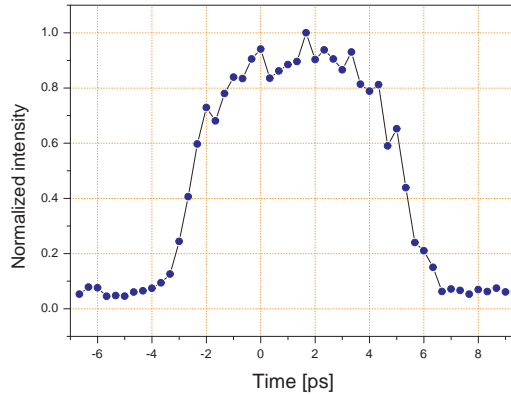


Figure 3: UV pulse time distribution measured by cross-correlation technique

pulse length over a range from 2 to 10 ps to control the charge and peak current. The target is actually a 10 ps FWHM flat top pulse, which is predicted to be the optimum profile for emittance compensation in S-band photoinjectors such as SPARC. Also very short rise and fall times are required (defined as 10 to 90% of the maximum of intensity), definitely shorter than 1 ps. The flat top pulse can be obtained starting from a gaussian or a hyperbolic secant intensity profile, as far as a spectral modulation is applied to both amplitude and phase of the pulse. In order to perform such a phase manipulation two different techniques are envisioned, using a liquid crystal mask or an acousto-optic birefringent crystal. The phase modulation is achieved by varying the optical path of different spectrum components. Here we report the recent results obtained using an acousto-optic crystal (DAZZLER by FASTLITE) for the generation of ps-long laser pulses with flat-top time profile.

During a previous experiment a low energy square laser pulse has been obtained using the DAZZLER acousto-optic (AO) programmable dispersive filter. To generate nC level charge this pulse has to be amplified and converted to UV wavelengths. This consideration motivated further investigations at the Source Development Laboratory (SDL) of the Brookhaven National Laboratory. In the experimental set-up the AO filter were extensively tested using a frequency tripled high energy Ti:Sa laser system. The DAZZLER was installed at the exit of the 10 nm bandwidth oscillator before the stretcher, two amplifiers, compressor and the third harmonic generator. The filter was mounted in the single passage configuration to perform only amplitude modulation of the spectral components. To achieve pulse's duration up to 10 ps a non-complete compression was realized. The filter was used to compensate the phase and amplitude distortion due to the chirped pulse amplification and the non-linear harmonic generation. The non-linear response of these manipulations strongly enhanced even small modulation in the input pulse. For AO filter optimization feedback loop from the measurements was implemented. The characterization of the shaped pulse was carried out using optical based techniques in the time and spectral domain. In the Fig. 3 it is reported the UV intensity profile measured by multi-shot cross-correlation. As shown in the figure the rise and fall time are about 1 ps and ripples are limited to 25%. The pulse length can be increased changing the compression factor.

2.3 Design and First RF measurements results of a X-Band Structure

To get rid of the presence of non-linear components in the beam particle distribution along the longitudinal phase space the insertion of an X-band accelerating section is necessary. A suitable structure, operating on the π standing wave mode, has been designed to obtain a 5 MV accelerating voltage. It is a 9 cells structure fed by a central waveguide coupler or two external antennas at the ends cells. The 2D profile of the structure has been obtained using the codes SUPERFISH and OSCARD2D while the coupler has been designed using the HFSS code. A copper prototype has been realized to perform the experimental tests at room temperature, see Fig. 4. During the experimental test great relevance was given to the bench optimization in order to minimize systematical errors and to better understand the measurement uncertainty. Exciting the structure by the central coupler we excite 5 over 9 possible modes because we impose a non-zero field in the central cell. On the other hand exciting the structure from the antennas, all the modes can be excited for measurement purpose. The quality factor Q and the form factor R_{sh}/Q of the operating π mode have also been measured. With the bead-pull technique the longitudinal electric field behavior on axis has been measured. The theoretical predictions are in excellent agreement with the experimental test.



Figure 4: *SPARC* prototype of the nine cells IV Harmonic cavity.

2.4 Low Energy Beam Diagnostic

To assess the performance of the photo-injector the beam emittance compensation process will be tested as first. The measurement of the transverse emittance oscillation in the drift after the gun exit will be performed for different values of the bunch charge. A double minima behavior is expected, as shown in Fig. 2; the optimum beam matching to the booster is located on the second relative maximum. To measure the beam emittance oscillation after the gun exit a dedicated movable emittance measurement station has been designed, as shown in Fig. 5. The measurement is based on the multislit technique: the beam is sliced into well-separated sampling beamlets by means of an intercepting mask. The slits convert the space charge dominated incoming beam, ($E = 6$ MeV), into several emittance-dominated beams that drift to a detection screen. Numerical

simulation of the measurement have been performed with PARMELA to optimize the device mechanical assembly parameters, (slit width and spacing, distance between multislit mask and output screen), on the basis of analytical guidelines.

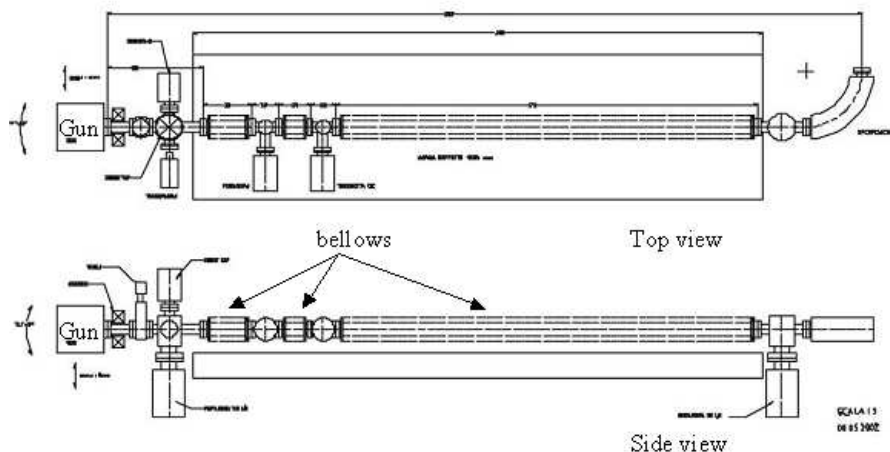


Figure 5: *Movable beam transverse emittance measurement station. A pepperpot and a screen are connected with three bellows in order to scan the emittance along 1m long drift at the exit of the RF gun.*

2.5 High Energy Beam Diagnostic

The characterization of the longitudinal and transverse phase space of the beam at the exit of the third LINAC section, ($E = 150\text{MeV}$), is a tool to verify and tune the photo injector performance. The underneath difficulty is that, for example, the bunch length of the SPARC beam is well beyond the commonly used instrumentation capabilities. By means of an RF deflector it is possible to measure the bunch length and, together with the help of a dispersive system, the longitudinal beam phase space can be completely reconstructed. A schematic layout of the measurement is reported in Fig. 6. The effect of the RF deflector is the following: the RF deflector voltage (the integrated transverse kick) is null in the longitudinal center of the bunch and gives a linear transverse deflection to the bunch itself. If we consider the beam distribution and a drift space of length L after the deflector, the transverse kick results in a transverse displacement of the centroid of the bunch slice. This displacement is proportional to the slice longitudinal offset and RF voltage. A voltage of 1.0 MV has been chosen for the RF deflector, obtaining a resolution of about 2%. A sketch of the longitudinal phase space measurement setup is shown in Fig. 7. In this scenario, the bunch is vertically deflected by the RF deflector and horizontally by a magnetic dipole. The dispersion properties of the dipole allow to completely characterizing the energy distribution of the bunch and the total longitudinal phase space can be displayed on the screen. The transverse phase space characterization is obtained measuring the beam slice emittance in both the transverse planes. As mentioned before, the slice emittance is the transverse emittance of a short time interval (slice) of the microbunch. It can be measured using a beam with a linear energy-time correlation, or chirp; the chirp is combined with the quadrupole scan technique to determine the emittance

of the slices along the bunch. This type of energy-time correlation can be provided by the RF deflector or by use of the dispersive system. Using the RF deflector the horizontal slice emittance ε_x can be measured either on the transfer lines or on the dogleg of SPARC.

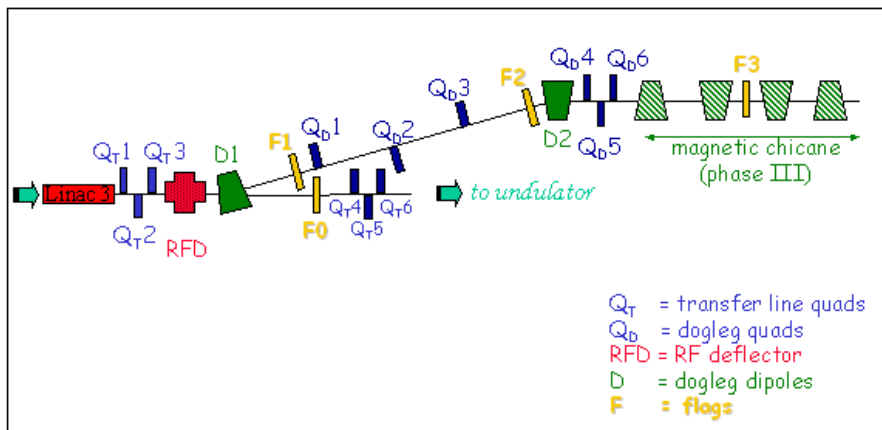


Figure 6: SPARC measurement layout for high energy beam characterization, starting from the third accelerating section.

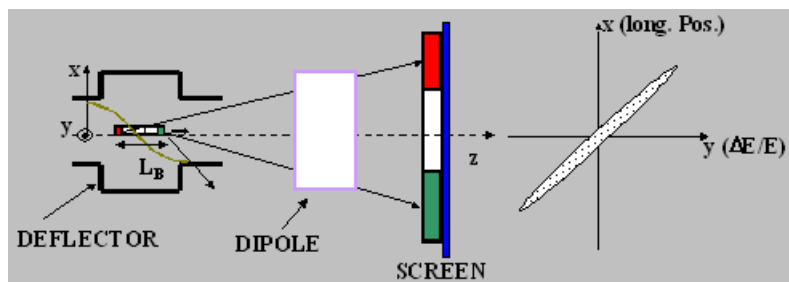


Figure 7: Schematic design of the longitudinal phase space measurement setup, using an RF deflector and a dipole magnet.

2.6 Study of SASE FEL

The FEL SASE experiment will be conducted using a permanent magnet undulator made of 6 sections, each 2.13 m long, separated by 0.36 m gaps hosting single quadrupoles which focus in the horizontal plane. The undulator period is set at 3.0 cm, with an undulator parameter $k_w = 1.4$. Simulations performed with GENESIS show an exponential growth of the radiation power along the undulator. Almost 108 Watts can be reached after 14 m of total undulator length. Preliminary evaluations of the radiation power generated into the non-linear coherent odd higher harmonics show that 107 and 7×10^5 W can be reached on the third and fifth harmonics, respectively.

2.7 Study of a Seeding experiment at SPARC

Besides the Self Amplified Spontaneous Emission (SASE) scheme the FEL can be operated as an amplifier of an external seed signal, and in this case the coherence properties are determined by the seed characteristics while the FEL radiation has significantly lower intensity fluctuations. The Harmonic Generation process in an FEL can also be exploited to widen the wavelength range of operation toward the shorter wavelengths. The two concepts, of seeding and harmonic generation, can be coupled in a single device capable of providing both temporally and spatially coherent radiation at short wavelengths, with significantly reduced intensity fluctuations in a more compact and less expensive configuration.

Sources based on high order harmonics generated in gas with high power Ti:Sa lasers pulses represent promising candidates as seed sources for FELs for several reasons, as spatial and temporal coherence, wavelength tunability and spectral range, which extends down to the 10^{-9} m wavelength scale. In this arrangement, an external laser source is seeded into a modulator, i.e. an undulator where a periodic energy modulation is induced in the electron beam. This modulation occurs with the periodicity of the seed wavelength, the successive beam evolution in a dispersive section induces the conversion of the energy modulation into a density modulation and consistent emission of radiation at higher order harmonics with longitudinal and transverse coherence reproducing those of the laser seed. On SPARC a chamber will be installed devoted to the generation of a short pulse (few tens of fs) of high order harmonics generated in a crystal (400 nm and 266 nm) and in a gas (266nm, 160 nm, 114nm, 88nm), to be seeded in the SPARC FEL. Diagnostics of the output radiation in terms of spectrum and pulse duration provides relevant information about the FEL amplification process. The SPARC configuration is monitored by diagnostic stations located in between the undulator sections with the opportunity to follow the dynamics along the pulse propagation in different FEL regime.

2.8 Study of Bunch Compression Techniques

A second phase of the SPARC project is planned to beam dynamics studies relative to the bunch compression systems. To exploit the RF compression technique, based on the velocity bunching (VB) scheme, a dedicated accelerating section will be inserted downstream the RF gun. First simulations results obtained with Parmela are shown in Fig. 8. A peak current $I_{peak} \simeq 320$ A is reached on one slice, and the 50 % of the beam shows $I_{slice} > 200$ A, while the slice emittance is lower than $1 \mu\text{m}$ for the 80 % of the bunch. At the same time a standard magnetic chicane will be installed in a parallel beam line (“14° dogleg”), see Fig. 1, to allow experimental investigations of CSR induced effects on emittance degradation and surface roughness wake-field effects.

2.9 Study of Further Experiments at SPARC

Two main R&D activities are further foreseen: 1) the plasma acceleration of electron beams by means of laser excited plasma waves, 2) the development of a monochromatic and tunable X-ray source, (20-1000 keV), via Thomson scattering of laser pulse in the visible region on relativistic electron beam. In Tab. 1 the main beam requirements are reported. Two additional beam lines are planned on this purpose: the design and optimization is presently under study.

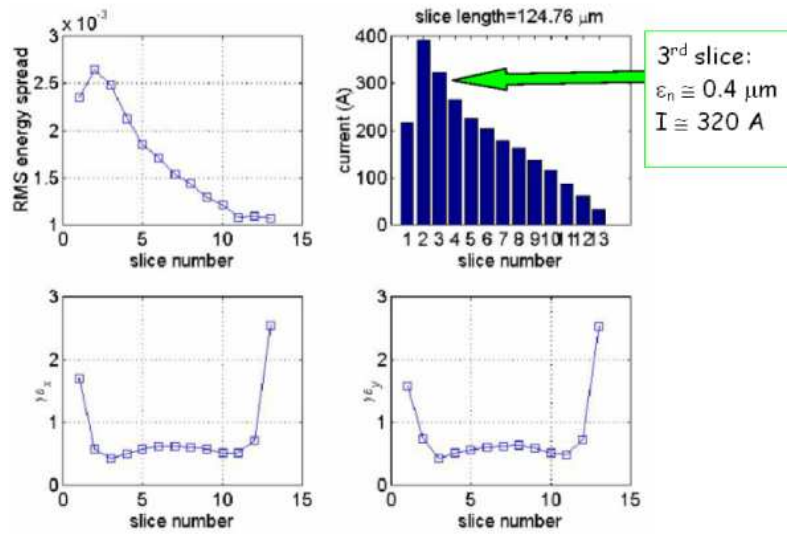


Figure 8: *Slice analysis through the compressed bunch. Top left: energy spread; top right: current distribution; bottom left: horizontal emittance, bottom right: vertical emittance.*

Application	Q (nc)	E (MeV)	σ_t (ps)	ϵ_n (μm)	$\sigma_{\psi/\gamma}$ (%)
FEL-SASE	1	150	3	2	0.1
Plasma-Acc	0.025	100-200	0.025	0.1	0.2
Monochr. X	1-3	30-200	3	2-5	0.2-0.1

Table 1: *Beam relevant parameters for the three main applications included in the SPARC project.*

References

1. D. Alesini *at al.*, (The SPARX Study Group), “Status of the SPARC project”, contributo a European Particle Accelerator Conference 2004, pp. 399-401, Lucerne, Switzerland, JULY 2004, anche SPARC- GE - 04/001, Frascati, 13 Luglio 2004.
2. D. Alesini *at al.*, (The SPARX Study Group), “Design study for advanced acceleration experiments and monochromatic X- ray production at SPARC”, European Particle Accelerator Conference, Lucerne, Switzerland, JULY. (pp. 695-697), anche SPARC GE - 04/001, Frascati, 13 Luglio 2004.
3. M. E. Biagini *at al.*, “SPARC Photoinjector Working Point Optimization, Tolerances and Sensitivity to Errors”, contributo a European Particle Accelerator Conference 2004, pp. 396-398, Lucerne, Switzerland, July 2004, anche SPARC GE - 04/001, Frascati, 13 Luglio 2004.

4. M. Ferrario, V. Fusco, M. Migliorati, L. Palumbo, B. Spataro, "Wake Fields Effects in the SPARC Photoinjector", contributo a European Particle Accelerator Conference 2004, pp. 405-407, Lucerne, Switzerland, JULY 2004, anche SPARC GE - 04/001, Frascati, 13 Luglio 2004.
5. I. Boscolo *at al.*, "Laser Temporal Pulse Shaping Experiment for SPARC Photoinjector", contributo a European Particle Accelerator Conference 2004, pp. 1300-1302, Lucerne, Switzerland, JULY 2004, anche SPARC GE - 04/001, Frascati, 13 Luglio 2004.
6. M. Boscolo *at al.*, "Design Study of a Movable Emittance Meter Device for the SPARC Photoinjector", contributo a European Particle Accelerator Conference 2004, pp.2622-2624, Lucerne, Switzerland, July 2004, anche SPARC GE - 04/001, Frascati, 13 Luglio 2004.
7. D. Alesini *at al.*, "An RF Deflector Design for 6d Phase Space Characterization of the Sparc Beam", contributo a European Particle Accelerator Conference 2004, pp.2616-2618, Lucerne, Switzerland, July 2004, anche SPARC GE - 04/001, Frascati, 13 Luglio 2004.
8. D. Alesini *at al.*, "The Design of a Prototype RF Compressor for High Brightness Electron Beams", contributo a European Particle Accelerator Conference 2004, pp. 698-700, Lucerne, Switzerland, July 2004, anche SPARC GE - 04/001, Frascati, 13 Luglio 2004.
9. M. Ferrario, J. Rosenzweig, J. Sekutowicz, "An Ultra-high Brightness, High Duty Factor", Superconducting RF Photoinjector, contributo a European Particle Accelerator Conference 2004, pp. 402-404, Lucerne, Switzerland, JULY 2004, anche SPARC GE - 04/001, Frascati, 13 Luglio 2004.
10. A. Renieri *at al.*, "Status Report on SPARC Project", contributo a Free Electron Laser Conference 2004, pp. 163-166, Trieste, Italy, 29 August 3 September 2004, anche SPARC - GE - 04/003, Frascati, 17 Settembre 2004.
11. D. Alesini *at al.*, (The SPARX Study Group), "The SPARX Project : R&D Activity towards X-rays FEL Sources", contributo a Free Electron Laser Conference 2004, pp.407-410, Trieste, Italy, 29 August 3 September 2004, anche SPARC - GE - 04/003, Frascati, 17 Settembre 2004.
12. A. Ghigo *at al.*, "Preliminary Results Using an Acousto-optic Dispersive Filter for laser Pulse Shaping", LS-04/001, 15/01/2004.
13. F. Sgamma, "The SPARC Project Alignment Procedures", ME-04/001, 22/09/2004.
14. L. Pellegrino, U. Rotundo, "Misura di Vibrazioni Meccaniche per SPARC", ME-04/002, 23/11/2004.
15. M. Ferrario, V. Fusco, M. Migliorati, L. Palumbo, B. Spataro, "Off-Axis Beam Dynamics in the Homdyn Code", BD-04/001, 20/01/2004.
16. M. Boscolo, M. Ferrario, S. Reiche, "Studies of Gaussian Pulse Shaping at SPARC", BD-04/002, 25/10/2004.

YEAR 2004 FRASCATI PUBLICATIONS

Available at www.lnf.infn.it

1 – Frascati Physics Series

Volume XXXIII

Bruno Touschek Memorial Lectures

M. Greco, G. Pancheri

Frascati, May 11, 1987

ISBN – 88-86409-40-0

Volume XXXIV – Special Issue

*Les Rencontres de Physique de la Vallée d'Aoste –
Results and Perspectives in Particle Physics*

M. Greco

La Thuile, Aosta Valley, February 29 – March 6, 2004

ISBN – 88-86409-42-7

Volume XXXV

Heavy Quarks And Leptons 2004

A. López

San Juan, Puerto Rico, 1–5 June 2004

ISBN – 88-86409-43-5

Volume XXXVI

DAΦNE 2004: Physics at Meson Factories

F. Anulli, M. Bertani, G. Capon, C. Curceanu-Petrascu, F.L. Fabbri, S. Miscetti

Frascati, June 7–11, 2004

ISBN – 88-86409-53-2

2 – LNF–Frascati Reports

LNF–04–01 (P)

S. Bianco (on behalf of the BTeV Coll.)

Status of BTeV experiment at the Fermilab Tevatron

Presented at the Intern. Conf. on Physics at LHC, Vienna (Austria) 2004

LNF–04–02 (P)

S. Di Matteo, Y. Joly, A. Bombardi, L. Paolasini, F. de Bergevin, and C. R. Natoli

Observation of Local Chiral–Symmetry Breaking in Globally Centrosymmetric Crystals

Phys. Rev. Lett. 91 257402 (2003)

LNF–03–03 (IR)

D. Hampai, S.B. Dabagov, and G. Cappuccio

PolyCAD: A New X–Ray Tracing Code for Cylindrical Polycapillary Optic

LNF–03–04 (IR)

M. Cestelli Guidi, A. Marcelli, A. Nucara and P. Calvani

Infrared Spectra Normalization at SINBAD

LNF–03–05 (P)

E. Basile F. Bellucci M. Bertani S. Bianco M.A. Caponero F. Di Falco F.L. Fabbri
F.Felli M. Giardoni A. La Monaca G. Mensitieri B. Ortenzi M. Pallotta A. Paolozzi
L. Passamonti D. Pierluigi A. Russo S. Tomassin

*Study of Tensile Response of Kapton and Mylar Strips to AR and CO₂ Mixtures for the
BTeV Straw Tube Detector*

Presented by F. Di Falco at 10th Vienna Conf. on Instrumentation 16–21 Feb 2004,
Vienna, Austria

LNF–04/06 (IR)

A. Marcelli, G. Cibin and A. Raco

*Progetto e Realizzazione di un Manipolatore Micrometrico a sei Gradi di Liberta' per
Spettroscopia a Bassa Temperatura in Alto Vuoto*

LNF–04–07 (IR)

S.V. Bulanov, T. Esirkepov, P. Migliozzi, F. Pegoraro, T. Tajima, F. Terranova

Neutrino Oscillation Studies with Laser–Driven Beam Dump Facilities

LNF–04–08 (IR)

AA.VV.

Activity Report 2003

LNF–04–09 (IR)

C. Catena, D. Pomponi, G. Trenta, F. Celani, P. Marini, G. De Rossi, E. Righi

Acqua Pesante (D₂O) Irradiata: Dal Reattore Nucleare Alla Cellula

LNF-04-10 (NT)

M. Bassan, L. Quintieri

Progetto di una Sospensione Meccanica a Bassa Frequenza di Risonanza per Masse Cilindriche

LNF-04-11 (NT)

Marco Cordelli, Agnese Martini, Luciano Trasatti

PICCA – a PIC demo board for LabVIEW courses

LNF-04-12 (P)

M. Agnello, G. Beer, L. Benussi, M. Bertani, S. Bianco, E. Botta, T. Bressani, L. Busso, D. Calvo, P. Camerini, P. Cerello, B. Dalena, F. De Mori, G. D'Erasmus, D. Di Santo, F.L. Fabbri, D. Faso, A. Feliciello, A. Filippi, V. Filippini, E.M. Fiore, H. Fujioka, P. Gianotti, N. Grion, A. Krasnoperov, V. Lucherini, S. Marcello, T. Maruta, N. Mirfakhrai, O. Morra, A. Olin, E. Pace, M. Pallotta, M. Palomba, A. Pantaleo, A. Panzarasa, V. Patichio, S. Piano, F. Pompili, R. Rui, G. Simonetti, H. So, S. Tomassini, R. Wheadon, A. Zenoni

First results on hypernuclear spectroscopy from the FINUDA experiment at DAΦNE

Presented By M. Bertani at MESON 2004, 8th International Workshop On Meson Production, Properties And Interactions,(June 2004 Crakow, Poland)

LNF-04-13 (P)

L. Benussi (on behalf of the FOCUS Coll.)

Focus Measurements of Masses And Widths of Excited Charm Mesons $D_{2^{}}$ And Evidence for Broad States*

Presented at MESON04 (Cracow Poland 2004)

LNF-04-14 (P)

S. Bianco (on behalf of the FOCUS Coll.)

New Focus Results On Charm Physics

Presented at Les Rencontres de Physique de la Vallée d'Aoste - Rencontre and Perspectives in Particle Physics, La Thuile, Aosta Valley, February 29- March 6, 2004

LNF-04-15 (P)

S. Bianco

Hot Topics In Charm Physics

Presented at Second PANDA Workshop, Frascati 2004

LNF-04-16 (P)

I.I. Bigi

Per Aspera ad Astra' — A Short Essay on the Long Quest for CP Violation

It will appear in the Proceedings of the Conference 'Time & Matter 2000'

LNF-04-17 (P)

D. Benson, I.I. Bigi, N. Uraltsev

On 'Bias' Corrections to the Photon Energy Moments in $B \rightarrow X_s + \gamma$

LNF-04-18 (P)

Accelerator Division

Papers presented at EPAC 2004

Contributions to the 9th European Particle Accelerator Conference (EPAC 2004)

LNF-04-19 (P)

E. Basile, F. Bellucci, L. Benussi, M. Bertani, S. Bianco, M.A. Caponero, D. Colonna, F. Di Falco, F.L. Fabbri, F. Felli, M. Giardoni, A. La Monaca, G. Mensitieri, B. Ortenzi, M. Pallotta, A. Paolozzi, L. Passamonti, D. Pierluigi, C. Pucci, A. Russo, G. Saviano, S. Tomassini

A New Configuration for a Straw tube-Microstrip Detector

Presented by E. Basile at the IEEE NSS Conference, Rome, October 19 2004

LNF-04-20 (P)

B.V. Robouch, E.M. Sheregii, A. Kisiel

Statistical Analysis Of Inter-Ionic Distances And Occupation Preferences In Ternary Zincblende And Wurzite Structured Crystals

Proceedings 11th International Conf. on Phonon Scattering in Condensed Matter - Phonons2004, St Petersburg, Russia, July 25-30, 2004 Phys. Stat. Sol. (2004) (in press)

LNF-04-21 (IR)

B.V. Robouch, A. Kisiel, E. Burattini, I. Kutcherenko, L.K. Vodopyanov

Local Structure Properties of $Ga_{1-x}Al_xN$ Epitaxial Layer

LNF-04-22 (P)

F. Terranova, A. Marotta, P. Migliozi, M. Spinetti

High Energy Beta Beams without Massive Detectors

Submitted to the European Physical Journal C

LNF-04-23 (P)

B.V. Robouch, E.M. Sheregii, A. Kisiel

Statistical Strained-Tetrahedron Model Of Local Ternary Zincblende Crystal Structures

Proceedings: 32nd ITEPh Winter School and 7th International Moscow School of Physics, 16-26/Feb/2004, Otradnoe-Moscow, Russia

LNF-04-24 (IR)

M. Anelli, B. Buonomo, G. Mazzitelli and P. Valente

A Scintillating-fiber Beam Profile Monitor for the DAΦNE BTF

LNF-04-25 (IR)

E. Basile, F. Bellucci, L. Benussi, M. Bertani, S. Bianco, M. A. Caponero, D. Colonna, F. Di Falco, F.L. Fabbri, F. Felli, M. Giardoni, A. La Monaca, G. Mensitieri, B. Ortenzi, M. Pallotta, A. Paolozzi, L. Passamonti, D. Pierluigi, C. Pucci, A. Russo, G. Saviano, S. Tomassini

Novel Approach for an Integrated Straw Tube–Microstrip Detector

LNF-04-26 (IR)

D. Babusci, C. Curceanu(Petrascu), S. Dell'Agnello, G. Delle Monache, M.A. Franceschi, M. Ricci, R. Vittori

Select Experimental Trends in Astro–Particle Physics in Space

LNF-04-27 (IR)

M. Incurvati, C. Sanelli

A Power Supply Study for the Ramping Dipoles of the Synchrotron Ring of the CNAO Project

LNF-04-28 (IR)

A. Cecchetti, B. Dulach, D. Orecchini, G. Peiro, F. Terranova

Chemical and Magnetic Characterization of the Steels for the Opera Spectrometer

LNF-04-29 (P)

F. Ronga

Neutrino Long Base Line Experiments in Europe

Published on: Presented at the Conference NOW 2004, Otranto, 12-17, September 2004

LNF-04-30 (IR)

E. Burattini, A. De Sio, F. Malvezzi, A. Marcelli, F. Monti, E. Pace

Caratterizzazione di un Fotoconduttore Basato su Singolo Cristallo di Diamante 1b Mediante Luce di Sincrotrone

3 – INFN Reports

INFN-AE-04-01

Barbara Famoso, Francesco Riggi

A Proposal For Cosmic Ray Studies Involving Collaborations Between Higher Education, Research Sites and Local Area High Schools

INFN-AE-04-02

G.A.P. Cirrone, G. Cuttone, S. Donadio, V. Grischine, S. Guatelli, P. Gumplinger, V. Ivanchenko, M.Maire, A. Mantero, B. Mascialino, P. Nieminen, L. Pandola, S. Parlati, A. Pfeiffer, M.G. Pia, L. Urban

Precision Validation of Geant4 Electromagnetic Physics

INFN-AE-04-03

S. Donadio, S. Guatelli, B. Mascialino, A. Pfeiffer, M.G. Pia, A. Ribon, P. Viarengo

A Software Toolkit For Statistical Data Analysis

INFN-AE-04-04

L. Beaulieu, J.F. Carrier, F. Castrovillari, S. Chauvie, F. Foppiano, G. Ghiso, S. Guatelli, S. Incerti, E. Lamanna, S. Larsson, M.C. Lopes, L. Peralta, M.G. Pia, M. Piergentili, P. Rodrigues, V.H. Tremblay, A. Trindade

Overview of Geant4 Application in Medical Physics

INFN-AE-04-05

P. Cirrone, S. Donadio, S. Guatelli, A. Mantero, B. Mascialino, L. Pandola, S. Parlati, M.G. Pia, P. Viarengo, F. James, A. Pfeiffer, A. Ribon

Code-testing of Statistical Test Implementations

INFN-AE-04-06

Franca Foppiano, Susanna Guatelli, Jakub Moscicki, Maria Grazia Pia, Michela Piergentili
From Dicom Togrid: A Dosimetric System For Brachytherapy Born From Hep

INFN-AE-04-07

Stefania Donadio, Susanna Guatelli, Barbara Mascialino, Andreas Pfeiffer, Maria Grazia Pia, Alberto Ribon, Paolo Viarengo

Data Analysis in Hep: A Statistical Toolkit

INFN-AE-04-08

G.A.P. Cirrone, S. Donadio, S. Guatelli, A. Mantero, B. Mascialino, S. Parlati, A. Pfeiffer, M.G. Pia, A. Ribon, P. Viarengo

A Goodness-of-Fit Statistical Toolkit

INFN-AE-04-09

Stefania Donadio, Susanna Guatelli, Barbara Mascialino, Andreas Pfeiffer, Maria Grazia Pia, Alberto Ribon, Paolo Viarengo
A Statistical Toolkit for Data Analysis

INFN-AE-04-10

Antonio Codino, François Plouin
The Extension and Shape of the Collecting Zones of the Galactic Cosmic Rays From Helium to Iron

INFN-AE-04-11

Susanna Guatelli, Maria Grazia Pia
The Geant4 REMSIM Simulation for Dosimetry in Interplanetary Manned Space Missions

INFN-AE-04-12

Angela Badalà, Roberto Barbera, Giuseppe Lo Re, Armando Palmeri, Alberto Pulvirenti, Giuseppe S. Pappalardo, and Francesco Riggi
Reconstruction of the $K^(892)0$ Resonance Signal in Pp Collisions at the LHC Regime Through the Alice Detector*

INFN-AE-04-13

Barbara Famoso, Paola La Rocca and Francesco Riggi
Long Term Monitoring of Cosmic Ray Flux And Atmospheric Pressure: Estimation of the Barometric Coefficient by a Simple Geiger Counter

INFN-AE-04-14

Paola La Rocca and Francesco Riggi
Are Small Single Geiger Counters Able to Show up Cosmic Daily Variation Effects? A Case Study for Educational Investigations

INFN-BE-04-01

Simone Cialdi, Ilario Boscolo
A Shaper for Providing Long Laser Waveforms

INFN-TC-04-01

V. Carassiti, F. Evangelisti, M. Furini, L. Landi, M. Melchiorri, S. Squerzanti G. Ciullo, P. Ferretti-Dalpiaz, P. Lenisa
Il Ciclo di Costruzione della Target Cell del Recoil Detector dell'Esperimento HERMES

INFN-TC-04-02

G. Avellino, S. Beco, B. Cantalupo, A. Maraschini, F. Pacini, S. Monforte, M. Pappalardo, D. Kouril, A. Krenek, Z. Kabela, L. Matyska, M. Mulac, J. Pospisil, M. Ruda, Z. Salvat, J. Sitera, M. Vocu, F. Giacomini, E. Ronchieri, A. Gianelle, R. Peluso, M. Sgaravatto, M. Mezzadri, F. Prelz, A. Guarise, R. Piro, A. Werbrouck, D. Colling

Supporting the Development Process of the DataGrid Workload Management System Software with GNU autotools, CVS and RPM

INFN-TC-04-03

Tullio Macorini, Claudio Strizzolo, Lucio Strizzolo

Una Struttura di Autenticazione Centralizzata per Diversi Gruppi di Sistemi LINUX, Realizzata con NIS e ISPEC

INFN-TC-04-04

A. Galata' L. Ciavola, F. Consoli, S. Gammino, S. Marletta

Comparison of ECR Ion Source Performance for Different Microwave Generators

INFN-TC-04-05

Matteo Sassi

Study of a Pure Object Programming Language for Reliable System Development

INFN-TC-04-06

E. Acerbi, G. Baccaglioni, G. Cartegni, M. Sorbi, G. Volpini

Detection of Turn-to-turn Insulation Failures in the Toroidal ATLAS Coils after Cold Mass Assembling

INFN-TC-04-07

Antonio Ordine

Nbn: A Fast, Low Cost, Mini Data Acquisition System for Nuclear Physics

INFN-TC-04-08

Domenico Diacono, Giacinto Donvito

Realizzazione di un Web Server Sicuro con User Mode Linux

INFN-TC-04-09

Progetto: V. Carassiti, F. Evangelisti; Calcoli struttura e azionamenti: V. Carassiti; Disegni: F. Evangelisti; Installazione degli azionamenti: M. Furini, L. Landi, M. Melchiorri, S. Squerzanti; Comandi e controlli degli azionamenti: R. Malaguti, S. Mantovani, C. Pennini

Cloud Radar: Radar Airborne per Misure in Nube, Note di Calcolo sul Sistema di Puntamento

INFN-TC-04-10

Claudio Strizzolo

Un Layout piu' Accessibile per il Sito WEB della Sezione di Trieste dell' INFN

INFN-TC-04-11

Antonio Anastasio

Realizzazione di un Sisema di Movimentazione dei Bersagli per un Laser a 1KH

INFN-TC-04-12

Vincenzo Masone

La Controller Board dello Spettrometro di Muoni dell' esperimento Opera

INFN-TC-04-13

Lucio Rossi, Massimo Sorbi

Qlasa: A Computer Code For Quench Simulation In Adiabatic Multicoil Superconducting Windings

INFN-TC-04-14

Linda Imbasciati, Lucio Rossi, Massimo Sorbi, Piero Spillantini

Optimization of Superconducting Coils for Solar Cosmic Rays Protection During Interplanetary Missions

INFN-TC-04-15

Sergio Andreozzi, Daniele Bonaccorsi, Vincenzo Ciaschini, Alessandro Cavalli, Flavia Donno, Sergio Fantinel, Federica Fanzago, Antonia Ghiselli, Alessandro Italiano, Mirco Mazzucato, Andrea Sciaba, Heinz Stockinger, Gennaro Tortone, Marco Verlatto, Cristina Vistoli

Pilot Production Grid Infrastructure For High Energy Physics Applications

INFN-TC-04-16

Sergio Andreozzi

GLUE Schema Implementation for the LDAP Data Model

INFN-TC-04-17

Riccardo Veraldi, Francesca Del Corso

Implementazione di un VPN Server Utilizzando il Cisco VPN Concentrator 3005

INFN-TC-04-18

Sergio Andreozzi, Vincenzo Ciaschini, Luca dell'Agnello

An Abstract Model of the Virtual Organization Membership Service

Glossary

These are the acronyms used in each status report to describe personnel qualifications other than Staff Physicist:

Art. 15	Term Contract (Technician)
Art. 23	Term Contract (Scientist)
Ass.	Associated Scientist
Ass. Ric.	Research Associate
Bors.	Fellowship holder
Bors. PD	Post–Doc Fellow
Bors. UE	European Community Fellow
Dott.	Graduate Student
Laur.	Undergraduate Student
Osp.	Guest Scientist
Perfez.	Post–Laurea Student
Resp.	Local Spokesperson
Resp. Naz.	National Spokesperson
Specializ.	Post–Laurea Student
Tecn.	Technician